THE UNIVERSITY of ADELAIDE

Hydrothermal liquefaction of biosolids

By

Jasim Mohammed Jasim Al-juboori

Thesis submitted for the degree of Doctor of Philosophy

School of Chemical Engineering, and Advanced Materials

Faculty of Engineering Computer & Mathematical Sciences

The University of Adelaide, Australia

November 2021

Contents

Executive summary

Hydrothermal liquefaction (HTL) is a promising thermochemical conversion process to convert biosolids into renewable crude oil. HTL process can be achieved at temperatures between 200 to 350°C, pressures between 50 to 250 bar, and residence time between 1 and 60 minutes. The HTL produces four phases: renewable crude oil, aqueous, gaseous and solid phases. For the process to be upgraded to an industrial scale, it is needed to gain a better understanding of the HTL of biosolids. However, there is limited information to validate the effects of the interactions between the biosolid content under HTL reaction conditions on the yield and the composition of the produced renewable crude oil.

The primary objective of this research is to provide a better understanding of the HTL of biosolids, which was achieved through the following detailed objectives. The first objective is to quantify the variability in the biosolids composition to determine the chemical compositions of biosolids. The second objective is to understand how this variable biosolids feedstock behaves through HTL, especially to measure the effects of organic compounds of biosolids: lipids, proteins, carbohydrates, and lignins on the HTL yields. The third objective is to provide a new understating of the characterisation of HTL products from biosolids by identifying the effects of biosolid components and the HTL conditions on both the distributions of the HTL products' yields and on the qualities of renewable crude oil. The fourth objective is to assess the use of biosolids with dominant organic fraction via different reaction temperatures and residence times on the composition and fractions of the produced renewable crude oil.

From the results of the experiments, biosolids have different characters that affect the yield and quality of renewable crude oil. Applying a Van Krevelen diagram to compare biosolids with other biomass indicated that only some biosolids samples have similar characteristics to that of biomass. The difference in the characteristic of the organic content of biosolid samples could

depend on several reasons, such as the sources of the biosolids and the treatment process. The effects of the biosolids' composition on the HTL yield show that lipids and proteins have positive impacts on the renewable crude oil yield, while carbohydrates and insoluble lignin led to an increase in the solid residue. The renewable crude oil contained a high amount of high-boiling point materials in comparison with low-boiling point materials for all biosolids samples used in this study. The effect of the operating conditions, such as temperature was significant. The renewable crude yield usually increases with an increase in temperature until a specific temperature is reached, at which point the renewable crude yield starts to decrease. Various residence times also affected renewable crude oil yields significantly. The optimal residence times depended on the biosolids content and temperature.

The HTL of biosolids with different organic fractions resulted in different renewable crude oil compositions, which contained a complex mixture of >300 major compounds that were identified using Gas chromatography-mass spectroscopy analyser. The predominant components identified from the lipid, protein, carbohydrate and lignin constituents were cyclic terpanes and terpenes, along with nitrogenous, oxygenated, and phenolic components. Based on the boiling point of the produced compounds, high gasoline and naphtha-like and high diesel-like yields were produced from biosolid samples with high lipid and protein content, while the kerosene-like best yield was generated from a high lipid sample. A significant gas oil-like yield was produced from the high lipid and carbohydrate biosolid samples, while a high yield of wax, lubricating oil and vacuum gas oil-like contents were generated from the high lignin sample. In summary, the results of the outcomes of this work and the methods used to analyse the chemical compositions of biosolids can form a significant facet of future industrial development of HTL of biosolids, particularly in commercial plants design and management.

Finally, it is hoped that the methods presented here, especially the methods used to analyse the chemical compositions of biosolids and the outcomes of this work, especially regarding the composition of the produced renewable crude oil, can form a significant facet of future industrial development of the HTL of biosolids.

Declaration

I certify that this work contains no materials which have been accepted for the award of any other degree or diploma, in my university or other tertiary institution, to Jasim Mohammed Jasim Al-juboori, and, to my best knowledge and belief, contains no material previously published or written by any other person, except where due reference has made in the text. In addition, I certify that no part of this work will, in the future, be used in a submission in my name, for any other degree or diploma in any university or other tertiary institution, without the prior approval of the University of Adelaide, and where applicable, any partner institution responsible for the joint-award of this degree.

I acknowledge that the copyright of published works contained within this thesis resides with the copyright holder(s) of those works.

I also give permission for the digital version of my thesis to be made available on the web, via the University's digital research repository, Library Search and also through web search engines, unless permission has been granted by the University to restrict access for a period of time.

I acknowledge the support I have received for my research through the provision of an Australian Government Research Training Program Scholarship.

Jasim Mohammed Jasim Al-juboori

8 November 2021
Date

Acknowledgements

The compilation of this thesis would not have been achieved without the guidance, support, advice, and contribution of many people. I would like to acknowledge and thank the following people. I greatly appreciate the help and would like to say huge thanks to:

- My supervisors, Dr Philip van Eyk, Prof. David Lewis and Prof. Peter Ashman from the School of Chemical Engineering and Advanced Materials, Faculty of Engineering, Computer and Mathematical Sciences, the University of Adelaide for the scientific and personal support that they have given me throughout the PhD and my personal life.
- Dr Tony Hall from the School of Physical Sciences, the University of Adelaide for his assistance in the analytical techniques.
- Dr Rosmala Lewis for providing the biosolids feedstock.
- I am profoundly grateful to Dr Alison-Jane Hunter for proofreading the thesis.
- A huge thank you to my family, mother, father, and friends for always being there and supporting during my PhD research.
- Finally, I owe my deepest gratitude to my late wife, Dr Amira Elmadahm, for her love, understanding, encouragement, affection, constant support and patience even on the most challenging time. She supported me without any complaint or regret, which enabled me to complete my PhD work. But most of all, thank you for being my best friend. I owe you everything.

Preface

This thesis is submitted as a portfolio of publications according to the 'Specifications for Thesis 2020' of the University of Adelaide. The main body of this thesis includes three papers that were prepared for publication. The three papres form a series of work that investigated the effect of biosolids content treated under optimal HTL conditions and the resultant renewable crude oil composition:

1) The effect of biochemical composition on the renewable crude oil produced from hydrothermal liquefaction of biosolids

   Jasim M. Al-juboori, David M. Lewis, Peter J. Ashman, Tony Hall and Philip J. van Eyk.

2) Elucidation of the effect of reaction conditions and biosolids' composition on conversion to renewable crude oil via hydrothermal liquefaction

   Jasim M. Al-juboori, Reem Obeid, David M. Lewis, Tony Hall and Philip J. van Eyk.

3) Characterisation of chemical properties of the produced organic fractions via hydrothermal liquefaction of biosolids

   Jasim M. Al-juboori, David M. Lewis, Tony Hall and Philip J. van Eyk.

List of abbreviations and symbols

AFDW	Ash-free dry weight
CHNO&S	Carbon, hydrogen, nitrogen, oxygen, and sulphur
CO	Carbon monoxide
CO_2	Carbon dioxide
d.a.f.	Dry ash free
GC-MS	Gas chromatography-mass spectrometry analysis
g	Gram
g	times gravity force
HBP	High-boiling point
HC	High carbohydrate
HL	High lipid
HLG	High lignin
HP	High protein
HTL	Hydrothermal liquefaction
H_2	Molecular hydrogen
H_2O	Water
LBP	Low-boiling point
LC	Low carbohydrate
LL	Low lipid
LLG	Low lignin
LP	Low protein
mg	Milligram
mL	Millilitre
mm	Millimicron
N_2	Nitrogen
OM	Organic matter
SRA	Source rock analyser
TEA	Techno-economic analysis
TGA	Thermogravimetric analysis
TOC	Total organic carbon

vol.%	Volume fraction
wt.%	Mass fraction
µL	Microlitre
µm	Micrometre

To the soul of my wife

Amira Elmadahm

With love and eternal appreciation

CHAPTER 1

INTRODUCTION

1. The motivation of the work

The increase in energy demand over the past few decades, which is also associated with a decline in oil reserves and rapid global population growth, has increased the global interest in producing alternative renewable energy[1, 2]. This interest is accompanied by many environmental problems caused by the by-products from wastewater treatment plants, such as sludge and biosolids[3]. At present, the world relies on fossil fuels as the main sources of energy to keep up with the continuously increasing energy demands. For example, more than 89% of the energy demands in the United States are supplied by fossil fuels[4]. However, global fossil fuel resources continue to decrease. Oil reserves, for example, are estimated to provide energy for about 50 more years, while other energy resources, like coal, may only provide energy for about 132 years[5]. Therefore, the sustainability of energy resources represents a key global issue, and there is a pressing need to develop alternative forms of energy to help meet global energy demands.

Simultaneously, the rapid population increase has led to unmanageable quantities of human waste, such as biosolids, which is a problematic waste for the water industry. For example, the annual global production of biosolids in 2011 was about 17 billion tonnes and is expected to reach 27 billion tonnes by 2050[6]. The wastewater treatment plants in Australia produces more than 330,000 dry tonnes of biosolids annually[7]. Furthermore, the United States alone produces more than 7,100,000 dry tonnes of biosolids annually[8]. The accumulation of the annual global production of biosolids represents a critical environmental problem[1]. The current treatment processes for biosolids are very expensive. The United States, for example, spends more than $2 billion per annum to treat and manage about five to seven million tonnes of biosolids[1]. Therefore, developing sustainable processes to produce renewable crude oil using the ever-

increasing quantities of biosolids could provide a solution for both protecting the environment and providing green energy. For these significant ongoing concerns, the research into alternative sustainable renewable energy has expanded worldwide[9].

Many researchers have attempted to produce alternative sources of energy to reduce the dependence on fossil fuels[10, 11]. At present, the production of renewable crude oil from biosolids appears to be a promising sustainable alternative fuel[12, 13] because it, especially via the hydrothermal liquefaction (HTL) process, has a low oxygen content and high heating value[14]. Also, renewable crude oil generates significantly fewer greenhouse gas emissions in comparison with fossil fuels and could be carbon-neutral if produced efficiently[15, 16]. So, producing renewable crude oil from biosolids could be a significant step forward for sustainable green energy, which has greater benefits for both the energy industry and the environment. However, the production of renewable crude oil from biosolids via the HTL process is a relatively new technology, which will benefit from further research.

1.1 Novelty

Renewable crude oil production via the HTL process is still in the beginning stages, and there is no deep understanding of the fundamental knowledge of the HTL of biosolids. Although much research has been done about the HTL of biomasses, such as microalgae, minimal fundamental information is available in the literature about the HTL of biosolids, which is a more complicated feedstock because biosolids composition varies widely, and it is essential to understand the effect of biosolids composition on the quality and quantity of the produced renewable crude oil. Also, there is not much information in the literature on assessing the biosolids composition for producing renewable crude oil, and the composition of biosolids is

fundamentally important because it affects the HTL reactions and the renewable crude oil composition.

The principal objective of this thesis is to improve the understanding of the behaviour of variable biosolids contents through the HTL process, especially to identify the optimum HTL conditions and the effects of biosolids compounds, which are lipids, proteins, carbohydrates and lignins, on the HTL yields and the quality of the produced renewable crude oil, and to determine the nature of the produced renewable crude oil at different boiling points. The better understanding of the HTL of biosolids would allow gaining a better reactor design for the HTL commercial plants and ultimately reduce the cost of production. The results of characterising renewable crude oil are also necessary to optimise the economy of the conversion of biosolids into renewable crude oil and to provide a possible procedure to manipulate the desired products, especially to meet the specifications of the existing fuel.

1.2 Scope and structure of the thesis

The aim of this thesis is to develop a greater understanding of the HTL of biosolids to produce the highest yield and quality of renewable crude oil. While a significant number of studies have been undertaken about the HTL of biomasses, such as microalgae, however hardly any studies have been undertaken in the literature about the HTL of biosolids. This research will provide fundamental information for any future commercial scaling of the technology. Based on the knowledge gaps, these are the detailed objectives of the thesis:

- Providing a critical review of the literature relating to the HTL of biosolids, which requires further research since there is a lack of specific information in the literature about the HTL of biosolids, and this will be discussed in chapter two. Besides providing background information about the HTL of biosolids, the emphasis of this chapter is on two main aspects of the HTL process: (1) the biomass composition and (2) the process conditions.

- Describing the methods utilised to characterise the biosolids' content and their modes of modification. A detailed description was provided of the experiments HTL of biosolids under different conditions. The experimental apparatus used is described, together with the methods used to determine and analyse feedstock and renewable crude oil. This represents chapter three of the thesis.

- Providing developed and modified methods for measuring the biosolids' content, which consists of proteins, lipids, carbohydrates, and lignins, as well as measuring the inorganic content. The work also provides a clear understanding of the biosolids' characterisation and how the biosolids' composition affects the products yield and the

quality of the resultant renewable crude oil, along with how to determine the level of produced renewable crude oil at different boiling points. These represent the first and second objectives, which are presented as a journal article in chapter four.

- Providing a new understanding of the characteristics of HTL products made from biosolids and assesses the effects of different operating parameters and different biosolids' compositions on the yields of HTL products made from biosolids and characterising the boiling point fractions of the renewable crude produced. A simulated distillation of the renewable crude oil is also utilised to establish the approximate renewable crude oil fractions. This represents the third objective, which is presented as a journal article in chapter five.

- Assessing the use of biosolids with dominant organic fraction, such as lipids, proteins, carbohydrates and lignins via different HTL conditions, as a function of temperature, residence time to identify their effects on the composition, quality and fractions of the produced renewable crude. The original source of the renewable crude oil fractions was determined and measured to understand the contribution of biosolids' individual components under specific HTL conditions on the renewable crude oil fractions. So, the subcritical reaction conditions can be optimised depending on biosolids composition to maximise the target fuel. This represents the fourth objective, which is presented as a journal article in chapter six.

- The conclusions of the research, along with the recommendations for future work in this area of research are presented in chapter seven.

CHAPTER 2

LITERATURE REVIEW

2. Introduction

The purpose of this chapter is to identify and review the relevant scientific knowledge relating to HTL and biosolids, supported by information reported on other biomass used in HTL processes. The scientific literature is dominated by HTL papers using microalgae, which is an expensive feedstock. Therefore, there is a need to explore other relevant feedstocks for HTL processes, such as biosolids, as illustrated in Figure 1. The literature review emphasises two main aspects of the HTL process: the variations in biomass composition on the HTL process, and the effects of the HTL reaction parameters. In addition, the biomass composition and reaction parameters are considered in terms of the reaction pathways to understand their effects on the yield distribution and composition of the produced renewable crude oil and by-products (Figure 1).

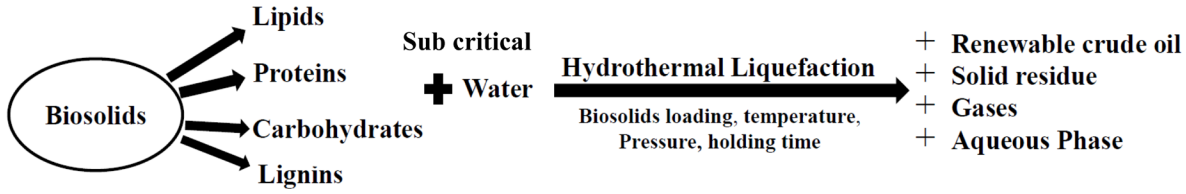

Figure 1: Simplified overview of the HTL of biosolids.

2.1 Biosolids background

The sources of wastewater sludge are generally households' human waste, along with municipal, agricultural and food-processing industry waste, including those from arborous and field crops[17]. Biosolids as a term was introduced by the wastewater industry in the early 1990s in order to identify the quality of the sludge's treatment[18-20]. Thus, biosolids are sewage sludge after it has undergone further treatment, such as stabilisation, composting, and digestion in wastewater treatment plants, to decrease the pathogens and volatile organic matter[21, 22]. In fact,

biosolids can only be classified as such once they meet the requirements of approved biosolids management guidelines, such as managing the health safety aspects of biosolids handling, managing the contamination of biosolids, managing the risk on the human, animal health and environmental, food safety risks, legal risks, and preventing the waste from the needs for any further necessary treatment[21].

2.1.1 Biosolids characterisation

According to the US Environmental Protection Agency[20], biosolids are a mix of water and organic substances derived from carbon, hydrogen, oxygen, and inorganic substances, which are rich in nutrients, and represent an agglomeration of different substances. Each wastewater treatment plant produces specific, unique biosolids of variable composition. The nature of the biosolids, therefore, varies according to the origin of the processed waste, and the waste treatment methods. The Australian Bureau of Statistics[21] reported that the biosolids' solids content could range from 15% to 90%. The biomass composition's organic contents contain lipids at 6 - 30%, proteins at 20 - 30%, carbohydrates, cellulose, hemicellulose at 20 - 40% of the biomass, lignins at 6 %, and ash[23-25]. The dry basis biomass contains 30 - 60% carbon, 30 - 40% oxygen, and 5 - 6% hydrogen, depending on the ash content[21]. The Australian Water Association[21] also reported that a typical biosolids composition contains 1% nitrogen, 1% phosphorus, 1% micro-nutrients, 6% inert matter, 12% organic matter, 80% water and 2% other compounds.

The biosolids' composition can be further classified as follows[20, 21, 26-30].

1) Macronutrients (organic), such as sulphur, phosphorus, potassium, and nitrogen.
2) Six semi-volatile organics and polycyclic aromatic hydrocarbons.
3) Flame retardants, such as PFAS.

4) Bacteria, bio-toxins, viruses, pathogenic protozoa, and parasitic worms.
5) Micronutrients, such as manganese, zinc, magnesium, iron, copper, boron, calcium, and molybdenum.
6) Traces of metals and synthetic organic compounds, such as selenium, chromium, silver, cadmium, nickel, aluminium, lead, mercury, and arsenic.
7) Pharmaceuticals products, such as antibacterial pesticides, ciprofloxacin, diphenhydramine, triclosan, triclocarban, steroids, and hormones.
8) Nanomaterials: materials that are engineered at the ultra-fine molecular scale.

Therefore, it is clear that the composition of biosolids is highly variable. There is a lot of scientific work reported on biosolids, but is limited regarding using biosolids for energy production, and there is minimal fundamental information available in the scientific literature regarding the composition of biosolids. The composition of biosolids is fundamentally important because it will affect the processes and reactions. Therefore, the variation in biosolids' contents requires a wide range of analytical tools to permit analysis of their composition. This is important for accurate characterisation when assessing their value in renewable crude production.

Usage of biosolids

Traditionally, the majority of biosolids produced globally have been used for agricultural purposes and/or spread over land[31] because of their high organic content, which provides nutrients to crops[32, 33]. For this reason, approximately 55% of biosolids have typically been used for agricultural purposes, as a fertiliser or for distressed land restoration, and approximately 30% are sent for landfill. The remainder has been used in a variety of applications, which include incineration, forestry, and biogas production[21, 34].

Biosolids can contain materials that make them unsuitable for agricultural applications. For example, biosolids from sewage sludge waste are generally high in ammonium and have a high soluble salt content[35, 36]. Biosolids produced from manure waste and food residues are usually rich in nutrients but also have a high salt content, which can increase salinity levels in soils[37-39]. Additionally, heavy metals can be present in biosolids, depending upon the origin of the waste. Therefore, the use of biosolids in agriculture can pose many environmental challenges[40], and there is scope for more effective management and regulation as well as the ongoing production of biosolids requires to develop sustainable solutions.

The environmental concerns about biosolids

The traditional reuse of biosolids in agricultural applications has become increasingly more restricted in many countries, including the USA and Europe, because of the potentially negative impact upon the environment[41]. There are many environmental concerns connected with traditional methods, such as resource depletion, greenhouse gas emissions and soil pollution. For example, the overuse of biosolids for agricultural purposes is causing over-fertilisation on soils, which leads to the pollution of surface water and groundwater[21]. Also, using biosolids for agricultural purposes has other potential environmental risks, such as an excessive increase in trace elements, which can cause contamination from soluble phosphorus and increased nitrogen levels in subsurface and groundwater. Air quality can also be affected by the emission of noxious gasses[42]. In Australia, for example, there have been several persistent issues facing the biosolids' management industries, such as community acceptance, dewatering, health risks and greenhouse gas emissions[43]. Therefore, the recovery and recycling of biosolids represent an important step towards developing a sustainable environmental system, but more research is needed to bring the emerging technologies to commercial reality.

Sustainable environmental management of biosolids

In recent decades, sustainable energy and the environment have become major issues of concern in the world. One of the negative effects on the environment is biosolids. Biosolids represent a problematic waste for the water industry because they are very costly to manage, keep growing in size and are ubiquitous. Because of their potential adverse effect on the environment, developing methods for disposing of biosolids in a sustainable environmental manner has become a pressing issue. While biosolids can cause environmental harm, if processed appropriately, they can provide a rich resource of renewable energy, without causing environmental damage.

Many techniques have been used to produce renewable energy, such as wind power, solar power and biofuels[12, 13]. In this context, biomass, which includes biosolids, represents a significant and sustainable source of organic carbon for renewable crude oil production[44, 45], particularly because of the large, ongoing, annual production of biosolids, its renewability, and its high energy density, which is considered to be carbon-neutral[46]. Therefore, there is a compelling case to develop an energy-efficient process for the sustainable production of renewable crude oil from biosolids. An effective treatment process could simultaneously protect the environment and move the world closer to operating on renewable energy alone.

Many process technologies can be used to recover energy from biosolids, such as gasification, pyrolysis, direct combustion, and thermal processes. However, one of the significant barriers that these methods face is the need for the drying step of the biosolids, which requires time, cost, and energy to be implemented[1]. Because HTL does not involve a drying step, HTL could be a promising thermochemical technology to convert high moisture biosolids into renewable

crude oil[47-49]. Especially, biosolids are an appropriate feedstock for hydrothermal liquefaction because they are produced in a wet waste at small particle size, which is perfect for HTL process. HTL of biosolids, therefore, has the potential economic competitive. However, few techno-economic analysis (TEA) studies are available on the HTL of biomass to evaluate the economic feasibility. Li *et al.*[191] reported that the produced renewable crude oil cost via the HTL of wet waste ranges from $2.65/gge to $4.93/gge, with an uncertainty range from −29% to 35%. While another preliminary TEA analysis by Snowden-Swan *et al.*[192] estimated a different cost for the produced renewable crude oil via the HTL of sludge ranges from $3.8/gge to $4.9/gge. However, there is a need for more data on HTL of biosolids so that TEA analyses can be undertaken to evaluate the potential economic competitive of the HTL of this feedstock.

Although much is known about the HTL of different biomasses, such as microalgae, the HTL of biosolids is at a relatively early stage of research and development, and there is a need to quantify the performance of biosolids through HTL, which is more complicated because the composition of biosolids is highly variable. It is important to understand the effect of different variables of the biosolids composition on the quality and quantity of the produced renewable crude oil to be able to optimise and assess the appropriateness of the HTL for managing biosolids.

2.2 Hydrothermal liquefaction background

Many conversion processes have been developed to recover energy from waste biomass over several decades. The main thermochemical technologies for processing biomass are gasification, pyrolysis and combustion[1]. None of these processes has had wide commercial success, largely due to the need for a dewatering step, which, according to Darvodelsky[50], represents a third of the total expenses of the biosolids' production cost of around $100-300

per tonne in Australia. Therefore, the economics of renewable crude oil production from biomass via gasification, pyrolysis, and combustion suffer from the high cost of the dewatering process.

Hydrothermal liquefaction has the ability to convert any wet biomass like biosolids into renewable crude oil without the need for a drying step[7, 51, 52] and therefore potentially save energy in comparison with other thermochemical processes. According to Savage *et al.*[53], the dewatering process for drying biological solids requires a level of energy, which exceeds that required for the HTL of biomass with a 30% w/w water content. Similarly, Singh *et al.*[54] reported that the dewatering process could consume about 80% of the produced energy through the HTL processes. So, the energy-savings and potential cost savings generated by removing the dewatering process make the production of renewable crude oil from biosolids via the HTL process potentially less expensive[53]. As a result, HTL could be an applicable approach to produce energy from biosolids. However, further understanding is required for the HTL of biosolids to maximise the renewable crude oil and minimise its losses.

2.2.1 Hydrothermal liquefaction

HTL is a thermochemical conversion process that causes the thermal disintegration of any organic feedstock, like biosolids, into renewable crude oil at subcritical conditions[7, 51, 52, 55]. Generally, biomass conversion from solid form to liquid oil is not a spontaneous process. Fossil fuels, for example, need millions of years to be produced through geochemical processes, converting largely vegetative biological material into crude oil[4]. HTL processing occurs in minutes or hours, yet the HTL process mimics the simulates fossil fuel production processes that occur in the earth over millions of years[56]. Similarly, the HTL process leads to the thermal disintegration of feedstock into renewable crude oil using a solvent, typically subcritical water,

to break down the solid biopolymeric structure[57]. The HTL conditions and water content create a highly reactive medium, supporting the breakdown of the chemical bonds, which leads to the reformation of organic compounds[10]. HTL in general, rapidly hydrolyses, decomposes, and breaks down wet biomass into fragments of small molecules of various organic compositions[58-60]. Re-polymerisation turns the unstable fragments into various oily compounds[61-63]. However, various parameters influence the product yields, alongside the composition of the biomass. Therefore, it is necessary to characterise the influence of the HTL conditions, as well as the biomass composition in order to optimise the economy of the conversion of biomass into renewable crude oil.

The HTL processes are subject to various parameters that interact together to convert biomass into renewable crude oil, such as temperature, pressure, particle size, heating rate, and residence time, as well as the concentration of biomass and the biomass content[64-66]. HTL operates at subcritical conditions by using water at a moderate temperature of 200 to 375°C and high pressure of 50 to 250 bar[1, 44], as shown in Figure 2. At these conditions, water acts like a solvent, which leads to the breakdown of organic material through the HTL reactions at varying residence times (minutes or hours)[17, 57, 67-70]. Much research has been done on supercritical water HTL, which is very important, but the problem working at the supercritical point is that the construction of the reactor's materials would become too expensive. HTL production involves four phases: renewable crude oil, solid residue, gases, and aqueous phase[71]. The change in the HTL processing conditions influences biosolids' conversion into renewable crude oil, which is the desired product along with the other phases[55, 72]. According to Beckman and Elliott[73], changes in the key parameters have a significant impact on the produced products. However, the HTL of biosolids involves many uncertainties, such as understanding the influence of operation conditions, and further research is required for

specific feedstocks to gain the knowledge that could help to increase the yields and quality of renewable crude oil.

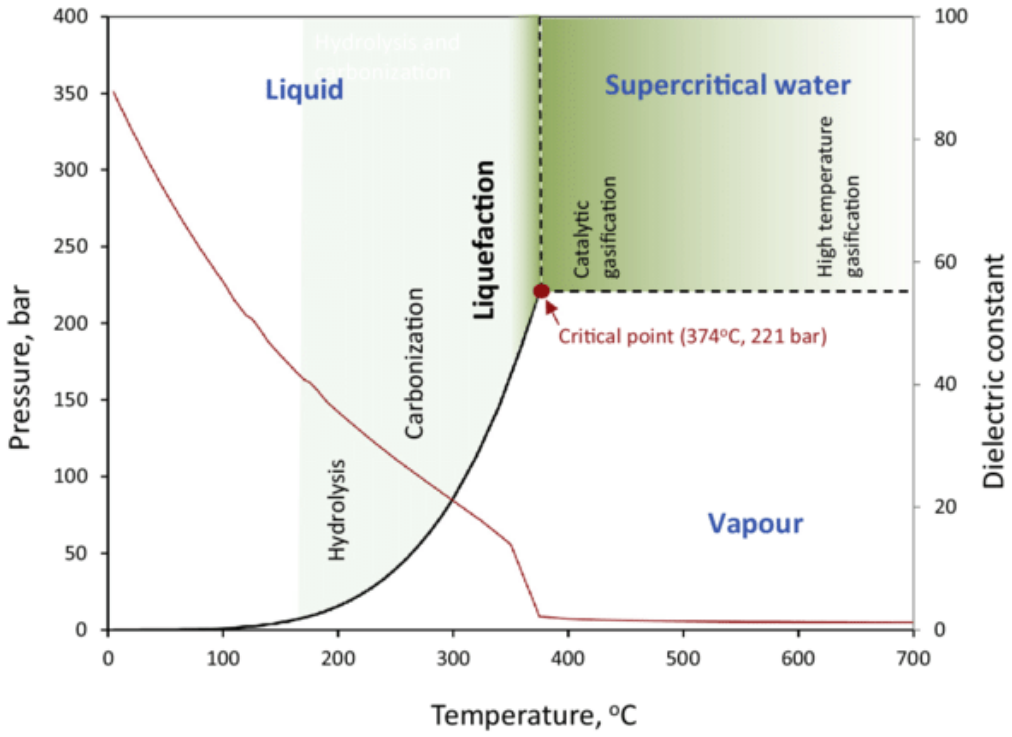

Figure 2: Phase diagram of HTL conditions and static dielectric constant 200 bar (reproduced from Tran[74]).

Review of the existing scientific literature provides limited information about the processes of HTL when using biosolids as feedstocks to produce renewable crude oil. The composition of microalgae contains proteins, carbohydrates, and lipids[60, 69], which is similar to the organic content of biosolids, which also contains lignins. Microalgae with various components were tested under HTL conditions in water with the absence of a catalyst[75, 76]. The yields of renewable crude oil from microalgae were about 20 to 40 wt.% depending on the microalgae composition[77, 78]. However, the main focus of the previous reported research of HTL of microalgae was to optimise the reaction conditions, such as the residence time, temperature, and heating rate, to maximise the renewable crude oil yield[79, 80]. The effects of different

compositions of biosolid have not been studied, and there is minimal fundamental information available in the scientific literature on the performance of biosolids through HTL, which is complicated because the composition of biosolids are highly variable. Key objectives of this research project are to study the effect of biosolids content and operating conditions on the distribution of the products and the quality and quantity of the renewable oil produced.

There are many different types of waste that have been used in the HTL process besides microalgae, such as sludge[17]. Suzuki *et al.*[81] used HTL to study several kinds of sewage sludge at 300°C and 120 bar. They found that the composition of sludge does not have a noticeable effect on the elemental composition and the heating value of the renewable crude oil. However, in many situations, the renewable crude oil yields from the HTL of microalgae were around 15% greater than the content of lipids[75]. This means that the proteins and carbohydrates contributed to the formation of renewable crude oil, which biosolids are rich in both. The similarity between biosolids' composition with other biomass, such as microalgae and sludge, could be used to compare and predict the general behaviour of biosolids. However, the HTL of biosolids is complicated because biosolids' composition is highly variable, which could affect the quality and the yields of the renewable crude oil. According to Brown *et al.*[82] and Garcia Alba *et al.*[76], the quality of the renewable crude oil is mostly subject to the quality of biomass and the process conditions. So, it is also important to identify the effects of the biosolids' composition and the HTL conditions on both the distributions of the HTL products' yields and on the qualities of renewable crude oil. However, comparing the outcomes of different research, especially the recovery of renewable crude oil, aqueous, gas, and solid fractions, is difficult because the various studies have different biomass compositions, process conditions, and different reactors configurations[26].

The following section contains a summary of the HTL of biosolids based on studies using microalgae, sewage sludge, and woody biomass. The review is focused on the effects of the biomass compositions and HTL conditions on the HTL product distribution and yields.

2.3 Biomass types

HTL could be a flexible technology in terms of using different feedstocks and different reaction conditions. Biomass, therefore, represents a great source of renewable energy[83]. However, biomass types are varied widely, and therefore represents the most concerning element of HTL technology[1] because of their effect on the yields and the quality of renewable crude oil. Most studies reported in the scientific literature have focused on the conditions of the HTL parameters with less focus on the effects of biomass composition, in particular biosolids. Understanding the HTL of a single component is easier than understanding the mixture of different compounds that contain ill-defined compounds. Biosolids represent a mixture of highly variable organic components, which react together through a similar chemical reaction pathway. For this reason, any change in the condition of the chemical processes is linked to a change in behaviour of one or more of the organic compounds, which can lead to dominating the energy conversion in the HTL process[83]. Therefore, making HTL technology more economically feasible requires an understanding of the effect of different variables of the biosolids composition on the product quality to be able to optimise the HTL process.

2.3.1 Lipids

Lipids represent the major non-polar compounds[84]. Lipid is insoluble at room temperatures; however, lipids tend to be soluble with any increase in temperature in the presence of solvents[57]. The dielectric constant of water at HTL operating conditions leads to great

miscibility, which enables the stabilisation of the structure of the triglycerides, causing the formation of glycerol (glycerol contains methanol, fatty acids and salts)[60]. However, the continuation of glycerol degradation will lead to the production of a stream of acetaldehydes, CO_2, CO, H_2, propionaldehyde, formaldehyde, acrolein, ethanol, and allyl alcohol[84]. Therefore, in many cases in the HTL process, the conversion of glycerol does not increase the renewable crude oil yield because it converts to a water-soluble compound[85].

Lipids, in general, contain a wide group of various categories of molecules, such as oils, sterols, fats and phospholipids[86]. The main constituent of lipids is triglycerides-esters, which are the main content of oils. The HTL reaction pathways of the lipids are relatively uncomplicated[86]; hydrolysis is the major reaction for lipids at low temperatures[86]. The hydrolysis turns the triglycerols into fatty acids and glycerol[87]. Hydrolysis also turns the phosphate esters into fatty acids and phosphoric acid[87]. Any increases in temperature will form fatty acids from alkanes and alkenes, depending on the HTL process conditions[86]. The presence of ammonia could also lead to the generation of amides from the combination of ammonia and fatty acids[86]. Therefore, it is essential to understand the behaviour of different lipids compounds during the HTL of biosolids and their effects on the composition of the produced renewable crude oil to optimise the HTL process depending on the target fuel.

2.3.2 Proteins

Protein is a major component of biomass, including biosolids, and consists of many compounds of peptides that are reformed to amino acids polymers during the HTL process[88]. The amino acids represent the main structure of proteins; however, they are heterogeneous[88]. Therefore, the amino acids' degradation is complex and represents a great challenge because they behave differently during the HTL, which leads to producing different compounds. The strong peptide

chain for the proteins is subjected to decarboxylation. During the deamination reaction in HTL processing, they form aldehydes, amines, acids, and hydrocarbons[55]. The continuous degradation of an amino acid leads to the production of iso-butyric, n-butyric, propionic, acetic and carboxylic acids[88]. In addition, the cyclisation and condensation of the protein molecules produce aromatic amide molecules, pyrroles, pyrazines, and indoles[89]. In general, in the HTL process, the hydrolysis of protein is mostly slow below 230°C; however, the hydrolysis of protein is significantly increased above 250°C[90]. Therefore, it is important to select a suitable temperature for the HTL of biosolids with high protein content, as it can be affected by other components of the biosolids, such as carbohydrates, during the HTL process.

2.3.3 Carbohydrate

Carbohydrate fraction consists of glucose, cellulose and hemicellulose[91]. During the HTL process, the degradation of carbohydrates predominantly results in glucose monomers and other saccharides, which are often then subject to further degradation[92]. However, because of the difference in the structure of the starch and cellulose, the hydrolysis results may vary significantly. For example, the main fractions of glucose consist of starch polymers, which are decomposed more easily than cellulose. According to Wang[86], in the HTL process, glucose is decomposed completely below 240°C. On the other hand, cellulose has a long chain polysaccharide with high polymerisation and high molecular weight[88]. The composition of cellulose is a natural polymer that is held by strong intermolecular hydrogen bonds[93]. Cellulose is non-polar at room temperature; however, cellulose is soluble with any rise in temperature[94]. The crystalline structure of the cellulose makes it insoluble in water. Despite this, during the HTL process, the cellulose rapidly decomposes and dissolves due to the strong bonds' breakdown with the increase in temperature during the HTL process[49]. According to Rogalinski

et al.[95], cellulose is fully converted between 280 to 310°C, while the starch is hydrolysed significantly faster during the same HTL process.

Hemicellulose is a branched structure heteropolymer containing hexose and pentose as a polymer[88]. The hemicellulose composition is an amorphous polymer containing a straight-chain skeleton of glucomannan and xylan[96]. The hemicellulose's contents have many types, such as grassy and woody biomass, which contain mannan, xylan, galactan and glucan[93]. Unlike cellulose, hemicellulose is a hetero-polysaccharide due to side groups' presence and non-uniformity; therefore, hemicellulose has a weak structure and low resistance to intramolecular hydrogen bonding, which enables easy disintegration of the molecules[60]. The hydrolysis of the hemicellulose is usually severe and tends to have an easy miscibility characteristic[97]. Hemicellulose is hydrolysed rapidly becoming amorphous at temperatures above 180°C[98]. Thus, the presence of hemicellulose generally leads to an increase in the renewable crude oil yield[60, 97], because the weak structure of hemicellulose has low resistance to the increase of temperature during the HTL process.

2.3.4 Lignin

Lignin mostly exists in willow, switchgrass, and agricultural residuals, such as wheat, corn stover, wood waste, rice straw, and the trees' cell walls[60]. Lignin is a natural polymer and represents an aromatic compound, which is composed of basic building blocks that link through ether bonds, such as the hydroxyl and ethoxy group and phenyl-propane[53, 97, 99]. Lignin is usually decomposed during the HTL process to phenolics, which is the most valuable compound for phenol production[100]. The lignin generally has a similar morphological characteristic to hemicellulose, along with low solubility, which is similar to cellulose[88]. Lignin also has a great ability to store energy because of its strong cell wall structure[101], which

produces a higher heating value than hemicellulose and cellulose[102, 103]. The decay rate of lignin is very slow, which makes lignin resistant to degradation during the HTL process, and this is a significant feature of lignin that contrasts with other compounds, such as hemicellulose and cellulose[88]. Also, lignin has a high polymerisation degree and complex interlinkage, which increase its decomposition limitations[60]. Therefore, lignin degrades at different temperatures, which are generally higher than the temperature required by other organic compounds, such as protein and lipid.

Hemicellulose, cellulose and lignin are linked together via hydrogen and covalent bonding. Ramsurn and Gupta[104] reported that the biopolymers in lignocellulose degrade at various temperatures; for example, in hemicellulose at 180 to 290°C, cellulose at 240 to 350°C and lignin at 280 to 500°C. So, it is clear that the hemicelluloses are solubilised first at low-temperatures to form the renewable crude, while cellulose and lignin are liquefied at higher temperatures and pressures.

2.3.5 Effects of biosolids compositions

The various composition of biosolids significantly affect the HTL process, which, in turn, is affected by the operating conditions. Many researchers have focused on using a simple model compound in the HTL process instead of real biomass to avoid the problems that are associated with the heterogeneity and the complexity of biomass contents. The HTL process operates through a range of complex reactions and transformations under subcritical conditions. The conversion of biomass in the HTL process includes the hydrolysis and decomposition of the biomass into water-soluble oligomers followed by the breakup of intermolecular and intramolecular hydrogen bonds into simple monomers in the presence of a solvent[59, 60]. The HTL processes start with solvolysis of the biomass, which disintegrates the fractions of

biomass, then move into thermal depolymerisation into smaller fragments[94, 105]. The re-polymerisation turns the unstable fragments into various oily compounds[63, 71, 94].

In general, the renewable crude oil produced by HTL can have many positive properties, such as a low moisture content, high heating value, and low oxygen content; however, the produced renewable crude oil can also have negative properties, such as relatively low stability, corrosive activity, and high viscosity[106, 107]. Therefore, the complexity in the HTL of biosolids, such as the effect of different biosolids' composition on the HTL process, requires further research focus in order to gain a better understanding of the yields and quality of the renewable crude oil, and the distribution of the product[62]. Neither of these elements has been reported sufficiently in the scientific literature. It is very important to develop an efficient process for the HTL of biosolids in order to optimise the quality and quantity of the produced renewable oil.

2.3.6 Reaction pathways for the HTL of biosolids

The HTL of biosolids undergoes a series of complex reactions, which has not been clearly explained in the scientific literature to date. In general, biosolids is first decomposed and then depolymerised into small fractions of compounds[88]. The fragments will then degrade after into smaller compounds by dehydration, dehydrogenation, deoxygenation and decarboxylation[55]. However, at the end of the HTL process, the complex chemicals could be synthesised by repolymerisation[88]. The small compounds are usually highly reactive; therefore, they are polymerised to produce four products, which are the renewable crude oil, solid residue, gas and the aqueous phase[88]. The produced renewable crude oil in the repolymerisation usually consists of alcohols, ketones, esters, aldehydes, phenols, and acids[105], which could be varied depending on the biomass composition and the HTL conditions[88].

Biosolids are naturally a complex mixture of many components, such as lipids, proteins, carbohydrates, and lignins; therefore, the reaction mechanisms in the HTL process of biosolids are also complex[108]. The biosolids components during the HTL process interact through different reactions. Cellulose, hemicellulose and lignin compounds have hard crystallinity structures, which make the biomass conversion a more complex process. Despite the rich carbon and hydrogen source, the lignocellulose products via the HTL process are highly affected by its significant amount of oxygen because the high amount of oxygen contents causes poor stability in the produced renewable crude oil[109]. Hietala *et al.*[110] have reported a kinetic model for the HTL process of biomass; however, the accurate pathways of the HTL of biosolids remain unclear because of the complexity of the biosolids and the potential for infinite intermediate reactions. The significant steps for the reaction pathway of HTL, which include depolymerisation, decomposition and recombination, are explained hypothetically below.

2.3.6.1 Depolymerisation of the biosolids

Biomass depolymerisation represents the subsequent dissolving of the macromolecules using their chemical and physical properties[88]. The biopolymers of cellulose and hemicellulose contribute positively to the renewable crude oil's thermal stability[111]. Depolymerisation assists in dissolving the lignocellulose and overcoming the difficulties in their properties, which simulates the natural chemical processes of producing fossil fuels[88]. In general, the key parameters, such as temperature and pressure, break up the long-chain polymers containing carbon, oxygen, and hydrogen into short-chain hydrocarbons[112]. The energy in organic materials is usually recovered in the presence of water[88].

2.3.6.2 Decomposition of the biomass

The decomposition of biomass monomers occurs in several ways, such as cleavage, dehydration, decarboxylation and deamination[88]. The decomposition consists of the loss of water molecules via dehydration, and the loss of CO_2 molecules via decarboxylation, which is followed by the removal of the amino acid content via deamination[79]. The critical role of the dehydration and decarboxylation is that they assist in removing the oxygen from biomass in the form of H_2O and CO_2[88]. The biomass that contains macromolecules is mostly hydrolysed, producing monomers and polar oligomers[113]. Water at subcritical conditions breaks down the hydrogen-bonded cellulose, causing the formation of glucose monomers[88]. The fructose is more reactive than the glucose because it degrades quickly to many different products depending on the reaction process, such as reverse-aldol defragmentation, hydrolysis, dehydration, isomerisation, rearrangement and recombination reactions[114]. The major products of degradation, including glycolaldehyde, phenols, polar organic molecules, organic acids and furfurals, are highly soluble in water[88].

2.3.6.3 Recombination and repolymerisation

Recombination and repolymerisation represent the third step for the biomass components in the HTL process when they start to recombine the produced components again and reproduce solid products. The repolymerisation step occurs because of the lack of a hydrogen compound during the HTL process[55]. The availability of hydrogen in the organic components during the HTL process leads to an increase in the yield of the stable molecular weight species from the free radicals. The unavailability of hydrogen could happen because of the high concentration of free radicals, which causes recombined or repolymerised small fragments to form high molecular weight char compounds[39]. The conflict between the decomposition and

repolymerisation reactions is associated with different biomass conversion effects, which depends on the biomass's compositions. However, this conflict could be addressed by combining two parameters, particularly temperature and residence time to control the HTL process. Therefore, it is essential to gain accurate knowledge of the HTL process alongside accurate biosolids' compositions to optimise the HTL process to produce the desirable quality of the renewable crude oil.

2.4 The HTL reaction conditions

The output of HTL is distributed across four phases, namely the solid residue, gases, an aqueous phase, and the renewable crude oil. The HTL products are significantly influenced by various parameters that interact together to convert biosolids into renewable crude oil. Important parameters include the particle size of the biosolids, temperature, heating rate, pressure, residence times, solvents, and the biomass-to-solvent ratio[65, 66]. Therefore, it is necessary to understand the influence of the HTL conditions on the conversion process, especially on renewable crude oil production.

2.4.1 Temperature

Biosolids are generally composed of many bonds that must be broken down through the HTL process to produce renewable crude oil. An energy-efficient method is needed to overcome the energy barrier required to break down the biosolids' chemical composition to produce lower molecular weight species bonds. Temperature is the dominant operating parameter in the HTL process. In general, increasing the HTL process temperature from 250 to 350^{o}C leads to an increase in the renewable crude oil yield. One of the significant effects of using high temperatures around 350^{o}C is to improve the biomass conversion, such as the lignocellulosic

fraction cleavage and fragmentation, which leads to an increase in the renewable crude oil production[115]. Similarly, Shakya *et al.*[116], reported that increasing the temperature in the HTL of microalgae to 350ºC produced the best yield of renewable crude oil, which was around 48% Wt%. The HTL of biosolids at low temperatures around 250ºC is usually endothermic, while the HTL of biosolids at high temperatures around 350ºC becomes exothermic[10]. Therefore, the effect of using high temperatures in the HTL of biosolids may be valuable in order to increase the yields of the produced renewable crude oil[115]. However, more research is required to determine the optimum operating temperatures.

The appropriate optimum operating temperature for renewable crude oil production may vary as the biomass composition varies[116]. For example, the optimum temperature range for cellulose, and hemicelluloses is 300 to 330ºC, whereas lignin may require higher temperatures to break down the biosolids' bonds and increase the renewable crude oil production[10]. Shakya *et al.*[116], in a study of the HTL of microalgae, reported that the HTL of high carbohydrate-containing microalgae found an increase in the renewable crude oil yield at higher temperatures of 300 and 350°C, in contrast, in high protein-containing microalgae, the renewable crude oil yield was higher at a lower temperature of 250°C, and therefore the HTL conditions could be optimised depending on the biosolids composition. Added to that, high temperatures above 350ºC cause increased gas, which tends to reduce the renewable crude oil yield[63]. Thus, temperatures between 300 to 350ºC would appear to be the most effective for the decomposition of biosolids. The optimum temperature within the range is likely to depend on the specific composition of each type of biosolid.

Previous studies of HTL have shown an increase in the conversion of woody biomass into renewable crude oil with an increase in the HTL temperature[66] but only up to a certain point

when the yield remains at the same amount or may drop again. Beyond a certain point, further temperature increases lead to a reduction in the renewable crude oil yields[25, 117, 118]. For example, Liu and Zhang[119] reported that the renewable crude oil yields from pinewood via HTL in the presence of water increased with temperature up to 300°C, but beyond 300ºC, the renewable crude oil yield began to decrease. Sun *et al.*[117], also showed that the highest renewable crude oil yields from the HTL of Paulownia wood were obtained at 300°C and increasing the temperature above 300°C led to a decrease in yield. Further research by Singh *et al.*[54] reported that an increase in the HTL temperature to 300°C when using rice straw showed a significant increase in the renewable crude oil yield; however, beyond 320°C, the renewable crude oil yield started to decrease because char formation was favoured at high temperatures. As a generalisation, a temperature around 300°C would appear to be close to optimum for the conversion of woody biomass via the HTL process. However, for specific types of biomass, temperatures up to 350°C may produce better renewable crude oil yields, as suggested by other researchers[120, 121]. Therefore, it is clear that utilising high temperatures does not necessarily mean that high renewable crude oil yields will be produced.

In contrast with the studies discussed above, Xu and Lancaster[122], who investigated the HTL of pulp sludge, obtained the highest yields at 250ºC, which was the lowest temperature studied in their work. While Xiu *et al.*[123] indicate that increasing the temperature during the HTL of swine manure from 260 to 340ºC leads to an increase in the renewable crude oil yield. Another important point is that according to Biller *et al.*[64] decreasing the temperature of the HTL process from 350 to 300°C leads to a reduction in energy consumption of 22%, whilst the reduction in the renewable crude oil yield may only be decreased by 3%. Therefore, it is clear that selecting the HTL reaction temperature must be depended on the biomass' composition as it has a significant effect on the renewable crude oil yield.

There are several explanations for the limiting effects of increasing the temperature on the HTL process. For example, Wang *et al.*[25] stated that there is a competition between two reactions in the HTL process: one being hydrolysis and the other being repolymerisation. The relative rate of this reaction changes with temperature, leading to decreasing yields at high temperatures[25, 122]. Furthermore, the reduction in the renewable crude yield of the HTL of woody biomass beyond 300°C could be related to the dominating secondary reaction and Bourdard gas reactions, which are associated with the recombination of the free radicals into char at higher temperatures[10, 66]. Molten *et al.*[124] and Goheen and Marten[125] explained the connection between the temperature and the degradation of hemicellulose and lignin as being that they are endothermic at low temperatures but exothermic at high temperatures. Xu and Etcheverry[122], attributed the decrease in the renewable crude oil yield to the enhancement of char formation at higher temperatures. Therefore, to summarise the above dissection, intermediate temperatures around 300°C could be the best temperatures to convert most of the biomass via the HTL process; however, more research is needed to determine the optimum temperature for producing the best renewable crude oil yield via the HTL of biosolids.

Using different temperatures in the HTL of the same biomass may lead to different yields. For example, the HTL of microalgae could have different yields depending on the operating temperatures. Jin *et al.*[126] reported that an increase in temperature in the HTL of microalgae led to a decrease in the solid residue because of the gradual conversion of organic materials in the biomass. According to Brown *et al.*[82], the optimum temperature for the HTL of biomass like microalgae is around 350°C. However, Jin *et al.*[126] stated that increasing the temperature above 340°C led to an increase in the yield of solid residue because of the polymerisation or condensation reactions of intermediate oils to form heavier higher-molecular-weight compounds like char, which is retained in the solid residue. Other researchers found similar

results for the HTL of microalgae, which showed that the renewable crude oil yield increased at the beginning of an increase in the temperature[127, 128]; while it stabilised or decreased when it reached a certain temperature[129, 130]. However, using a low-temperature blow 250ºC does not mean the automatic production of high renewable crude oil yields. For example, the renewable crude oil yield at moderate temperatures like 275°C also shows a decrease because of the partial breakdown of biomass components[92]. So, an intermediate temperature, such as 300 to 350°C could lead to higher renewable crude oil yield[120, 121].

In conclusion, the temperature has a vital role in increasing the renewable crude oil yield until a certain point is reached, whereupon further increases in temperature lead to decreases in the yield. Therefore, it is essential to understand the effects of temperature on the HTL of biosolids with different compositions, and the produced products.

2.4.2 Pressure

Pressure is another critical parameter in the HTL process because it assists in maintaining water in the liquid phases and in avoiding the two-phase system, which would result in an increase in energy costs[131]. According to Chan *et al.*[132], an increase in pressure leads to effective extraction of biomass. Supporting this view, Behrendt *et al.*[133] reported that high pressure in the HTL process results in a greater production of liquids than gases. By maintaining pressure during HTL, the rate of biomass dissolution can be controlled, which may enhance the favourable reaction pathways for the production of renewable crude oil[10]. The pressure also increases the solvent density. A high-density medium could penetrate the biomass components, which leads to improvements in decomposition and extraction[134]. However, increasing the pressure above a certain point could lead to many negative effects. For example, the high pressure could lead to an increase in solvent density and solubility, which would prevent the

fragmentation of the C-C bond[135]. A continuous increase in pressure, especially when using temperatures above 350ºC, could increase the effect of the surroundings on the molecules' properties, which then causes a decrease in the renewable crude oil yield[132]. Therefore, it is important to avoid using high pressure during the HTL process.

A combination of high temperatures above 350ºC and high pressures above 250 bar can also lead to a decrease in the dielectric constant, forcing hydrocarbons to be more water-soluble[60]. The polarity of any water molecules would be reduced because of more evenly-shared electrons between the hydrogen atoms and oxygen[1]. The dissociation increase of water to OH− ions and H makes the hot, compressed water a perfect medium for acid- or base-catalysed reactions[136]. There would be a low possibility that a reaction could happen between the free radicals and the produced gas molecules, which would cause either high char yields or a high gas yield. However, the pressure has little effect on liquid renewable crude oil[132]. Therefore, it is important to keep the pressure as low as possible and avoid any variation of pressure in the HTL process to obtain the best renewable crude yield. For this reason, in this work, it was found to be preferable to apply pressure at 200 bar in order to gain the best renewable crude oil yield and avoid either producing high char yields or a high gas yield.

2.4.3 Residence time

The residence time has a low to moderate effect on the overall HTL process, such as biomass conversion and product yields. During HTL processing, it is desirable to have short residence times because a longer residence time would decrease the renewable crude oil yield[10, 137]. In the HTL process, short residence times are standard practice, but it is preferable to have long residence times at low temperatures. Short residence times degrade biomass effectively

because the hydrolysis and decomposition rates are relatively fast[67, 138]. According to Faeth *et al.*[48], 66% Wt of renewable crude oil recovery from *Nannochloropsis sp.* was achieved with a 1 min residence time. Faeth *et al.*[48] and Garcia Alba *et al.*[76] concluded that the maximum renewable crude oil yields were obtained with residence times between 1 to 5 minutes. Therefore, the HTL process could have an economic attraction to produce renewable crude oil because the reaction time is very short, which could be around 1 minute. However, more research is required to evaluate the economic possibilities of using a short reaction time during the HTL process.

There is much information in the scientific literature on assessing the residence time. However, conflicting research has been undertaken about the residence times, where the researchers reported several results for the renewable crude oil yield. Many researchers state that increases in the residence time led to an improvement in the renewable crude oil yield until a maximum is reached, after which any further increase led to diverse results[122, 139]. There are a few explanations about the negative effects of long residence times, which is up to 1 hour. For example, according to Xu and Lancaster[122], a potential explanation for stabilisation or a decrease in the renewable crude oil yield during long residence times is that the liquid products are cracked to gases or lead to the formation of solid residue through crystallisation, condensation, and re-polymerisation. Another explanation is that the long residence time enables the production of dominating secondary and tertiary reactions, and they lead to the formation of gases or aqueous or solid residues from heavy intermediates, which then cause a reduction in the renewable crude oil yield[120].

There are many studies into the effects of residence time on the HTL of microalgae, and they found similar outcomes when comparing their results with the woody biomass results. For

example, the solid residue yield was decreased with any increase in the residence time; however, any further increase in the residence time will lead to increases in the yield of the solid residue[122]. The explanation for the increase in the solid residue was related to the further reaction of the oil intermediates and the subsequent cracking and polymerisation[140]. Thus, any further increases in the residence times after the renewable crude oil reaches its maximum yield will show a decline in the renewable crude oil yield[141]. Therefore, it is essential to optimise the residence times to obtain the most effective destruction of the organic contents in the waste biomass[142] because the residence times could determine the biosolids' conversion and the composition of the products[10].

To obtain more knowledge about the effect of residence times on HTL, many researchers have focused on this issue; however, they obtained different results, which could be related to many reasons, such as using different HTL conditions and different biomass composition. For example, Zhang *et al.*[143] and Ye *et al.*[118] reported that the optimal residence time for the HTL of native grassland perennials was 1 minute. Qu *et al.*[144], on the other hand, indicated that the optimum residence time for the HTL of *Cunninghamia lanceolata* was 10 minutes. Other researchers explained that the differences in results were related to the operating temperatures. According to Li *et al.*[139], the residence time effect is closely associated with the temperature; for example, the HTL of rice stalk has different yields, which depend on any change of temperature and residence time[139]. Li *et al.*[139] also reported that the optimal residence time was 90 minutes at 250°C and 60 minutes at 325°C. Therefore, it is essential to select an appropriate residence time for a given temperature in order to obtain desirable yields.

Researchers have investigated the connection between the residence time and temperature. The renewable crude oil yield, for example, was increased at a temperature below 180°C, with an

increase in residence time; however, in the HTL temperature range 250 - 280°C, long residence times led to a reduction in the renewable crude oil yield because of the secondary reactions[145]. In general, the renewable crude oil yield at 300°C increased with an increase in residence time up to 60 minutes, at which point it started decreasing[146]. According to Gai *et al.*[147], the decrease was caused by the repolymerisation and recondensation of the renewable crude oil, while the renewable crude oil yield at 250°C increased with an increase in residence time up to 60 minutes, when the decrease is caused by the dominant reactions, which involve secondary cracking[148]. The residence time for oil mill wastewater at 250 - 300°C is 30 minutes and any further increase in time after 30 minutes leads to an increase in the gas and solid residue yields, which may be linked to the competition between the hydrolysis and depolymerisation reactions[65].

The biomass' composition could represent another concerning factor, and many results record the link between using different types of biomass and the optimum residence time. For example, according to Jin *et al.*[126], the optimum residence time was 20 minutes for the HTL of *Spirulina platensis*, while according to Shuping *et al.*[128], the optimum residence time was 50 minutes for the HTL of *Tertiolecta*. Valdez *et al.*[80] indicate that the best results for the HTL of *Nannochloropsis sp.* is a short residence time of 10 minutes. Qu *et al.*[144] also found the same results for the HTL of *Cunninghamia lanceolata* and concluded that 10 minutes lead to the highest renewable crude oil yields. Therefore, the biomass' composition could represent another concerning factor when selecting the optimum residence time. Other examples to explain the effect of the biomass' content on the required residence time were the optimum residence time for the HTL of swine manure at 15 minutes[123], and for corn stalk at 30 minutes[149]. Lu *et al.*[150] also examined different residence times for the HTL of reed and corn stovers and indicated that the residence time has a significant effect on the yield of the products,

especially on the yield of solid residue. Therefore, it is evident that there is no single optimum residence time because the best yields not only depend on the residence time but also on a range of parameters, such as temperature and the biomass' composition.

2.4.4 Heating rate

The effect of the heating rate in the HTL process has been reported widely in the scientific literature. According to Akhtar and Amin[10], the heating rate during the HTL process has no or minimal effect on product distributions. Kamio *et al.*[151] also have tested cellulose during the HTL process and reported no effect from using different heating rates in terms of the renewable crude oil yield. The low effect of heating rates on the renewable crude oil yield could be connected to the type of the solvent used because solvent could behave as a transfer medium and extraction in the HTL process[39].

On the other hand, according to other scientific research, the heating rate could have a clear impact on the renewable crude oil yield and the distribution of the products. For example, Brand *et al.*[46] preferred using a fast heating rate during the HTL process because it could reduce the inevitable degradation and recombination of the initial products. Zhang *et al.*[152] also reported that increasing the heating rate from 5 to 140 ºC/min for the HTL of aspen wood leads to an increase in yield from 50 to 70%, which was also accompanied by a reduction in gaseous and solid products. However, according to Pandey *et al.*[131], using high heating rates leads to a decrease in the renewable crude oil yield because of the domination of the secondary reactions, which produce high gas yields, but assist in inhibiting the char formation. Biller *et al.*[64] also came to a similar conclusion with any increase in heating rates; however, the reduction in the renewable crude oil yield in their experiments was not significant. In contrast, Zhang *et al.*[152] reported that using a slow heating rate leads to high renewable crude oil yield; however,

according to Pandey *et al.*[131], slow heating rates lead to char residue formation because the slow heating rates lead to secondary reactions. Thus, it is clear that the use of heating rates could be subject to the influences of other parameters and biomass contents. For example, Akhtar and Amin[10] reported that using large variations of high heating rates does not have a real effect on the renewable crude oil yield. Therefore, it is advisable to use moderate heating rates to achieve some critical aspects, such as minimising the secondary reactions and overcoming the limitations of heat transfer and reducing the operational energy cost, which then helps produce a high renewable crude oil yield[46].

2.4.5 Particle size

The particle size of biosolids could be one of the critical parameters in the HTL process. The importance of any reduction in the particle size is that it may enhance the solubility, accessibility and penetration of heat on biosolids, which can improve the conversion rate[114]. However, grinding the biosolids to small sizes increases the costs in the HTL process[153]. Therefore, the location of an optimal particle size for biosolids could lead to better renewable crude oil yields at low cost. According to Akhtar and Amin[10], the best particle size for biomass could be 4-10 mm. However, Akhtar and Amin[10] also, reported that the HTL process is relatively insensitive to the particle size. For example, Zhang *et al.*[143] reported that a reduction in particle size did not lead to an increase in the renewable crude oil yield at 350ºC. Thus, biosolids' particle size may have a low influence on the HTL process, because the properties of the solvent in the HTL nullify the effect of particle size on the renewable crude oil yield, since the solvent in the HTL behaves as an extractant and as a heat transfer medium[10]. Therefore, to summarise the literature, the HTL process does not require excessive particle size reduction, and using an optimum particle size should increase the renewable crude oil yield at low cost.

2.4.6 Solvents

According to the scientific literature, solvents play an essential role in the HTL of biomass. The solvent's role is to assist in overcoming the transfer limitations of the heat, which make the HTL relatively dependant on heating rates and particle sizes[10]. According to the scientific literature, many solvents could be utilised in the HTL of biomass. Durak and Aysu[154] reported that the HTL of biomass could greatly depend on the type of solvents, which also affect the product yields and their contents. Among all the other solvents that could be utilised in the HTL process, water is the most commonly used because water serves as a great solvent, a reactant for hydrolysing the protein and carbohydrate and even a catalyst or catalyst precursor. In addition, water is the least expensive and most environmentally friendly solvent[1, 155]. However, the HTL process involves a series of complex reactions that lead to changes in the water's physical properties, such as solubility, density, and dielectric constant[90]. Therefore, many biomass compounds may not be water-soluble at ambient conditions but could be readily solubilised in hot water[105]. Moreover, the HTL temperature and pressure maintain the water in the liquid phase, which enhances the associated reactions. Another important benefit of using water in HTL is that water in its native or dissociated form assists in catalysing the hydrolysis and other reactions[136].

Apart from water, other organic solvents could be utilised in the HTL, such as methanol and ethanol[119]. The use of methanol and ethanol, for example, could lead to the production of high renewable crude oil yields[156]. However, according to Cheng *et al.*[157], the use of methanol and ethanol on HTL on pine sawdust leads to the opposite result and causes a reduction in the renewable crude oil yield, whilst hot-compressed water leads to a better renewable crude oil yield. In biomass like wood, the HTL process could be equally effective with the use of water or other organic solvents when applying the optimum parameters. However, it is preferable to

treat biomass like microalgae with alcohols because water is not an effective solvent in this case[156, 158]. Furthermore, utilising a combination of solvents, such as water and methanol or ethanol, can be chosen. Therefore, it is important to select the appropriate solvent for each specific biomass because the selection depends on both the biomass' composition and the operating conditions.

2.4.7 Biomass-to-water ratio

Researchers have examined the effect of the ratio of biomass to solvent because it strongly affects the yield of renewable crude oil and the residue yields. Water represents a part of all the biomass content, such as wood, sludge, biosolids and algae; therefore, it is important to evaluate the overall biomass to water ratio[1].

In the HTL of biomass, water has a triple role: firstly, acting as a reactant, then solvent, and finally a catalyst. For these reasons, the ratio of water to biosolids constitutes an important parameter, because the solvents extract the components of biomass, thereby enhancing the biomass dissolution[10]. According to Sato *et al.*[159], a high amount of water is appropriate for renewable crude oil production, which is probably because of the extraction enhancement of using a denser solvent medium. Also, the high amounts of solvents reduce the gas yield and the solid residue[160, 161]. According to Akhtar and Amin[10], this reduction could be related to the increase in the extraction of biomass components. Also, the high amount of solvent assists in pumping the biomass through the reactor during the HTL process[162]. However, according to Jin *et al.*[126] increasing the microalgae to water ratio has a certain capacity, and any further increase will lead to a decrease in the renewable crude oil yield and an increase in the yield of solid residue. Also, according to Jin *et al.*[126] and Qu *et al.*[144], the use of high water to microalgae ratio is undesirable because it leads to negative effects on energy efficiency during HTL, as the

increase in water requires more energy per unit to heat the biomass. In addition, high solvent ratios are undesirable because large amounts of solvent lead to wastewater treatment problems and require higher energy inputs[10]. Therefore, it is important to avoid the overuse of solvents during the HTL process.

On the other hand, according to Cheng *et al.*[157], utilising smaller biomass to water ratio could lead to a higher renewable crude oil yield. However, Jindal *et al.*[155] reported that a low biomass-to-solvent ratio leads to a low renewable crude oil yield because of the limited mix between water and biomass, which also led to an increase in the solid residue. The high amount of biomass may also make the water less influential on the biomass' molecules, which may inhibit the biomass components' dissolution[10]. Therefore, a decrease in the water-to-biomass ratio may not lead to an increase in the renewable crude oil yield[10].

To summarise, Jindal *et al.*'s[155] study of different biomass-to-water ratios suggested that the effect of biomass' (sawdust)-to-water ratio was almost negligible. However, it is clear that there is an optimal biomass-to-water ratio, which is dependent on many factors, such as the type of biomass. It is, therefore, important to select an appropriate biomass-to-water ratio that is suitable for the HTL of biosolids.

2.4.8 Effect of water on HTL processing

Water could be the most appropriate medium for dissolving organic molecules because of its ability to make reactions occur in a single phase, and this behaviour leads to higher reaction rates, which are followed by hydrolysis reactions[66, 163]. The water transition phase to its organic form leads to the precipitation of salt because of the reduction in solubility[164]. The water viscosity usually decreases with any temperature increase, which leads to a better mass transfer

and high diffusion coefficient[165, 166]. The water behaviour in the HTL process has two phases, the first phase is a preparation period generating a radical pool, and the second phase includes free-radicals' reactions. Both phases depend on process parameters[49]. The low density of water supports the free-radical reactions, while the high density of water dominates the mechanism for ionic reactions[167]. Beyond this, water has a triple role; firstly, acting as a reactant, then solvent, and finally, a catalyst. Therefore, water is a solvent that may well play an essential role in the HTL of biosolids.

2.5 Research need

The increase in demands of fossil fuels in the past decades, due to rapid global population growth has led to many problems, such as increasing energy costs, and environmental degradation. Biosolids are a problematic waste for the water treatment industry because they are costly to manage, keep increasing in size, and are ubiquitous. These concerns have increased the research for alternative renewable energy sources. The utilisation of biosolids for the production of renewable crude oil has many positive aspects, such as the product quantity of the biosolids, which is an essential factor for selecting any technologies for research[43]. Biosolids are an appropriate feedstock for the HTL process because of their sustainability, high productivity and carbon-neutrality, and they are produced in a wet waste at small particle size, which is ideal for HTL. These factors are significant when developing any product for commercial sale. Thus, the need for high-quality management of the produced biosolids could be combined with developing a more efficient alternative renewable energy technology. HTL is a thermochemical conversion process that offers a solution to manage wastewater biosolids by converting biosolids to green renewable crude oil.

A review of the above scientific literature reveals that previous researchers have made significant and substantial contributions to the HTL process of biomass, such as microalgae. The HTL of biosolids, however, is yet to receive sufficient research attention and requires more research when using biosolids for renewable energy production. Based on all the scientific literature that was presented, these are the key research gaps as illustrated below:

Biosolids are more complicated because the composition of biosolids is highly variable. There is limited information in the literature reporting about the organic composition of biosolids for renewable energy, and some of these studies have reported on a range of compositions of biosolids. This is at least partly because the organic content of biological biosolids varies widely, depending on the waste treatment process and the sources of biosolids. Although accurate methods to characterise the organic content of biosolids are necessary for HTL processes, there are no agreed standards or methods to do so for renewable crude energy. Therefore, identifying the amount of the individual components of the organic materials in biosolids represents a fundamental step in the HTL process because each biosolids' component behaves differently with each change to the HTL parameters. This will be fundamental information for any future commercial scaling of the technology. In addition, there is a need to identify the effects of biosolid components and the HTL conditions on both the distributions of the HTL products' yields and the renewable crude yield and quality. It is also important to identify the optimum HTL conditions and biosolids compositions to produce the maximum yield and quality of the renewable crude oil from the biosolids via the HTL process. Previously, some biomasses were studied to investigate their reaction pathway during the HTL process. However, the exact pathways for the biosolids' content, lipids, proteins, carbohydrates, and lignins, and their behaviour during different HTL processes still require more research. In particular, to understand their effect on the composition of the renewable oil produced.

2.6 The aim of the thesis

Based on the literature that was presented. The aim of this research is to develop a greater understanding of the HTL of biosolids to predict the optimum yield and quality of renewable crude oil. This study will provide fundamental information for any future commercial scaling of the technology. The gaps are associated with the primary objective presented in Chapter one, and the methodology that was used to get the data to fill the research gaps is presented in chapter three. These are the detailed objectives of this study:

1. To quantify the variability in biosolids composition by modifying the existing and novel analytical techniques to determine the chemical compositions of biosolids, which represent the fundamental stage of the HTL process.

2. To provide a better understanding of the behaviour of the variable composition of biosolids through the HTL process, especially to measure the effects of four main organic compounds of biosolids, which are lipids, proteins, carbohydrates and lignins on the HTL products yield; specifically, the produced renewable crude oil at different boiling point fractions, in particular, to determine the quantity and the quality of the produced renewable crude oil. This represents the second objective of the research, which will be combined with the first objective to present a journal article in Chapter four.

3. To provide new insight into the effects of biosolid components and the HTL conditions on both the distributions of the HTL products' yields and on the qualities of renewable crude oil. This represents the third objective of the research, which is presented as a journal article in Chapter five.

4. To assess the use of biosolids samples with different biochemical composition via different HTL reaction conditions, as a function of temperature, residence time at the subcritical reaction, to identify their effects on the composition, quality, and the fractions of the produced renewable crude oil in order to maximise the target fraction of the produced renewable crude oil. This represents the fourth objective of the research, which is presented as a journal article in Chapter six.

The following chapter addresses the quantification of the variability in biosolids' composition by modifying the existing and novel analytical techniques to determine biosolids' chemical compositions. This will lead to understanding how this variable feedstock behaves through HTL, especially to determine the effects of biosolids on the quantity and the quality of the produced renewable crude oil. Also, the used methods to produce and analyse renewable crude oil are addressed.

CHAPTER 3

MATERIALS AND METHODS

3. Materials and methods

The general methodology used for the experimentation is presented in this chapter, which is divided into two sections. In the first section, there is a detailed description of the existing methods from the literature and the modified methods that were used to gain the experimental data to address the identified research gaps. The second section outlines the results gained from the modified methods that were used to analyse the biosolids' composition.

3.1 Feedstock analysis

The Melbourne Water Corporation provided biosolids from different stockpiles at the Western Treatment Plant in Werribee, Victoria Australia (Figure 3). Fifty-nine different samples were collected randomly from different stockpiles of biosolids. The collected biosolids samples differed in age, their position of exposure to sunlight, and the depth of the samples taken from the stockpiles. In this research, the youngest twenty-one samples were selected for further investigation, because of the availability of recorded information of the applied wastewater treatment process on the produced biosolids on the last fifteen years at Melbourne Water, which could provide a better understanding about the HTL of biosolids especially for the design of the commercial-scale plant. Out of the 21 selected samples, samples 1- 19 were approximately ten years old, whilst samples 20 and 21 were three years old, which represents the biosolids stockpiles at the Western Treatment Plant in Werribee, Victoria Australia. All the tests in this research were done in triplicate.

Figure 3: Biosolids stockpiles at the Western Treatment Plant in Werribee, Victoria Australia[168].

3.1.1 Biosolids' characteristics

Samples of biosolids were analysed using modified methods to determine their characterisation in terms of the inorganic and organic composition, which included quantification of the lipid, carbohydrate, protein and lignin (soluble and insoluble) content, and the major elementals of biosolids: carbon, hydrogen, nitrogen, oxygen and sulphur. The reason for modifying the standard methodology for analysis biosolids sample was because of the difficulties in dissolving the biosolids in the solvent due to the long years that biosolids were left outdoors facing the weather and its changes. So, the analytical methods were needed to be modified in order to find an accurate measurement to determine the composition of biosolids, which will be explained in more details in the following sections.

Organic content and moisture content

Quantification of the organic and inorganic fractions of the biosolids was determined using a modification of the ash-free dry weight basis (daf) (AFDW) method from the Laboratory Manual of the Central Analytical Laboratory, Natural Resources Research Institute, University of Minnesota-Duluth (USA)[169]. This method involves:

1. Placing a Pecombust Whatman GF/C filter (47 mm diameter, nominal pore size 1.2 μm) covering it with foil in the furnace at 80°C for 1 hour to remove the initial moisture from the put filter.
2. Cooling the filter in a vacuum desiccator and weighing the pre-combusted filters to a decimal point on an analytical balance.
3. Placing the biosolids on the filter. Initially, the dry weight of biosolids involves using 1.5g at 80°C in the oven for 8 hours to measure the amount of moisture, then oxidising the samples in a muffle furnace at 450°C for 8 hours to measure the AFDW.
4. In these experiments, there was no need to wash the biosolids with 20 mL volumes of ammonium bicarbonate solution, as was done in the original method, due to the low amount of absorbed salt in biosolids, since the biosolids are from non-marine sources.
5. The calculations of the dry weight and ash-free dry weight were undertaken by using the following Equations, respectively.

Dry Weight (DW) = (Mass dried – Mass tare)/mass sample Eq 1

Ash Free Dry Weight (AFDW) = (Mass dried – Mass ash)/ mass sample Eq 2

The moisture content was calculated using the following equation.

((initial weight – final weight) / final weight) X 100 =

Lipid content

The standard methodology commonly used to assess lipids content is an inaccurate method when used to determine lipids content in biosolids, because of the difficulties in dissolving the biosolids in the solvent due to the long years that biosolids were left outdoors facing the weather and its changes. So, an analytical method was needed to be modified in order to find an accurate measurement to determine the lipid content in biosolids. In this work, the lipid content of biosolids was determined through a modification of the Folch method[170], which included extraction of lipids, separation of lipids, and the determination of the lipids, as explained in the following steps:

1. The determination of lipid content requires the preparation of an extraction solution (500 mL glass Schott bottle). Firstly, add 200 mL of methanol, followed by 100 mL of chloroform, followed lastly by 80 mL of demineralised water.
2. Prior to the HTL experiments, the dried biosolids samples were ground and sieved to particle size for 142 μm. The particle size of the biosolid samples analysis was measured using a particle size analyser from Malvern Panalytical Limited, UK.
3. Then collect 100g of the biosolids sample for lipid analysis and use 1.5g of the biosolids' sample for each 50 mL falcon tube.
4. Then, pour the water from the tubes following centrifugation and discard while keeping the biosolids pellet. Next, add 5 mL of extraction solution to each tube and mash the biosolids pellet with a glass stirring rod until no visible lumps remain. Add the lid to each falcon tube and centrifuge at 3000×g for 15 minutes.
5. The biosolids will be forced to the bottom with the chloroform layer above it (which contains the lipids) and the water layer on the top. With a glass Pasteur pipette, carefully extract the upper water layer from each tube.

6. Drying some 10 mL clean glass phials at 100ºC for a minimum of 1 hour and allow them to cool. After that, transfer the chloroform layer from each Falcon tube to the glass phials and add a further 3 mL to each phial.
7. Giving each phial a swirl and allow for phase separation to occur, then removing the upper layer with a fine glass pipette and evaporate the samples under a fume hood at 35 to 40ºC.
8. The difference from the original method was made by using dried biosolids samples, which were ground and sieved to particle size for 142 μm. The reason for the ground and sieved of biosolids was the age of biosolids, which was more than 13 years old with the effect of the exposure of sunlight. The sunlight effect has made the biosolids very hard to resolve in organic solvents, especially biosolids contain a high amount of inorganic materials.
9. Another difference from the original method was the use of 1.5g of the sample of biosolids to each 50 mL falcon tube instead of a 50 mL sample. The reason is that biosolids are solids materials and usually contain a low amount of lipids, which necessitates an increase in the sample weight in order to be measured.
10. The samples were centrifuged at 3000×g for 15 minutes instead of 5 minutes to separate the water from the lipids. Also, there was no need to add sea-sand to the experiments, used in the original method to break down the microalgae cells[171]. The lipid content of biosolids was determined as follows:

Lipids weight = Test tubes with only lipids (g) – Empty test tubes weight (g)

Lipids percentage % = (Lipids weight (g) / Biosolids weight (g)) X 100

Protein content

The estimate of the protein content in the biosolids was based on the total nitrogen content, which, according to Fujihara *et al.*[172], is the most practical method for determining the protein content. This method is based on the concept that the lipids and carbohydrates do not contain nitrogen and all the nitrogen in the biosolids originates in the proteins alone. The nitrogen content was measured using elemental analysis of the biosolids, via a Perkin Elmer 2400 Series II CHNO&S analyser operated in CHNS mode. The quantity of the protein was calculated by multiplying by a factor (N x 6.25). This factor represents the most accurate factor for plant and animal proteins[173], which is corresponded to the average nitrogen content of 16% in the pure protein[173, 174].

Carbohydrate content

Carbohydrate is one of the main contents of biosolids[175]. There are several methods to determine the carbohydrate content in biomass. In general, the carbohydrate in biomass can be measured using the phenol-sulphuric acid method. This process is based on the Dubois *et al.*[176] method, which is the most reliable method to measure the carbohydrate content in biomass[177, 178]. However, the carbohydrate content in biosolids cannot be measured using the original method because of the difficulties in dissolving the biosolids in sulphuric acid, which can lead to inaccurate measurements[179]. Especially carbohydrate content required to be dissolved in the solvent in order to be measured by the selected UV-VIS wavelength range. Hence, biosolids require an accurate method to determine their carbohydrate content, particularly in the presence of other organic materials like lipids, proteins and lignins, and other inorganic content. The solution to this problem could be found by treating the biosolids as a soil, due to the similarity in the organic matter levels and inorganic contents between soil and biosolids[180]. Safařík and

Šantrůčková[179] report the most suitable method to determine the carbohydrate content in the soil, and this makes it the best method to measure the composition of the carbohydrate in biosolids due to the similarity in the organic matter levels between biosolids and soil, as explained in the following steps.

The Safařík and Šantrůčková[179] method to measure the carbohydrate content in biosolids is based on measuring the colour development in phenol-sulphuric acid. The determination was achieved by hydrolysing 25 mg of biosolids into 100 µL of the 12 M sulphuric acid, using a colorimetric tube for 16 hours at room temperature. This was followed by adding 2.4 mL of water, then the samples were heated in a boiling water bath at 80ºC for 8 hours. The next step was to mix 0.5 mL of the hydrolysate biosolids with 0.5 mL of water, then add 1 mL of 5% phenol solution, which was followed rapidly by injecting 5 mL of the sulphuric acid directly against the liquid surface to get good mixing of the solutions[177]. According to Montgomery[181] and Dolson *et al.*[182], the temperature rises immediately from 80 to 110ºC. The generated heat will complete the chromogen development to produce a stable yellow-orange chromogen with absorbances at 485 nm.

The samples were vortexed for about 10 seconds and then left for 1 hour at room temperature. In the blank, the hydrolysate was replaced by water. This period was also enough for the temperature and colour for the blank to approximately equalise. Then the obtained absorbance from the biosolids samples was measured at 485 nm on the Shimadzu (UV-VIS 1601) spectrophotometer against the blank after warming up the UV-VIS for at least an hour[182]. The difference between the two readings was used to calculate the carbohydrate content. As can be seen in Table A1 in Appendix A, the preparation of standard samples was made by pipetting 1 mL of carbohydrate (a sugar solution containing 100µg glucose) into a colorimetric tube and

then adding 1 mL of 5% phenol. 5 mL of concentrated sulphuric acid rapidly, which was then allowed to stand for 25 minutes. The tube was shaken and then allowed to stand for a further 5 minutes. Also, a 'blank' was made by repeating the above process but replacing the sugar solution (Glucose) with distilled water. The standard curve can be seen in Figure 4.

Both cuvettes were filled with the 'blank' and inserted into the spectrophotometer and the absorbance reading set at zero. The cuvette closest to the front of the spectrophotometer was removed and the contents discarded. The cuvette rinsed with the standard. The rinse was discarded, and the cuvette was refilled with the standard. This improved the results by reducing any dilution errors and any differences in the optical properties of individual cuvettes. Then the absorbance (%ABS) of the standard was measured by selecting an operating wavelength of 485nm. Starting with a sugar concentration of 50 µg /mL and the performing phenol-sulphuric acid reaction as outlined above, the absorbance was measured. The process was repeated, increasing the sugar concentrations up to 200 µg/mL. A standard curve was constructed by plotting absorbance against sugar (Glucose) concentration. The standard curve, as shown in Figure 4, can be used to determine the carbohydrate concentration of unknown samples.

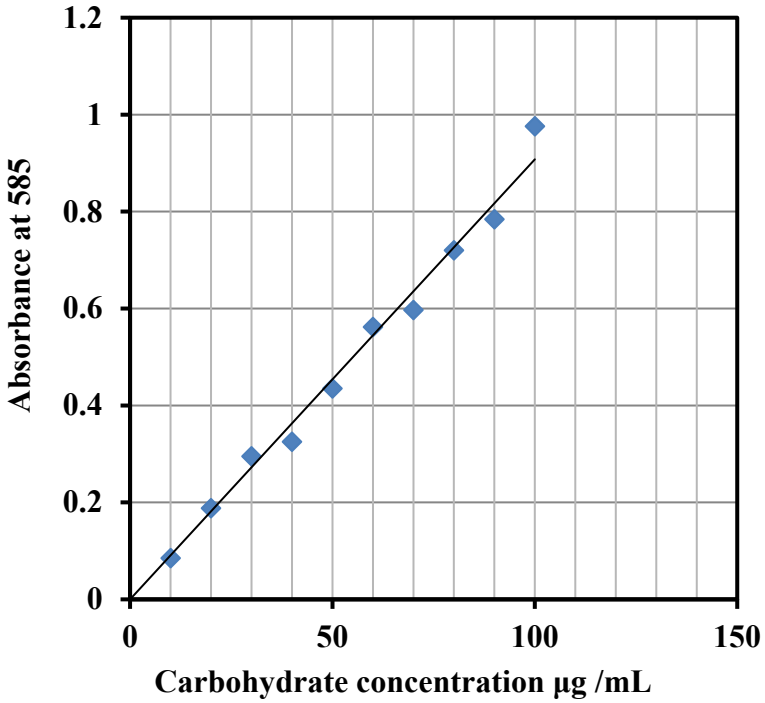

Figure 4: Standard curve for determining carbohydrate concentration.

The calculation was undertaken by putting the average of the absorbance into the equation to solve for concentration in micrograms per mL. The actual measured concentration must be multiplied by 10, since the carbohydrate measured in the samples were prepared by adding 100 µg of the original sample to 900 µg of water to give a 10x dilution, as shown in the example provided in Table A2 in Appendix A.

However, the results obtained from these experiments indicate that the carbohydrate content of biosolids was only 1%, though by doubling the amount of sulphuric acid used, the result increased to 2%. These were unlikely to be reliable because, according to the literature, the carbohydrate content in biosolids is around 15 to 18%[25]. As a result, this method required further modification in order to achieve an accurate result. Therefore, factorial design experiments were applied to measure the carbohydrate content in biosolids, using three amounts of sulphuric acid: 100, 550 and 1000 µL, three acid residence times to dissolve the

biosolids were 1, 4.5 and 8 hours, and three different residence times of the boiling water bath were 1, 4.5 and 8 hours. The optimum conditions were using 550 µL sulphuric acid, 4.5 hours of acid residence time and 4.5 hours of boiling water bath residence time, as discussed further in Chapter 4.

Lignin content

Lignin is one of the organic contents of biosolids. It influences the yields and quality of the HTL products. Therefore, the determination of lignin is very important for renewable crude oil production via the HTL process. The lignin content can be measured using the following method. The quantitation of lignin was undertaken by using the Klason lignin and acid-soluble lignin methods[183]. The differences from the original method were that 25 mg of the biosolids sample were placed in 550 µL sulphuric acid for 4.5 hours with no heating, followed by heating in a boiling water bath at 80ºC for a further 4.5 hours so as to dissolve the biosolids effectively, as occurred in the earlier carbohydrate method. The next step was measuring the acid-soluble lignin content, which was determined using UV-Visible analysis, based on the absorbance value at 205 nm. The wavelength represents the difference between measuring the lignin and the carbohydrate content, which was determined using UV-Visible analysis, based on the absorbances at 485 nm for the carbohydrate and at 205 nm for the lignin.

The final step used an oven and a muffle furnace to measure the insoluble lignin content. Biosolids were placed in a muffle furnace, the following program was set; the temperature was ramped from room temperature to 105ºC and held for 12 minutes, then the temperature was increased to 250ºC at 10 ºC/min and held for 30 minutes. Finally, the temperature was increased again to 575 ºC at 20 ºC/min and held for 180 minutes. Afterwards, the temperature was allowed to drop to 105ºC and held at 105ºC until the samples were removed. The acid-insoluble

residue and acid-soluble ash content were calculated. The lignin content was then calculated by subtracting the acid insoluble ash content from the acid-insoluble residue content.

Analysis of the major elements of biosolids

The biosolids samples were also analysed for the major elements, including carbon, hydrogen, nitrogen, oxygen, and sulphur, using a Perkin Elmer 2400 Series II CHNO&S analyser operated in CHNS mode. The oxygen content was calculated by subtraction from the total mass of carbon, hydrogen, nitrogen, and sulphur[184, 185]. The renewable crude oil was also analysed for the major elements, using the same method.

Particle size

The biosolids, as received, were dried in an oven at 45ºC until they reached a constant mass. Prior to the HTL experiments, the dried biosolids samples were ground and sieved with a mesh size of 142 μm.

The particle size of the biosolid samples analysis was measured using a particle size analyser from Malvern Panalytical Limited, UK[186]. The Malvern Mastersizer 2000 measures particle size based on static light scattering principle in conjunction with the Mie theorem183. Biosolid samples were dispersed in a dispersion medium (water). The dispersion unit in the particle size analyser determined how much sample was dispersed in the water by measuring the fraction of light lost during scattering. The software uses the scattering data to calculate the particle sizes distribution for the biosolid samples.

3.2 Hydrothermal Liquefaction of biosolids

The biosolids samples were ground and sieved to a particle size for 142 µm. The HTL of the biosolids experiments were carried out in triplicate in a high-pressure batch reactor. Figure 5 shows a photograph of the reactor setup, which is explained in detail in Chapter 4. The HTL experiments were undertaken by filling the batch reactor with reactants to 50% volume of the reactor, which was 5.5 mL. This volume represents a 30% of biosolids in the presence of water. Then, after adding the reactants, the reactor was sealed from the top. After filling, the reactor was charged and purged with nitrogen three times to remove any residual air from inside the reactor, and also to be certain that there was no drop in the pressure, so the reactor would hold the pressure during the HTL process. The charged nitrogen inside the reactor was 90 bar to make the pressure reach 200 bar at a reaction temperature of 250 to 350ºC. The top of the reactor was then closed and placed in the heated fluidised bath. The nitrogen-filled reactor was weighed to determine the added nitrogen mass.

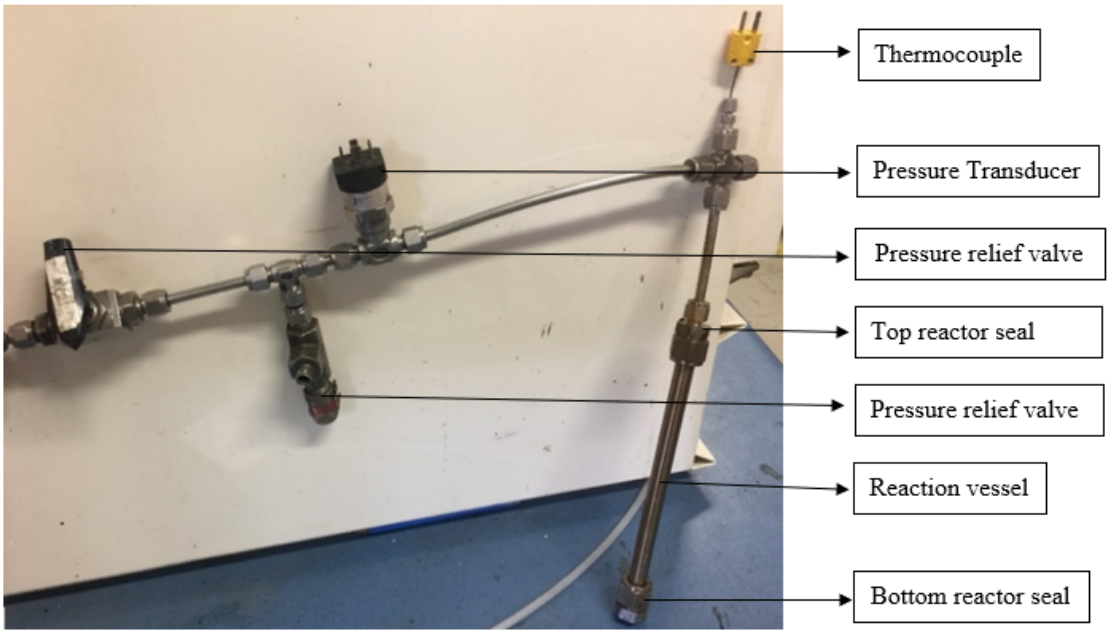

Figure 5: Batch high- pressure reactor.

The batch reactor was placed in a Techne SBL-2D fluidised bed with a Techne-9D temperature controller to heat the reactor to the required temperature, as shown in Figure 6. The desired holding time was set to between 5 - 60 minutes, with the timing started when the reactor temperature initially reached 98% of the reaction temperature. The heating rate was 80 ºC/min. The selected reaction temperatures were maintained between 250 to 350ºC. The advantage of using subcritical reaction conditions (250 to 350ºC) in the HTL of biosolids instead of supercritical reaction conditions is that the design of the commercial-scale plant at supercritical conditions will be very expensive and required a lot of maintenance due to the high temperatures and high pressures, which is in contrast with the concept of this research. The objectives of this research are to provide the best knowledge to be optimised at the industrial scale to produce renewable crude oil at a commercial price. It is important to note that with the temperature increase, the pressure was expected to increase to around 200 bar when the isothermal holding time started. At the completion of the reaction holding time, the reactor was removed from the bed, and it was gradually air-cooled to 70ºC using a ventilator located in the top of the reactor. The reactor was weighed before and after the experiments. Then the gas was released to determine the gas yield.

Figure 6: Techne SBL-2D fluidised bed.

The remaining reactor contents were separated by opening the reactor and decanting the aqueous phase into one 50 mL falcon centrifuge tube, and collecting the remaining solid material in another centrifuge tube, which contained the solid residue and the renewable crude oil. The reactor was then cleaned with a known volume of water, with the washings added to the decanted aqueous phase solid material. In most cases, the solids and the viscous renewable crude oil were bound together. The produced solids were dried in an oven at 40ºC for 72 hours and then the weight was quantified. The resulting solid product contained both solid residue and renewable crude oil. Quantifying the amount of renewable crude oil in the obtained solids was carried out by using the thermal desorption and the pyrolysis of organic matter method. The difference in the total mass of solids, renewable crude oil and gas from the original biosolids mass was used to determine the aqueous phase yields.

3.3 Analysis of the renewable crude oil

The composition of renewable crude oil mostly depends on the source of the biosolids and the HTL reaction conditions. The composition of renewable crude oil will have many differences from fossil oil, which should be addressed[187]. The analysis of the produced renewable crude oil via the HTL of biosolids was conducted using the following methods.

3.3.1 Thermal desorption and pyrolysis of organic material

The used Weatherford Instruments Source Rock Analyser (SRA) method to determine the organic material (OM) and unconverted fractions of the produced renewable crude oil via the HTL of biosolids is discussed in more detail in Chapter 4.

3.3.2 Thermogravimetric analysis

The characterisation of the renewable crude oil fractions assists in understanding the potential procedure to produce the desired products. Thermogravimetric analysis (TGA) method has been used to characterise the renewable crude fractions, which can be separated by particular boiling points, as has been done by Garcia-Perez *et al.*[188]. A simulated distillation of the renewable crude oil using a Netzsch simultaneous thermal analyser (STA) 449 F5 Jupiter was undertaken to obtain the approximate fuel fractions, using the ranges given by the ASTM[189]. This provides further insight into conversions of the renewable crude oil with temperature and time. So, the reaction conditions can be understood, and therefore reactions can be controlled depending on the target fuel. The boiling point profile for the TGA analysis of the renewable crude oil was conducted from 40 to 1010ºC, using an N_2 flow rate of 20 mL/min and a heating rate of 10 °C/min. The fuel fractions from TGA represent the percentage of the renewable crude oil with a boiling point in the range of gasoline and naphthas at 80 to 205°C, kerosene at 205

to 255°C, diesel at 205 to 290°C, gas oil at 255 to 425°C and wax, lubricating oil and vacuum gas oil at 425 to 600°C.

3.3.3 Gas chromatography-mass of the renewable crude oil

The used gas chromatography-mass analysis method of the produced renewable crude oil via the HTL of biosolids is discussed in more detail in Chapter 6.

3.4 Results of the development methods

3.4.1 Organic and inorganic materials content

A modified method of the ash-free dry weight basis (daf) method was tested to determine its reliability for the quantification of the organic and inorganic fractions for biosolid samples. The average result of the organic percentage in the biosolids samples was 29±0.2%, and the average result of the inorganic percentage in the biosolids samples was 71%.

3.4.2 The lipids content in the biosolids

In this work, a modified method of the Folch method[170] was tested to determine its reliability for the quantification of the lipids content of biosolids samples. The result for the lipid content in the biosolids samples was 3.9+03%, and the lipid percentage in the organic materials of the biosolids was 12.9%. An ash-free dry weight basis (daf) test was also undertaken for the products that remained after the lipid experiment to determine its reliability for the quantification of the lipid content. The differences between the results of the organic content before and after the test for lipid content were ~4%, which was similar to the lipid content that was recorded in the lipid test. This proved that the procedure for the lipid test provided an accurate result.

3.4.3 The protein content in biosolids

The analysis of the biosolids samples using the CHNOS[184, 185] method shows that the percentage of protein in the biosolids was 11.5%, and in the organic content of biosolids was 39.5%.

3.4.4 The CHNO&S analysis of the biosolids

Fifty-nine biosolids samples were analysed for samples that were collected from different biosolids stockpiles from the Western Treatment Plant in Werribee, Melbourne, Australia, which can be found in Table A3 in Appendix A. The analysed data for the ultimate analysis shows that each sample of biosolids is unique, and the change in the content of the individual components do not affect each other. The differences in the results of biosolids composition could be due to several factors, such as wastewater treatment processes, retention times, and the age and chemical composition of the sludge[41, 190], which are discussed in more detail in Chapter 4. In this research, of the fifty-nine samples, twenty-one samples were selected based on the age because of the availability of recorded information of the applied wastewater treatment process on the produced biosolids on the last fifteen years, which could provide a better understanding about the HTL of biosolids. Samples 1- 19 were approximately ten years old, whilst samples 20 and 21 were three years old.

3.4.5 The carbohydrate and lignin results

The results of the modified methods for carbohydrate[179] and lignin[183] are discussed in more detail in Chapter 4.

3.4.6 Biosolids particle size

As seen in the data presented in Figure 7, the majority of the biosolid particle sizes lie within a range of 30 - 600µm, with an average particle size of 142 µm. The utilised method to ground of biosolids was explained in the method section.

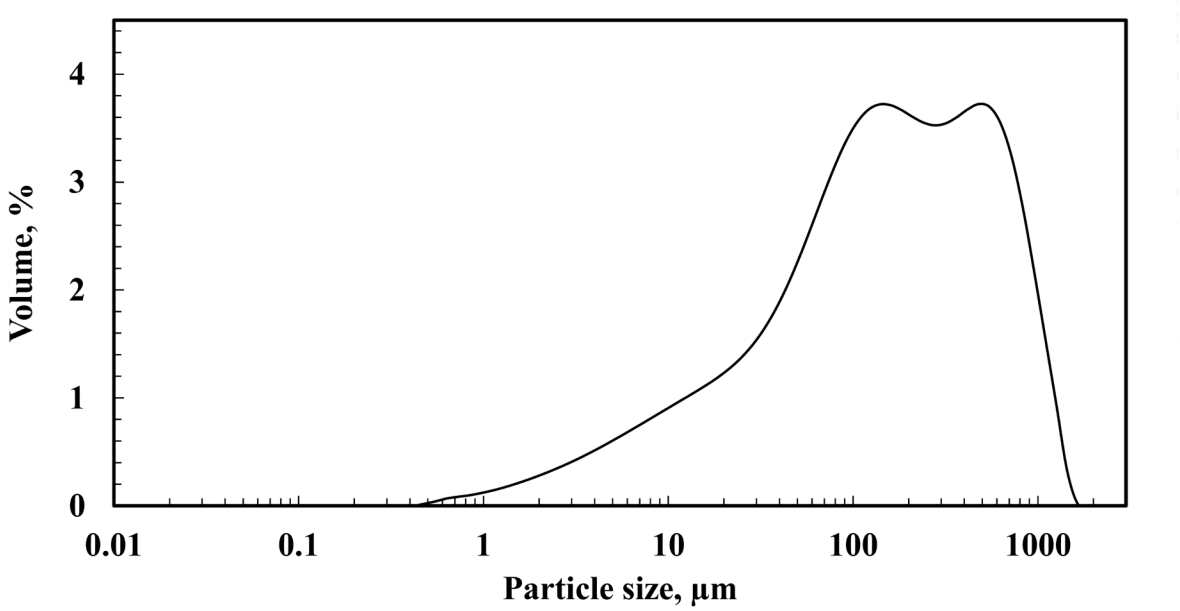

Figure 7: The particle size of biosolids (µm).

3.5 Conclusion

The analysis of the biosolids samples demonstrated the potential of using biosolids for renewable crude oil production because they are rich in organic content. The preliminary objective of this chapter was to develop analytical methods to quantify the biosolids content. The difference in the organic content of the collected biosolids samples was related to the difference in age, their position of exposure to sunlight, and the depth of the samples taken from the stockpiles. In this research, the youngest Twenty-one samples were selected for further investigations, because of the availability of recorded information of the applied

wastewater treatment process on the produced biosolids on the last fifteen years at Melbourne Water, which could provide a better understanding about the HTL of biosolids especially for the design of the commercial-scale plant. The average result of the organic percentage in the biosolids samples was ~30%. The lipid percentage in the organic materials of the biosolids was approximately 13% with protein content ~40% and carbohydrate content ~35% and lignin content ~12%. Biosolids, therefore, represent an appropriate feedstock for producing renewable crude oil via HTL because of their sustainability, and high productivity, and they are produced as a wet waste with small particle sizes that are rich in organic content, which is perfect for HTL feedstocks.

The following chapter address research gaps that arose from this research. In particular, the quantification of the variability in the composition of biosolids to provide a better understanding of the behaviour of the variable composition of biosolids through HTL.

CHAPTER 4

THE EFFECT OF BIOCHEMICAL COMPOSITION ON THE RENEWABLE CRUDE OIL PRODUCED FROM HYDROTHERMAL LIQUEFACTION OF BIOSOLIDS

Jasim M. Al-juboori [a], David M. Lewis [a], Peter J. Ashman [a], Tony Hall [b] and Philip J. van Eyk [a,*]

[a] School of Chemical Engineering & Advanced Materials, University of Adelaide, Adelaide, SA 5005

[b] School of Physical Sciences, University of Adelaide, Adelaide, SA 5005

** Corresponding Author: philip.vaneyk@adelaide.edu.au*

Statement of Authorship

Title of Paper	The effect of biochemical composition on the renewable crude oil produced from hydrothermal liquefaction of biosolids
Publication Status	☐ Published ☐ Accepted for Publication ☐ Submitted for Publication ☑ Unpublished and Unsubmitted work written in manuscript style
Publication Details	

Principal Author

Name of Principal Author (Candidate)	Jasim Al-juboori		
Contribution to the Paper	HTL reactor design and methods HTL batch experiments completed Methods developed for analysing the composition of biosolids HTL products separation and yields quantification completed Writing and editing		
Overall percentage (%)	80%		
Certification:	This paper reports on original research I conducted during the period of my Higher Degree by Research candidature and is not subject to any obligations or contractual agreements with a third party that would constrain its inclusion in this thesis. I am the primary author of this paper.		
Signature		Date	19/08/2021

Co-Author Contributions

By signing the Statement of Authorship, each author certifies that:

i. the candidate's stated contribution to the publication is accurate (as detailed above);

ii. permission is granted for the candidate in include the publication in the thesis; and

iii. the sum of all co-author contributions is equal to 100% less the candidate's stated contribution.

Name of Co-Author	David Lewis		
Contribution to the Paper	Concept development Assistance with analysis and interpretation of data Drafting of paper		
Signature		Date	19/AUG/2021

Name of Co-Author	Peter Ashman		
Contribution to the Paper	Concept development Assistance with analysis and interpretation of data Drafting of paper		
Signature		Date	19/8/21

CHAPTER 4 - THE EFFECT OF BIOCHEMICAL COMPOSITION ON THE RENEWABLE CRUDE OIL PRODUCED FROM HYDROTHERMAL LIQUEFACTION OF BIOSOLIDS

Name of Co-Author	Tony Hall		
Contribution to the Paper	Method design and analysis using Source Rock Analyser		
Signature		Date	19/08/2021

Name of Co-Author	Philip van Eyk		
Contribution to the Paper	HTL reactor design and methods Concept development Assistance with analysis and interpretation of data Drafting of paper		
Signature		Date	19/08/2021

CHAPTER 4 - THE EFFECT OF BIOCHEMICAL COMPOSITION ON THE RENEWABLE CRUDE OIL PRODUCED FROM HYDROTHERMAL LIQUEFACTION OF BIOSOLIDS

Abstract

Biosolids are potentially a highly productive source of renewable crude. Hydrothermal liquefaction (HTL) is a promising technique to convert biosolids into renewable crude oil. However, challenges exist with optimising the HTL of biosolids, such as identification of the composition of biosolids and the resultant effect on the produced renewable crude. The objectives of this work are to develop and modify methods to analysecomer the composition of biosolids and to quantify the effect of biosolids' composition and specific reaction conditions on product distributions derived from HTL. Biosolids with varying compositions were processed using HTL in a batch reactor under controlled operating conditions. The analysis of the biosolids' composition showed that few biosolids samples are close to the composition of biomass content, and the majority of the biosolids samples differ in composition from biomass when compared using the Van Krevelen diagram. The results also show that those biosolids with higher lipid and protein content exhibit an increase in the renewable crude yield with a larger content of low-boiling point components. However, biosolids with higher carbohydrate and insoluble lignin content produce lower renewable crude oil yield with a higher content of high-boiling point components and an increased mass fraction of solid residue.

Keywords: Hydrothermal liquefaction, Biosolids characterisation, Reaction conditions, Renewable crude oil, HTL yields.

1. Introduction

The world currently relies on fossil fuels to meet the growth in energy demand. For example, more than 80% of the energy demand in the United States is met using fossil fuels[1]. However, fossil fuel resources are facing decline, so the increase in global energy demand has increased the desire for alternative renewable energy[2]. Oil reserves are only estimated to provide energy for about fifty years, and it is estimated that coal can only provide energy for 132 years[3]. The increase in global energy demand is also connected with many environmental problems, some of which is caused by rapid population growth, such as the effects of the by-products from wastewater treatment plants, particularly sludge and biosolids[4]. Biosolids represent a problematic by-product from the water industry because they are costly to manage, in term of treatment processes and the scale of biosolid stockpiles are increasing widely. The annual global production of biosolids in 2011 was about 17 billion tonnes and is expected to reach 27 billion tonnes by 2050[5]. In 2010, the Chinese city of Shanghai alone produced about 294,000 dry tonnes of biosolids[6]. The USA currently spends about two billion dollars annually on treating about five to seven million tonnes of biosolids[7]. The combination of the decline in fossil fuel reserves and the negative environmental effects of biosolids has created the need for alternative renewable treatment technology[8], with a greater focus on integrating sustainability by using the large continuing annual production of biosolids as a possible valuable source for renewable energy[9]. However, the development of appropriate technology to generate green energy is still in its infancy and requires more research.

One method of conversion researchers has investigated is to convert the organic material of biomass into renewable crude oil using HTL. HTL of biosolids, therefore, could be a promising technology to convert biosolids into renewable crude oil by precluding the drying pre-treatment

step, which exceeds the energy requirement for the HTL of biosolids with a 30% w/w water content[10-12]. HTL is a thermo-chemical process that converts biosolids under moderate temperatures, from 250 to 350ºC, and high pressure, from 50 to 200 bar, into renewable crude oil[13-16]. The products from the HTL process include renewable crude oil, an aqueous phase, solid residue, and a gaseous product[17]. Majority of the previous investigations have been undertaken on other feedstocks, such as biomass, microalgae and food waste[18]. The effect of model compounds and biomass content in the HTL products have been investigated and reported in the scientific literature. However, different sources of biomass or model compounds have produced different product distributions, especially in renewable crude. For example, Zhang *et al*.[19] stated that 58%, 79% and 29% of renewable crude oil yields were gained from the HTL of Kraft pine, lignin and switchgrass, respectively at 374ºC, 220 bar and 10 minutes residence time. Furthermore, the renewable crude oil yields from model compounds also ranged widely. According to Teri *et al*.[20], the HTL of sunflower oil and castor oil, soy protein and albumin, and polysaccharides were 90 wt%, 30 to 35 wt% and 10 to 15 wt%, respectively at 300 to 350°C and residence time from 10 to 90 minutes. Therefore, it is clear that renewable crude oil yields are fluctuated and dependant on the biomass composition, which may be affected by different HTL conditions[19]. Moreover, the scientific literature has minimal fundamental information about the performance of biosolids through HTL process. Therefore, the HTL of biosolids requires more research to get a better understanding of the effects of HTL conditions and the biosolids composition on the renewable crude oil yield and the distribution of the products, which is essential to optimise and promise the design of the commercial-scale plant.

One of the major aims in developing the HTL process is to maximise renewable crude oil recovery and minimise its losses. According to Garcia Alba *et al*.[21], the low rates of recovery of renewable crude oil could be influenced by the conditions of the process and the exact composition of the biomass. There is minimal fundamental information available in the scientific literature about the composition of biosolids for renewable energy production, which is more complicated because the composition of biosolids is highly variable. The differences in the chemical composition of biomass - and therefore biosolids - could have significant effects on the HTL process and the resulting renewable crude oil because each biosolid's component behaves differently with the changing HTL parameters[22]. The renewable crude oil composition also could be influenced by the proportion of the carbohydrates, proteins, lipids and lignin[23]. So, it is important to understand the effect of different variables of the biosolids composition on the quality and quantity of the renewable oil produced. However, there is not sufficient scientific literature on assessing the composition of biosolids. This is unexpected because much work has been done on biosolids but not for producing renewable energy, and the composition of biosolids is fundamentally important because it affects the reactions. Therefore, identifying the amount of the individual components of the organic materials of the biosolids, including carbohydrates, proteins, lipids, lignin, and inorganic material, is critical because it is the primary stage of renewable crude oil production and could help to explain the quantity and nature of the resulting renewable crude oil.

Biosolids have their origins in widely varying sources, both household and industrial[4, 24]. A review of the scientific literature reveals that limited information has been reported about the organic composition of biosolids, although some of these studies have reported a range of organic compositions of biosolids. For example, Wang *et al*.[25] reported that the composition of

biosolids contains 7 to 35% lipids, 20 to 30% proteins and 15 to 18% carbohydrates. Similarly, Parmar *et al*.[26] stated that biosolids consist of about 50% proteins, 20% carbohydrates, and the remainder is bacterial biomass. Most of these studies ignore the lignin content and report the carbohydrate content by subtraction. Also, there is not much scientific literature on assessing the composition of biosolids, especially in relation to the use of biosolids for renewable energy production. Although accurate methods to characterise the organic content of biosolids are necessary for the HTL processes, to date, there are no agreed standards or methods to do so. This is at least partly because the organic content of biological biosolids varies widely depending on the waste treatment process[27].

The existing scientific literature provides clear knowledge about the composition of other biomass like microalgae, which include proteins, carbohydrates and lipids[18, 28]. Many microalgae components have been tested under HTL conditions, but in many situations, the renewable crude oil yields were about 15% more than the lipid content[21]. This implies that renewable crude oil must also be derived from proteins and carbohydrates, in which biosolids are rich[23]. Suzuki *et al*.[29] tested several kinds of sewage sludge at 300ºC and 120 bars. They found that the composition of sludge does not have a noticeable effect on either the elemental composition or the heating value of the obtained renewable crude oil. However, the variations between the composition of microalgae and biosolids raise many questions about the above result. The composition of biosolids is more complicated because it is highly variable, and it is important to understand the effect of different variables of the biosolids composition on the quality and quantity of the renewable oil produced. Also, understanding the HTL of biosolids is essential to optimise and promise the design of the commercial-scale plant. Therefore, it is essential to discover appropriate analytical methods to identify the biosolids components, such

as lipids, proteins, carbohydrates, lignins and solid residues, in order to gain a better understanding of the effect of different components of biosolids on the quality and the distribution of the products from the HTL of biosolids.

Carbohydrates are one of the main contents of biosolids[26]. Hence, there is a need for an accurate method to determine the carbohydrate content of biosolids, particularly in the presence of other biological materials like proteins, lipids and lignin and the high inorganics content. In general, carbohydrates can be measured by using the phenol-sulphuric acid method. This process is based on the Dubois method[30], which represents the most reliable, reproducible, easiest and most sensitive method to measure the carbohydrates' content in biomass[31, 32]. However, the carbohydrate content in biosolids cannot be measured by using the original method due to the difficulties of dissolving the biosolids in sulphuric acid, which can lead to inaccurate measurements[33]. In addition, according to Ashwell[34] and Shetlar and Masters[35], the phenol-sulphuric acid method could be affected by several components, such as proteins and lipids, even though they have a small effect on absorption curves. However, Lourenço *et al*.[36] report that the proteins and amino acids do not interfere with the procedures of this method. Furthermore, the result of the carbohydrate content could be affected by the amount of water, which could stop the reaction completely, especially before adding the sulphuric acid[37].

There have been a few attempts to optimise the phenol-sulphuric acid method, which could be a practical method to determine the carbohydrates content. For example, Buysse and Merckx[38] adjusted the amount of phenol that could be used for carbohydrates mixtures of sucrose, fructose, and glucose. However, according to Chow and Landhäusser[39], this method did not report the optimisation of a mixture of all dominant carbohydrates. In addition, Rose *et al*.[40]

described a method to digest starch by using enzyme mixtures of α-amylase and amyl glucosidase. However, there was no test to determine the completeness of digestion in their method. Chow and Landhäusser[39] also report that using an enzyme to digest the starch was not possible in the phenol-sulphuric acid because the concentration of the sulphuric acid hydrolysed the enzyme and therefore provided an unreliable outcome. However, there was a method to measure the carbohydrates content in the soil used by Safařík and Šantrůčková[33], which could be the most suitable method to determine the carbohydrate content in the biosolids due to the similarity in the organic and inorganic contents between soil and biosolids. Given the above-combined problems, a direct method to determine the carbohydrate content in biosolid is still not available and needs further research.

Outputs from the HTL of biosolids are significantly affected by the initial composition of the biosolid feedstock, which can vary significantly due to a range of factors. This research aims to provide a better understanding of the characterisation of biosolids feedstock by reporting proximate and ultimate analyses of biosolids along with their composition, such as mass % of carbohydrates, lipids, proteins and lignins. In addition, H/C and O/C ratio of feed materials are also provided. To achieve this aim, the key objectives of this work are to develop and modified analytical techniques to quantify the individual component of the organic materials and inorganic composition of the biosolids. The main aim of the work is to provide a clear understanding of the biosolids' characterisation and how the different biosolids' composition affects the HTL yields of organic crude oil, aqueous fraction, and solid residue and gases products, at specified temperature and pressures, and to determine the nature of the produced renewable crude oil at different boiling points.

2. Materials and methods

2.1 Feedstocks

The biosolids were provided by Melbourne Water, Western Treatment Plant, Werribee, Victoria, Australia. Twenty-one different samples were collected randomly from different biosolids stockpiles. The biosolids samples differed in sunlight position, ages and depth. Samples 1- 19 were approximately ten years old, whilst samples 20 and 21 were three years old. All the tests in this project were completed in triplicate.

2.2 Biosolids characteristics

The inorganic and organic content of the biosolids samples were investigated, including quantification of the lipid, carbohydrate, protein, and lignin (soluble and insoluble) content, and the major elements; carbon, hydrogen, nitrogen, oxygen and sulphur.

2.2.1 Organic content and the moisture content

Quantification of the organic and inorganic fractions of the biosolids was determined using a modification of the ash-free dry weight (AFDW) method from the Lab Manual of the Central Analytical Laboratory, Natural Resources Research Institute, University of Minnesota-Duluth[41]. Initially, 1.5g of the biosolids was dried at 80°C in an oven for 8 hours to measure the amount of moisture, then oxidised in a muffle furnace at 450°C for 8 hours to measure the AFDW. In these experiments, there was no need to wash the biosolids with 20 mL volumes of ammonium bicarbonate solution, as was undertaken in the original method, due to the low level of absorbed salt on the cell surface, since the biosolids are from non-marine sources.

2.2.2 Lipid content

The lipids content of biosolids was evaluated by modification of the Folch method[42]. The process included the extraction of lipids, lipids separation, and the determination of the lipids, as explained in the following steps. The determination of lipid content requires preparing an extraction solution (500 mL glass Schott bottle); firstly, adding 200 mL of methanol, followed by 100 mL of chloroform, and lastly by 80 mL of demineralised water. Prior to the HTL experiments, the dried biosolids samples were ground and sieved to particle size for 142 μm. The particle size of the biosolid samples analysis was measured using a particle size analyser from Malvern Panalytical Limited, UK. Then 100g of the biosolids sample was collected for lipid analysis, using 1.5g of the biosolids sample for each 50 mL falcon tube. The water was poured from the tubes following centrifugation and discarded while keeping the biosolids pellet. Then 5 mL of extraction solution was added to each tube, and the biosolids pellet was mashed with a glass stirring rod until no visible lumps remained. A lid was added to each falcon tube, and it was centrifuged at 3000×g for 15 minutes. The biosolids are forced to the bottom, with the chloroform layer above containing the lipids. The water layer is on the very top. Then with a glass Pasteur pipette, the upper water layer is carefully extracted from each tube. Some clean glass 10 mL phials are dried at 100ºC for a minimum of 1 hour and allow to cool. After that, the chloroform layer is transferred from each Falcon tube to the glass phials, and a further 3 mL is added to each phial. Each phial is swirled to allow for phase separation to occur, then the upper layer is removed with a fine glass pipette, and the samples are evaporated in a fume hood at 35 to 40ºC. The difference from the original method was made by using dried biosolids samples, which were ground and sieved to particle size for 142 μm. The reason for the ground and sieved of biosolids was the age of biosolids, which was more than 13 years old with the effect of the exposure of sunlight. The sunlight effect has made the biosolids very hard to

resolve in organic solvents, especially biosolids contain a high amount of inorganic materials. Also, in this work, we used 1.5g of the biosolids sample in each 50 mL falcon tube, instead of a 50 mL sample. The reason is that biosolids are solids materials and usually contain a low amount of lipids, which require an increase in the sample weight in order to be measured. The samples were centrifuged at 3000×g for 15 minutes instead of 5 minutes to separate the water from the lipids. Also, there was no need to add sea-sand to the experiments, as was used in the original method, to break down the microalgae cells[43].

2.2.3 Carbohydrate content

The carbohydrate content was initially determined using a modified version of the method described by Safařík and Šantrůčková[33], which is based on the measurement of the development of the colour in the phenol-sulphuric acid. The same method was used to determine the carbohydrate content in biosolids after sulphuric acid hydrolysis: placing 25 mg of the biosolids samples into a colourimetric tube, then adding 100 μL of the 12 M sulphuric acid. After hydrolysis, the samples are kept at room temperature for 16 hours, then 2.4 mL of water was added. Next, the samples were heated on a boiling water bath at 80ºC for 8 hours. However, at first, it was found that the carbohydrates content of biosolids was only 1%, though by doubling the amount of sulphuric acid used, the result increased to 2%. These are most unlikely to be reliable results because according to the scientific literature, the carbohydrate content in biosolids is around 15 to 18%[25]. As a result, this method required further modification in order to obtain an accurate result. Therefore, factorial designs experiments were applied to determine the content of carbohydrate in the biosolids, using three amounts of sulphuric acid: 100, 550 and 1000 μL, three residence times for the acid to dissolve the biosolids, for 1, 4.5 and 8 hours, and three different residence times to use the boiling water

bath, for 1, 4.5 and 8 hours. The experiments demonstrated that the optimum conditions were to use 550 µL sulphuric acid, 4.5 hours of acid residence time and 4.5 hours of boiling water bath residence time, as discussed further in Section 3.2.

2.2.4 Protein content

The estimate of the protein content in the biosolids was based on the total nitrogen content, which, according to Fujihara *et al*.[44], is the most practical method for determining the protein content. This method is based on the concept that the lipids and carbohydrates do not contain nitrogen and all the nitrogen in the biosolids originates in the proteins. The nitrogen content was measured by analysis of the biosolids using elemental analysis, achieved using a Perkin Elmer 2400 Series II CHNO&S analyser operated in CHNS mode. The quantity of the protein was calculated by multiplying by a factor of 6.25. This factor represents the most accurate factor for the plant and animal proteins, which is corresponded to average nitrogen content of 16% in the pure protein[45, 46].

2.2.5 Lignin content

Lignin quantification was conducted using the Klason lignin and acid-soluble lignin test[47]. The method was modified with 25 mg of the biosolids sample digested in 550 µL sulphuric acid for 4.5 hours with no heating, followed by heating at 80ºC in a boiling water bath for a further 4.5 hours, similar to the carbohydrate method dissolve the biosolids more effectively. The acid-soluble lignin content was quantified using Shimadzu UV-visible spectrophotometer (UV-1601) analysis, based on the absorbance value at 205 nm. The acid-insoluble lignin was quantified by mass using a muffle furnace. Biosolids were placed in the muffle furnace, heated

from room temperature to 105ºC and held for 12 minutes, then ramped to 250ºC at 10 ºC/min and held for 30 minutes, and finally ramped to 575ºC at 20 ºC/min and held for 180 minutes. The samples were cooled to 105ºC until removed. The acid-insoluble residue and acid-soluble ash content were calculated. The lignin content was then calculated by subtracting the acid insoluble ash content from the acid-insoluble residue content.

2.2.6 The analysis of the major elementals of biosolids

The biosolids samples were also analysed for the major elements, carbon, hydrogen, nitrogen, oxygen, and sulphur, using a Perkin Elmer 2400 Series II CHNO&S analyser, operated in CHNS mode. The oxygen content was calculated by its subtraction from the total mass of carbon, hydrogen, nitrogen, and sulphur[47].

2.3 Hydrothermal liquefaction of biosolids

Prior to the HTL experiments, the biosolids samples were ground and sieved to a median particle size of 142 μm, which was measured using a particle size analyser (Malvern Mastersizer 2000). The HTL experiments were performed in triplicate on the biosolids samples in a high-pressure batch reactor, as used previously in our laboratory[48]. The HTL experiments were conducted by filling the batch reactor to a 50% volume of the reactor, which was 5.5 mL, as presented in Figure 1. The dry biosolids percentage was 30% by mass in the presence of water. The reactor was sealed after adding the reactants. After filling, the reactor was charged and purged with nitrogen three times to remove the residual air from inside the reactor. The charged nitrogen inside the reactor was 90 bar to make the pressure reach 200 bar at the reaction temperature of 350ºC. The nitrogen-filled reactor was weighed to determine the added nitrogen

mass. The top of the reactor was then sealed.

The batch reactor was next placed in a Techne SBL-2D fluidised bed, with a Techne-9D temperature controller to heat the reactor to the required temperature. The desired holding time was set at 20 minutes, because this could be the most enhanced reaction kinetics time to improve the desired product yields[49], with the timing started when the reactor temperature first reached 98% of the reaction temperature. The heating rate was 80 ºC/min, as measured in the preliminary experiments. The selected temperature, 350ºC, was maintained for the specific residence time of 20 minutes. It is important to note that with the temperature increase, the pressure increased to 200 bar when the isothermal holding time started. At the completion of the reaction holding time, the reactor was removed from the bed, and it was gradually air-cooled to 70ºC using the flow of cool air. After reaching 70ºC, the reactor was drenched in cold water. The reactor was weighed before and after the experiments. The gas was then released to determine the gas yield, which represented the first step of the procedure for separating HTL products, which also contained renewable crude oil, aqueous and solid residue.

The remaining reactor contents were separated by opening the reactor, decanting the aqueous phase into a centrifuge tube and collecting the remaining solid material in another centrifuge tube, which contained the renewable crude oil and the solid residue. The reactor was then cleaned with 50 mL water, with the washings added to the decanted aqueous phase solid material. The solids residue and the viscous renewable crude oil were bound together. The produced solids and oil mixture were dried in an oven at 40ºC for 72 hours until it reached a constant weight and then weighed. Quantifying the amount of renewable crude oil in the obtained solids was implemented by using the thermal desorption and pyrolysis of organic

matter method, as discussed in Section 2.4. The difference in the total mass of solids, renewable crude and gas from the original biosolids mass was used to determine the aqueous phase yields.

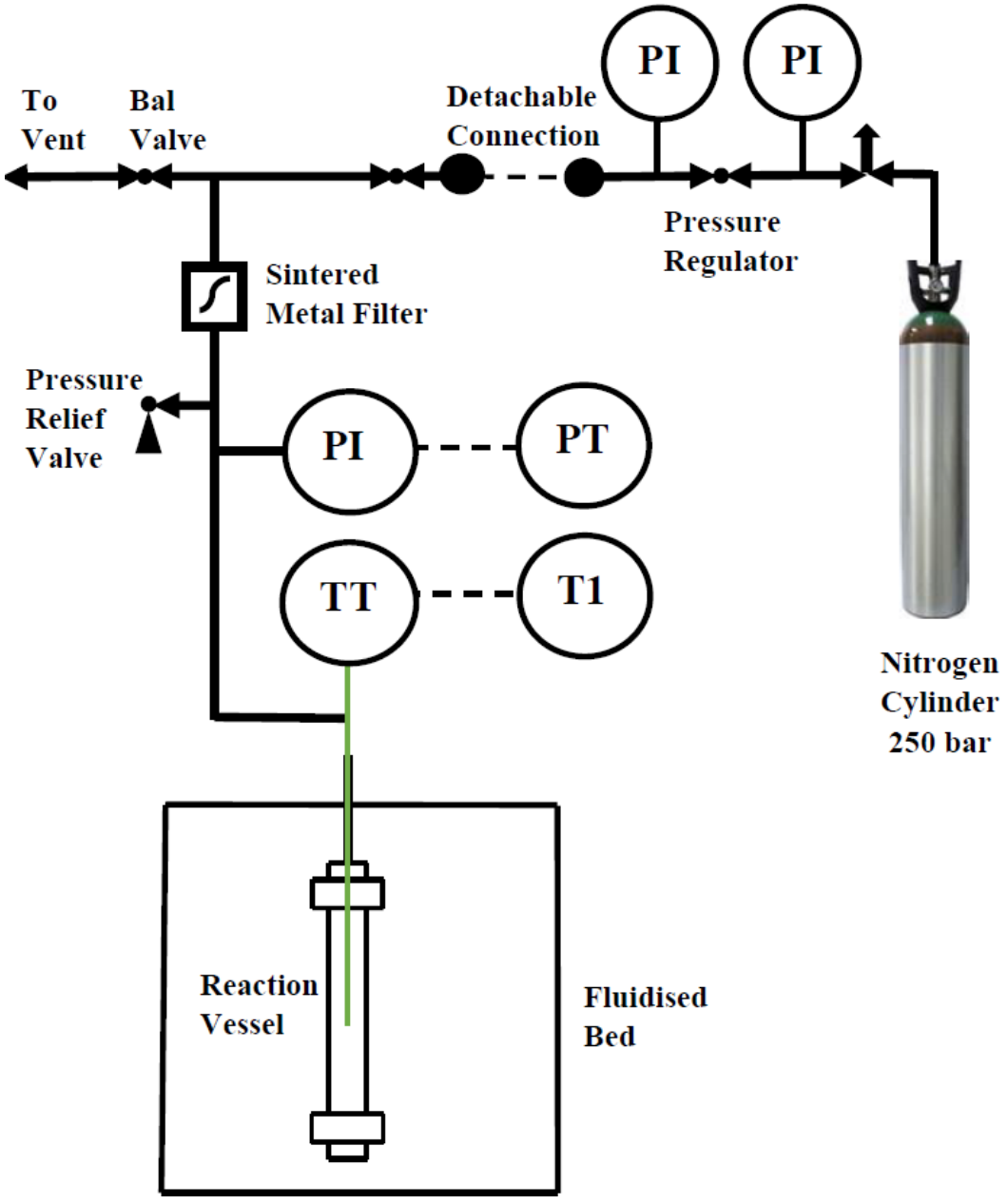

Figure 1: The configuration of the HTL reactor. PT: Pressure Transducer. PI: Pressure Indicator. TT: Thermocouple. TI: Temperature Indicator.

2.4 Thermal desorption and pyrolysis of organic matter

A Weatherford Instruments Source Rock Analyser (SRA) was used to evaluate the organic matter (OM) in the biosolids samples (the residual renewable crude oil and unconverted fractions). The OM was quantitatively assessed by heating the samples to a programmed temperature in a controlled atmosphere with detection by either a flame ionisation detector (hydrocarbons) or infra-red spectrometry CO_2 & CO. Quantification of total organic content was conducted against the Weatherford Certified References Standard 533.

The biosolids were pulverised and passed through a 40-mesh sieve. 20 to 40 mg of each sample was then accurately weighed, loaded into SRA crucibles and placed in the SRA auto-sampler carousel. The crucible was then transferred from the auto-sampler tray to the SRA pedestal and loaded into the oven base and purged under helium carrier gas (99.9999% Ultra-pure Grade) at 120ºC for 90, seconds before being raised fully into the furnace and held isothermally at 300ºC for 3 minutes. During the thermal extraction, free hydrocarbons (S1 fraction) were volatilised and quantitatively detected using the FID detector and reported as milligrams per gram of biosolids.

Following the thermal extraction, pyrolysis was conducted by increasing the oven temperature at 25 ºC/min to 600ºC. The hydrocarbons generated from the pyrolytic degradation of the kerogen in the biosolids (S2 fraction) represent the generative potential of the residual OM. The hydrocarbons were detected by the FID and reported as milligrams per gram of biosolids. Free CO_2 simultaneously liberated during the pyrolysis of the OM between 300ºC and 400ºC (S3 fraction) was also determined by detection in the IR cells and reported as milligrams per gram of the biosolids.

In the final oxidation stage, following the end of pyrolysis, the oven was cooled to 400ºC, and the carrier lines were switched to CO_2 free instrument grade air and purged for 5 minutes. The oven was then increased to 540ºC at a maximum heating rate and held isothermally for 15 minutes. The residual inert OM (S4 fraction) was converted to CO and CO_2 during the oxidation stage and detection in the IR cells and reported as milligrams per gram of the biosolids.

3. Results and discussion

3.1 Biosolids characteristics

The organic and inorganic contents of the biosolids samples were quantified for the twenty-one samples using the AFDW. As shown in Appendix B (Figure S1), the organic content in the biosolids samples was associated with the biosolids' age and ranged from 18 to 45%. The samples with the highest organic content were the three-year-old samples, and the lowest organic content was found in the ten-year-old samples. Several reasons might account for the differences in the amounts of organic content in the biosolids. For example, the dissolved organic matter in biosolids depends on both the quality and the quantity of the wastewater resource and the levels and the types of the wastewater treatment[50, 51]. Also, the original sources of biosolids are not from households alone but include waste from food-processing, animals, plants, commercial, and industrial sources[4, 24]. Therefore, the organic content in the biosolids differs widely.

The moisture content in the biosolids samples also had a wide range: from 3 to 9%. The main reason for the variation in the biosolids' moisture is associated with the initial treatment process

of biosolids. For example, the biodegradability of the waste-activated sludge is related to its age, and therefore the age of biosolids[52], while most of the other types of sludge depend on the chemical sludge and the wastewater process[53]. Also, several factors can lead to differences in the moisture content of the biosolids. These factors could be age, depth, and the position of the samples in relation to the sun.

3.2 The Biochemical composition of the biosolids

The outcome of the experiments that were used to determine the carbohydrate content can be seen in Figure 2, which shows that the carbohydrate content of 100 µL of the sulphuric acid at 1-hour acid residence time and boiling water bath time was about 4%, and increased to around 8% at 8 hours' boiling water bath residence time, it remained low at around 4% for the 4.5 hours of acid residence time and boiling water bath residence time. The carbohydrate with 8 hours of acid residence time and boiling water bath residence time of between 1-8 hours reached 4%.

The results of the experiments show that the content of the carbohydrate at 550µL sulphuric acid reached 13% at 4.5 hours' boiling water bath residence time and acid residence time and then dropped again to around 4% with the increase of the boiling water bath time and acid time hours. The reason for the decrease in the carbohydrate content is the dehydration of the carbohydrate. Sulphuric acid is known for its ability to perform in three different ways; firstly, as an acid, secondly, as a dehydrating agent and thirdly as an oxidising agent[54]. According to Dolson *et al*.[37], the dehydration of carbohydrate when reacted with concentrated sulphuric acid will lead to char formation from the carbohydrate. Also, according to Nagasawa *et al*.[55] after 4 hours, around 94% of the carbohydrate will dissolve in the sulphuric acid. However, the

continuity of the reaction leads to char formation from the carbohydrate and the creation of solid materials that cannot be read by the UV-VIS. As a result, in this experiment, the most accurate result was 12.8%. This was gained in the 550 µL sulphuric acid, after 4.5 hours of acid residence time and the 4.5 hours of boiling water bath residence time. An additional test was also undertaken to confirm the result of the carbohydrates content via the carbohydrate modified method. A sample with the same content of biosolid was created and used to determine the accuracy of the carbohydrate modified method. The result of the carbohydrates content for the created sample was 13.1%, which was very close to the result obtained from the biosolids. Therefore, the modified carbohydrate method was used to determine the content of the carbohydrate in the biosolids.

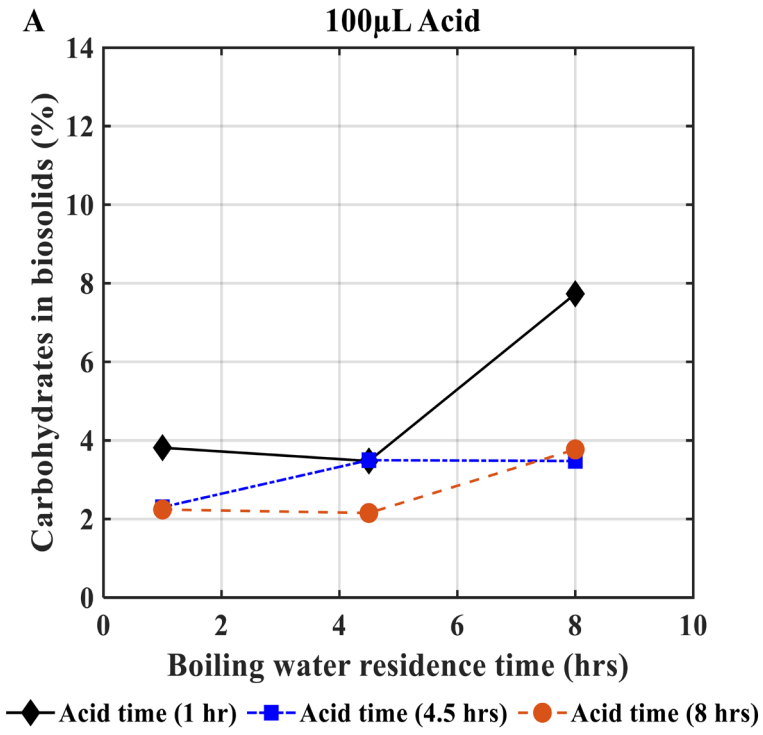

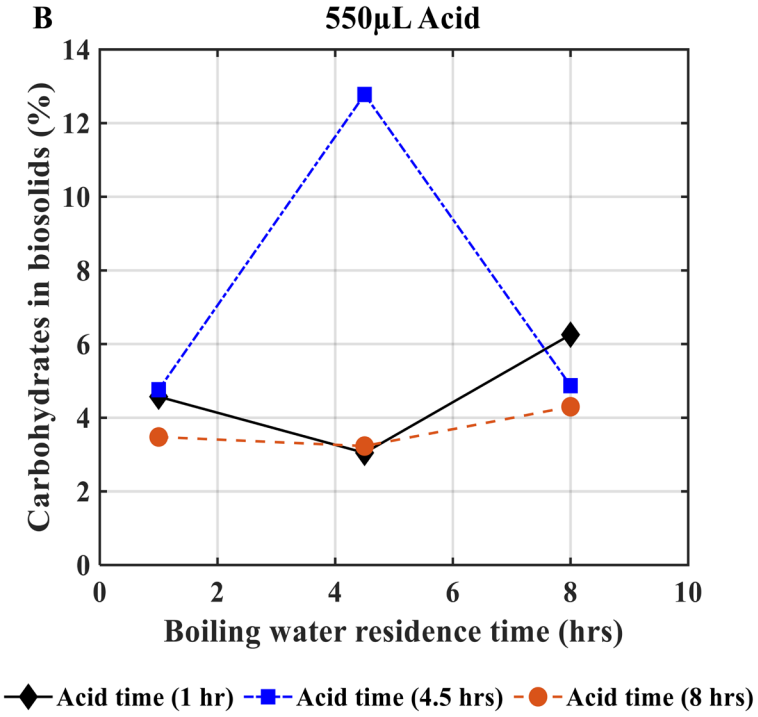

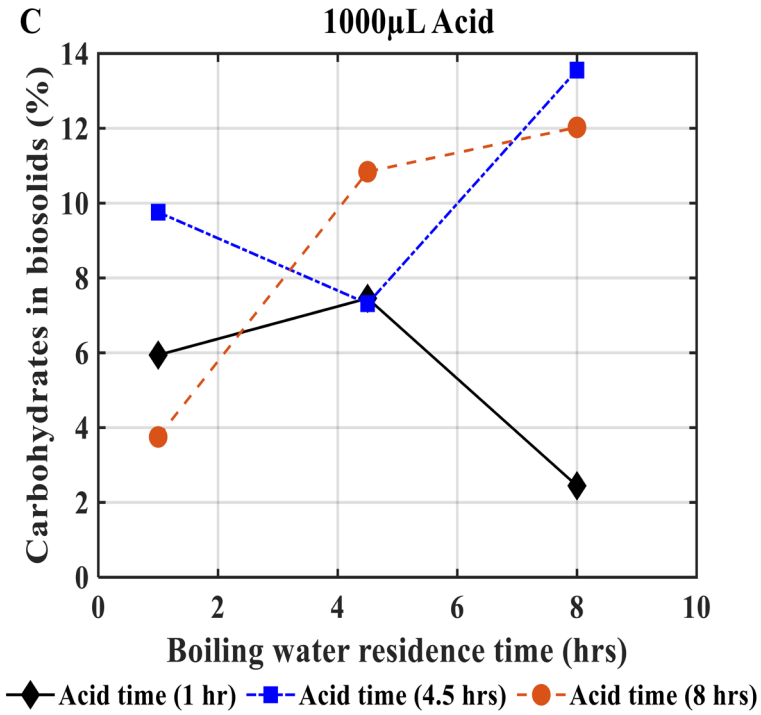

Figure 2: Carbohydrate content in biosolids at three amounts of sulphuric acid: 100, 550 and 1000 µL, three acid residence times: 1, 4.5 and 8 hours, and three different residence times of the boiling water bath: 1, 4.5 and 8 hours.

The biochemical composition of the organic materials of biosolids consists of various compounds, as shown in Figure 3. Firstly, the lipids ranged from 2 to 32%. According to the scientific literature, lipids mainly consist of triglycerides-esters, which are the main contents of oils[56]. Also, according to Wang[57], lipids contain various categories of molecules, such as oils, sterols, fats and phospholipids. Secondly, the carbohydrates ranged from 21 to 46%, and according to Gollakota *et al*.[58], they can consist of different compounds, such as cellulose, which has a long chain polysaccharide with high polymerisation and high molecular weight, or hemicellulose, which is a branched structure hetero-polymer containing hexose and pentose as a polymer. Thirdly, the protein ranged between 20 to 48% and can contain many chains of peptide that are reduced to amino acid polymers[58]. Fourthly, the soluble lignin ranged between 9 to 32%, and the insoluble lignin ranged between 3 to 6%. Lignin is a natural polymer and represents an aromatic compound, which is composed of basic building blocks linked through ether bonds, such as those of the hydroxyl and ethoxy group and phenyl-propane[59, 60]. This makes it clear that the biosolid samples had very different biochemical compositions. Analysis of the biochemical composition data shows that the individual components of the biosolids do not affect each other, and each biosolid sample has a different organic content from the others, which is mainly connected with the original biological nature of the biosolids, and the processed waste.

The variation in the percentage of the biosolids content is associated with the origin of the biosolids and the treatment process. The dissolved organic materials of biosolids are predominantly dependent both qualitatively and quantitatively on the origin of wastewater and the treatment types[50, 61]. There are two main important types of sludge produced by the wastewater treatment plants. Firstly, is the primary sludge, which is produced from the bottom

of the primary sedimentation. Secondly, waste-activated sludge is gained from the activated sludge system[62]. The quality of the primary sludge is mostly dependent on the retention time in the sedimentation tank, which means the wastewater treatment process has no effect on the organic materials[63]. Therefore, biosolids retain most of the organic contents during this process. However, the biodegradability of the waste-activated sludge is dependent on using aeration and biological treatment to remove the carbonaceous materials from sludge[52], which reduces the organic contents of the biosolids. It was for these reasons that in 2012, the US Environmental Protection[27] reported that the composition of biosolids represents an agglomeration of different substances because each wastewater treatment plant produces specific and unique biosolids of widely variable composition. Therefore, the characteristics of biosolids also differ widely[52]. So, knowing the individual component of biosolids represents an important stage in the HTL process, which usually needs to be optimised, depending on the biosolids' composition.

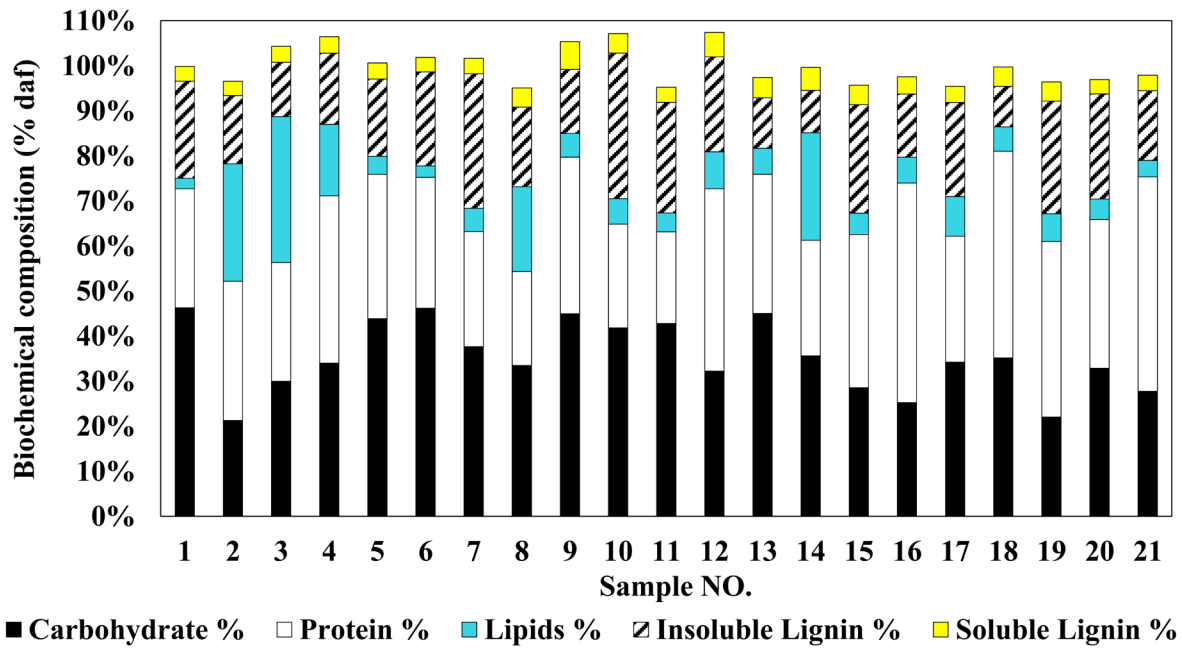

Figure 3: The Biochemical composition (% daf) of the biosolids includes carbohydrate, protein, lipid, insoluble and soluble lignin.

3.3 The ultimate analysis of the biosolids

The ultimate analysis of the major elements of biosolids includes carbon, hydrogen, nitrogen, oxygen and sulphur. The results for the twenty-one samples are shown in Figure 4. The carbon ranged between 26 and 59%, the hydrogen ranged between 5 and 12%, the nitrogen ranged between 3 and 7%, the sulphur ranged between 2 and 4%, and the oxygen ranged between 19 and 61%. Analysis of the data shows that the ultimate analysis of each sample is unique, and the amount of the individual components does not affect the rest of the components. These results were different from the Australian Bureau of Statistics[64], which reported that the dry basis biomass contains 30 - 60% carbon, 30 - 40% oxygen, and 5 - 6% hydrogen, depending on the ash content. However, neither of these elements has been reported sufficiently in the scientific literature. Therefore, the ultimate analysis of biosolids required more attention, especially for renewable energy production.

The differences in the results of the ultimate analyses of the biosolids could be dependent on several factors, such as retention times, wastewater treatment processes, the age and the chemical composition of the sludge[52, 53, 65]. For example, the initial treatment process and the biosolids' resources are the main causes of the changeable content of the carbon and nitrogen in biosolids. Królak *et al*.[66] reported the differences between the ultimate analyses of the rural and municipal plants were that the carbon and nitrogen content in the sludge of the rural plant were higher than in the municipal plant, and that was primarily due to the different technologies that were applied in sewage treatments. For example, the biological treatment in the rural wastewater plant led to the removal of the carbonaceous materials from sludge, reducing the sludge carbon content, while in the municipal plant there was enhanced nitrogen removal that led to reducing the nitrogen content[66]. Furthermore, the protein content also led to an increase

in the nitrogen levels in the biosolids[23]. Therefore, it is clear that the sources of biosolids and the initial treatment processes were the main reasons for the differences in carbon and nitrogen; thus, each sample requires careful and accurate measurement methods to determine the biosolids' content.

Analysis of the biosolids samples shows that they have different oxygen content. The differences in the oxygen content of the biosolids can be related to the treatment processes. For example, biosolids produced from the biological process receive anaerobic digestion, which occurs in the absence of oxygen to break down the biodegradable material[67], which leads to a decrease in the chemical oxygen and biochemical oxygen content[68]. The result is that the produced biosolids will have low oxygen content. Also, the degradation of the organic material can occur aerobically with the presence of oxygen, or anaerobically without oxygen[69]. For this reason, some wastewater plants use oxygen or air in the treatment[70]. Bacteria and fungi also generally enhance the ability to degrade organic pollutants by producing oxygenises and so assist in pollutant oxidation[68]. This leads to an increase in the oxygen content in the produced biosolids. Therefore, the oxygen content level can be low or high in biosolids samples, depending on the treatment process.

The importance of accurately measuring the nitrogen and oxygen contents in the biosolid samples is related to the contents' effects on renewable crude oil composition. High nitrogen and oxygen content results in low HHV values of the renewable crude oil extracted from biosolids compared with that in petroleum crudes[71, 72]. Also, biosolids with high oxygen compounds raise a serious concern because they can polymerise, and this causes storage instability[73]. Therefore, it is essential to determine the oxygenated compounds before the

renewable crude oil upgrading processes, especially because the hydrogen consumption and operation severity are mainly dependent on the concentration of oxygenated compounds present in the renewable crude oil[74]. Therefore, it is clear that understanding the elemental composition of biosolids could lead to a better understanding of the yields and quality of the renewable crude oil, and the distribution of the product[75].

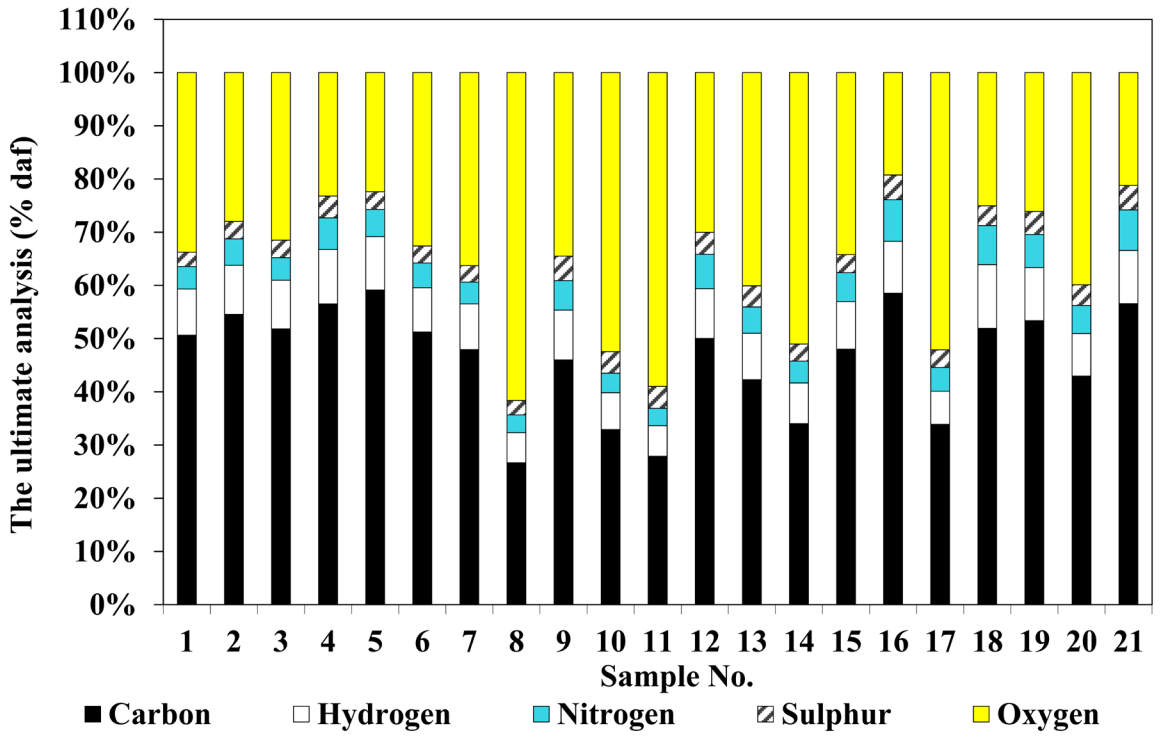

Figure 4: The ultimate analysis (% daf) of the biosolids includes carbon, hydrogen, nitrogen, sulphur and oxygen.

By applying the Van Krevelen diagram, as used by McKendry[76], the H/C and O/C ratio of a biosolid with another biomass can be compared, as shown in Figure 5. The comparison provides a clear vision that some biosolid samples have similar characteristic to that of biomass, while the majority of the biosolid samples differ characteristically from other types of biomass. The comparison between the biosolid samples and sewage sludge data obtained from the

scientific literature showed they vary in their composition. The difference in the characteristic of the organic content of biosolid samples could depend on several reasons, such as the sources of the sewage sludge and the treatment process[77-83]. Therefore, biosolids require more research to gain a better understanding in order for them to be used in the HTL process.

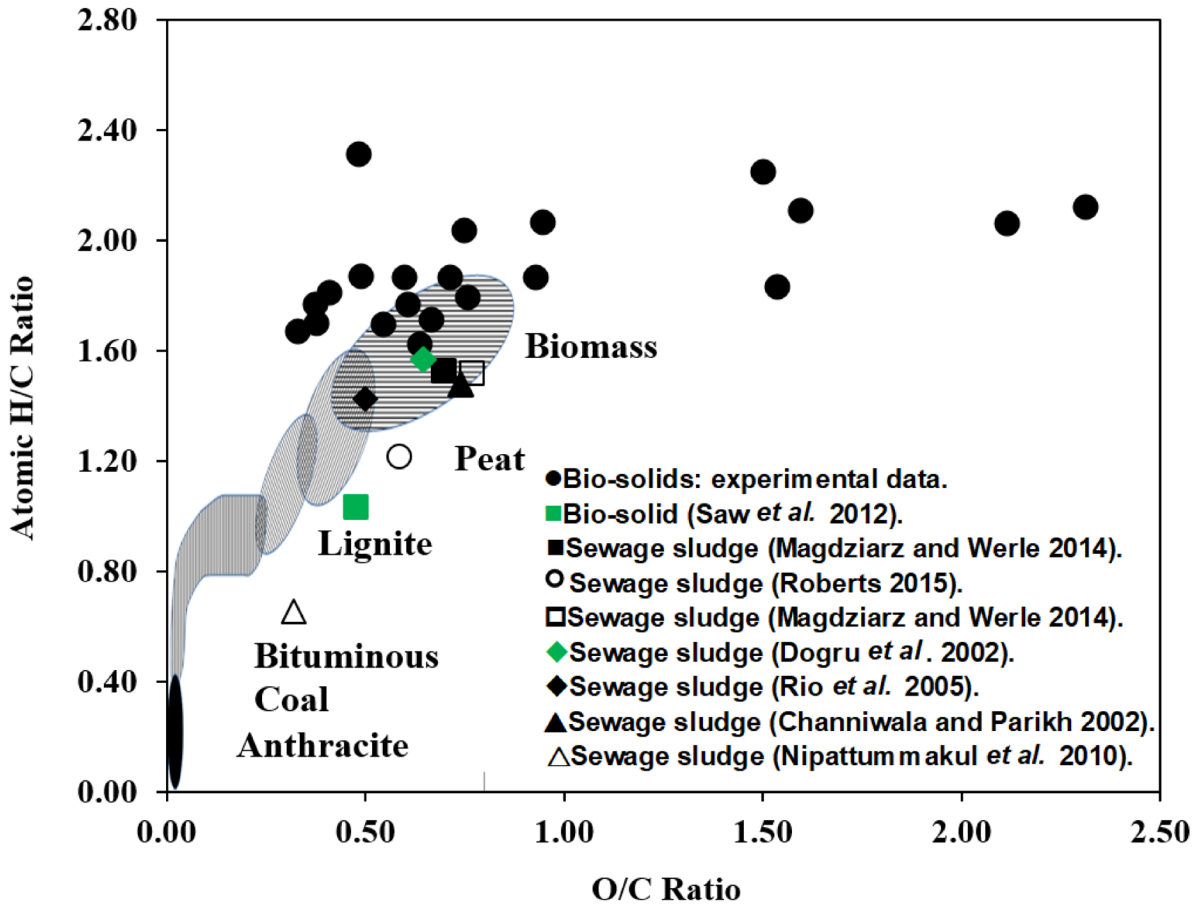

Figure 5: H/C and O/C ratio for biosolid (Van Krevelen diagram).

3.4 Renewable crude oil yields from biosolids

The results obtained from the analysis of the twenty-one different samples of biosolids varied widely in terms of the organic content. However, there were some samples that could be compared in terms of the amount of organic composition, such as the highest and lowest levels

of the individual components of the organic content. When used in the HTL process, these samples can provide a clear comparison of the obtained results in terms of the effects of the highest individual component and its interaction with the other components. In this research, the selected biosolids samples HC, LC, HP, LP, HL, LL, HLG and LLG, represent the samples that have the highest and lowest carbohydrates, proteins, lipids and lignins contents respectively, as shown in Figures 3. The inorganic and organic materials and the properties of the major elements of the selected biosolids samples, including carbon, hydrogen, nitrogen, oxygen and sulphur, are reported in Figures 4 and in Appendix B (Figure S1).

In order to discover the optimal composition of biosolids, the HTL of biosolids with different compositions was measured at 350ºC and 20 minutes to understand the effects of different biosolids' composition in the products, especially the renewable crude oil yield. The products from HTL include renewable crude oil, an aqueous stream, a solid residue and a gaseous product[84]. The yield of the HTL products obtained from the biosolids is represented in Figure 6. The renewable crude oil yields ranged between 8 to 12%, and it is clear that the amount of renewable crude oil increased with the increase in lipids and decreased with the increase in carbohydrates and lignins. The yields of the solids residues ranged between 9 and 17%, and the biosolids samples had mostly similar results due to their high content of carbohydrate and lignin. However, it was noticeable that low carbohydrate content led to a decrease in the yield of the solids' residues. The gas yields ranged between 51 and 16%. They increased with the increase in proteins and decreased with the increase in carbohydrates and lignins. The aqueous phase yields ranged between 23 and 58%, and was generally high, except with the protein sample from which most of the yield went to the gas yield.

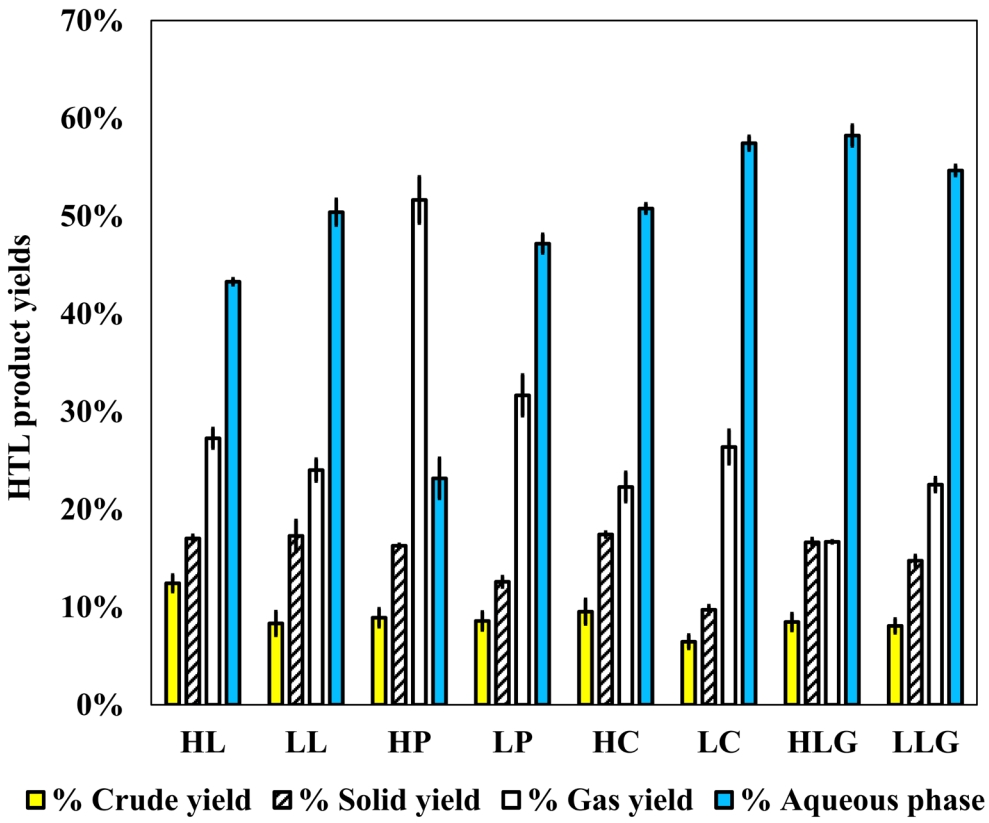

Figure 6: The HTL results in the biosolids at 350°C and 20 minutes.

The HTL reactions were performed at subcritical conditions. According to the scientific literature, biomass - including biosolids - dispersion into water starts at 100°C, followed by hydrolysis above 150°C, which leads to the disintegration of the cellulosic and hemicellulosic of the carbohydrate into monomeric chains[22]. The slurry then begins to react via the HTL process at 200°C[85]. At 250°C, the renewable crude oil from the protein is gained from the amino acids, which react via decarboxylation, producing hydrocarbons, amines, carbonic acid and aldehydes, or via a deamination reaction which leads to the production of organic acids and ammonia[22, 28]. According to Gollakota *et al.*[86], any further reaction of the amino acid leads to the production of various products, such as n-butyric acid, iso-butyric acid, propionic acid, acetic acid and carboxylic acid. In addition, the reactions between the carbohydrates and the

proteins have a significant effect on the HTL process because these reactions lead to the production of organic compounds that contain nitrogen[87]. For example, the polycyclic nitrogenous compounds formed in the HTL process are produced through Maillard reactions between carbohydrates and amino acids[88], which usually happen at 260°C[89]. Therefore, according to Peterson *et al*.[88], increasing the temperature above 260°C could decompose the Melanoidin-like polymers and turned them into pyrazines and pyrroles, causing an increase in the renewable crude oil yield. However, biosolid samples have different organic components, which react together through the HTL reaction and produce yields of various products, as explained below.

The renewable crude oil yield showed that it was influenced by the ratio of the initial composition of the biosolids[23]. As shown in Figure 6, the highest renewable crude oil yield gained from the HL sample was 12%. This result is similar to the results of other researchers. For example, He *et al*.[90] and Wang[57] reported that sludge - which has a high lipid content - yields the highest renewable crude oil in the HTL process. In general, lipids are a positive factor for the renewable crude oil yield but are not necessary for the quality of the renewable crude oil[91]. According to Biller and Ross[23], lipids produce around 80% of the renewable crude oil yields. However, the renewable crude oil yield in this research was mostly affected by other compounds, like carbohydrates and lignins. According to the scientific literature reported, most of the renewable crude oil yield from the HL sample could be obtained from lipid and fatty acids, which were the predominant reactants of the HTL[92]. In addition, the dielectric constant of water in the HTL process stabilises the triglyceride structures, which causes the formation of glycerol[28]. However, the glycerol conversion cannot increase the amount of renewable crude oil because of its conversion to a water-soluble compound[93]. Continuous glycerol degradation

produces acetaldehydes, propionaldehyde, formaldehyde, ethanol, and allyl alcohol[94], which could lead to increases in renewable crude oil depending on the conditions of the process[57].

The lowest renewable crude oil yield was 6.4% from the LC sample, which also contains high insoluble lignin content. According to Vardon[91] and Do Couto *et al*.[95], biomass rich in lignin and carbohydrates leads to the production of a low renewable crude oil yield. The reason is that lignin usually experiences limited decomposition due to its high degree of polymerisation[28]. There are several explanations for the decrease in renewable crude oil with an increase in carbohydrate and lignin. For example, the Bourdard gas reactions and the dominating secondary reaction (Maillard reaction will start at 240 ºC) are connected with the recombination of the free radicals into char[96]. Wang *et al*.[25] also reported that competition between the hydrolysis and repolymerisation reactions is the reason for the decrease in renewable crude oil when process temperatures are above 300°C. Added to that, according to Demirbaş[97], the low lignin content in biomass leads to high conversion of carbohydrates into soluble products, similar to the results that were gained in this research, as found in samples 5 and 20. Therefore, it can be concluded that the only small part of the lignin content in biosolid samples was converted to renewable crude oil; especially since most of the lignin in biosolids is an insoluble form which does not readily react to form renewable crude oil.

The highest solid residue yield was 17%, which was gained from the HC sample. According to Wang[57], the HTL of carbohydrates produced more than 40% of the solid residue. According to Yin and Tan[98], using temperatures above 300°C leads to a negative effect on the renewable crude oil yield because the hydroxymethylfurfural could be converted to a solid residue. A similar result was found for the HLG sample, which also produced a high solid residue of 16%.

The increase in the solid residue could also be connected to the further reaction of the intermediate oil and polymerisation reactions of intermediates to form the solid residue[99]. Another reason could be the dominant reactions and the secondary cracking, which lead to the formation of solid residues from heavy intermediates[100, 101]. For these reasons, the amount of solid residue produced was high in the HLG sample, while the lowest solid residue yield - derived from the LC sample - was 9%. However, the LC sample also contains a high protein content, under which conditions, according to Wang[57], the presence of the lipids and proteins alongside the carbohydrates leads to significantly decreased yields of solid residue. Therefore, it is clear that the carbohydrates and insoluble lignin have negative impacts on renewable crude oil yields and require more research. For example, more catalyst might reduce the negative effects on the renewable crude oil yield, while lipids and proteins have a positive impact on renewable crude oil.

The protein content generally is a positive factor for the renewable crude oil yield[57]. Biosolids rich in protein are desirable because they lead to a higher renewable crude oil yield[91]. However, the renewable crude oil yield from the HP sample was usually less than the HL sample due to its high gas yields. In this research, the highest gas yield from the biosolids samples was 51%, which was gained from the HP sample. The explanation is that using a high temperature like 350ºC leads to secondary and tertiary reactions, which increase the gases formation from heavy intermediates and lead to a reduction in the renewable crude oil yield[10, 101]. The lowest gas yield of 16% was gained from the HLG sample, which also contains a high carbohydrate content. Sample HLG also contained the highest aqueous yield, which means that the insoluble lignin and carbohydrate led to a decrease in the gas yield and an increase in the aqueous yield. For example, the highest aqueous phase yield of 58% was gained from the HLG sample, which

was similar to the high carbohydrate content sample. According to Ying *et al.*[102], the highest aqueous percentages were connected to saccharification and lead to the formation of water-soluble components. On the other hand, the lowest aqueous phase yield of 23% was gained from the HP sample. According to Wang[57], mixing proteins with lipids leads to a decrease in the aqueous yield. However, the protein content leads to an increase in gas yields. Therefore, the high protein and high lignin content in the HP sample caused a decreased aqueous yield and an increased gas yield.

According to the scientific literature, some biomass produced high renewable crude oil yield. For example, the HTL of organosolv lignin produced 79% of renewable crude at 374ºC, 220 bar and 10 minutes residence time[19]. However, Valdez *et al.*[103] gained 5 to 25 Wt% renewable crude oil yield from rich organic biomass like microalgae, which seems low yields. Therefore, other studies attempted to increase renewable crude oil yields by applying catalysts during the HTL of biomass. Shuping *et al.*[104], for example, applied 5% of Na_2CO_3 as a catalyst via the HTL of algae at 360ºC, and 50 minutes but the yields of the renewable crude oil was only 25%. In addition, the renewable crude oil yield from the HTL of the organic content of aspen wood and glycerol were 20 to 30% respectively, which gained by using 4% of potassium carbonate as a catalyst[105]. Song *et al.*[106] also examined the HTL of corn stalk by adding 1.0 wt% of Na_2CO_3, and determined that using catalyst increased the renewable crude oil yield from (33 to 47%); however, they did not provide any explanation about the effect of using catalyst on the HTL products. Other researchers also applied dichloromethane or acetone phase in the HTL separation process, which could lead to an increase in the yields of the renewable crude oil[19, 20].

In this work, the age of biosolids samples was around 13 years old. The organic content in the biosolids samples was low, which were related to several reasons, such as the original sources of biosolids[4, 24], the dissolved organic matter in biosolids, which depends on both the quality and the quantity of the wastewater resource and the levels and the types of the wastewater treatment[50, 51]. For these reasons, biosolids contain a high content of inorganic content, which is around 60%. The organic content of biosolids contains a high percentage of insoluble lignin and carbohydrates, which leads to reduce the renewable crude oil yields. Therefore, the produced renewable crude oil from biosolids could be low in comparison to other biomass, such as microalgae. In addition, the insoluble lignin and carbohydrates content in biosolids is mostly high and will not break down in the selected key parameters that were used in this research. The presence of lignin in biomass is a less desirable component for HTL and is related to lower renewable crude oil yield[91]. The high carbohydrate and lignin content of sludge and biosolids leads to low renewable crude oil yields[91]. However, producing renewable crude oil from biosolids could be a great solution to address the decline in the fossil fuel reserves and climate change. Therefore, these results provide a better understanding of biosolids during the HTL.

3.4.1 Renewable crude oil characteristics

The Source Rock Analysis (SRA) was applied to evaluate the residual crude oil in the biosolids. The results in Figure 7 represent the proportions for the renewable crude oil, at the low-boiling point (LBP>80ºC), and the high-boiling point (80ºC<HBP<600ºC) based on SRA measurements. Where boiling point represents the amount of energy required to separate a liquid molecule from its gaseous molecule. In general, the low-boiling point materials have shorter hydrocarbon molecules, which have weaker intermolecular forces. Therefore, they are

highly volatile and highly flammable. While, the high-boiling point materials have large molecules because they have very strong chemical bonds between atoms, and high energy is needed to break them apart.

The low-boiling point materials' highest yield of renewable crude oil was around 4%, at its LBP. This was gained from the HL sample and is similar to the results reported by Biller *et al.*[107]. The low-boiling point materials' lowest yield in the renewable crude oil was 1% at its LBP. This was gained from the LC sample. However, this sample also contained a high amount of insoluble lignin content. On the other hand, the high-boiling point materials' highest yield of renewable crude oil at its HBP was around 8%. This was gained from the HL sample. The high-boiling materials' lowest yield of renewable crude oil at HPB was around 5%. This was gained from the LC sample. In general, the low-boiling point material in the renewable crude oil yield from biosolids at the LBP was less than the high-boiling point material. Also, as shown in Figure 6 and Figure 7, the biosolids' composition affected not only the renewable crude oil yield but also led to differing boiling materials in the renewable crude oil. Therefore, biosolids at these conditions require more research to find ways in which to increase the low boiling materials at the LBP and simultaneously reduce the high boiling materials.

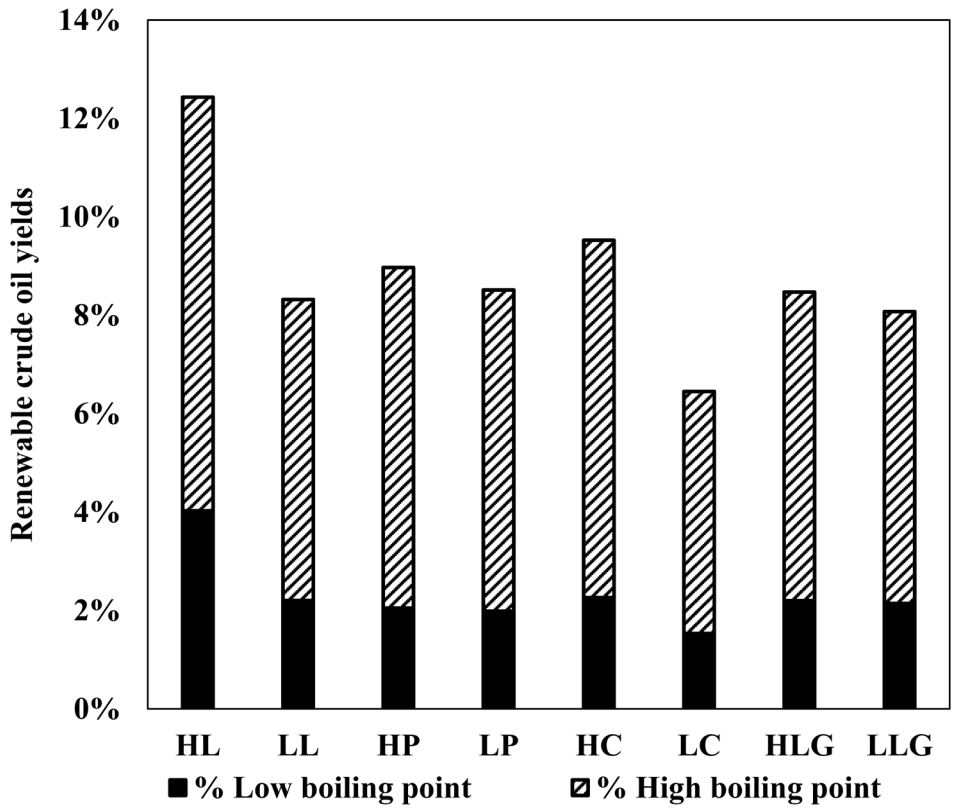

Figure 7: The renewable crude oil yields from biosolids at low and high boiling points.

4. Conclusion

Biosolids represent a sustainable feedstock source for renewable crude oil production through the HTL process. However, biosolids have different characters that affect the yield and quality of renewable crude oil. Biosolids, for example, have different organic content, which is associated with the biosolids' age. The chemical composition of the biosolids was also changed due to the various sources and the initial treatments. Therefore, applying a Van Krevelen diagram to compare biosolids with other biomass indicated that only some biosolids samples have similar characteristic to that of biomass, while the majority of the biosolid samples differ characteristically from other types of biomass. The difference in the characteristic of the organic content of biosolid samples could depend on several reasons, such as the sources of the

sewage sludge and the treatment process. The effects of the biosolids' composition on the HTL yield show that lipids and proteins have positive impacts on the renewable crude oil yield, while carbohydrates and insoluble lignin had negative effects on the renewable crude oil yield, which led to an increase in the solid residue. The quality of the renewable crude oil also shows it is affected by the composition of the biosolids. The renewable crude oil contained a high amount of high-boiling point materials in comparison with low-boiling point materials for all biosolids samples used in this study.

5. Author information

Corresponding Author:

Dr Philip van Eyk.

School of Chemical Engineering and Advanced Materials

Faculty of Engineering, Mathematical and Computer Sciences

University of Adelaide

Adelaide, South Australia 5005

+61 8 8313 6081

philip.vaneyk@adelaide.edu.au

The manuscript was written through the contributions of all authors. All authors have given approval to the final version of the manuscript.

6. Acknowledgements

The authors would like to acknowledge Dr Rosmala Lewis and Melbourne Water, Werribee, Victoria, Australia for providing the feedstocks.

Funding: This work was supported by the Australian Research Council and Southern Oil Refining Pty Ltd [Grant numbers LP150101241].

7. Abbreviations

HTL, hydrothermal liquefaction; AFDW, ash-free dry weight; SRA, source rock analyser; OM, organic matter; HC, high carbohydrate; LC, low carbohydrate; HP, high protein; LP, low protein; HL, high lipid; LL, low lipid; HLG, high lignin; LLG, low lignin; LBP, low-boiling point; HBP, high-boiling point.

8. References

1. Consumption, R. E., Electricity: Preliminary Statistics 2009. *Energy Information Administration* **2010,** *14*.

2. Ullah, K.; Ahmad, M.; Sofia; Sharma, V. K.; Lu, P.; Harvey, A.; Zafar, M.; Sultana, S.; Anyanwu, C. N., Algal biomass as a global source of transport fuels: Overview and development perspectives. *Progress in Natural Science: Materials International* **2014,** *24* (4), 329-339.

3. Tully, A., BP's latest estimate says world's oil will last 53.3 years. Diperoleh: 2015.

4. Dimitriadis, A.; Bezergianni, S., Hydrothermal liquefaction of various biomass and waste feedstocks for biocrude production: A state of the art review. *Renewable and Sustainable Energy Reviews* **2017,** *68*, 113-125.

5. Karak, T.; Bhagat, R.; Bhattacharyya, P., Municipal solid waste generation, composition, and management: the world scenario. *Critical Reviews in Environmental Science and Technology* **2012,** *42* (15), 1509-1630.

6. Lee, D.; Spinosa, L.; He, P.; Chen, T., Sludge production and management processes: case study in China. *Water science and technology* **2006,** *54* (5), 189-196.

7. Meeroff, D. E., Effects of ionizing radiation in wastewater treatment and residuals processing. **2001**.

8. Elliott, D., Thermochemical processing of biomass. Chichester, UK: John Wiley & Sons Ltd: 2011.

9. Jones, C. W.; Agrawal, P. K., Hydrogen production from biomass. Google Patents: 2011.

10. Akhtar, J.; Amin, N. A. S., A review on process conditions for optimum bio-oil yield in hydrothermal liquefaction of biomass. *Renewable and Sustainable Energy Reviews* **2011,** *15* (3), 1615-1624.

11. Cantrell, K.; Ro, K.; Mahajan, D.; Anjom, M.; Hunt, P. G., Role of thermochemical conversion in livestock waste-to-energy treatments: obstacles and opportunities. *Industrial & engineering chemistry research* **2007,** *46* (26), 8918-8927.

12. Babeker, T. M. A.; Chen, Q., Heavy Metal Removal from Wastewater by Adsorption with Hydrochar Derived from Biomass: Current Applications and Research Trends. *Current Pollution Reports* **2021**, 1-18.

13. Albrecht, K. O.; Zhu, Y.; Schmidt, A. J.; Billing, J. M.; Hart, T. R.; Jones, S. B.; Maupin, G.; Hallen, R.; Ahrens, T.; Anderson, D., Impact of heterotrophically stressed algae for biofuel production via hydrothermal liquefaction and catalytic hydrotreating in continuous-flow reactors. *Algal research* **2016,** *14*, 17-27.

14. Mørup, A. J.; Becker, J.; Christensen, P. S.; Houlberg, K.; Lappa, E.; Klemmer, M.; Madsen, R. B.; Glasius, M.; Iversen, B. B., Construction and commissioning of a continuous

reactor for hydrothermal liquefaction. *Industrial & Engineering Chemistry Research* **2015,** *54* (22), 5935-5947.

15. Devi Venkatachalam, C.; Raam Ravichandran, S.; Sengottian, M., Lignocellulosic and algal biomass for bio-crude production using hydrothermal liquefaction: Conversion techniques, mechanism and process conditions: A reivew. *Environmental Engineering Research* **2021**.

16. Kandasamy, S.; Zhang, B.; He, Z.; Chen, H.; Feng, H.; Wang, Q.; Wang, B.; Ashokkumar, V.; Siva, S.; Bhuvanendran, N., Effect of low-temperature catalytic hydrothermal liquefaction of Spirulina platensis. *Energy* **2020,** *190*, 116236.

17. Frank, E. D.; Elgowainy, A.; Han, J.; Wang, Z., Life cycle comparison of hydrothermal liquefaction and lipid extraction pathways to renewable diesel from algae. *Mitigation and Adaptation Strategies for Global Change* **2013,** *18* (1), 137-158.

18. López Barreiro, D.; Prins, W.; Ronsse, F.; Brilman, W., Hydrothermal liquefaction (HTL) of microalgae for biofuel production: State of the art review and future prospects. *Biomass and Bioenergy* **2013,** *53*, 113-127.

19. Zhang, B.; Huang, H.-J.; Ramaswamy, S., Reaction kinetics of the hydrothermal treatment of lignin. In *Biotechnology for Fuels and Chemicals*, Springer: 2007; pp 487-499.

20. Teri, G.; Luo, L.; Savage, P. E., Hydrothermal treatment of protein, polysaccharide, and lipids alone and in mixtures. *Energy & fuels* **2014,** *28* (12), 7501-7509.

21. Garcia Alba, L.; Torri, C.; Samorì, C.; Van Der Spek, J.; Fabbri, D.; Kersten, S. R. A.; Brilman, D. W. F., Hydrothermal treatment (HTT) of microalgae: Evaluation of the process as conversion method in an algae biorefinery concept. *Energy and Fuels* **2012,** *26* (1), 642-657.

22. Toor, S. S.; Rosendahl, L.; Rudolf, A., Hydrothermal liquefaction of biomass: A review of subcritical water technologies. *Energy* **2011,** *36* (5), 2328-2342.

23. Biller, P.; Ross, A., Potential yields and properties of oil from the hydrothermal liquefaction of microalgae with different biochemical content. *Bioresource technology* **2011,** *102* (1), 215-225.

24. Nagwekar, P. R., Removal of Organic Matter from Wastewater by Activated Sludge Process-Review. *International Journal of Science, Engineering and Technology Research (IJSETR)* **2014,** *3* (5), 1260-1263.

25. Wang, L. K.; Shammas, N. K.; Hung, Y.-T., *Biosolids treatment processes*. Springer: 2007; Vol. 6.

26. Parmar, N.; Singh, A.; Ward, O., Enzyme treatment to reduce solids and improve settling of sewage sludge. *Journal of Industrial Microbiology and Biotechnology* **2001,** *26* (6), 383-386.

27. US Environmental Protection, A. Biosolids: Frequently Asked Questions. <http://water.epa.gov/polwaste/wastewater/treatment/biosolids/genqa.cfm> (accessed 1 May).

28. Peterson, A. A.; Vogel, F.; Lachance, R. P.; Fröling, M.; Antal Jr, M. J.; Tester, J. W., Thermochemical biofuel production in hydrothermal media: A review of sub- and supercritical water technologies. *Energy and Environmental Science* **2008,** *1* (1), 32-65.

29. Suzuki, A.; Nakamura, T.; Yokoyama, S.; Ogi, T.; Koguchi, K., Conversion of sewage sludge to heavy oil by direct thermochemical liquefaction. *Journal of Chemical Engineering of Japan* **1988,** *21* (3).

30. Dubois, M.; Gilles, K. A.; Hamilton, J. K.; Rebers, P. t.; Smith, F., Colorimetric method for determination of sugars and related substances. *Analytical chemistry* **1956,** *28* (3), 350-356.

31. Liu, D.; Wong, P.; Dutka, B., Determination of carbohydrate in lake sediment by a modified phenol-sulfuric acid method. *Water research* **1973,** *7* (5), 741-746.

32. Masuko, T.; Minami, A.; Iwasaki, N.; Majima, T.; Nishimura, S.-I.; Lee, Y. C., Carbohydrate analysis by a phenol–sulfuric acid method in microplate format. *Analytical biochemistry* **2005,** *339* (1), 69-72.

33. Safařík, I.; Šantrůčková, H., Direct determination of total soil carbohydrate content. *Plant and Soil* **1992,** *143* (1), 109-114.

34. Ashwell, G., Colorimetric analysis of sugars. *Methods En-zymol.* **1957,** *3*, 73-105.

35. Shetlar, M.; Masters, Y. F., Use of thymol-sulfuric acid reaction for determination of carbohydrates in biological material. *Analytical Chemistry* **1957,** *29* (3), 402-405.

36. Lourenço, S. O.; Barbarino, E.; De-Paula, J. C.; Pereira, L. O. d. S.; Marquez, U. M. L., Amino acid composition, protein content and calculation of nitrogen-to-protein conversion factors for 19 tropical seaweeds. *Phycological Research* **2002,** *50* (3), 233-241.

37. Dolson, D. A.; Battino, R.; Letcher, T. M.; Pegel, K.; Revaprasadu, N., Carbohydrate dehydration demonstrations. *Journal of chemical education* **1995,** *72* (10), 927.

38. Buysse, J.; Merckx, R., An improved colorimetric method to quantify sugar content of plant tissue. *Journal of Experimental Botany* **1993,** *44* (10), 1627-1629.

39. Chow, P. S.; Landhäusser, S. M., A method for routine measurements of total sugar and starch content in woody plant tissues. *Tree physiology* **2004,** *24* (10), 1129-1136.

40. Rose, R.; Rose, C. L.; Omi, S. K.; Forry, K. R.; Durall, D. M.; Bigg, W. L., Starch determination by perchloric acid vs enzymes: evaluating the accuracy and precision of six colorimetric methods. *Journal of Agricultural and Food Chemistry* **1991,** *39* (1), 2-11.

41. Ameel, J.; Ruzycki, E.; Axler, R., Analytical chemistry and quality assurance procedures for natural water samples. Central Analytical Laboratory. *Natural Resources Research Institute Technical Report NRRI/TR–98/03 revised annually* **1998**.

42. Folch, J.; Lees, M.; Sloane Stanley, G., A simple method for the isolation and purification of total lipids from animal tissues. *J biol Chem* **1957,** *226* (1), 497-509.

43. Zhu, C.; Lee, Y., Determination of biomass dry weight of marine microalgae. *Journal of applied phycology* **1997,** *9* (2), 189-194.

44. Fujihara, S.; Kasuga, A.; Aoyagi, Y., Nitrogen-to-protein conversion factors for common vegetables in Japan. *Journal of food science* **2001,** *66* (3), 412-415.

45. Maclean, W.; Harnly, J.; Chen, J.; Chevassus-Agnes, S.; Gilani, G.; Livesey, G.; Warwick, P. In *Food energy–Methods of analysis and conversion factors*, Food and agriculture organization of the united nations technical workshop report, 2003; pp 8-9.

46. Mariotti, F.; Tomé, D.; Mirand, P. P., Converting nitrogen into protein—beyond 6.25 and Jones' factors. *Critical reviews in food science and nutrition* **2008,** *48* (2), 177-184.

47. Hatfield, R. D.; Jung, H. J. G.; Ralph, J.; Buxton, D. R.; Weimer, P. J., A comparison of the insoluble residues produced by the Klason lignin and acid detergent lignin procedures. *Journal of the Science of Food and Agriculture* **1994,** *65* (1), 51-58.

48. Obeid, R.; Lewis, D. M.; Smith, N.; Hall, T.; van Eyk, P., Reaction Kinetics and Characterization of Species in Renewable Crude from Hydrothermal Liquefaction of Mixtures of Polymer Compounds To Represent Organic Fractions of Biomass Feedstocks. *Energy & Fuels* **2019,** *34* (1), 419-429.

49. Zhang, L.; Champagne, P.; Xu, C. C., Bio-crude production from secondary pulp/paper-mill sludge and waste newspaper via co-liquefaction in hot-compressed water. *Energy* **2011,** *36* (4), 2142-2150.

50. Daims, H.; Taylor, M. W.; Wagner, M., Wastewater treatment: a model system for microbial ecology. *Trends in biotechnology* **2006,** *24* (11), 483-489.

51. Sonune, A.; Ghate, R., Developments in wastewater treatment methods. *Desalination* **2004,** *167*, 55-63.

52. Spinosa, L.; Vesilind, P. A., *Sludge into biosolids*. IWA publishing: 2001.

53. Hecht, N. L.; Duvall, D., *Characterization and utilization of municipal and utility sludges and ashes*. National Environmental Research Center, Office of Research and Development, US Environmental Protection Agency: 1975; Vol. 1.

54. Kim, D.-Y.; Nishiyama, Y.; Wada, M.; Kuga, S., High-yield carbonization of cellulose by sulfuric acid impregnation. *Cellulose* **2001,** *8* (1), 29-33.

55. Nagasawa, K.; Tohira, Y.; Inoue, Y.; Tanoura, N., Reaction between carbohydrates and sulfuric acid: Part I. Depolymerization and sulfation of polysaccharides by sulfuric acid. *Carbohydrate Research* **1971,** *18* (1), 95-102.

56. Mol, J., Catalytic metathesis of unsaturated fatty acid esters and oils. *Topics in Catalysis* **2004,** *27* (1-4), 97-104.

57. Wang, Z., Reaction mechanisms of hydrothermal liquefaction of model compounds and biowaste feedstocks. Zhang, Y., Ed. ProQuest Dissertations Publishing: 2011.

58. Gollakota, A. R.; Reddy, M.; Subramanyam, M. D.; Kishore, N., A review on the upgradation techniques of pyrolysis oil. *Renewable and Sustainable Energy Reviews* **2016,** *58*, 1543-1568.

59. Saisu, M.; Sato, T.; Watanabe, M.; Adschiri, T.; Arai, K., Conversion of lignin with supercritical water− phenol mixtures. *Energy & Fuels* **2003,** *17* (4), 922-928.

60. Savage, P.; Levine, R.; Huelsman, C., Hydrothermal processing of biomass. *Thermochemical conversion of biomass to liquid fuels and chemicals* **2010**, 192-221.

61. Henze, M.; Harremoes, P.; la Cour Jansen, J.; Arvin, E., *Wastewater treatment: biological and chemical processes*. Springer Science & Business Media: 2001.

62. Appels, L.; Baeyens, J.; Degrève, J.; Dewil, R., Principles and potential of the anaerobic digestion of waste-activated sludge. *Progress in energy and combustion science* **2008,** *34* (6), 755-781.

63. Fernandes, F.; Von Sperling, M.; Vitorio Andreoli, C.; Ronteltap, M., *Sludge treatment and disposal*. IWA publishing: 2007.

64. Statistics, A. B. o. Waste Management Services. <http://www.abs.gov.au/ausstats/abs@.nsf/lookup/8698.0Glossary12009-10>. (accessed 2 May).

65. Seehar, T. H.; Toor, S. S.; Sharma, K.; Nielsen, A. H.; Pedersen, T. H.; Rosendahl, L. A., Influence of Process Conditions on Hydrothermal Liquefaction of Eucalyptus Biomass for Biocrude Production and Investigation of the Inorganics Distribution. *Sustainable Energy & Fuels* **2021**.

66. Królak, E.; Filipek, K.; Biardzka, E., Comparative analysis of sewage sludge from two sewage treatment plants: in Mrozy and Siedlce (Mazowieckie Province)/Porównawcza analiza osadów ściekowych z dwóch oczyszczalni ścieków w Mrozach i Siedlcach (województwo mazowieckie). *Ochrona Środowiska i Zasobów Naturalnych-Environmental Protection and Natural Resources* **2013,** *24* (2), 57-61.

67. Kalogo, Y.; Monteith, H., *Energy and resource recovery from sludge*. IWA Publishing: 2012.

68. Zheng, C.; Zhao, L.; Zhou, X.; Fu, Z.; Li, A., Treatment technologies for organic wastewater. In *Water Treatment*, Intech: 2013.

69. Scott, J. P.; Ollis, D. F., Integration of chemical and biological oxidation processes for water treatment: review and recommendations. *Environmental Progress* **1995,** *14* (2), 88-103.

70. Ogilvie, D., *National study of the composition of sewage sludge*. Drainage Managers Group, a subgroup of the New Zealand Water and Wastes Association: 1998.

71. Speight, J. G., *Handbook of petroleum product analysis*. John Wiley & Sons: 2015; Vol. 182.

72. Vardon, D. R.; Sharma, B.; Scott, J.; Yu, G.; Wang, Z.; Schideman, L.; Zhang, Y.; Strathmann, T. J., Chemical properties of biocrude oil from the hydrothermal liquefaction of Spirulina algae, swine manure, and digested anaerobic sludge. *Bioresource technology* **2011,** *102* (17), 8295-8303.

73. Adjaye, J. D.; Sharma, R. K.; Bakhshi, N. N., Characterization and stability analysis of wood-derived bio-oil. *Fuel Processing Technology* **1992,** *31* (3), 241-256.

74. Furimsky, E.; Massoth, F. E., Deactivation of hydroprocessing catalysts. *Catalysis Today* **1999,** *52* (4), 381-495.

75. Zhang, L.; Xu, C. C.; Champagne, P., Overview of recent advances in thermo-chemical conversion of biomass. *Energy Conversion and Management* **2010,** *51* (5), 969-982.

76. McKendry, P., Energy production from biomass (part 2): conversion technologies. *Bioresource technology* **2002,** *83* (1), 47-54.

77. Channiwala, S. A.; Parikh, P. P., A unified correlation for estimating HHV of solid, liquid and gaseous fuels. *Fuel* **2002,** *81* (8), 1051-1063.

78. Dogru, M.; Midilli, A.; Howarth, C. R., Gasification of sewage sludge using a throated downdraft gasifier and uncertainty analysis. *Fuel Processing Technology* **2002,** *75* (1), 55-82.

79. Magdziarz, A.; Werle, S., Analysis of the combustion and pyrolysis of dried sewage sludge by TGA and MS. *Waste management* **2014,** *34* (1), 174-179.

80. Nipattummakul, N.; Ahmed, I. I.; Kerdsuwan, S.; Gupta, A. K., Hydrogen and syngas production from sewage sludge via steam gasification. *International Journal of Hydrogen Energy* **2010,** *35* (21), 11738-11745.

81. Rio, S.; Faur-Brasquet, C.; Coq, L. L.; Courcoux, P.; Cloirec, P. L., Experimental design methodology for the preparation of carbonaceous sorbents from sewage sludge by chemical activation—application to air and water treatments. *Chemosphere* **2005,** *58* (4), 423-437.

82. Roberts, D., Characterisation of chemical composition and energy content of green waste and municipal solid waste from Greater Brisbane, Australia. *Waste management* **2015,** *41*, 12-19.

83. Saw, W.; McKinnon, H.; Gilmour, I.; Pang, S., Production of hydrogen-rich syngas from steam gasification of blend of biosolids and wood using a dual fluidised bed gasifier. *Fuel* **2012,** *93*, 473-478.

84. Elliott, D. C.; Biller, P.; Ross, A. B.; Schmidt, A. J.; Jones, S. B., Hydrothermal liquefaction of biomass: Developments from batch to continuous process. *Bioresource Technology* **2015,** *178*, 147-156.

85. Yokoyama, S.; Matsumura, Y., The Asian biomass handbook: a guide for biomass production and utilization. *Thermochemical conversion of biomass, 1st (Ed) part* **2008,** *4*, 71.

86. Gollakota, A.; Kishore, N.; Gu, S., A review on hydrothermal liquefaction of biomass. *Renewable and Sustainable Energy Reviews* **2018,** *81*, 1378-1392.

87. Kruse, A.; Maniam, P.; Spieler, F., Influence of proteins on the hydrothermal gasification and liquefaction of biomass. 2. Model compounds. *Industrial & Engineering Chemistry Research* **2007,** *46* (1), 87-96.

88. Peterson, A. A.; Lachance, R. P.; Tester, J. W., Kinetic evidence of the Maillard reaction in hydrothermal biomass processing: glucose− glycine interactions in high-temperature, high-pressure water. *Industrial & Engineering Chemistry Research* **2010,** *49* (5), 2107-2117.

89. Deniel, M.; Haarlemmer, G.; Roubaud, A.; Weiss-Hortala, E.; Fages, J., Energy valorisation of food processing residues and model compounds by hydrothermal liquefaction. *Renewable and Sustainable Energy Reviews* **2016,** *54*, 1632-1652.

90. He, W.; Li, G.; Kong, L.; Wang, H.; Huang, J.; Xu, J., Application of hydrothermal reaction in resource recovery of organic wastes. *Resources, Conservation and Recycling* **2008,** *52* (5), 691-699.

91. Vardon, D., Hydrothermal liquefaction for energy recovery from high-moisture waste biomass. **2012**.

92. He, P.; Gu, G.; Shao, L.; Zhang, Y., Research on low temperature thermo-chemical conversion to oil process for sewage sludge. In *Water Science and Technology*, 2000; Vol. 42, pp 301-308.

93. Lehr, V.; Sarlea, M.; Ott, L.; Vogel, H., Catalytic dehydration of biomass-derived polyols in sub-and supercritical water. *Catalysis Today* **2007,** *121* (1-2), 121-129.

94. Bühler, W.; Dinjus, E.; Ederer, H.; Kruse, A.; Mas, C., Ionic reactions and pyrolysis of glycerol as competing reaction pathways in near-and supercritical water. *The Journal of supercritical fluids* **2002,** *22* (1), 37-53.

95. do Couto Fraga, A.; de Almeida, M. B. B.; Sousa-Aguiar, E. F., Hydrothermal liquefaction of cellulose and lignin: a new approach on the investigation of chemical reaction networks. *Cellulose* **2021**, 1-18.

96. Gupta, V. G.; Tuohy, M.; Kubicek, C. P.; Saddler, J.; Xu, F., *Bioenergy research: advances and applications*. Newnes: 2013.

97. Demirbaş, A., Effect of lignin content on aqueous liquefaction products of biomass. *Energy Conversion and Management* **2000,** *41* (15), 1601-1607.

98. Yin, S.; Tan, Z., Hydrothermal liquefaction of cellulose to bio-oil under acidic, neutral and alkaline conditions. *Applied Energy* **2012,** *92*, 234-239.

99. Özçimen, D.; Karaosmanoğlu, F., Production and characterization of bio-oil and biochar from rapeseed cake. *Renewable energy* **2004,** *29* (5), 779-787.

100. Sasaki, M.; Adschiri, T.; Arai, K., Fractionation of sugarcane bagasse by hydrothermal treatment. *Bioresource Technology* **2003,** *86* (3), 301-304.

101. Sugano, M.; Takagi, H.; Hirano, K.; Mashimo, K., Hydrothermal liquefaction of plantation biomass with two kinds of wastewater from paper industry. *Journal of Materials Science* **2008,** *43* (7), 2476-2486.

102. Ying, G.; CHEN, H.-p.; Jun, W.; Tao, S.; Hai-Ping, Y.; Xian-Hua, W., Characterization of products from hydrothermal liquefaction and carbonation of biomass model compounds and real biomass. *Journal of Fuel Chemistry and Technology* **2011,** *39* (12), 893-900.

103. Valdez, P. J.; Tocco, V. J.; Savage, P. E., A general kinetic model for the hydrothermal liquefaction of microalgae. *Bioresource Technology* **2014,** *163*, 123-127.

104. Shuping, Z.; Yulong, W.; Mingde, Y.; Kaleem, I.; Chun, L.; Tong, J., Production and characterization of bio-oil from hydrothermal liquefaction of microalgae Dunaliella tertiolecta cake. *Energy* **2010,** *35* (12), 5406-5411.

105. Abu El-Rub, Z.; Bramer, E. A.; Brem, G., Review of catalysts for tar elimination in biomass gasification processes. *Industrial & engineering chemistry research* **2004,** *43* (22), 6911-6919.

106. Song, C.; Hu, H.; Zhu, S.; Wang, G.; Chen, G., Nonisothermal catalytic liquefaction of corn stalk in subcritical and supercritical water. *Energy & fuels* **2004,** *18* (1), 90-96.

107. Biller, P.; Riley, R.; Ross, A., Catalytic hydrothermal processing of microalgae: decomposition and upgrading of lipids. *Bioresource technology* **2011,** *102* (7), 4841-4848.

CHAPTER 5

ELUCIDATION OF THE EFFECT OF REACTION CONDITIONS AND BIOSOLIDS' COMPOSITION ON CONVERSION TO RENEWABLE CRUDE OIL VIA HYDROTHERMAL LIQUEFACTION

Jasim M. Al-juboori [a], Reem Obeid [a], David M. Lewis [a], Tony Hall[b] and Philip J. van Eyk.a [a,*]

[a] School of Chemical Engineering & Advanced Materials, University of Adelaide, Adelaide, SA 5005

[b] School of Physical Sciences, University of Adelaide, Adelaide, SA 5005

** Corresponding Author: philip.vaneyk@adelaide.edu.au*

Statement of Authorship

Title of Paper	Elucidation of the effect of reaction conditions and biosolids' composition on conversion to renewable crude oil via hydrothermal liquefaction
Publication Status	☐ Published ☐ Accepted for Publication ☐ Submitted for Publication ☑ Unpublished and Unsubmitted work written in manuscript style
Publication Details	

Principal Author

Name of Principal Author (Candidate)	Jasim Al-juboori
Contribution to the Paper	HTL reactor design and methods HTL batch experiments completed Methods developed for analysing the composition of biosolids HTL products separation and yields quantification completed Thermogravimetric analysis to determine crude oil faction completed Writing and editing
Overall percentage (%)	80%
Certification:	This paper reports on original research I conducted during the period of my Higher Degree by Research candidature and is not subject to any obligations or contractual agreements with a third party that would constrain its inclusion in this thesis. I am the primary author of this paper.
Signature	Date 19/08/2021

Co-Author Contributions

By signing the Statement of Authorship, each author certifies that:

i. the candidate's stated contribution to the publication is accurate (as detailed above);

ii. permission is granted for the candidate in include the publication in the thesis; and

iii. the sum of all co-author contributions is equal to 100% less the candidate's stated contribution.

Name of Co-Author	Reem Obeid
Contribution to the Paper	Construction of model Drafting of paper
Signature	Date 19/08/2021

Name of Co-Author	David Lewis
Contribution to the Paper	Concept development Assistance with analysis and interpretation of data Drafting of paper
Signature	Date 19/08/2021

Name of Co-Author	Tony Hall		
Contribution to the Paper	Method design and analysis using Source Rock Analyser		
Signature		Date	19/08/2021

Name of Co-Author	Philip van Eyk		
Contribution to the Paper	HTL reactor design and methods Concept development Assistance with analysis and interpretation of data Drafting of paper		
Signature		Date	19/08/2021

Abstract

Hydrothermal liquefaction (HTL) represents a practical technology that converts biosolids into renewable crude oil. However, more research is required to understand the produced renewable crude oil via the HTL of biosolids. HTL of biosolids in a small-scale batch reactor identified that the HTL reaction conditions and biosolids content affect renewable crude oil yield, ranging from 21 to 26%, where the highest yield was obtained at 250^{o}C and 20 mins. The renewable crude oil fractions were also affected by the HTL reaction conditions and biosolids content. Based on the boiling point, biosolid with a high-lipid content produced the maximum potential gasoline and naphtha-like yield, while high-carbohydrate biosolid content generated the highest potential kerosene-like yield. The potential gas oil-like, wax, lubricating oil-like fractions were significantly high for all the biosolid samples. A developed bulk kinetic model to predict the product fractions showed the trends in product fractions with various reaction times and temperatures.

Keywords: Hydrothermal liquefaction; Biosolids contents; HTL reaction parameters, Renewable crude quality; Product distribution.

1. Introduction

The recent decline in easily-accessible petroleum reserves has increased the need and desire for alternative sources of energy[1]. This desire is also driven by global population growth, which has caused many environmental concerns, such as sludge and biosolids waste disposal[2]. Waste disposal from the water industry, such as biosolids stockpile is growing globally, and they are costly to manage and regulate. The combination of environmental degradation caused by waste from the water industry and the negative environmental effect of using fossil fuels on global warming and climate change has imposed the requirement for alternative renewable energy[3]. These concerns have led to the expansion of research on alternative renewable energy sources worldwide.

Biosolids are sustainable due to their large, ongoing, annual production. For example, Australia produces about 330,000 dry tonnes of biosolids annually[4]. Also, the USA alone produces about 7,100,000 dry tonnes of biosolids annually from around 16,500 wastewater treatment plants[5]. 90% of the global utilisation of biosolids is for agricultural purposes[6]. However, the overuse of biosolids for agricultural purposes creates many challenges, such as over-fertilisation, which leads to pollution of the land's surface and groundwater[7]. Therefore, biosolids require environmentally friendly management and regulation.

The high annual productivity and carbon-neutral content of biosolids have attracted attention as promising energy alternatives to fossil fuel, especially for renewable crude oil[8]. Many processes can be used to recover energy from biomass; however, selecting efficient conversion processes to convert biosolids to energy represents a significant research challenge[9]. Many types of conversion processing, including gasification, pyrolysis, and direct combustion,

involve thermal processes that require a costly drying step in the case of wet feedstock[2]. According to Savage *et al.*[10], the energy required to dry biological solids exceeds the energy requirement for the HTL of biomass with a 30% w/w water content. HTL, therefore, could be an attractive thermochemical approach to convert high moisture biosolids into renewable crude oil that would be equivalent to conventional crude by precluding the drying pretreatment[11-15]. However, not enough is yet understood about the reaction processes and the HTL conditions of biosolids to make it successful. The HTL process, therefore, requires more research and development to maximise the renewable crude yield from biosolids, which is essential to optimise and promise the design of a commercial scale plant.

Conversion of organic matter from solid form to liquid renewable crude oil via HTL is not a spontaneous process. HTL processing occurs in a short time and leads to the thermal disintegration of biosolids into renewable crude oil[16]. However, various operational parameters influence the efficacy of the HTL process. During the HTL process, biosolids react with hot water at a temperature of 250 to 350°C and a pressure between 50 to 300 bar for anywhere between 10 to 60 minutes, with biomass containing 20% to 30% mass, to generate a highly reactive environment[17-21]. These conditions keep water in the liquid phase. This is essential because the water is the reactant that supports the conversion of biosolids to renewable crude oil[22, 23]. According to Beckman and Elliott[24], any changes in the key parameters, such as the residence time and reaction temperature, significantly impact the HTL products, which are renewable crude, solids, gas and aqueous products. The effect of using different conditions in the renewable crude oil yield of the HTL of biomass, such as swine manure and microalgae have been investigated and reported in the scientific literature[25-29]. They reported that the renewable crude oil yields ranged widely from 5 to 61% due to the effect of the HTL reaction

conditions and the biomass compositions. However, the operational conditions for HTL process and the recovery of renewable crude oil from biosolids are not clearly understood and more research is required to understand the effects of the operating conditions, including temperature and residence time when using complex biomass materials, such as biosolids.

According to the scientific literature, there are several explanations for the effects of increasing temperatures on renewable crude yields. For example, the renewable crude yield reduction could be related to the dominating secondary reaction and Bourdard gas reactions[25]. Wang *et al.*[29] stated that the competition between the two reactions in the HTL process - the hydrolysis and repolymerisation reactions - could be the reason for the decrease in renewable crude yield with any increase in temperature beyond 300°C. Also, according to Jin *et al.*[30], increases in yields of solid residue could be explained by the tendency for polymerisation or condensation reactions of intermediates to form heavier higher-molecular-weight compounds like char, which is retained in the solid residue. However, the effect of temperature on the renewable crude yield of the HTL of biosolids is not yet clearly understood and more research is required.

Renewable crude oil from the HTL of biosolids can be gained at different reaction times. For example, the renewable crude oil yield from the HTL of lipids can be decreased with increased residence time. According to Xu and Lancaster[31], the decrease in the renewable crude oil yields with the increase in residence times is related to the formation of a solid residue via crystallisation, condensation, and re-polymerisation. Also, the long residence times in the HTL of lignin could lead to secondary and tertiary reactions dominating, which could convert heavy intermediates either into liquids or residues species[32, 33]. However, the short reaction times in the HTL of carbohydrate lead to increase renewable crude oil yield. According to Sasaki *et*

al.[32], the short reaction times degrade carbohydrate effectively because the hydrolysis and the decomposition are relatively fast in the HTL process. Therefore, more research is required to understand the process that leads to the production of different yields during the HTL of biosolids in order to optimise the target yield.

The influence of biosolids' composition on HTL processes represents one of the most challenging research areas for renewable crude oil production because of the wide range of biosolids' compositions. Conversion of biosolids to renewable crude oil in the HTL process requires the break-down and reformation of a range of chemical bonds. During the HTL process, the dispersion of the water-soluble part of biomass into the water is known to start at 100°C, which is followed by subsequent hydrolysis above 150°C. This leads to the disintegration of the hemicellulosic and cellulosic fractions of the biomass into monomeric chains[23]. Then, at 200°C, the biomass slurry undergoes the HTL reaction[34]. However, biosolids are a mixture of many organic components that react together through different conditions. The organic contents in the biosolids typically have a composition containing: 6% to 30 % lipids, 20% to 30% proteins, 20% to 40% carbohydrates, and around 6% lignin[29, 35, 36]. Typical biosolids on a dry basis can also contain 30% to 60% carbon, 30% to 40% oxygen, and 5% to 6% hydrogen[29]. The inorganic elements in biosolids contain chlorine, nitrogen and sulphur[37]. This leads to the production of different yields of products. Most of previous research on the HTL process has been undertaken on other biomass, such as food waste and microalgae[38-40]. According to Obeid *et al.*[41], the renewable crude oil yield could be varied depending on the biomass source. For example, the yields of renewable crude oil from microalgae and digested sludge were about 5 to 25% depending on the biomass composition[42-44]. However, the scientific literature has minimal fundamental information about the performance of biosolids through

HTL. Therefore, understanding the effect of biosolid's compositions on the HTL process requires more research to make HTL technology more economically feasible, which has not yet been studied or reported in the scientific literature.

Although the chemistry that leads to the production of different yields during the HTL process of biosolids is not yet clear, there are several explanations about the effect of the organic component on the HTL process. According to Goheen[45], the effects of reaction temperature on the HTL of carbohydrates are related to the connection between temperature and hemicellulose degradation. The aqueous yield from carbohydrates could also be increased with the increase in temperature. According to Sakaki *et al.*[46], saccharification and carbonisation are the main steps for HTL degradation of cellulose, which, according to Ying *et al.*[47], causes a minor decomposition that leads to the formation of water-soluble sugars, followed by the carbonisation of water-soluble sugars. In addition, the gas yield from carbohydrate at 300°C and 30 minutes residence time led to a negative effect on the renewable crude oil yield because the hydroxymethylfurfural formation (HMF) was converted to gas and solid phases[48].

The renewable crude oil from protein at 250°C could be gained by hydrolysing the protein into amino acids, which could further react via decarboxylation[23, 49]. This produces aldehydes, amines, carbonic acid and hydrocarbons, or it can be achieved via a deamination reaction, which produces organic acids and ammonia. According to Gollakota *et al.*[9], the continuous degradation of an amino acid leads to the production of iso-butyric acids, n-butyric acid, propionic acid, acetic acid and carboxylic acids. Also, the cyclisation and condensation of the molecules lead to the production of aromatic amide molecules, pyrrole, pyrazine and indoles[50].

Renewable crude oil from lipids can be produced at a low temperature. Around 80% of renewable crude oil yields can be gained from hydrolysis of the lipids at 250°C, such as is reported in work by Biller and Ross[51] and Wang[52]. However, the renewable crude yield from the lipids can be decreased with increased residence time, which may be caused by the repolymerisation and recondensation of renewable crude[53]. The temperature also has a negative effect on the renewable crude oil yield from lignin. According to Xu and Etcheverry[54], the renewable crude oil yield from lignin can be decreased increased temperature because of the char formation's enhancement. The high yields of solid residue from lignin could be related to the condensation reactions of intermediates to form char[30]. Therefore, it is essential to understand the influence of biosolids' composition on the HTL processes and renewable oil crude oil.

Another critical point is the renewable crude oil composition, which is naturally affected by the HTL process and biosolids' composition. It is possible that the desired products could be produced by manipulating critical key parameters[34]. Compositions of renewable crude oil must be identified to gain a better understanding of the HTL od biosolids, which will enable fuel yields to be targeted. However, biosolids have not received enough research attention in this area, unlike other biomass like algae. In previous work, researchers have distinguished light and heavy renewable crude fractions by using the same biomass. For example, Valdez *et al.*[55] identified different yields of light and heavy renewable crude oil using different HTL conditions on the same strain of algae. Characterising renewable crude fractions could assist in understanding a possible procedure to manipulate the desired products. One of the reliable methods of assessing crude yields from biosolids is the thermogravimetric analysis (TGA) method. TGA has been used to characterise the renewable crude fractions, which can be

separated by a particular boiling point, as has been achieved by Garcia-Perez *et al.*[56]. This research measured the appropriate HTL conditions to obtain desirable yields.

The quantitative kinetics reaction is another important aspect because it enables the prediction of the yields of each product phase in the HTL of biosolids, which is currently limited in the scientific literature. However, kinetic models for the HTL of soy protein and algae have been presented[55, 57, 58]. These papers reported modelling work that contained a set of the first-order differential equations for the obtained experimental data from laboratories' scale batch reactors. Also, Li *et al.*[59] have developed a multicomponent additivity model for the HTL of microalgae from experiments set at 300 °C and 30 minutes. In addition, first-order kinetic models were developed for different temperatures to gain Arrhenius parameters[55, 57, 59-61]. The feed concentration in these models led to the determination of the product fractions. The model was applied to predict the HTL product yield from manure and sludge with some accepted accuracy, although further research is required because of the limitations in the available data in terms of reaction conditions, reactants, and product yields from these biomass sources. In this research, the product phase yields were predicted using these models for the HTL of the individual components of biosolids including, lipids, proteins, lignins, and carbohydrates; however, a further development model was required to predict the HTL yields for feedstocks with different fractions, such as biosolids under varying HTL reaction conditions.

Basically, biosolid compositions are highly variable. The produced products from the HTL of biosolids are significantly affected by the composition of biosolids and HTL reaction conditions. This research aims to provide a new understating of the characterisation of HTL products from biosolids. This research's principal objective is to utilise the optimum HTL

conditions and biosolids compositions to produce the best yield and quality of renewable crude oil via the HTL process. To achieve this aim, the key objectives are to assess the effects of different operating parameters, particularly reaction temperatures and residence times, and different biosolid compositions, which include lipids, proteins, carbohydrates and lignins on the yields of HTL products and to characterise the boiling point fractions of the produced renewable crude oil. A bulk kinetic model was developed for the HTL of biosolids, with varying fractions of lipids, proteins, carbohydrates and lignins to predict the product fraction yields.

2. Materials and methods

2.1 Feedstocks

The Melbourne Water Corporation supplied biosolids from stockpiles at the Western Treatment Plant in Werribee, Victoria, Australia. Biosolids were collated randomly from twenty-one different biosolids stockpiles. The collected biosolid samples differed in age, the depth of the samples taken from the stockpiles, and their position in exposure to sunlight. All the tests undertaken in this work were done in triplicate.

2.2 Biosolids characteristics

In previous research (Al-juboori *et al.* 2019), twenty-one biosolids samples were analysed using modified methods developed from the following techniques. The biosolids' organic and inorganic materials were measured using the Dry-Ash Free basis (daf) method[62]. The lipid content in the biosolids was determined by using the Folch method[63]. The protein content was estimated based on the total nitrogen content, which, according to Fujihara *et al.*[64], is the most practical method for determining protein content in plant and animal products. The

conventional method for lignins quantification was undertaken using the Klason lignin and acid-soluble lignin test[65]. The carbohydrate content was measured using the Safařík and Šantrůčková method[60]. Analysing the biosolids' major elements, including carbon, hydrogen, nitrogen, oxygen, and sulphur was carried out using a Perkin Elmer 2400 Series II CHNO&S analyser. Oxygen was calculated by subtracting the oxygen content from the total mass of carbon, hydrogen, nitrogen, and sulphur[65]. In this research, as can be seen in Tables 1 and 2, the selected biosolids samples (dry ash-free basis, daf) HC, HP, HL, and HLG represented the samples that have a high content of one of the organic materials, namely carbohydrates, proteins, lipids and lignins.

Table 1: The biochemical composition (% daf) of the biosolids.

Trial	Organic%	Inorganic%	Moisture%	Carbohydrate%	Protein%	Lipids%	Insoluble Lignin%	Soluble Lignin%
HC	33	63	4	44	32	4	17	4
HP	38	58	4	25	49	6	14	4
HL	36	59	5	30	26	32	12	4
HLG	26	70	4	42	23	6	32	4

Table 2: The ultimate analysis (% daf) of the biosolids.

Sample	Carbon%	Hydrogen%	Nitrogen%	Sulphur%	Oxygen%
HC	59	10	5	3	22
HP	59	10	8	5	19
HL	52	9	4	3	31
HLG	33	7	4	4	52

2.3 Hydrothermal liquefaction of biosolids

Biosolids were firstly dried in a Memmert 400 Drying Oven at 45ºC until a constant mass weight was attained. The biosolid samples were ground before the HTL experiments and sieved to particle size (142 μm). The particle size of the biosolid samples was measured using a

particle size analyser (Malvern Mastersizer 2000). HTL experiments were performed in triplicate on the biosolid samples in a high-pressure batch reactor by loading 1.65 g of biosolids and 3.85 g water. The HTL reactor was filled to 50% volume, which was 5.5 mL. The sealed reactor then was filled and purged with nitrogen three times to remove residual air from inside the reactor. The charged nitrogen was 90 bar to make the pressure reach 200 bar at the required reaction temperature.

The batch reactor was placed in a Techne SBL-2D fluidised bed with a Techne-9D temperature controller preheated in a sand bath set to 250, 300 and 350°C and kept for 20, 40, and 60 minutes. The holding time was set to start when the reactor temperature initially reached 98% of the reaction temperature. The heating rate was 80 ºC/min. It is important to note that the pressure was expected to increase to around 200 bar with the temperature increase when the isothermal holding time started. At the completion of the reaction holding time, the reactor was removed from the bed and was gradually air-cooled to 70ºC using a ventilator located at the top of the reactor. After reaching 70ºC, the reactor was drenched in cold water. The reactor was weighed before and after the experiments. Then the gas was released to determine the gas yield.

The reactor's remaining contents were separated by opening the top of the reactor and collecting the solid materials, which contained the renewable crude oil and the solid product in a centrifuge tube after decanting the aqueous phase into another centrifuge tube. The water was then used to clean the reactor, and the washings were added to the decanted aqueous phase solid material. In most cases, the viscous renewable crude oil and the solids residue were bound together. The produced solids products were dried in an oven at 40ºC for 72 hours and then quantified. The resulting solid product contained renewable crude oil and solid residue.

Quantifying the amount of renewable crude oil in the obtained solids product was performed by using the thermal desorption and pyrolysis of organic matter method. The difference in the final measure quantified the aqueous phase yields.

2.4 Thermal desorption and pyrolysis of organic matter

This analysis was consistent with previous work in Chapter Four. The methods here have been given in brief. To detect organic matter (OM) in biosolid, Weatherford's Instruments Source Rock Analyser (SRA) was employed for pyrolysis measurements. Detected by a flame ionisation detector (hydrocarbons) or infra-red spectrometry CO_2 & CO by heating the samples in a controlled atmosphere. Samples were pulverised, sifted, 20 to 40 mg loaded into SRA crucibles, placed in the auto-sampler carousel, moved to the pedestal, loaded into the oven base, purged under helium carrier gas at 120^{o}C for 90 seconds, raised into the furnace and held isothermally at 300^{o}C for 3 minutes. Free hydrocarbons (S1 fraction) were volatilised, detected using the FID detector reported as milligrams per gram of biosolids. Pyrolysis was conducted by increasing the temperature to 600^{o}C. The hydrocarbons generated from the kerogen's pyrolytic degradation (S2 fraction) represents the residual OM's productive potential, S3 represents the released carbon dioxide from the OM. In the oxidation stage, the oven was cooled to 400^{o}C, the carrier lines were switched to CO_2, purged for 5 minutes, temperature increased to 540^{o}C and held isothermally for 15 minutes. The residual inert OM (S4 fraction) converted to CO and CO_2 during this stage detected in the IR cells, reported as milligrams per gram of the biosolids.

2.5 Analysis of the produced renewable crude

A simulated distillation of the renewable crude oil, using a Netzsch simultaneous thermal analyser (STA) 449 F5 Jupiter, was utilised to establish the approximate fuel fractions, using the ranges given by the ASTM[66]. The boiling point profile for the TGA analysis of the renewable crude oil was conducted from 40 to 1010ºC, using an N_2 flow rate of 20 mL/min and a heating rate of 10 C/min. The fuel fractions from the TGA represented the renewable crude oil percentage, with the boiling point in the range of gasoline and naphthas-like 80 to 205°C, kerosene-like 205 to 255°C, diesel-like 205 to 290°C, gas oil-like 255 to 425°C and wax, lubricating oil and vacuum gas oil-like 425 to 600°C.

2.6 Kinetic pathways

The kinetic pathways were used to define the biosolids kinetics during the HTL process, as shown in Figure 1, and were determined from experiments with model compounds in the previous work[66]. To obtain the kinetic parameters for the kinetic pathways, as shown in Figure 1, the MATLAB function ODE45 was employed as the solver for the ordinary differential equations in Equations 1-8. The parameters were fit via a least-squares algorithm with the MATLAB function lsqcurvefit. The bounds for the kinetic parameters were set between 0 and 1. The errors in the Arrhenius parameters in Table 3 were calculated from the standard deviation of the 95% confidence interval, using the MATLAB function polyconf for the Arrhenius parameters calculated by polyfit as described previously[41].

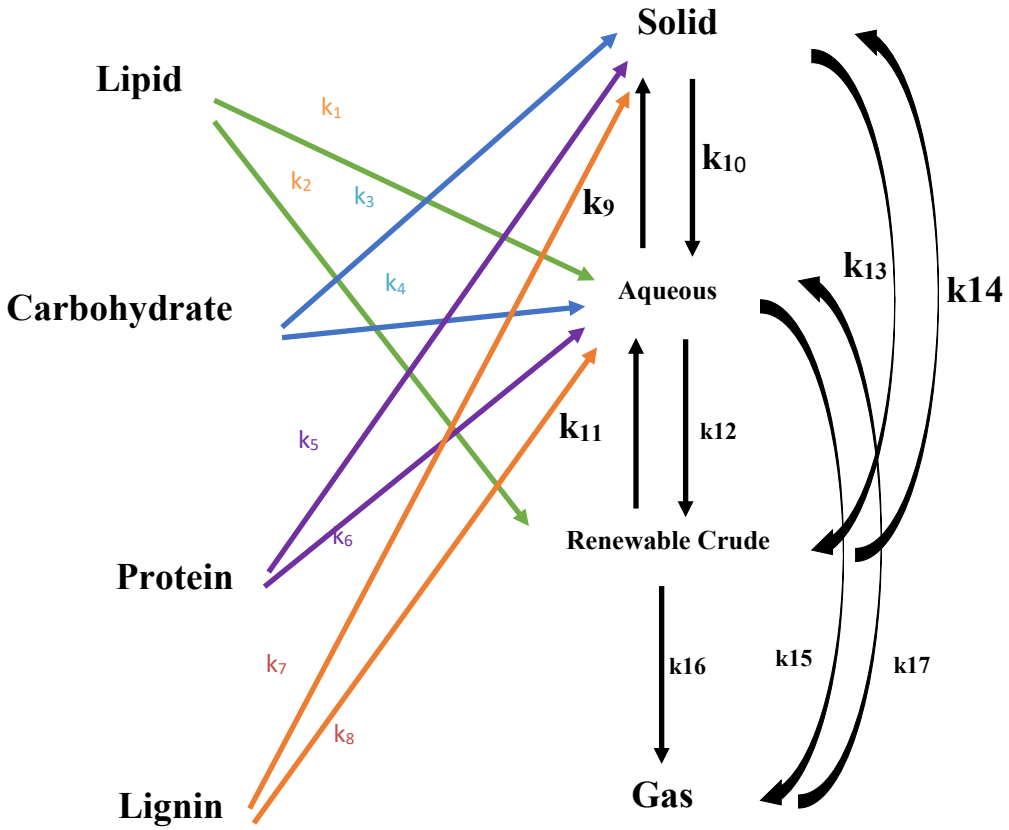

Figure 1: Kinetic pathways for biomass model compounds derived from model compounds taken from[41].

(1) $\frac{dx_1}{dt} = -(k_1 + k_2)x_1$

(2) $\frac{dx_2}{dt} = -(k_3 + k_4)x_2$

(3) $\frac{dx_3}{dt} = -(k_5 + k_6)x_3$

(4) $\frac{dx_4}{dt} = -(k_7 + k_8)x_4$

(5) $\frac{dx_5}{dt} = -(k_{10} + k_{13})x_5 + k_3x_2 + k_5x_3 + k_7x_4 + k_9x_6 + k_{14}x_7$

(6) $\frac{dx_6}{dt} = -(k_9 + k_{12} + k_{15})x_6 + k_1x_1 + k_4x_2 + k_6x_3 + k_8x_4 + k_{10}x_5 + k_{11}x_7 + k_{17}x_8$

(7) $\frac{dx_7}{dt} = -(k_{11} + k_{14} + k_{16})x_7 + k_2x_1 + k_{12}x_6 + k_{13}x_5$

(8) $\frac{dx_8}{dt} = -k_{17}x_8 + k_{15}x_6 + k_{16}x_7$

3. Results and discussion

3.1 The distribution of the HTL products

The product yields from the HTL of the four biosolid samples, HC, HP, HL and HLG, are shown in Figure 2. The values are based on a dry ash-free basis (daf). The effects of the reaction temperature and residence time on the HTL process were measured to understand their effect on the distribution yields to improve the renewable crude yields. The results showed that renewable crude yields were affected by the temperatures and residence time during the HTL process, as discussed below.

The highest renewable crude yield of biosolids was obtained from the HLG sample and was approximately 26% at 250ºC and 40 minutes. The high renewable crude yields from the HLG sample indicate that the lignin was significantly affected by other compounds like lipids and proteins, which leads to an increase in the lignin conversion to renewable crude oil. Once the conversion of biosolids from the HLG sample reached its maximum value at 250°C, further increases in temperature and residence time led to decrease renewable crude oil yield. The minimum solid residue produced from the HLG sample was achieved with a short residence time at 350ºC. However, the main product of the HTL of the HLG sample was an aqueous phase, which is similar to the result found by Obeid *et al.*[66]. The gas yield, on the other hand, increased with an increase in both temperature and residence time.

The HP sample's renewable crude yield was mostly consistent at 250°C to 300°C, without an increase in residence time. The renewable crude oil yield, however, showed a reduction at 350°C, with an increase as the residence time increased. The gas yield increased with an increase in the reaction temperature. It was mostly residence time that affected the gas yield at 250°C because most of the renewable crude oil at 250°C could be gained by hydrolysing the protein into amino acids[18]. The aqueous phase also was mainly influenced by the residence time. While the solid residue was affected by both temperature and residence time, it dropped at 300°C. However, it increased again when it reached 350°C.

At between 20 and 60 minutes at 250°C to 300°C, the HC sample's renewable crude yield was mostly consistent. However, it dropped with the increase in temperature, and the residence time did not show any effect. The yield of the solids' residue was decreased with the increase in temperature. However, it showed an increase with an increase in residence time; behaviour which is opposite to that in the aqueous and gases phases. On the other hand, the renewable crude yield from the HL sample showed that the highest yield was gained at the lowest temperature, and it decreased with the increase in residence time. However, it was relatively constant for the other temperatures. The gas yield was mostly affected at 250°C to 300ºC, with an increase in residence time. The solid residue decreased with an increase in residence time at 250ºC to increase again with time at 350ºC, which is in contrast with the aqueous phase.

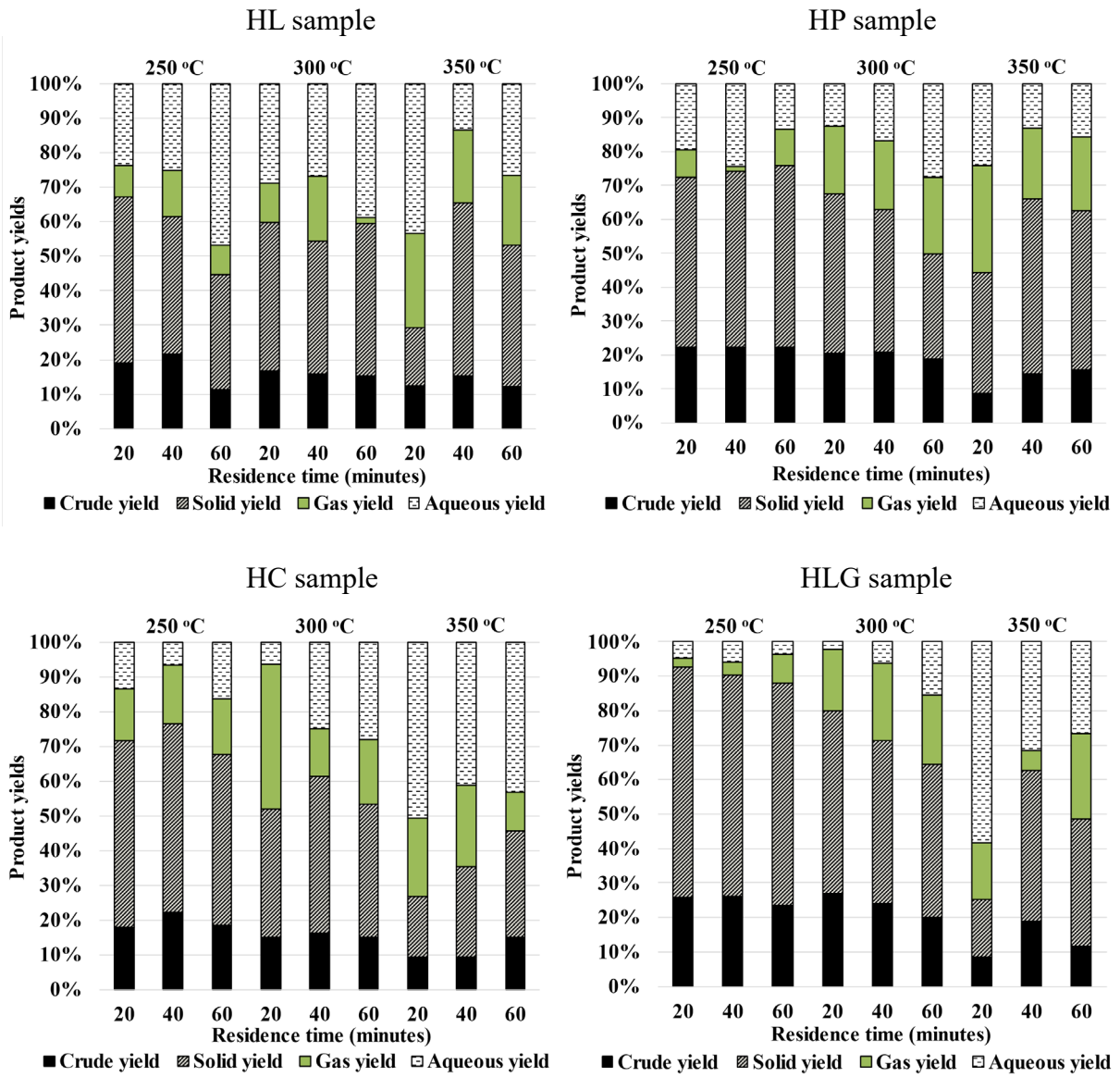

Figure 2: The HTL yields from biosolids at 250, 300 and 350°C reaction temperature and 20, 40 and 60 minutes residence time.

3.2 HTL reaction of components in biosolids

This section discusses the high amounts of the selected organic components in the HTL reaction of biosolids and their combined effect on the distribution of HTL products. In the HC sample, the highest renewable crude oil yields at 250°C and 40 minutes were around 22% but began to fall with the increase in temperature. The residence time did not show a significant effect on

the renewable crude, and increasing the residence time led to an increase in the conversion of the water-soluble intermediates, which led to an increase in the aqueous yield. According to Peterson *et al.*[49] and Wang[52], the renewable crude oil from carbohydrates at 250°C is mainly gained from hemicellulose and glucose but is followed by the decomposition of the cellulose at 300°C, as also reported by Peterson *et al.*[49]. At 350°C, the renewable crude yield dropped and remained consistent at 40 minutes. According to Akhtar and Amin[67], at 350°C, the cellulose may hydrolyse to polysaccharides. Saccharification will follow. However, increasing the temperature did not lead to an increase in the yield of renewable crude oil.

According to Molten *et al.*[68] and Goheen[45], the limiting effects of increased temperature on carbohydrate conversion are related to the connection between the temperature and hemicellulose degradation because hemicellulose has an endothermic reaction to pathways heat that impacts at low temperature, but has exothermic effects at high temperatures. The endothermic reaction occurs at low temperature (below 280ºC) due to the evaporation of monomolecularly adsorbed water, and the split-off of a hydroxyl group of hydrogen from the existing water in biosolids[69]. The endothermic reaction usually decreases with the increase of temperature, and the exothermic reaction occurs at high-temperature (320 to 360ºC)[45]. At high temperatures, the exothermic reaction occurs, and mostly increases with the increase of oxygen in biosolids samples due to the oxidation of the degraded fragments of hemicellulose[68, 70].

The aqueous yield from the HC sample shows an increase with the increase of temperature, due to the conversion of the water-soluble intermediates fractions of the carbohydrate into the aqueous phase[37.] The solid residue yield from the HC sample also increases with the increase of temperature until 300ºC is reached due to the conversion and repolymerization of the water-

soluble intermediates into water-insoluble products, which are yielded in the solid residue[37]. The HC sample's gas yield also increased to reach its maximum at 300ºC and 20 minutes and dropped thereafter. The high gas yields are possibly related to secondary decompositions, which become active at high reaction temperatures and cause the formation of gas[71]. Therefore, to obtain a high renewable crude yield from carbohydrate, it is important to inhibit the decomposition of lighter products[66].

The HC sample's renewable crude oil yield also showed no significant change with the increase in the residence time from 20 to 60 minutes. According to Sasaki *et al.*[32], short residence times degrade biosolids effectively because the hydrolysis and the decomposition rates are relatively fast in the HTL process. Also, a long residence time is not suitable because it decreases renewable crude oil yields[32, 67]. Therefore, it is desirable to have shorter residence times for a high carbohydrate content sample.

The HP sample's renewable crude oil yield was most consistent at 250°C to 300°C, when it was around 21%. According to previous work in the HTL of protein done by Peterson *et al.*[49] and Toor *et al.*[23], the renewable crude oil yield at 250°C could be gained by hydrolysing the protein into amino acids. However, renewable crude oil at 350°C shows a reduction with an increase in temperature. The explanation is that an increase in temperature leads to dominant secondary and tertiary reactions. These cause the formation of gases and aqueous or solid residues from heavy intermediates, resulting in a reduction of the renewable crude yield[13, 29]. Therefore, it is noticeable that the gas yield increases with an increase in the reaction temperature. For most of the previous research, gas yields from protein, such as brown algae and soy protein, were around 30 to 45%[72, 73]. However, the gas yields percentage from this

research were between 10% and 20%, which means that the other organic compounds affected the gas yields. On the other hand, the residence time did not affect the renewable crude oil yield from the HP sample at 250°C and 300°C. However, at 350°C, the renewable crude oil yields were significantly affected when using longer residence time. At 350°C and 20 minutes, the renewable crude yield was 9% and started to increase to 13% at 40 minutes and continued to increase until it reached 17% at 60 minutes.

The highest renewable crude oil yield from the HL sample was noticed at 250°C and mainly remained consistent at 40 minutes. According to previous research by Wang[29], most of the renewable crude yield at 250°C is gained from hydrolysis of the lipid, which is the predominant reaction for lipids at low temperatures. The increase in temperature led to a noticeable effect on renewable crude oil yields at 300°C and 350°C and then remained consistent. The HTL of lipids has been reported to produce around 80% renewable crude yields, as reported in work by Biller and Ross[51]. However, the renewable crude oil yield from the HL sample in this research was significantly lower, around 22%, which was mostly a result of the presence of other compounds in the biosolids, such as carbohydrate and lignin.

At 250°C and 350ºC, the renewable crude yield from the HL sample showed a decrease with an increased residence time. According to Gai *et al.*[53], the decrease could be caused by the repolymerisation and recondensation of renewable crude. For example, according to Xu and Lancaster[31], a potential explanation for stabilising or decreasing renewable crude yields due to overextended residence times is that the liquid products could be cracked to gases or form a solid residue through crystallisation, condensation, and re-polymerisation. Therefore, renewable crude yields are significantly affected by the high yields of the solid residues that

are produced from carbohydrates and lignins.

The renewable crude yield from the HLG sample mostly remained constant at 250°C, but the renewable crude oil dropped after 300°C. According to Xu and Etcheverry[54], the renewable crude yield from lignin can be decreased after 300°C because of the char formation's enhancement at higher temperatures. In this work, maximum solid residues were gained at low temperatures. Temperature increases lead to the distribution of the lignin product into the aqueous phase. Arturi *et al.*[74], for example, found that a high lignin content produced a higher yield in the aqueous phase.

The amount of solid residue produced was high in the HLG sample, which was associated with an increase in temperature. For example, the reduction of the renewable crude yield could be related to the recombination of the free radicals into char[25]. Wang *et al.*[29] state that the competition between the hydrolysis and repolymerisation reactions could lead to a decrease in renewable crude oil, along with an increase in temperature. Also, according to Jin *et al.*[30], increases in yields of solid residues could be related to the condensation reactions of intermediates to form char, which is retained in the solid residue. Therefore, the amount of solid residues produced was high in the HLG sample.

The residence time effects on the HLG sample were minimal for low temperatures but had a more pronounced effect for high temperatures. For example, at 300°C, the solid residue yield reduced with an increase in the residence time, and any further increase in the reaction temperature and residence time led to increases in the yields of the gas and aqueous phases. The explanation for the increase in the gas and aqueous phases could be related to the further

reaction of the intermediates' oil and the subsequent cracking[75]. Another explanation is that long residence times could lead to secondary and tertiary reactions dominating, which could convert heavy intermediates into liquids, gases, or residues species[32, 33].

3.3 Renewable crude characteristics

The SRA was used to evaluate the residual crude oil and OM in the biosolids. The results in Figure 3 represent the proportions for renewable crude oil, also shown in Figure 2, at a low-boiling point (LBP) and a high-boiling point (HBP) based on SRA measurements. The SRA results for biosolids samples before the HTL process show that biosolids samples have mostly similar low boiling materials at LBP, ranging from 1 to 2%. In comparison, the high boiling material at HBP was higher and ranging from 9 to 14%. The SRA results for the renewable crude of biosolids show that each biosolids sample produced renewable crude oil with different boiling materials, as discussed below.

The low boiling materials in the renewable crude oil from the HL sample at LBP were constant at 250ºC and around 3%. However, this increased with the increase in temperature and at 350ºC reached 6%. The residence time showed no effect at 250ºC, but at 350ºC, the low boiling materials in the renewable crude oil increased when the residence time was increased to 40 minutes. Conversely, the high boiling material in the renewable crude at HBP decreased from 16% to 7% with an increase in temperatures and residence time. Thus clear that the majority of the boiling material from the HL sample at low temperatures has a higher boiling point range. However, the boiling material in the renewable crude at LBP increased with an increase in temperature to 350ºC. This is similar to the results found by Biller *et al.*[76]. On the other hand, the low boiling material at LBP in the renewable crude from the HC sample increased with an

increase in temperature to reach 6%. The residence time did not affect the low boiling material at 250ºC and 300ºC, but it showed a significant increase in the low boiling material at 350ºC and 40 minutes. Furthermore, the high boiling material at HBP decreased from 16% to 5% with an increase in temperature and residence time. Therefore, it is clear that most of the boiling material from the HL and HC samples have a higher boiling point range at low temperatures, but the low boiling materials at LBP increased with any increase in temperature.

The boiling point distribution of the renewable crude oil that was gained from the HP sample indicates that renewable crude oil contains a large amount of high boiling material, which is similar to the results produced by Ross *et al.*[77] in the HTL of microalgae. The low-boiling point material at LBP remained constant at around 6% during the different conditions of the HTL process. However, the high boiling material at HBP decreased from 16% to 6% with the increase of temperature and residence time until 350ºC and 40 minutes when it showed a slight increase in the high boiling material at HBP at 350ºC and 40 minutes. On the other hand, the low-boiling point material at LBP in the HLG sample increased to 9% with an increase in temperature to 300ºC. The residence time showed no effect at 250ºC, but it decreased with an increase in residence time at 300ºC. Conversely, an increase in the low boiling materials with an increase in residence time showed at 350ºC. The high boiling materials at HBP from the HLG samples decreased from 19% to 6% with an increase in temperatures and residence time. In general, it was noticeable that the low boiling materials at LBP increased with an increase in both temperature and residence time.

The highest renewable crude oil yields from most biosolids samples were obtained at 250ºC and 20 minutes. However, this does not imply that this will be the highest extractible renewable

crude yields due to the low amount of the low boiling material at LBP. Therefore, the HTL of biosolids is most advantageous at 350ºC and 40 minutes, because the renewable crude oil at high temperatures gained better yields from the low boiling material at LBP. This result is similar to that found by Chen *et al.*[78] for the HTL of algal biomass.

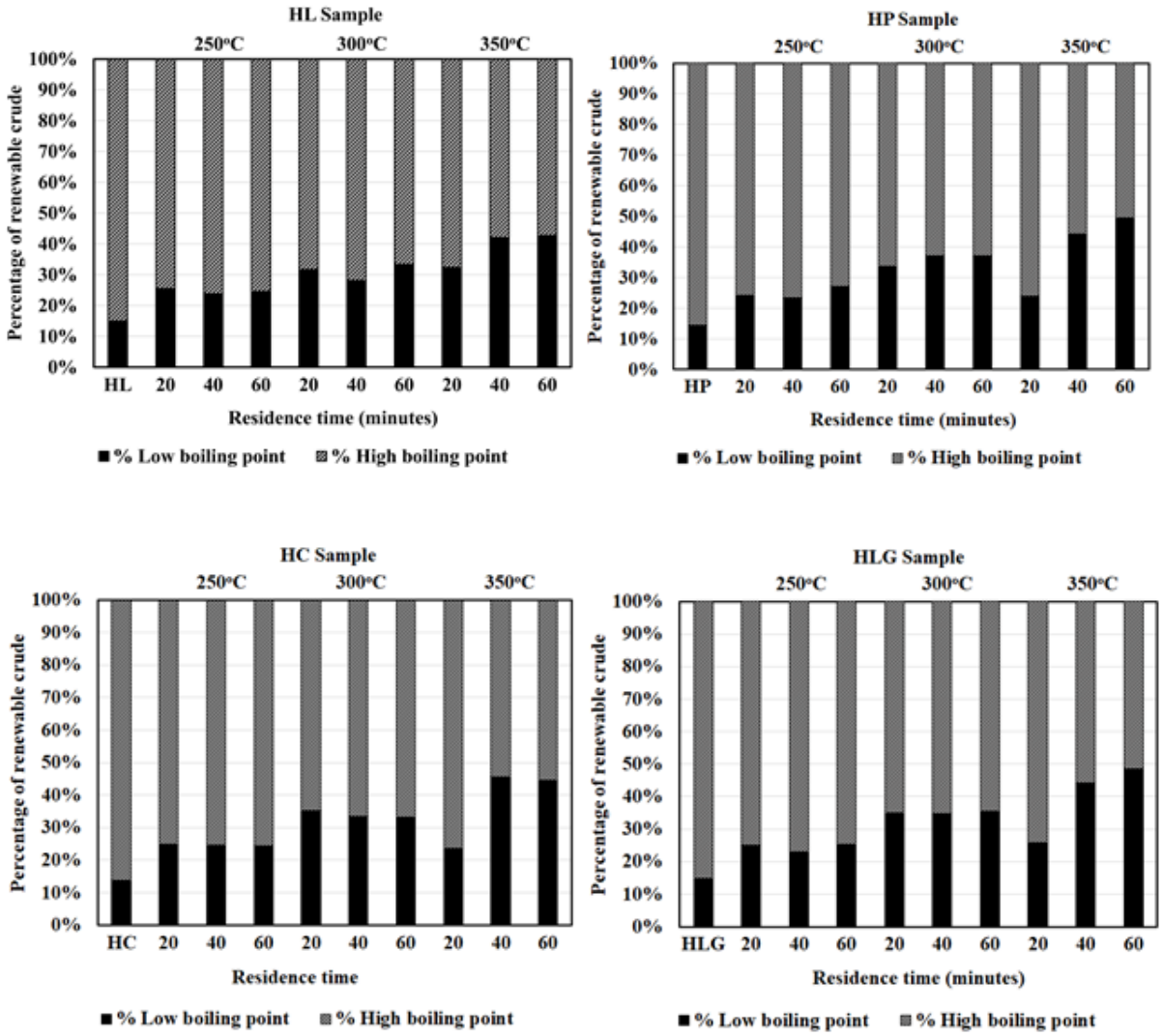

Figure 3: The proportion for the renewable crude yields at low and high boiling point for HL, HP, HC and HLG biosolids samples before the HTL process and at 250, 300 and 350ºC, and 20, 40 and 60 minutes HTL reaction conditions.

The distillation properties of renewable crude oil under different HTL conditions can be seen in Figure 4. The fraction of renewable crude oil within specific boiling point ranges, which correspond to the same boiling point ranges of the fractions of petroleum crude, was used to identify renewable crude oil properties. The gasoline and naphtha-like 80°C to 205ºC yields were the highest percentages in the renewable crude oil from the HL sample at around 9% at 250ºC and 20 minutes. However, this amount started to drop with an increase in temperature and residence time. In contrast, it increased with an increase in temperature and residence time for the HP sample to reach 8% at 350ºC and 60 minutes. The HC and HLG samples were similar in their behaviour but provided low yields. On the other hand, the highest kerosene-like 205°C to 255ºC yields from the renewable crude were mostly similar across all the samples, at around 10% at 350ºC and 20 minutes. The HP, HC and HLG samples showed an increase in the yields with an increase of temperature, while lipids had the opposite behaviour and 250ºC and 20 minutes were sufficient to gain the highest yield.

The diesel-like 205°C to 290ºC yields from all the samples were mostly similar, at around 15% at 250ºC and 20 minutes. The HP, HC and HLG samples did not experience any change with the changing conditions, and only the HL sample showed a decrease to 8% with an increase of residence time at 350ºC. This result is in contrast with other researchers, such as Biller *et al.*[79], for example, who reported that the HTL of lipids with longer residence times resulted in higher diesel-like yields and that this difference in behaviour was related to the composition of the biosolids, which contained a mix of different compounds that affected each other. Therefore, it is clear that 20 minutes and 250ºC are sufficient to produce the highest yields from most biosolids' samples.

The gas oil-like distillate range of 255°C to 425°C yields was generally high in all the samples, at around 50% at 250ºC and 20 minutes. The HP, HC and HLG samples showed a similar behaviour where the yields decreased with an increase in temperature, while the HL sample only showed a noticeable increase with an increase in residence time at 250ºC, from 20 to 60 minutes. On the other hand, the wax, lubricating oil and vacuum gas oil-like yields at 425°C to 600ºC from the HP, HC and HLG samples were mostly similar. They ranged between 25% and 33%. The best yields from the HL, HC and HLG samples were gained at around 350ºC and 60 minutes, while 250ºC and 20 minutes were enough to gain the highest yield from the HP sample.

From the above discussion, it can be observed that the results can provide further insights into the effects of the HTL conditions and biosolid compositions on the renewable crude oil composition, which can be controlled to produce the required fractions of renewable crude; it is, therefore, essential to optimise the HTL conditions regarding the biosolids composition. However, refining renewable crude oil on an industrial scale could lead to removing some elements, such as sulphur, oxygen and nitrogen. Several industrial processes were developed to upgrade these materials by diluting or converting the heavier components into lighter components, such as the hydrocarbon treatment[71]. Therefore, the fuel fractions' results could deviate from the predicted amounts in terms of these experiments, when TGA was used.

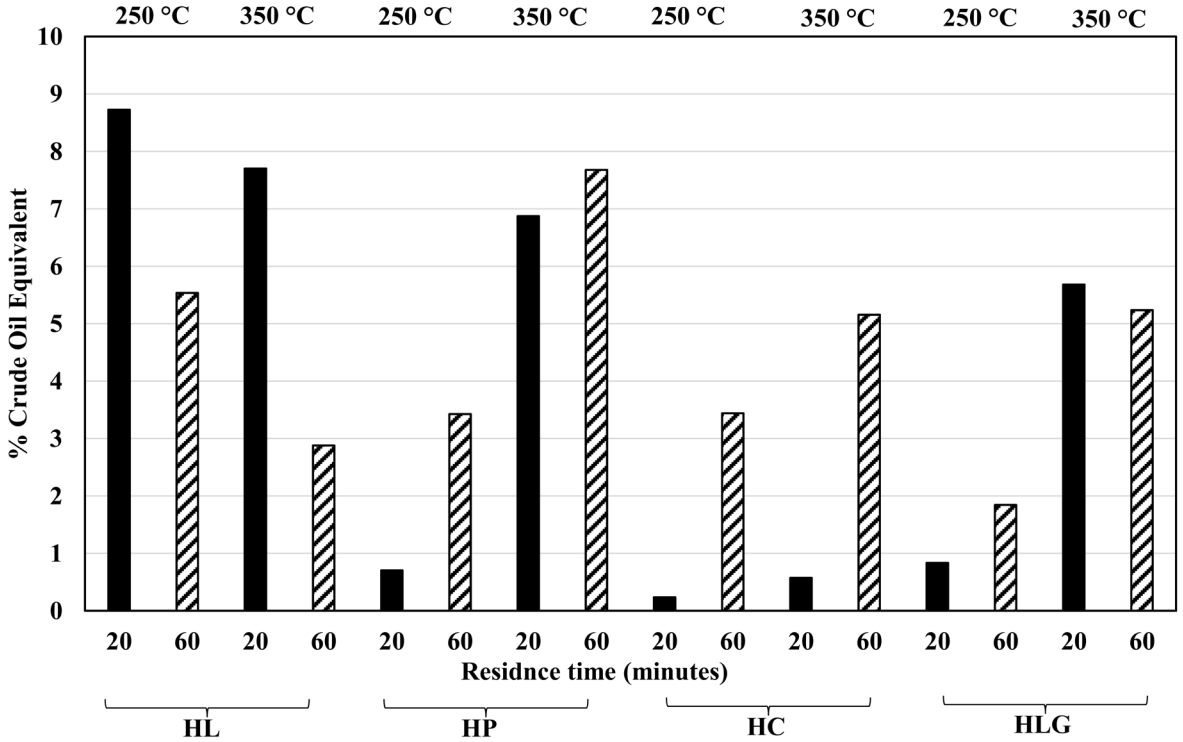

A. Gasoline and naphthas-like (80-205°C).

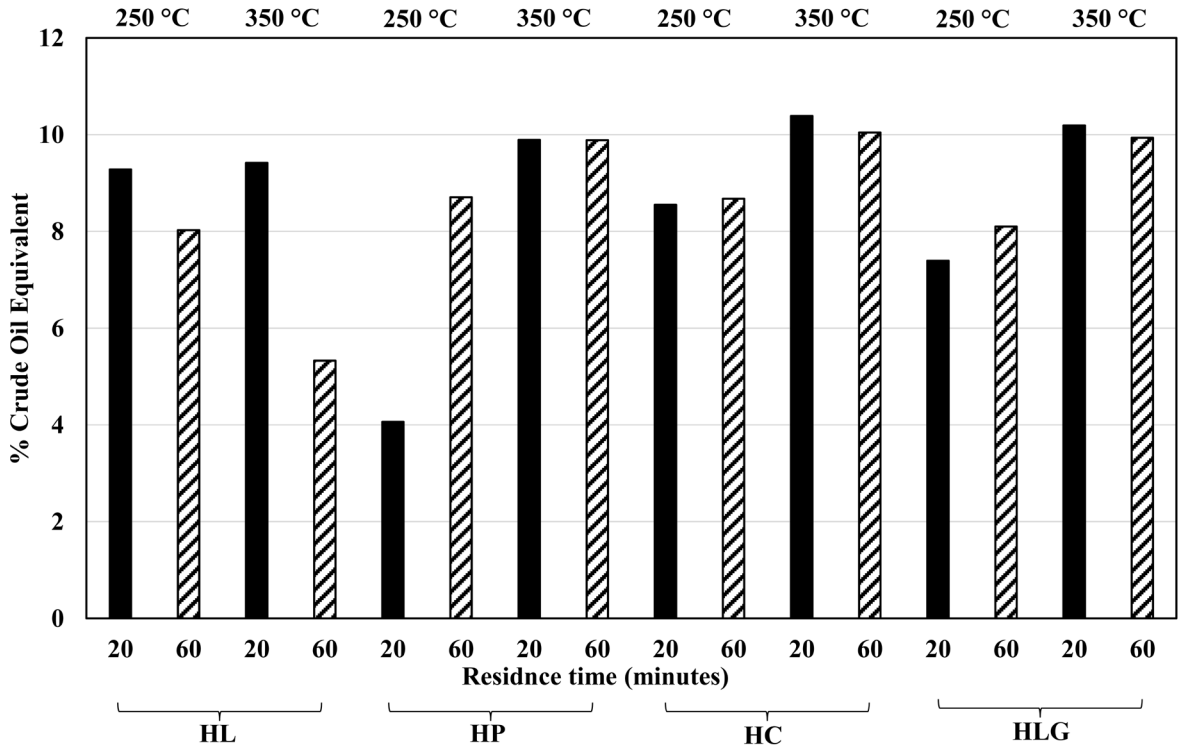

B. Kerosene-like (205-255°C).

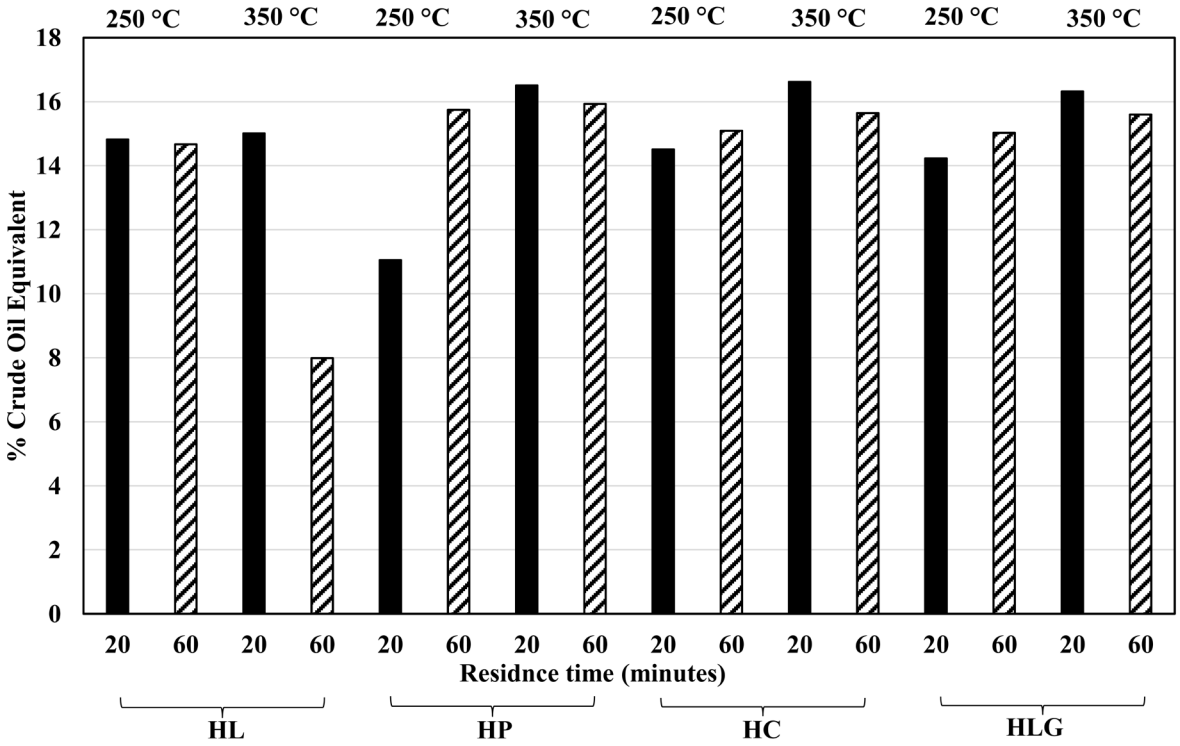

C. Diesel-like (205-290°C).

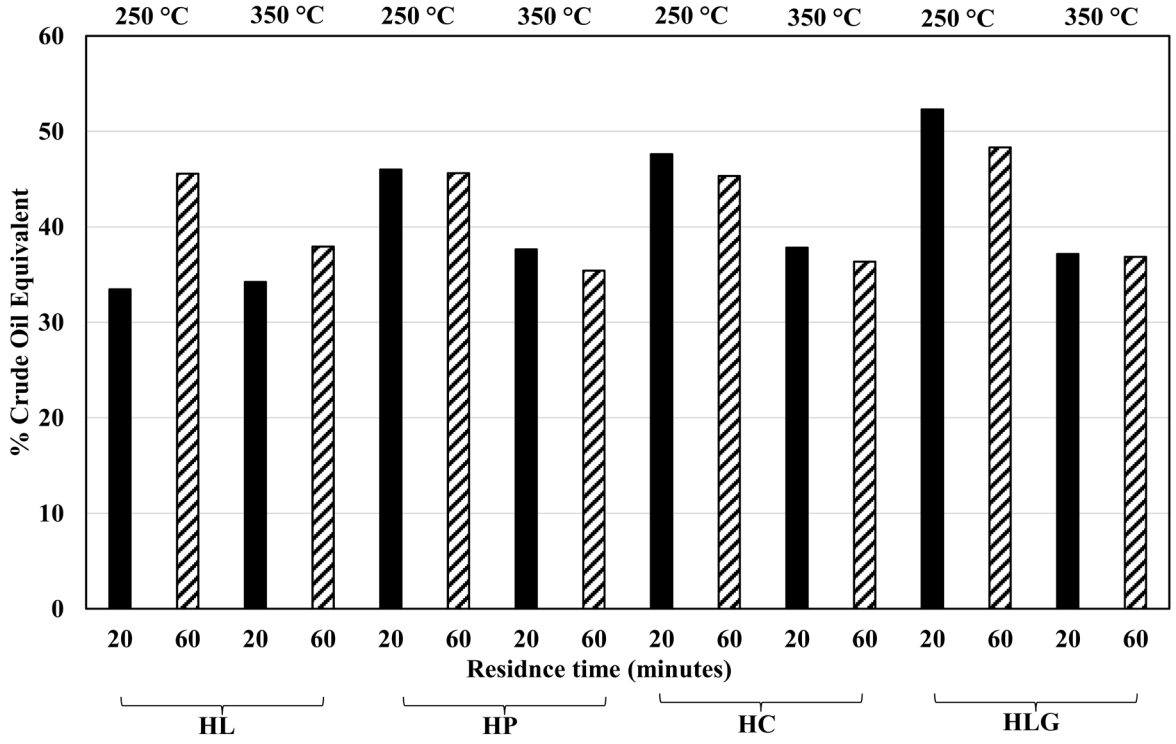

D. Gas oil-like (255-425°C).

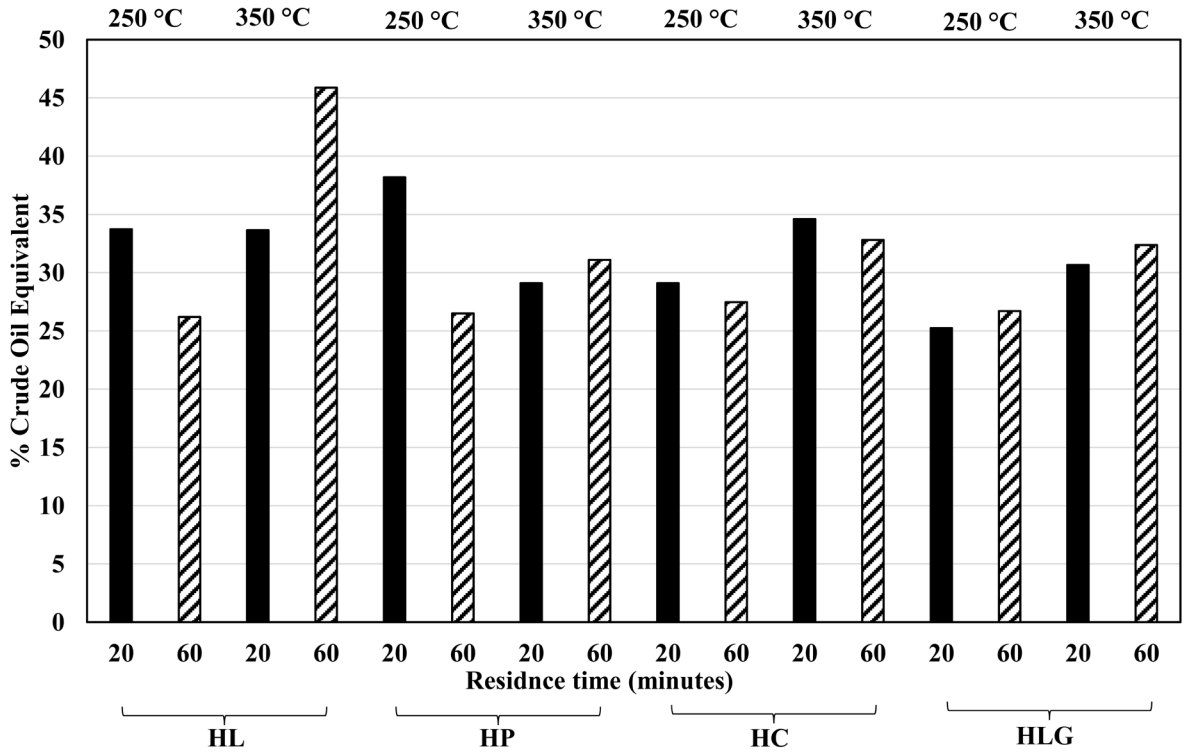

E. Wax, lubricating oil and vacuum gas oil-like (425-600°C).

Figure 4: Percentage of renewable crude in the boiling point ranges of petroleum fractions for the HTL product of biosolids at 250, 300 and 350°C reaction temperature and 20, 40, and 60 minutes residence time.

Numerical models were then applied to the kinetic pathways, using a method that was presented in Section 2.6. The kinetic models used to characterise the biosolids samples were plotted against the experimental yields in as can be seen in Figure 5, and Appendix C (Figure S1, S2, S3 and S4). As shown, the model predicts renewable crude yields with an error of less than 20%. The solids yield was predicted with an error of less than 25%. The gas yield was predicted with an error of less than 20%, and the aqueous yield was predicted with an error of less than 25%. These errors were significant and partially due to the large variation in the composition of the biosolids, which resulted in significant variations in the distribution of the products. The biosolids' composition affected the product distribution significantly, and the four biosolids

samples contained distinctly different compositions of carbohydrates, proteins, lipids and lignins. The trends in minimum variation with reaction time after 5 minutes at each reaction temperature for the four biosolid feedstocks are represented by the model.

The errors in Arrhenius parameters were significant in Table 3. This demonstrated that the HTL reactions were being oversimplified by the first order bulk kinetic model in Figure 5. Comparisons with the previous model developed for sewage sludge using this reaction scheme showed that the Arrhenius parameters deviate for the same reaction pathways by up to 130 kJ/mol[66]. This major variation in the two bulk kinetic models derived from the significant differences in product distributions. While the HTL of biosolids and sewage sludge both result in crude yields of 10 to 20%, the solid yields for biosolids were between 10 to 55% and the solid yields for sewage sludge were between 10 to 30%. Therefore, higher activation energies for converting solids to other product phases are seen in the biosolids model, when compared with the model for sewage sludge.

Other limitations for the model included the limited number of experimental data points for each sample of biosolids. The inorganic composition in the biosolids feedstock has also been found to affect the product distribution due to the catalytic and inhibitory effects of some inorganics inherent in the biosolids[80, 81]. However, in the tested biosolids samples, the amounts of the content of the metals were not enough to have a significant effect. The model was developed for experimental data, which was obtained using the methods described in this work. The reactor configuration, batch HTL experimental methods and product separation methods used have some effect on product compositions. Hence, the yields obtained from HTL using other methods could vary further from the model. Further experiments with different types of

biosolids at varying reaction conditions will allow the model to be further refined.

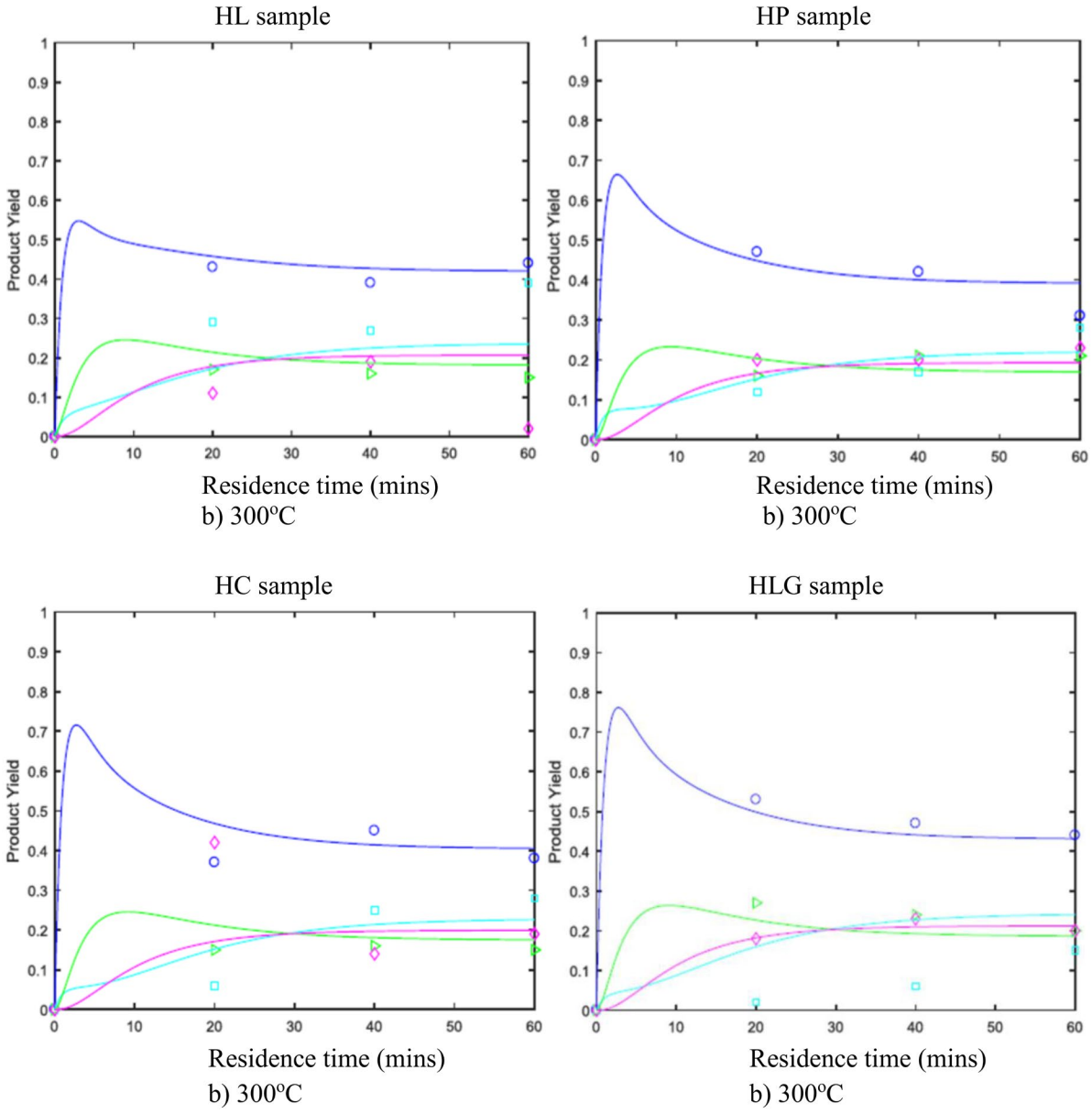

Figure 5: The bulk kinetic model with data for biosolids samples at 300ºC.

Table 3: Kinetic parameters fitted to the reaction pathways in Figure 1.

			k[°C](sec^{-1})				
Compound	Path	Reaction	Temperature (°C)			lnA	E_A (kJ/mol)
			250	300	350		
Bio-solids	1	Lipid to Aqueous	1.99	2.10	60.00	20.71±20.49	89.42±16.60
	2	Lipid to renewable crude	6.00	60.00	60.00	16.84±11.97	64.03±9.70
	3	Carbohydrate to solid	8.03	58.90	59.40	15.15±10.31	55.64±8.35
	4	Carbohydrate to aqueous	0.30	0.30	60.00	29.89±32.82	139.00±26.58
	5	Protein to solid	30.00	60.00	60.00	7.93±3.60	19.27±2.92
	6	Protein to aqueous	11.02	11.40	60.00	12.37±10.11	44.52±8.19
	7	Lignin to solid	8.03	58.90	59.40	15.15±10.31	55.64±8.35
	8	Lignin to aqueous	0.30	0.30	60.00	29.89±32.82	139.00±26.58
	9	Aqueous to solid	0.30	4.00	21.99	25.72±2.90	116.74±2.35
	10	Solid to aqueous	0.30	0.30	2.81	17.36±19.59	82.98±15.87
	11	Renewable crude to aqueous	0.32	0.33	15.70	21.76±23.73	102.35±19.22
	12	Aqueous to renewable crude	0.30	0.30	2.81	11.93±13.87	58.73±11.23
	13	Solid to renewable crude	0.30	6.99	27.56	27.42±7.87	123.55±6.38
	14	Renewable crude to solid	0.30	11.65	38.06	29.65±11.70	132.81±9.47
	15	Aqueous to gas	1.80	1.86	12.28	11.88±11.52	50.43±9.33
	16	Renewable crude to gas	0.30	4.59	27.39	1.47±3.12	13.85±2.53
	17	Gas to aqueous	2.99	6.14	36.42	66.68±66.68	16.24±16.24

4. Conclusion

The yield and quality of the produced renewable crude oil via the HTL of biosolids were affected by biosolids content and reaction conditions. In particular, the composition of biosolids significantly influenced the renewable crude composition. Increasing reaction temperature and residence times generally increased renewable crude yield. However, the optimum residence time depended on the biosolid content and reaction temperature. The simulated distillation by TGA indicated that the renewable crude oil fractions varied depending

on biosolids content and operating conditions. The gasoline and naphtha-like yield from HL and HP samples have an opposite response to increased temperature and residence time. The gas oil-like yield was high in all samples but declined with increased temperature. The kerosene-like, diesel-like, and wax lubricating oil-like yields were mostly similar across all the samples.

5. Author information

Corresponding Author:

Dr. Philip van Eyk.

School of Chemical Engineering & Advanced Materials

Faculty of Engineering, Mathematical and Computer Sciences

University of Adelaide

Adelaide, South Australia 5005

+61 8 8313 6081

philip.vaneyk@adelaide.edu.au

The manuscript was written with contributions from all the authors. All authors have given approval to the final version of the manuscript.

6. Acknowledgements

The authors would like to acknowledge Dr Rosmala Lewis and Melbourne Water, Werribee, Victoria, Australia for providing the feedstocks.

Funding: This work was supported by the Australian Research Council and Southern Oil Refining Pty Ltd [Grant numbers LP150101241].

7. Abbreviations

HTL, Hydrothermal Liquefaction; TGA, thermogravimetric analysis; Daf, dry-ash free; SRA, Source Rock Analyser; OM, organic matter; HC, high carbohydrates; HP, high proteins; HL, high lipids; HLG, high lignin; LBP, low-boiling point; HBP, high-boiling point.

8. References

1. Tekin, K.; Karagöz, S., Non-catalytic and catalytic hydrothermal liquefaction of biomass. *Research on Chemical Intermediates* **2013,** *39* (2), 485-498.

2. Dimitriadis, A.; Bezergianni, S., Hydrothermal liquefaction of various biomass and waste feedstocks for biocrude production: A state of the art review. *Renewable and Sustainable Energy Reviews* **2017,** *68*, 113-125.

3. Elliott, D., Thermochemical processing of biomass. Chichester, UK: John Wiley & Sons Ltd: 2011.

4. GOH, N.; SHORT, M. D.; BOLAN, N. S.; SAINT, C. P., Solutions for solid wastes. *Unmaking Waste 2015 Conference Proceedings* **2015**, 342-356.

5. Federation, W. E. Questions and Answers on Land Application of Biosolids. (accessed 01 May).

6. Statistics, A. B. o. Waste Management Services. <http://www.abs.gov.au/ausstats/abs@.nsf/lookup/8698.0Glossary12009-10>. (accessed 2 May).

7. Mahro, B.; Timm, M., Potential of biowaste from the food industry as a biomass resource. *Engineering in Life Sciences* **2007,** *7* (5), 457-468.

8. Kabir, G.; Hameed, B., Recent progress on catalytic pyrolysis of lignocellulosic biomass to high-grade bio-oil and bio-chemicals. *Renewable and Sustainable Energy Reviews* **2017,** *70*, 945-967.

9. Gollakota, A.; Kishore, N.; Gu, S., A review on hydrothermal liquefaction of biomass. *Renewable and Sustainable Energy Reviews* **2018,** *81*, 1378-1392.

10. Savage, P.; Levine, R.; Huelsman, C., Hydrothermal processing of biomass. *Thermochemical conversion of biomass to liquid fuels and chemicals* **2010**, 192-221.

11. Chiaramonti, D.; Prussi, M.; Buffi, M.; Rizzo, A. M.; Pari, L., Review and experimental study on pyrolysis and hydrothermal liquefaction of microalgae for biofuel production. *Applied energy* **2017,** *185*, 963-972.

12. Faeth, J. L.; Savage, P. E., Effects of processing conditions on biocrude yields from fast hydrothermal liquefaction of microalgae. *Bioresource technology* **2016,** *206*, 290-293.

13. Jain, A.; Balasubramanian, R.; Srinivasan, M., Hydrothermal conversion of biomass waste to activated carbon with high porosity: A review. *Chemical Engineering Journal* **2016,** *283*, 789-805.

14. Kumar, M.; Oyedun, A. O.; Kumar, A., A review on the current status of various hydrothermal technologies on biomass feedstock. *Renewable and Sustainable Energy Reviews* **2018,** *81*, 1742-1770.

15. Zhao, P.; Shen, Y.; Ge, S.; Yoshikawa, K., Energy recycling from sewage sludge by producing solid biofuel with hydrothermal carbonization. *Energy conversion and management* **2014,** *78*, 815-821.

16. Patil, V.; Tran, K.-Q.; Giselrød, H. R., Towards sustainable production of biofuels from

microalgae. *International journal of molecular sciences* **2008,** *9* (7), 1188-1195.

17. Elliott, D. C.; Biller, P.; Ross, A. B.; Schmidt, A. J.; Jones, S. B., Hydrothermal liquefaction of biomass: Developments from batch to continuous process. *Bioresource Technology* **2015,** *178*, 147-156.

18. Huber, G. W.; Iborra, S.; Corma, A., Synthesis of transportation fuels from biomass: Chemistry, catalysts, and engineering. *Chemical Reviews* **2006,** *106* (9), 4044-4098.

19. López Barreiro, D.; Prins, W.; Ronsse, F.; Brilman, W., Hydrothermal liquefaction (HTL) of microalgae for biofuel production: State of the art review and future prospects. *Biomass and Bioenergy* **2013,** *53*, 113-127.

20. Ramirez, J. A.; Brown, R. J.; Rainey, T. J., A review of hydrothermal liquefaction bio-crude properties and prospects for upgrading to transportation fuels. *Energies* **2015,** *8* (7), 6765-6794.

21. Shah, A. A.; Toor, S. S.; Conti, F.; Nielsen, A. H.; Rosendahl, L. A., Hydrothermal liquefaction of high ash containing sewage sludge at sub and supercritical conditions. *Biomass and Bioenergy* **2020,** *135*, 105504.

22. Chen, W.-T.; Wu, Z.; Si, B.; Zhang, Y., Renewable diesel blendstocks and bioprivileged chemicals distilled from algal biocrude oil converted via hydrothermal liquefaction. *Sustainable Energy & Fuels* **2020,** *4* (10), 5165-5178.

23. Toor, S. S.; Rosendahl, L.; Rudolf, A., Hydrothermal liquefaction of biomass: A review of subcritical water technologies. *Energy* **2011,** *36* (5), 2328-2342.

24. Beckman, D.; Elliott, D. C., Comparisons of the yields and properties of the oil products from direct thermochemical biomass liquefaction processes. *The Canadian Journal of Chemical Engineering* **1985,** *63* (1), 99-104.

25. Gupta, V. G.; Tuohy, M.; Kubicek, C. P.; Saddler, J.; Xu, F., *Bioenergy research:*

advances and applications. Newnes: 2013.

26. Hong, C.; Wang, Z.; Si, Y.; Li, Z.; Xing, Y.; Hu, J.; Li, Y., Preparation of bio-oils by hydrothermal liquefaction (HTL) of penicillin fermentation residue (PR): Optimization of conditions and mechanistic studies. *Science of The Total Environment* **2021,** *761*, 143216.

27. Minowa, T.; Yokoyama, S. y.; Kishimoto, M.; Okakura, T., Oil production from algal cells of Dunaliella tertiolecta by direct thermochemical liquefaction. *Fuel* **1995,** *74* (12), 1735-1738.

28. Shuping, Z.; Yulong, W.; Mingde, Y.; Kaleem, I.; Chun, L.; Tong, J., Production and characterization of bio-oil from hydrothermal liquefaction of microalgae Dunaliella tertiolecta cake. *Energy* **2010,** *35* (12), 5406-5411.

29. Wang, L. K.; Shammas, N. K.; Hung, Y.-T., *Biosolids treatment processes*. Springer: 2007; Vol. 6.

30. Jin, B.; Duan, P.; Xu, Y.; Wang, F.; Fan, Y., Co-liquefaction of micro-and macroalgae in subcritical water. *Bioresource technology* **2013,** *149*, 103-110.

31. Xu, C.; Lancaster, J., Conversion of secondary pulp/paper sludge powder to liquid oil products for energy recovery by direct liquefaction in hot-compressed water. *Water research* **2008,** *42* (6-7), 1571-1582.

32. Sasaki, M.; Adschiri, T.; Arai, K., Fractionation of sugarcane bagasse by hydrothermal treatment. *Bioresource Technology* **2003,** *86* (3), 301-304.

33. Sugano, M.; Takagi, H.; Hirano, K.; Mashimo, K., Hydrothermal liquefaction of plantation biomass with two kinds of wastewater from paper industry. *Journal of Materials Science* **2008,** *43* (7), 2476-2486.

34. Yokoyama, S.; Matsumura, Y., The Asian biomass handbook: a guide for biomass production and utilization. *Thermochemical conversion of biomass, 1st (Ed) part* **2008,** *4*, 71.

35. Mtui, G. Y., Recent advances in pretreatment of lignocellulosic wastes and production of value added products. *African Journal of Biotechnology* **2009,** *8* (8).

36. Sánchez, C., Lignocellulosic residues: biodegradation and bioconversion by fungi. *Biotechnology advances* **2009,** *27* (2), 185-194.

37. McKendry, P., Energy production from biomass (part 2): conversion technologies. *Bioresource technology* **2002,** *83* (1), 47-54.

38. Arun, J.; Gopinath, K. P.; SundarRajan, P.; Malolan, R.; Adithya, S.; Jayaraman, R. S.; Ajay, P. S., Hydrothermal liquefaction of Scenedesmus obliquus using a novel catalyst derived from clam shells: Solid residue as catalyst for hydrogen production. *Bioresource technology* **2020,** *310*, 123443.

39. Hao, B.; Xu, D.; Jiang, G.; Sabri, T. A.; Jing, Z.; Guo, Y., Chemical reactions in hydrothermal liquefaction of biomass and in catalytic hydrogenation upgrading of biocrude. *Green Chemistry* **2021**.

40. Leng, L.; Zhang, W.; Peng, H.; Li, H.; Jiang, S.; Huang, H., Nitrogen in bio-oil produced from hydrothermal liquefaction of biomass: A review. *Chemical Engineering Journal* **2020**, 126030.

41. Obeid, R.; Lewis, D.; Smith, N.; van Eyk, P., The elucidation of reaction kinetics for hydrothermal liquefaction of model macromolecules. *Chemical Engineering Journal* **2019,** *370*, 637-645.

42. Consumption, R. E., Electricity: Preliminary Statistics 2009. *Washington, DC: US Energy Information Administration* **2010**, 14.

43. Scott, J. P.; Ollis, D. F., Integration of chemical and biological oxidation processes for water treatment: review and recommendations. *Environmental Progress* **1995,** *14* (2), 88-103.

44. Suzuki, A.; Nakamura, T.; Yokoyama, S.; Ogi, T.; Koguchi, K., Conversion of sewage

sludge to heavy oil by direct thermochemical liquefaction. *Journal of Chemical Engineering of Japan* **1988,** *21* (3).

45. Goheen, D. W., Lignin Structure and Reactions. *Adv Chem Ser* **1965,** *59*, 205.

46. Sakaki, T.; Shibata, M.; Miki, T.; Hirosue, H.; Hayashi, N., Decomposition of cellulose in near-critical water and fermentability of the products. *Energy & Fuels* **1996,** *10* (3), 684-688.

47. Ying, G.; CHEN, H.-p.; Jun, W.; Tao, S.; Hai-Ping, Y.; Xian-Hua, W., Characterization of products from hydrothermal liquefaction and carbonation of biomass model compounds and real biomass. *Journal of Fuel Chemistry and Technology* **2011,** *39* (12), 893-900.

48. Yin, S.; Tan, Z., Hydrothermal liquefaction of cellulose to bio-oil under acidic, neutral and alkaline conditions. *Applied Energy* **2012,** *92*, 234-239.

49. Peterson, A. A.; Vogel, F.; Lachance, R. P.; Fröling, M.; Antal Jr, M. J.; Tester, J. W., Thermochemical biofuel production in hydrothermal media: A review of sub- and supercritical water technologies. *Energy and Environmental Science* **2008,** *1* (1), 32-65.

50. Yaylayan, V.; Kaminsky, E., Isolation and structural analysis of Maillard polymers: caramel and melanoidin formation in glycine/glucose model system. *Food chemistry* **1998,** *63* (1), 25-31.

51. Biller, P.; Ross, A., Potential yields and properties of oil from the hydrothermal liquefaction of microalgae with different biochemical content. *Bioresource technology* **2011,** *102* (1), 215-225.

52. Wang, Z., Reaction mechanisms of hydrothermal liquefaction of model compounds and biowaste feedstocks. Zhang, Y., Ed. ProQuest Dissertations Publishing: 2011.

53. Gai, C.; Li, Y.; Peng, N.; Fan, A.; Liu, Z., Co-liquefaction of microalgae and

lignocellulosic biomass in subcritical water. *Bioresource technology* **2015,** *185*, 240-245.

54. Xu, C.; Etcheverry, T., Hydro-liquefaction of woody biomass in sub-and super-critical ethanol with iron-based catalysts. *Fuel* **2008,** *87* (3), 335-345.

55. Valdez, P. J.; Tocco, V. J.; Savage, P. E., A general kinetic model for the hydrothermal liquefaction of microalgae. *Bioresource Technology* **2014,** *163*, 123-127.

56. Garcia-Perez, M.; Chaala, A.; Pakdel, H.; Kretschmer, D.; Roy, C., Characterization of bio-oils in chemical families. *Biomass and Bioenergy* **2007,** *31* (4), 222-242.

57. Hietala, D. C.; Faeth, J. L.; Savage, P. E., A quantitative kinetic model for the fast and isothermal hydrothermal liquefaction of Nannochloropsis sp. *Bioresource technology* **2016,** *214*, 102-111.

58. Sheehan, J. D.; Savage, P. E., Modeling the effects of microalga biochemical content on the kinetics and biocrude yields from hydrothermal liquefaction. *Bioresource technology* **2017,** *239*, 144-150.

59. Li, Y.; Leow, S.; Fedders, A. C.; Sharma, B. K.; Guest, J. S.; Strathmann, T. J., Quantitative multiphase model for hydrothermal liquefaction of algal biomass. *Green Chemistry* **2017,** *19* (4), 1163-1174.

60. Safařík, I.; Šantrůčková, H., Direct determination of total soil carbohydrate content. *Plant and Soil* **1992,** *143* (1), 109-114.

61. Vo, T. K.; Kim, S.-S.; Ly, H. V.; Lee, E. Y.; Lee, C.-G.; Kim, J., A general reaction network and kinetic model of the hydrothermal liquefaction of microalgae Tetraselmis sp. *Bioresource technology* **2017,** *241*, 610-619.

62. Ameel, J.; Ruzycki, E.; Axler, R., Analytical chemistry and quality assurance procedures for natural water samples. Central Analytical Laboratory. *Natural Resources Research Institute Technical Report NRRI/TR–98/03 revised annually* **1998**.

63. Folch, J.; Lees, M.; Sloane Stanley, G., A simple method for the isolation and purification of total lipids from animal tissues. *J biol Chem* **1957,** *226* (1), 497-509.

64. Fujihara, S.; Kasuga, A.; Aoyagi, Y., Nitrogen-to-protein conversion factors for common vegetables in Japan. *Journal of food science* **2001,** *66* (3), 412-415.

65. Hatfield, R. D.; Jung, H. J. G.; Ralph, J.; Buxton, D. R.; Weimer, P. J., A comparison of the insoluble residues produced by the Klason lignin and acid detergent lignin procedures. *Journal of the Science of Food and Agriculture* **1994,** *65* (1), 51-58.

66. Obeid, R.; Lewis, D. M.; Smith, N.; Hall, T.; van Eyk, P. J., Reaction kinetics and characterisation of species in renewable crude from hydrothermal liquefaction of mixtures of polymer compounds to represent organic fractions of biomass feedstocks. *Energy & Fuels* **2019**.

67. Akhtar, J.; Amin, N. A. S., A review on process conditions for optimum bio-oil yield in hydrothermal liquefaction of biomass. *Renewable and Sustainable Energy Reviews* **2011,** *15* (3), 1615-1624.

68. Molten, P.; Demmitt, T.; Donovan, J.; Miller, R., Mechanism of conversion of cellulose wastes to liquid in alkaline solution. *Energy from biomass and wastes III. Chicago, IL: Institute of Gas Technology* **1983,** *293*.

69. Ramiah, M., Thermogravimetric and differential thermal analysis of cellulose, hemicellulose, and lignin. *Journal of Applied Polymer Science* **1970,** *14* (5), 1323-1337.

70. Park, W. C.; Atreya, A.; Baum, H. R., Experimental and theoretical investigation of heat and mass transfer processes during wood pyrolysis. *Combustion and Flame* **2010,** *157* (3), 481-494.

71. Austin, D., Method to treat emulsified hydrocarbon mixtures. Google Patents: 2003.

72. Luo, L.; Sheehan, J. D.; Dai, L.; Savage, P. E., Products and kinetics for isothermal

hydrothermal liquefaction of soy protein concentrate. *ACS Sustainable Chemistry & Engineering* **2016,** *4* (5), 2725-2733.

73. Yang, D.; Jones, K. S., Effect of alginate on innate immune activation of macrophages. *Journal of Biomedical Materials Research Part A: An Official Journal of The Society for Biomaterials, The Japanese Society for Biomaterials, and The Australian Society for Biomaterials and the Korean Society for Biomaterials* **2009,** *90* (2), 411-418.

74. Arturi, K. R.; Toft, K. R.; Nielsen, R. P.; Rosendahl, L. A.; Søgaard, E. G., Characterization of liquid products from hydrothermal liquefaction (HTL) of biomass via solid-phase microextraction (SPME). *Biomass and Bioenergy* **2016,** *88*, 116-125.

75. Özçimen, D.; Karaosmanoğlu, F., Production and characterization of bio-oil and biochar from rapeseed cake. *Renewable energy* **2004,** *29* (5), 779-787.

76. Biller, P.; Friedman, C.; Ross, A. B., Hydrothermal microwave processing of microalgae as a pre-treatment and extraction technique for bio-fuels and bio-products. *Bioresource technology* **2013,** *136*, 188-195.

77. Ross, A. B.; Biller, P.; Kubacki, M. L.; Li, H.; Lea-Langton, A.; Jones, J. M., Hydrothermal processing of microalgae using alkali and organic acids. *Fuel* **2010,** *89* (9), 2234-2243.

78. Chen, W.-T.; Zhang, Y.; Zhang, J.; Yu, G.; Schideman, L. C.; Zhang, P.; Minarick, M., Hydrothermal liquefaction of mixed-culture algal biomass from wastewater treatment system into bio-crude oil. *Bioresource technology* **2014,** *152*, 130-139.

79. Biller, P.; Sharma, B. K.; Kunwar, B.; Ross, A. B., Hydroprocessing of bio-crude from continuous hydrothermal liquefaction of microalgae. *Fuel* **2015,** *159*, 197-205.

80. Obeid, R., Smith, N., Lewis, D.M., Hall, T. and van Eyk, P., 2022. A kinetic model for the hydrothermal liquefaction of microalgae, sewage sludge and pine wood with product

characterisation of renewable crude. *Chemical Engineering Journal*, *428*, p.131228.

81. Anastasakis, K.; Ross, A. B., Hydrothermal liquefaction of the brown macro-alga Laminaria Saccharina: Effect of reaction conditions on product distribution and composition. *Bioresource Technology* **2011,** *102* (7), 4876-4883.

CHAPTER 6

CHARACTERISATION OF CHEMICAL PROPERTIES OF THE PRODUCED ORGANIC FRACTIONS VIA HYDROTHERMAL LIQUEFACTION OF BIOSOLIDS

Jasim M. Al-juboori [a,*], David M. Lewis [a], Tony Hall [b] and Philip J. van Eyk [a]

[a] *School of Chemical Engineering & Advanced Materials, University of Adelaide, Adelaide, SA 5005*

[b] *School of Physical Sciences, University of Adelaide, Adelaide, SA 5005*

** Corresponding Author: Jasim.al-juboori@adelaide.edu.au*

Statement of Authorship

Title of Paper	Characterisation of chemical properties of the produced organic fractions via hydrothermal liquefaction of biosolids
Publication Status	☐ Published ☐ Accepted for Publication ☐ Submitted for Publication ☑ Unpublished and Unsubmitted work written in manuscript style
Publication Details	

Principal Author

Name of Principal Author (Candidate)	Jasim Al-juboori
Contribution to the Paper	HTL reactor design and methods HTL batch experiments completed Methods developed for analysing the composition of biosolids HTL products separation and yields quantification completed Interpretation of GC-MS results Writing and editing
Overall percentage (%)	80%
Certification:	This paper reports on original research I conducted during the period of my Higher Degree by Research candidature and is not subject to any obligations or contractual agreements with a third party that would constrain its inclusion in this thesis. I am the primary author of this paper.
Signature	Date 19/08/2021

Co-Author Contributions

By signing the Statement of Authorship, each author certifies that:

i. the candidate's stated contribution to the publication is accurate (as detailed above);

ii. permission is granted for the candidate in include the publication in the thesis; and

iii. the sum of all co-author contributions is equal to 100% less the candidate's stated contribution.

Name of Co-Author	David Lewis
Contribution to the Paper	Concept development Assistance with analysis and interpretation of data Drafting of paper
Signature	Date 19/8/2021

Name of Co-Author	Tony Hall
Contribution to the Paper	Method design and analysis using Source Rock Analyser and GC-MS Drafting of paper
Signature	Date 19/8/21

CHAPTER 6 - CHARACTERISATION OF CHEMICAL PROPERTIES OF THE PRODUCED ORGANIC FRACTION FROM BIOSOLIDS VIA THE HYDROTHERMAL LIQUEFACTION

Name of Co-Author	Philip van Eyk		
Contribution to the Paper	HTL reactor design and methods Concept development Assistance with analysis and interpretation of data Drafting of paper		
Signature		Date	20/8/21

CHAPTER 6 - CHARACTERISATION OF CHEMICAL PROPERTIES OF THE PRODUCED ORGANIC FRACTION FROM BIOSOLIDS VIA THE HYDROTHERMAL LIQUEFACTION

Abstract

Upgradable renewable crude oil produced from the hydrothermal liquefaction (HTL) of municipal wastewater sludge (biosolids) has the potential to be a sustainable feedstock to produce aviation fuels. A range of biosolids with different organic fractions was tested under controlled HTL operating conditions to quantify the quality of the produced renewable crude oil. The HTL results demonstrated that both the HTL reaction conditions and biosolids composition have significant effects on the chemical properties of the produced renewable crude oil. Gas chromatography-mass spectrometry (GC-MS) identified a complex mixture of >300 major compounds in the produced renewable crude oil. The predominant components identified from the lipid, protein, carbohydrate and lignin constituents were cyclic terpanes and terpenes, along with nitrogenous, oxygenated, and phenolic components. Based on the boiling point of the produced compounds, high gasoline and naphtha-like and high diesel-like yields were produced from biosolid samples with high lipid and protein content, while the kerosene-like best yield was generated from a high lipid sample. A significant gas oil-like yield was produced from the high lipid and carbohydrate biosolid samples, while a high-yield of wax, lubricating oil and vacuum gas oil-like contents were generated from the high lignin sample.

Keywords: Hydrothermal liquefaction, Biosolids composition, Sustainability, Aviation, Reaction conditions, Renewable crude oil.

1. Introduction

Prior to the discovery of fossil fuels, the world depended on biomass to fulfil energy demands. In the 19th century, the discovery of inexpensive fossil fuel led to global industrialisation[1], which led to petroleum fuel being the main dependent energy source. The continued dependence on fossil fuels must inevitably end in the foreseeable future due to the decline in fossil fuel resources[2]. This has accelerated the need for alternative sources of renewable energy, in particular heavy transportation fuels[3]. In addition, fossil fuel consumption is complemented by global climate change and other environmental pollution issues. Sustainable feedstocks are required to provide the energy needs for heavy transportation, which have a less environmental impact than fossil fuels and ultimately have a neutral carbon footprint and cost parity. Biomass sourced from waste could provide a sustainable feedstock for heavy transportation fuels, which could also lead to sustainable waste management practices for these wastes, i.e., a circular economy linking waste to sustainable fuels. Biosolids are a potential sustainable feedstock for heavy transportation fuels. In 2011, the annual global production of biosolids was over 17 billion tonnes[4], which provided significant waste management challenges. Biosolids, the by-products of conventional wastewater treatment processes, have been identified as an ideal candidate as an alternative energy source[5].

Many technologies can be applied to recover energy from waste, including biosolids, such as pyrolysis, gasification, and direct combustion; however, these technologies require a drying step, which requires a high energy input[5]. Over the last two decades, HTL has been applied to a wide range of wet biomass feedstocks with moisture contents ranging between 30 to 70 wt%, including biosolids, swine manure and microalgae[6-8]. HTL provides a promising

thermochemical process to convert biosolids into renewable crude oil at a subcritical condition[9], obviating the need for the dewatering stage.

The HTL process produces four phases: renewable crude oil, aqueous, gaseous and solid phases[10]. Renewable crude oil production via the HTL process can be achieved by breaking down biosolids' macromolecules and reforming them via dehydration and decarboxylation reactions at temperatures between 200 to 350°C, pressures between 50 to 250 bar, and residence time between 1 and 60 minutes[11-14]. The renewable crude oil yield from the HTL of biomass can range from 10 to 60 wt%[5]. The HTL process could be a progressive technology to produce reasonable yields of renewable crude oil from biosolids, which could be equivalent to conventional crude oil[15, 16] and provide a sustainable management option biosolids. However, more research is required to identify the effects of different biosolids' content on renewable crude oil composition, which has proven to be a significant challenge in optimising the HTL process and improving its economic viability.

The produced renewable crude oil via the HTL of biomass has many positive characteristics, such as low moisture and low oxygen contents, leading to an increase in its energy content[17]. However, there is a critical difference between fossil crude and renewable crude oil. The fossil crude consists of a mixture of liquid hydrocarbons created naturally under the earth's surface[18]. In comparison, renewable crude oil contains high heteroatom contents, mainly sulphur, nitrogenous and oxygenated compounds, which leads to the replacement of carbon in the molecular structure[19, 20]. This results in many undesirable fuel properties, such as polymerisation, oil acidity, corrosive activity, high viscosity, low storage stability, high-boiling distribution and combustion performance[21-23]. According to Jazrawi[24], HTL reaction conditions

and biomass composition strongly affect biomass conversion and product yields and lead to heteroatoms in the produced renewable crude. For example, processing high-nitrogen content feedstocks, such as high-protein microalgae, significantly increased the nitrogen levels of the renewable crude oil[25, 26]. Therefore, the complexity of the produced renewable crude oil represents an analytical challenge and requires more research to identify its characterisation. Additionally, renewable crude oil may likely require an upgrade process like hydro-deoxygenation to reach similar properties of transportation fuels[27-30].

Renewable crude oil properties produced via HTL are mostly dependent on the biomass content[31]. The organic content of biosolids varies widely, which greatly influences the renewable crude oil composition. Biosolids' qualities, specifically their biological and chemical composition, depend on the treated waste and treatment methods[32, 33]. Most of the analysed biosolids in the scientific literature differ in physical and chemical[34]. According to the scientific literature, biosolids consist of a mixture of organic content, typically having a composition of 6% to 30 % lipids, 20% to 30% proteins, 20% to 40% carbohydrates, and around 6% lignin[35-37]. Rural sewage sludge typically contains higher organic carbon and nitrogen than municipal waste, but its phosphorus content is lower than for municipal waste[34].

The effect of specific biomass composition on produced renewable crude oil via the HTL process has been investigated and reported in several studies[38-40]. For example, researchers reported that the composition of the produced renewable crude oil via the HTL of biomass, such as algae, manure, and sludge, was influenced by the ratio of the organic content of the biomass[41, 42]. The renewable crude oil from these investigations contained a range of chemical compounds, such as fatty acids, carboxylic acids, phenolic components, nitrogenous and non-

nitrogen compounds, ketones, aldehydes, alkanes, alkenes and their derivatives[43-45]. However, much of the scientific literature on the HTL has been on the conversion of individual model compounds, such as triacylglycerides, linoleic acid, glutamic acid, cellulose, glucose, guaiacol and alkali lignins. Fewer studies have been made regarding the produced components via a mixture of model compounds or biomass. Consequently, there is limited information to validate the effects of the interactions between the biosolid content under HTL reaction conditions on the renewable crude oil composition. The key objectives of the reported investigation were to assess the use of biosolids samples with a dominant organic fraction, such as lipid, protein, carbohydrate, or lignin via a range of HTL reaction conditions to quantify their effects on the composition of the produced renewable crude oil.

2. Materials and methods

2.1 Feedstocks

The Melbourne Water Corporation provided biosolid samples from the Western Treatment Plant in Werribee, Victoria, Australia. Twenty-one, different biosolids samples were randomly collected from various stockpiles. The collected biosolids samples differed in terms of sunlight position, age, and the samples' depth when taken from the stockpiles.

2.2 Biosolids' characteristics

The organic composition of the biosolid samples was quantified using modified methods:

- The organic and inorganic materials in the biosolids samples were quantified using the Dry-Ash Free basis (DAF) method[46].
- The protein content in the biosolids was estimated based on the total nitrogen content[47].

- The lipids content was measured using the Folch method[48].
- The carbohydrates content was quantified using the Safařík and Šantrůčková method[49].
- The conventional method for lignins quantification was determined using the Klason lignins and acid-soluble lignins test[50].

Analysing the major elements of biosolids, including carbon, hydrogen, nitrogen, oxygen, and sulphur was undertaken using a Perkin Elmer 2400 Series II CHNO&S analyser. Oxygen was calculated by subtraction. The selected biosolid samples were characterised as HC (high carbohydrate), HP (high protein), HL (high lipid), and HLG (high lignin) based on a dry-ash free basis. The biochemical composition (% DAF) of the biosolids varied widely. The HC sample comprised 63% inorganic material, 4% water and 33% organic material. The organic fraction was made up of 44% carbohydrate, 32% protein, 4% lipid, 16% insoluble lignin and 4% soluble lignin. The HP sample comprised 59% inorganic material, 4% water and 37% organic material. The organic fraction was made up of 25% carbohydrate, 49% protein, 6% lipid, 14% insoluble lignin and 4% soluble lignin. The HL sample comprised 59% inorganic material, 5% water and 36% organic material. The organic fraction was made up of 30% carbohydrate, 26% protein, 32% lipid, 12% insoluble lignin and 4% soluble lignin. The HLG sample contains insoluble lignin 32%, soluble lignin 4%, carbohydrate 42%, protein 23%, lipid 6%, inorganic content 70% and moisture 4%. At the same time, the elemental composition of the HC sample was 59% carbon, 10% hydrogen, 5% nitrogen, 22% oxygen, and 3% sulphur. In comparison, the HP sample contained 59% carbon, 10% hydrogen, 8% nitrogen, 19% oxygen, and 5% sulphur; the elemental composition of the HL sample was 52% carbon, 9% hydrogen, 4% nitrogen, 31% oxygen, and 3% sulphur, and the HLG sample was 33% carbon, 7% hydrogen, 4% nitrogen, 52% oxygen, and 4% sulphur.

2.3 Hydrothermal liquefaction of biosolids

The biosolid samples were first dried at 45ºC in a Memmert 400 Drying Oven until a constant mass weight was reached. Prior to the HTL experiments, the biosolid samples were ground and sieved to a particle size of less than (142 µm). The biosolid samples' particle size was quantified using a particle size analyser (Malvern Mastersizer 2000). HTL experiments were conducted in triplicate in a high-pressure batch reactor with 11 mL volume, filled with 5.5 g of the reactants. The reactor was loaded with 1.65 g of dried biosolids and 3.85 g of water. The total biosolids loading represented 30 wt % with 70 wt % water. The sealed reactor was filled and purged three times with nitrogen to remove any residual air from inside the reactor. The nitrogen was charged was 90 bar at the start of each experiment, which was adjusted to maintain the pressure at 200 bar for all HTL experiments at the required reaction temperature.

The HTL reactions of biosolids were undertaken at temperatures of 250, 300, and 350°C and reaction residence times of 5, 20 and 60 minutes. The batch reactor was placed in a Techne SBL-2D fluidised bed with a Techne-9D temperature controller and heated to the required reaction temperature. The batch reaction timer was set at 20, 40 or 60 minutes once the temperature reached 98% of the target temperature. At the completion of the reaction residence time, the reactor was removed from the fluidised bed and was gradually air-cooled to 70ºC using a ventilator located at the top of the reactor. The reactor was then quenched in cold water, dried and weighed (before and after the HTL experiment). The gaseous product (plus N_2) was released to determine the gas yield (by weight) produced from the HTL of biosolids. The gaseous product yield was calculated by subtracting the initial N_2 mass to the batch reactor from the total mass of the released gases.

The remaining content in the reactor vessel was separated by opening the reactor's top and collecting the products, which consisted of solids, an aqueous phase, and the renewable crude oil; in a centrifuge tube after decanting the aqueous phase into another centrifuge tube. The reactor was then cleaned with deionised water to remove any soluble oil and solids stuck to the reactor walls, and the washings were added to the decanted aqueous phase. In most cases, the viscous renewable crude oil and the solids residue were bound together.

The produced solid products were then dried in a Memmert 400 Drying Oven at 40^{o}C for 72 hours to remove moisture. The resulting solid product contained renewable crude oil and solid residue. The mass of the aqueous phase was determined by subtracting the final mass of the produced renewable crude oil, solid and gas phases from the mass of the biosolid mass initially loaded into the reactor. The yield of each product phase was calculated by dividing the mass of each product phase by the initial mass of the biosolids that were initially fed into the reactor.

2.4 Biocrude oil characterisation

2.4.1 Thermal desorption and pyrolysis of organic matter

A Source Rock Analyser (SRA) was employed to pyrolyse the produced solid phase and renewable crude oil to determine the organic matter (OM) content. The OM was quantitatively measured by heating the samples to a programmed temperature in a controlled atmosphere with detection by either a flame ionisation detector (hydrocarbons) or infra-red spectrometry CO_2 & CO. The measurement of the total organic content was based on the Weatherford Certified References Standard 533.

The samples were pulverised and passed through a 40-mesh sieve. 20 to 40 mg of the samples were weighed, loaded into SRA crucibles and placed in the SRA auto-sampler carousel. The crucible was then moved from the auto-sampler tray to the SRA pedestal, loaded into the oven base, and purged under helium carrier gas (99.9999% Ultra-pure Grade) at 120ºC for 90 seconds. The crucible was then raised into the furnace and held isothermally at 300ºC for 3 minutes. During thermal extraction, the free hydrocarbons (S1 fraction) were volatilised and quantitatively detected using the FID detector and reported as milligrams per gram of biosolids. Following the isothermal heating step, pyrolysis was conducted by increasing the oven temperature by 25 ºC/min to 600ºC. The hydrocarbons generated from the kerogen's pyrolytic degradation in the biosolids (S2 fraction) represent the residual OM's productive potential, and S3 represents the released carbon dioxide from the OM.

In the final oxidation stage, the oven was cooled to 400ºC, and the carrier lines were switched to CO_2 free instrument grade air and purged for 5 minutes. The oven temperature was then increased to 540ºC at a maximum heating rate and held isothermally for 15 minutes. The residual inert OM (S4 fraction) was converted to CO and CO_2 during the oxidation stage, detected in the IR cells and reported as milligrams per gram of the biosolids.

2.4.2 GC-MS of the renewable crude oil

GC-MS analysis was conducted on the renewable crude oil fractions, which was bound to the produced solid residue from the HTL of biosolids using an Agilent 5977B MSD and 7890 GC gas chromatograph-mass spectrometer fitted with a Quantum MSSV pyrolysis injector. A J&W Scientific DB-5MS (60 m × 0.25 mm inner diameter × 0.25 μm phase thickness) capillary column with helium carrier gas at 1 mL/min flow were utilised for compound separation.

Approximately 4 mg of the biosolids sample was loaded into pre-cleaned MSSV glass tubes, which had a sealed capacity of 100µL, sealed, and placed into the Quantum MSSV injector at 300°C. The tube was then taken through a fast-ramped GC heating cycle to remove any possible exterior organic components and allow desorption of the bound organic fraction. The tube was cracked open within the MSSV injector, and evolved components were cryofocused in liquid nitrogen on the capillary head for 1 minute before analysis. The temperature inside the oven was programmed at 35°C, which was then held for 1 minute, prior to a 10°C/min ramp to 300°C, which was held for 14 minutes. The mass spectrometer was operated in full scan mode from m/z 20 to 500 at approximately 3 scans per second. Agilent Chemstation software was utilised to determine the individual components and then compared with the NIST14 spectral library database.

2.4.3 Renewable crude oil fractions' distribution

The renewable crude oil fraction distributions were defined based on the organic geochemistry distributions for refined fossil fuels[51]. The fuel fractions of the renewable crude oil were based on the following boiling point ranges:

- Gasoline and naphthas-like being 80 to 205°C
- Kerosene-like 205 to 255°C
- Diesel-like 205 to 290°C
- Gas oil-like 255 to 425°C
- Wax, lubricating oil and vacuum gas oil-like 425 to 600°C

Retention time ranges for these boiling point distributions were assigned by reference to saturated hydrocarbon standards containing nC$_6$ to nC$_{40}$, where compounds below 3 minutes' retention time were classified as non-renewable crude oil. It should be noted that there were

retention time differences observed between the capillaries used in the analyses; both were J&W DB5-MS columns with dimension 60m x 0.25mm ID and 0.25um phase thickness, but the initial capillary from 2019 was older and had been replaced before the later analyses in 2020. As shown in Table 1, the second set of experiments include HL S, 250°C, 20 mins, 300°C, 20 mins and 350°C, 40 mins and 60 mins, HP S, 250°C, 60 mins, 300°C, 60 mins, 350°C, 20 mins and 40 mins, HC S, HLG S, 250°C, 20 mins, 300°C, 60 mins, 350°C, 40 mins. The remaining samples represent the first set. In addition, there was a noticeable difference between the data obtained from GC-MS and the data obtained from thermogravimetric analysis (TGA) in terms of determining the distribution of the renewable crude oil fractions. Because TGA is not an organic-specific methodology, inference of composition is based upon loss of mass alone and not on the chemical composition of the evolved product over the temperature range. Therefore, any additional mass loss was from non-organic components, such as dehydration of clays and thermal decomposition of carbonate phases. SRA data provides a quantification of the organic phase released from a sample, whilst GC-MS data allowed for characterisation of the individual chemical compounds produced as the renewable crude oil. As such, the combination of SRA and GC-MS should provide a more accurate representation of the actual composition.

Table 1: Hydrocarbon number ranges, retention time and associated boiling point, ranges of the renewable crude oil via the HTL of biosolids.

The renewable crude oil fractions	Hydrocarbon range	Retention time for analyses set 1	Retention time for analyses set 2
Gasoline and naphthas (80-205°C)	C4-C11	3 to 8.5	3 to 10.5
Kerosene (205-255°C)	C11-C15	8.5 to 15.5	10.5 to 17.8
Diesel (205-290°C)	C11-C20	8.5 to 22	10.5 to 24.7
Gas oil (255-425°C)	C15-C32	15.5 to 34	17.8 to 36.5
Wax, lubricating oil and vacuum gas oil (425-600°C)	>C30	>32	>34

3. Results and discussion

3.1 Identification of renewable crude oil compounds via GC-MS

Biosolids have different compositions with a wide range of organic constituents, such as lipids, proteins, carbohydrates and lignins, as well as their inorganic content. Compounds produced via HTL are influenced mainly by the ratio of organic fractions in the feedstock[52, 53]. Thus, the derived renewable crude oil consists of a complex mixture of compounds, which may also vary with different HTL operating parameters[54, 55]. Characterisation of produced compounds of the biosolids samples and its produced renewable crude oil via the HTL was carried out using GC-MS analysis. In this work, more than 300 major compounds were identified in the biosolids samples and their produced renewable crude oil. For each sample, 25 to 35 significant compounds were interpreted and reported, representing 50 to 90% of the total weight of renewable crude oil produced. The area under each chromatographic peak as a proportion of the total area represents the proportions of individual compounds in renewable crude oil. The major compounds identified in this study have also been founds by others, which were used for comparison. In general, the GC-MS analysis revealed that the predominant components identified were:

- From the lipids: cyclic terpanes and terpenes compounds, such as cholestane and cholestene, their isomers and homologues[56-58].
- From the proteins: nitrogenous compounds, including amines, pyrrolidones and pyrazines[59].
- From the lignins: phenolic components, such as phenol, methyl and methoxy phenols[60].
- From the carbohydrates: oxygenated compounds, such as complex phenols, aldehydes and ketones[60, 61].

The following section contains an analysis of the produced renewable crude oil composition via the HTL of biosolids. A comprehensive list of interpreted compounds identified by GC-MS is found in the supplementary data, including references to their assigned origins.

3.1.1 GC–MS of the HL sample and the produced renewable crude via the HTL process

GC−MS of the HL sample before the HTL was conducted, and the identified compounds are shown in Figure 1 and Table 2. The HL sample contained high lipids content compared to other biosolids samples. The main produced compounds were from lipid constituents with a smaller representation of compounds derived from the organic macromolecules of protein, carbohydrate and lignin. The primary lipid organic macromolecules generally broke down to produce cyclic terpanes and terpenes, and the protein constituents produced nitrogenous compounds. The interaction between the organic constituents generated a broad spectrum of oxygenated and deoxygenated compounds in minor amounts.

GC−MS of the produced renewable crude oil via the HTL of the HL sample revealed that similar components were produced but in varying proportions. The relevant data are shown in Figure 1 and Table 3, and Figure S1and Tables S1, S2, S3, S4, S5, S6, S7 and S8 of Appendix D. At 250°C and 20 minutes' residence time, the produced renewable crude oil components were generated mainly from the lipid constituents. Saisu *et al.*[62] reported similar results, concluding that more crude oil components were derived from the lipids. Because lipids hydrolysed more readily at low temperatures than other components[63], resulting in the breakdown of triglycerides to fatty acids and glycerol[64]. The second most abundant compounds

were nitrogenous compounds generated from protein, which was similar to the reported results by Vardon *et al.*[23] for the HTL of sludge. The interaction between the organic compounds produced small amounts of various compounds, including cyclic terpanes and terpenes, oxygenated aromatics, and carboxylic acids compounds.

A greater proportion of the lipid fraction was broken down by increasing the residence time to 40 minutes. Simultaneously, there was a reduction in the proportion of produced compounds attributable to the protein, carbohydrate and lignin fractions. In addition, there were compounds below the boiling point of crude oil generated from protein and carbohydrate via the Maillard reaction, such as nitrogenous compounds. At 60 minutes reaction time, the produced compounds from lipid, protein, carbohydrate and lignin constituents slightly increased, which was similar to that reported in the scientific literature[20, 42]. At reaction times of 20 and 40 minutes, similar amounts of compounds were produced with a boiling point below the boiling point of crude oil generated from protein, carbohydrate, and lignin. Also, the produced carboxylic acids and nitrogenous compounds decreased with the increase in reaction time due to the decrease in the conversion of protein and carbohydrate constituents[44, 65].

At 300°C reaction temperature, there was an increase in the produced components from the lipid fraction with smaller proportionate of compounds attributable to the protein, carbohydrate, and lignin fractions. At 60 minutes' reaction time, some produced compounds were below the boiling point of crude oil generated, such as carboxylic acids and nitrogenous compounds. At a reaction temperature of 350°C, increasing the residence time from 20 to 40 minutes led to a decrease in the produced components from the lipid constituents and an increase in the produced components from other organic content. However, increasing the

residence time to 60 minutes reversed this trend where the amount of the phenolics and nitrogenous compounds were increased. At 350°C and 40 minutes residence time, the interaction between the constituents of organic content produced significant amounts of oxygenated aromatics and nitrogenous and phenolic components.

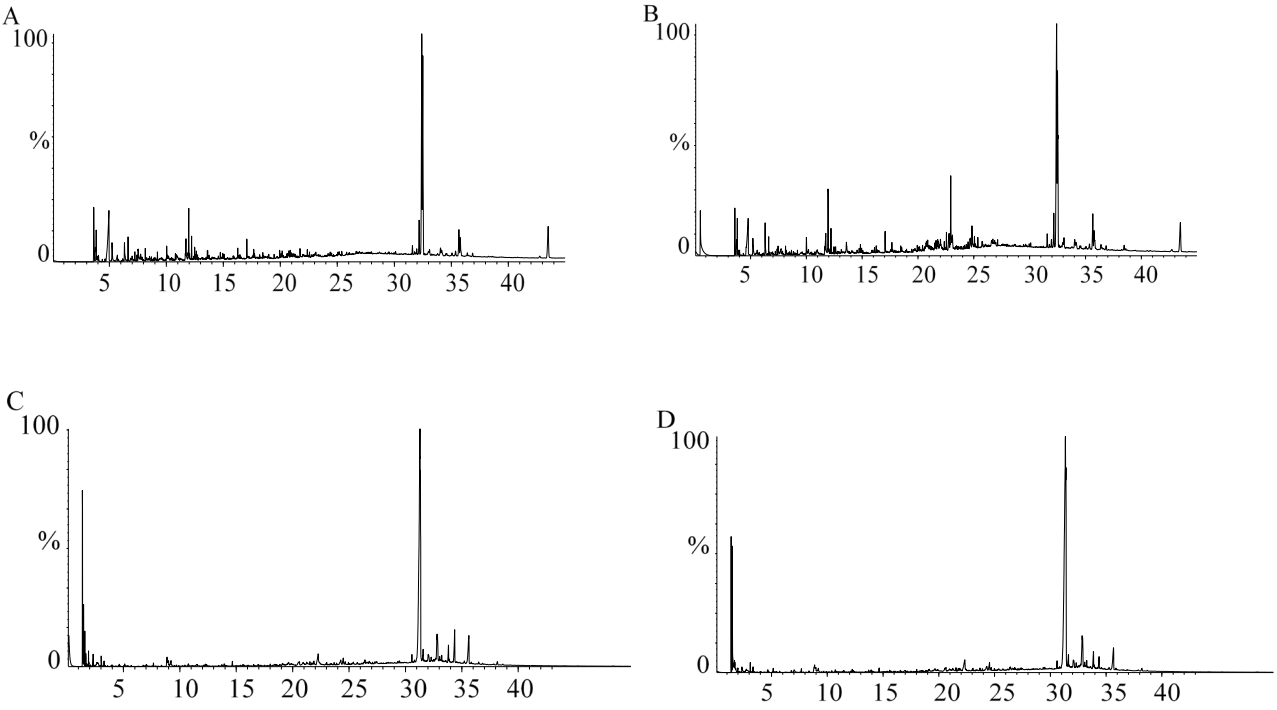

Figure 1: Chromatogram of GC-MS of HL sample: (A) before HTL process, (B) at 250ºC reaction temperatures and 20 minutes residence time, (C) at 250ºC reaction temperatures and 40 minutes residence time, (D) at 250ºC reaction temperatures and 60 minutes residence time.

Table 2: The major identified compounds in the HL sample before the HTL process using GC-MS analysis.

HL S							
No	**Retention time (mins)**	**Area**	**Area (%)**	**Compound name**	**Molecular formula**	**Molecular weight (g/mol)**	**Classification of compound**
1	3.624	10064483	3.83	Carbon dioxide	CO_2	44	Protein[64, 6]
2	3.773	3184850	1.21	Methanol	CH_3OH	32	Lignin[68]
3	3.837	4016503	1.53	Methanethiol	CH_4S	48	Probably bacterial products[122]
4	4.959	23586607	8.98	Acetic acid	CH_3COOH	60	Carbohydrate, Lignin[64]
5	5.226	4055888	1.54	2-Butanone	C_4H_8O	72	Carbohydrate[107]
6	5.696	1974664	0.75	Propanoic acid	$C_3H_6O_2$	74	Lipid, Protein[101]
7	6.327	4333720	1.65	Disulfide, dimethyl	$C_2H_6S_2$	94	Probably bacterial products[21]
8	6.636	2362051	0.90	Toluene	C_7H_8	92	Lipid, Protein, Carbohydrate[64]
9	7.523	3203731	1.22	Pyrazine, methyl-	$C_5H_6N_2$	94	Protein[44, 52]
10	7.748	2169557	0.83	Pentanoic Acid	$C_5H_{10}O_2$	102	Lipid[61]
11	10.023	2608745	0.99	Phenol	C_6H_6O	94	Protein, Carbohydrate, Lignin[29, 52, 106]
12	10.878	1682492	0.64	2-Pyrrolidinone, 1-methyl-	C_5H_9NO	99	Protein[29]
13	11.722	6039428	2.30	p-Cresol	C_7H_8O	108	Protein, Carbohydrate[64, 6]
14	11.967	7138334	2.72	2,5-Pyrrolidinedione, 1-methyl-	C_5H_7NO	113	Protein[64]
15	12.213	2535773	0.97	Methyl creatinine	$C_4H_7N_3O$	113	Protein[44]
16	13.623	2066441	0.79	2,5-Pyrrolidinedione, 1-propyl-	$C_7H_{11}NO_2$	141	Protein[64]
17	16.262	1801689	0.69	2,5-Pyrrolidinedione, 1-pentyl-	$C_9H_{15}NO_2$	169	Protein[45]
18	17.053	2724639	1.04	1H-Isoindole-1,3(2H)-dione,2-methyl-	$C_9H_7NO_2$	161	Protein[64]
19	31.582	1701667	0.65	Cholestene isomer (3?)	$C_{27}H_{46}$	370	Lipid[45, 52, 88, 106]
20	32.169	6827997	2.60	Cholestene isomer (4?)	$C_{27}H_{46}$	370	Lipid[45, 52, 88, 106]
21	32.404	55052547	20.97	Cholest-2-ene	$C_{27}H_{46}$	370	Lipid[45, 52, 88, 106]
22	32.49	43178822	16.44	Cholestane	$C_{27}H_{48}$	372	Lipid[45, 52, 88, 106]
23	35.663	6662707	2.54	Stigmastene isomer (2?)	$C_{29}H_{50}$	398	Lipid[51]
24	35.78	5218938	1.99	Stigmastane	$C_{29}H_{52}$	400	Lipid[88]
25	43.504	12444854	4.74	Dihydroxychloesterol	$C_{27}H_{46}O_3$	418	Lipid[17]
Total yields %			**82.51**				

Table 3: The major identified compounds of the produced renewable crude oil via the HTL process from the HL sample at reaction temperature of 250°C and residence time of 20 minutes using GC-MS analysis.

HL 250°C 20 Mins							
No	**Retention time (mins)**	**Area**	**Area (%)**	**Compound name**	**Molecular formula**	**Molecular weight (g/mol)**	**Classification of compound**
1	3.602	8686773	1.85	Carbon dioxide	CO_2	44	Protein[64, 6]
2	3.827	5925000	1.26	Methanethiol	CH_4S	48	Probably bacterial products[122]
3	4.799	24209945	5.15	Acetic acid	CH_3COOH	60	Carbohydrate, Lignin[64]
4	5.216	6056347	1.29	Propanoic acid	$C_3H_6O_2$	74	Lipid, Protein[101]
5	6.316	6830590	1.45	Disulfide, dimethyl	$C_2H_6S_2$	94	Probably bacterial products[21]
6	10.012	4072806	0.87	Phenol	C_6H_6O	94	Protein, Carbohydrate, Lignin[29, 52, 106]
7	11.754	8394147	1.79	p-Cresol	C_7H_8O	108	Protein, Carbohydrate[64, 6]
8	11.946	17625518	3.75	2,5-Pyrrolidinedione, 1-methyl-	C_5H_7NO	113	Protein[64]
9	12.213	3911829	0.83	Methyl creatinine	$C_4H_7N_3O$	113	Protein[44]
10	13.602	4578338	0.97	2,5-Pyrrolidinedione, 1-propyl-	$C_7H_{11}NO_2$	141	Protein[64]
11	17.063	3955699	0.84	1H-Isoindole-1,3(2H)-dione,2-methyl-	$C_9H_7NO_2$	161	Protein[64]
12	22.02	3319925	0.71	Phenol, 3,5-dimethoxy-	$C_8H_{10}O_3$	154	Protein, Carbohydrate, Lignin[19, 31, 86]
13	22.789	8412822	1.79	Biphenylol isomer	$C_{12}H_{10}O$	170	Lipid, Protein, Carbohydrate[31, 22]
14	22.939	18388496	3.91	n-Hexadecanoic acid	$C_{16}H_{32}O_2$	256	Lipid, Protein, Carbohydrate[12, 64]
15	23.089	3226678	0.69	5,10-Diethoxy-2,3,7,8-tetrahydro-1H,6H-dipyrrolo [1,2-a;1',2'-d] pyrazine	$C_{14}H_{22}N_2O_2$	250	Protein[74]
16	24.691	5333793	1.13	Oleic Acid	$C_{18}H_{34}O_2$	282	Lipid[22]
17	24.841	6430183	1.37	Octadecanoic acid	$C_{18}H_{36}O_2$	284	Lipid[22]
18	31.582	3614361	0.77	Cholestene isomer (3?)	$C_{27}H_{46}$	370	Lipid[45, 52, 88, 106]
19	32.169	9909523	2.11	Cholestene isomer (4?)	$C_{27}H_{46}$	370	Lipid[45, 52, 88, 106]
20	32.426	95019396	20.21	Cholest-2-ene	$C_{27}H_{46}$	370	Lipid[45, 52, 88, 106]

21	32.5	67744861	14.41	Cholestane	$C_{27}H_{48}$	372	Lipid[45, 52, 88, 106]
22	33.077	3783859	0.80	Cholestadiene isomer	$C_{27}H_{44}$	368	Lipid[45, 52, 88, 106]
23	35.663	11957051	2.54	Stigmastene isomer (2?)	$C_{29}H_{50}$	398	Lipid[51]
24	35.78	8167560	1.74	Stigmastane	$C_{29}H_{52}$	400	Lipid[88]
25	43.504	16349604	3.48	Dihydroxychloesterol	$C_{27}H_{46}O_3$	418	Lipid[17]
Total yields %			**75.68**				

3.1.2 GC–MS of the HP sample and the produced renewable crude via the HTL process

GC−MS of the HP sample before the HTL process was conducted and the identified compounds are illustrated in Figure S2 and Table S9 of Appendix D. The HP sample contained a high protein content in comparison with the other tested biosolids samples. However, the major produced compounds were from the lipid constituents and fewer than that from the constituents of other organic content. The produced compounds from the lipid and protein constituents were cyclic terpanes, terpenes, and nitrogenous compounds. This is similar to the scientific literature, where the protein constituents produce nitrogenous compounds, such as toluene and pyridine[66]. Also, amino acids broke down to ammonia, which is decarboxylated to produce amines and carbon dioxide[67]. At the same time, the primary organic macromolecules of carbohydrates broke down to produce oxygenated compounds. There were also cyclic terpanes, terpenes, deoxygenated compounds and phenolic components produced from the interactions between the organic content.

The identified compounds of the HP sample and its produced renewable crude oil via the HTL were similar but with a different distribution, as shown in Figure S2 and Tables S10, S11, S12, S13, S14, S15, S16, S17 and S18 of Appendix D. At 250°C reaction temperature and 20

minutes' residence time, the hydrolysis represented the major reaction of the lipid and protein constituents, which produces polymers across many reaction pathways[68]. However, the amounts of the produced compounds were mostly from lipid, with small amounts produced from other organic content. Similarly, Obeid *et al.*[69] reported that fatty acids were the main components in the crude oil at temperatures around 250°C associated with some products decomposed from amino acids. Increasing the residence time to 40 minutes did not show an important change in the produced compounds; however, there was a double increase in the amount of compounds below the boiling point of crude oil, such as nitrogenous and oxygenated compounds[70]. Increasing the residence time to 60 minutes led to an increase in the produced compounds from protein, carbohydrate, and lignin constituents and a decrease in the produced compounds from lipid constituents.

At 300°C reaction temperature, increasing the residence time led to a slight decrease in the produced compounds from lipid constituents and increased the produced compounds from other organic content. At 350°C reaction temperature, the amounts of the produced compounds from the lipid constituents did not show a significant change. In contrast, the amount of the produced compounds from the carbohydrate and lignin constituents decreased with the increase in residence time. However, the produced nitrogenous compounds from the protein constituents rose at 40 minutes before decreasing again at 60 minutes. Long residence times in the HTL of proteins allow the primary organic macromolecules to achieve decarboxylation, deamination, and to re-polymerise to longer chain hydrocarbons and aromatic ring-type structures, such as phenols and nitrogen heterocycles' indoles or pyrroles[42].

3.1.3 GC–MS of the HC sample and the produced renewable crude via the HTL process

GC−MS of the HC sample before the HTL process was conducted, and the identified compounds are shown in Figure S3 and Table S19 of Appendix D. The HC sample contained a high carbohydrate content in comparison with the other tested biosolids samples. However, the major produced compounds were from the lipid constituents and fewer than those from other organic content. The produced compounds from the lipid and protein constituents broke down into cyclic terpanes, terpenes, and nitrogenous compounds, while the lignin and carbohydrate constituents only produced phenolic components. The interaction between the organic content generated oxygenated compounds, cyclic terpanes and terpenes and phenolic components. It was noticeable that carboxylic acids formed the highest concentration of acetic acid due to the hydrolyses of cellulose, which degrades to produce carboxylic acids[44, 71].

GC−MS of the produced renewable crude oil from the HC sample was conducted. The identified compounds of the HC sample and its produced renewable crude oil via the HTL were similar but with a different distribution, as shown in Figure S3 and Tables S20, S21, S12, S23, S24, S25, S26, S27 and S28 of Appendix D. In contrast with the HP samples, at 250°C and 300°C reaction temperatures, the produced compounds from the carbohydrate, protein, and lignin constituents decreased with the increase in residence time, while at 350°C, they showed a slight increase with the increase in residence time. In contrast, the produced compounds from the lipid constituents showed an opposite behaviour and increased with the increase in residence time at 250°C, while they mostly sustained at 300°C and 350°C reaction temperatures, despite the increase in residence time.

At 250°C and 20 to 40 minutes' reaction time, similar compounds were produced from the lipid constituents, while the lignin and carbohydrate constituents only produced phenolic components and oxygenated aromatics. At the same reaction times, there were high amounts of compounds below the boiling point of crude oil, mostly produced from protein and bacteria. However, at 60 minutes' reaction temperature, there was a reduction in the amounts of compounds below the boiling point of crude oil. While at 350°C reaction temperature, the produced compounds below the boiling point of crude oil were increased with the increase in reaction time to 40 minutes before decreasing again at 60 minutes.

3.1.4 GC–MS of the HLG sample and the produced renewable crude via the HTL process

The identified compounds from HLG samples before the HTL process via the GC−MS analyser are shown in Figure S4 and Table S29 of Appendix D. The HLG sample contained a high lignin content compared with the other tested biosolids samples; however, the main compounds produced were from the lipid constituent, and fewer were derived from the constituents of other organic content, and included cyclic terpanes, terpenes, nitrogenous compounds, carboxylic acids and phenolic components.

GC−MS of the produced renewable crude oil from the HLG sample was conducted. The distribution of the identified compounds of the HLG sample and its produced renewable crude oil were similar but with a different distribution, as shown in Figure S4 and Tables S30, S31, S32, S33, S34, S35, S36, S37 and S38 of Appendix D. At 250°C reaction temperature, the produced compounds from the lignin, protein and carbohydrate constituents decreased with the

increase in residence time. At 300ºC, there was opposite behaviour, as the produced compounds from protein, carbohydrate and lignin constituents showed an increase in residence time, while the produced compounds from the lipid constituents showed a decrease with the increase in residence time. According to Kruse *et al.*[72], at 300ºC reaction temperature, the protein and carbohydrate reactions increased in residence time due to the increase in the produced nitrogenous compounds, such as pyrazines[73].

At 350°C, the produced compounds from lignin, protein and carbohydrate continued to increase in residence time to 40 minutes before decreasing again at 60 minutes. At 350°C reaction temperature and 20 minutes, it was noticeable that carbohydrate and lignin constituents produced different carboxylic acid and phenolic components. There were also oxygenated aromatic compounds, mainly formed from lignin constituents with considerable contribution from protein. It was also noticeable that at 250°C reaction temperature and 40 minutes' residence time, the produced compounds below the boiling point of crude oil were double the amount for 20 minutes' residence time where most of the compounds were generated from lignin and carbohydrate.

3.2 The yield of identified components in renewable crude oil

The renewable crude oil yields from the HC, HP, HL, and HLG samples were as follows; the values are based on a dry ash-free basis (daf):

- HL: 11 to 22 wt%
- HC: 10 to 22 wt%
- HP: 9 to 22 wt%
- HLG: 8 to 27 wt%

3.3 Renewable crude oils' distillation properties

The distillation properties of renewable crude oil from biosolids samples under different HTL conditions are illustrated in Figure 5. The renewable crude oil fractions at specific boiling points, which corresponded with the same boiling point ranges of the petroleum oil fractions, were applied to identify the renewable crude oil properties.

Gasoline and naphtha-like 80°C to 205°C

There was no significant change in the gasoline and naphtha-like yield from biosolids samples before the HTL process, and these ranged between 22 to 30%. The sources of the gasoline and naphtha-like yield varied depended on the biosolids' composition. Most of the gasoline and naphtha-like was produced from the carbohydrate, protein, and lignin constituents, with fewer contributions from the lipid constituents. However, in the HP and HLG samples, the constituents of proteins produced more gasoline and naphtha-like fractions than those produced in the HL and HC samples.

The gasoline and naphtha-like yield in the renewable crude oil also changed depending on the biosolids composition and HTL conditions. The gasoline and naphtha-like yield from the HL sample at 250°C and 300°C decreased from around 10% to less than 1% with the increase in residence time, where most gasoline and naphtha-like yield was generated from the protein, carbohydrate, and lignin. At 350°C, the gasoline and naphtha-like yield increased from 0.6 to 19% with increased residence time to 40 minutes, before dropping again to 12% at 60 minutes, where the yield generated from the degradation of the organic macromolecules from the lipid, protein, carbohydrate, and lignin. The gasoline and naphtha-like yield from the HP sample at

250°C and 300ºC had an opposite behaviour to the HL sample and increased from around 1 to 10% with increased residence time, with most gasoline and naphtha-like yield produced from the carbohydrate and lignin constituents. At 350°C, the gasoline and naphtha-like yields were similar to the HL sample yield at the same HTL conditions, as they increased from 9 to 17% with increased residence time to 40 minutes, before dropping again to less than 1% at 60 minutes, where most of the yield generated from carbohydrate and lignin. The gasoline and naphtha-like yields in the produced renewable crude oil from the HC sample were generally very low, and the maximum yield only reached 3%. The gasoline and naphtha-like yields from the HLG sample at 250°C had the same behaviour as the HL sample, which decreased from 20 to 1% with increased residence time, with most gasoline and naphtha-like composition generated from the lipid, protein and lignin. At 300ºC, the yield slightly increased from 2 to 6% with the increase in residence time. At 350°C, the gasoline and naphtha-like yields increased from 0.7 to 15% with increased residence time to 40 minutes, before dropping again to 2% at 60 minutes, with most of the yield generated from the protein, carbohydrate, and lignin.

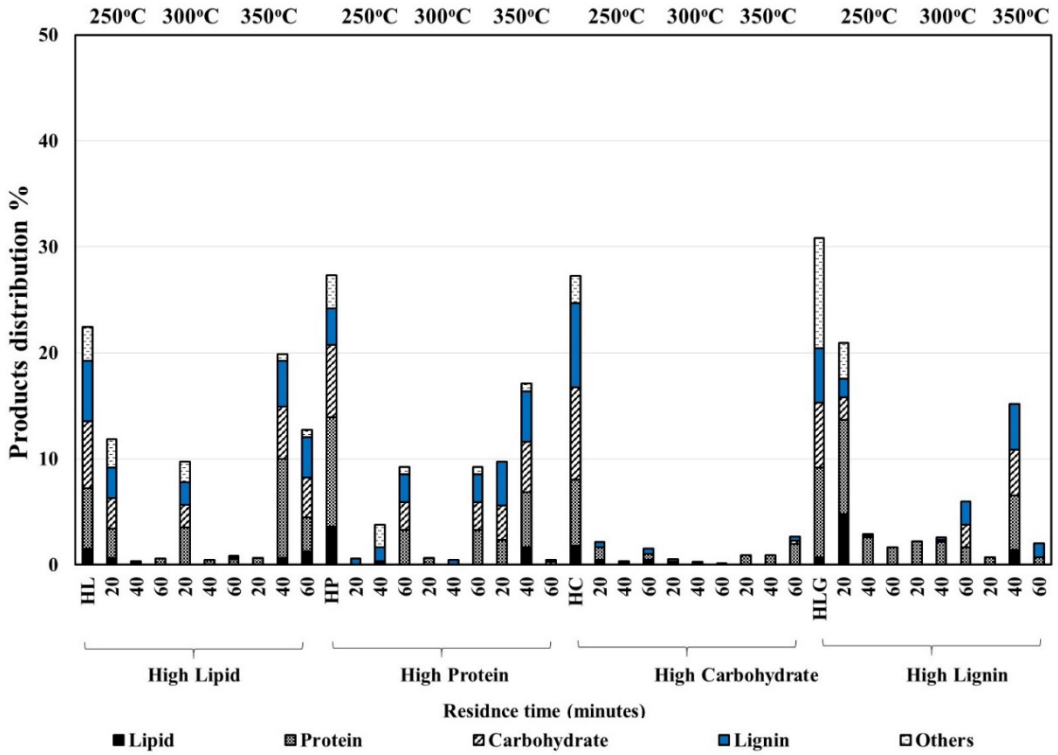

A. Gasoline and naphthas-like (80-205°C).

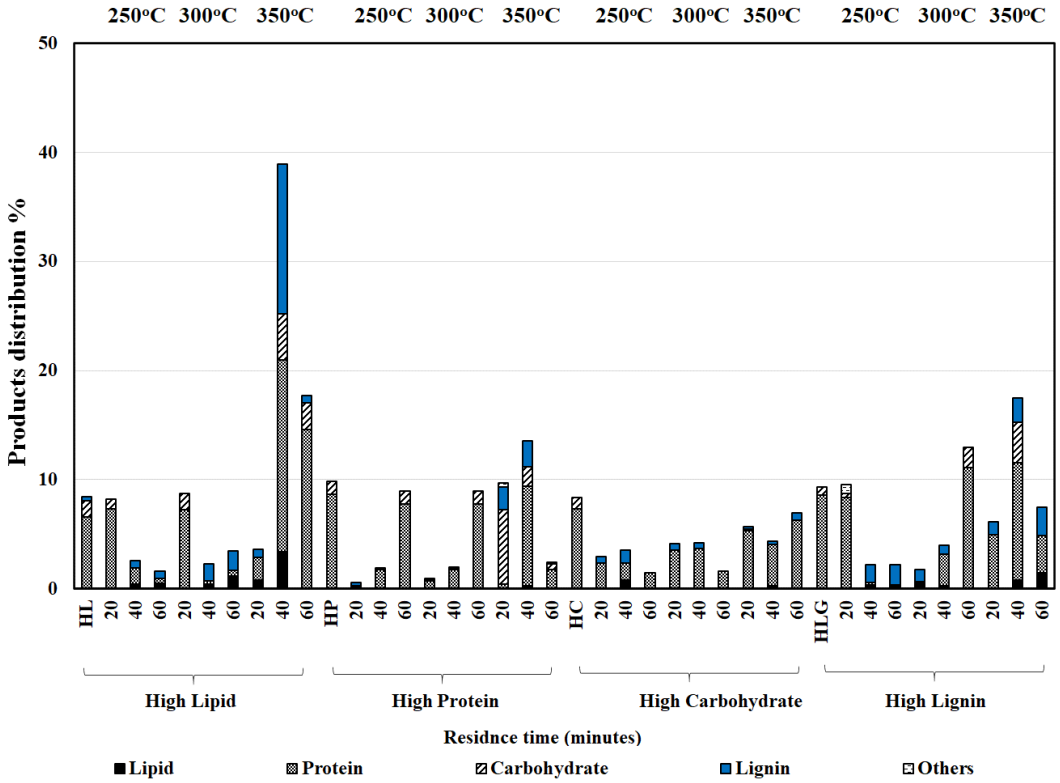

B. Kerosene-like (205-255°C).

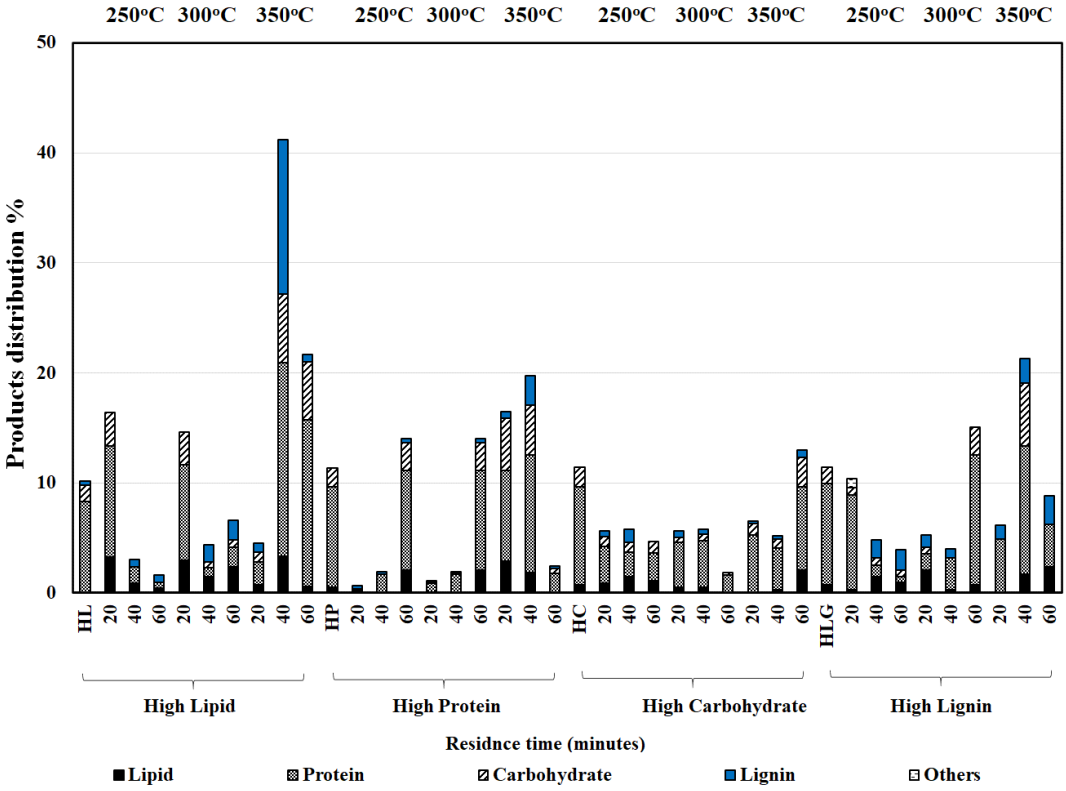

C. Diesel-like (205-290°C).

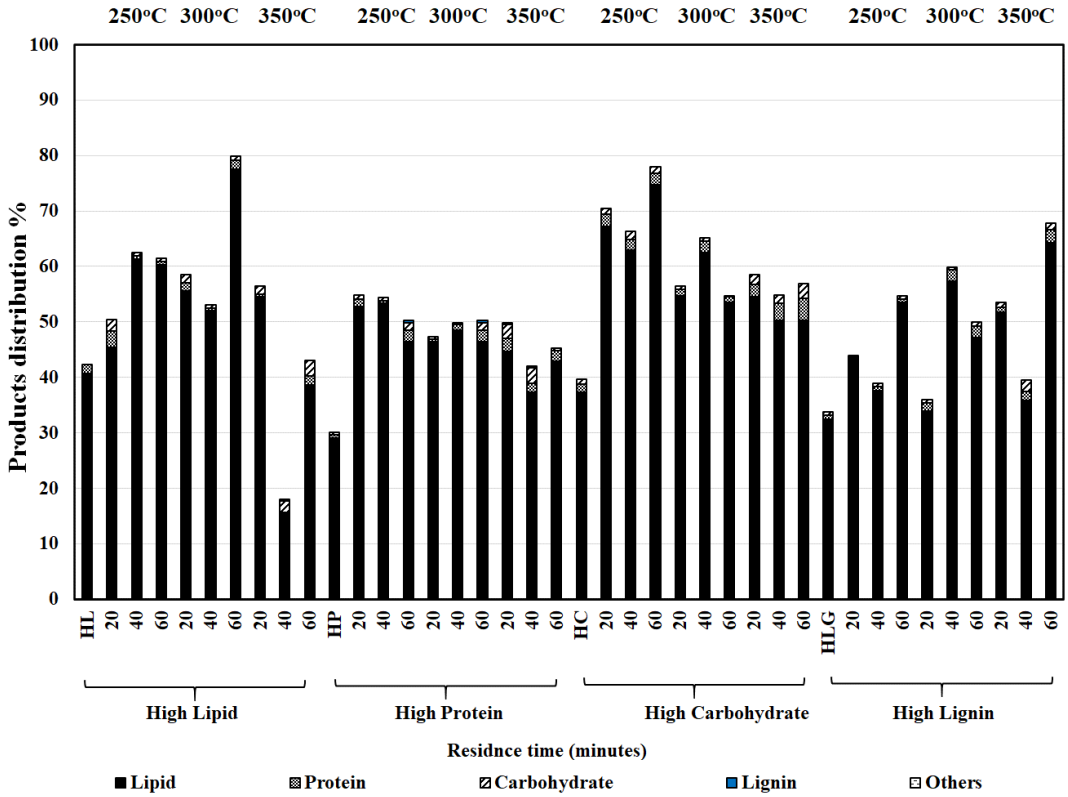

D. Gas oil-like (255-425°C).

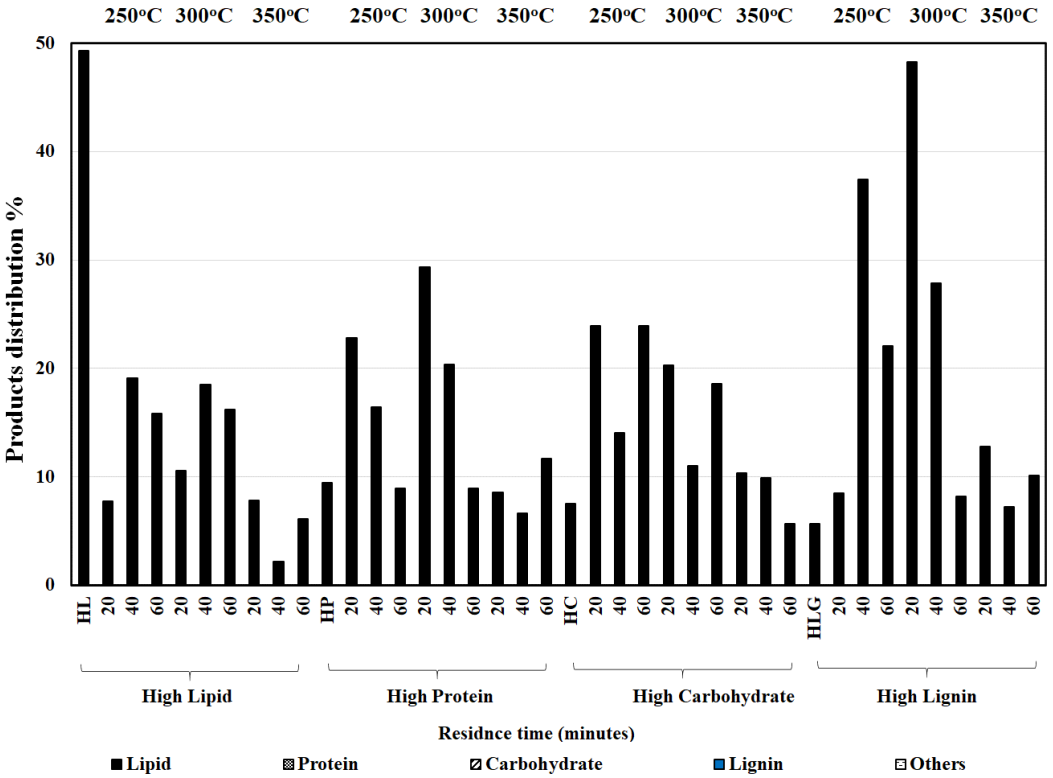

E. Wax, lubricating oil and vacuum gas oil-like (425-600°C).

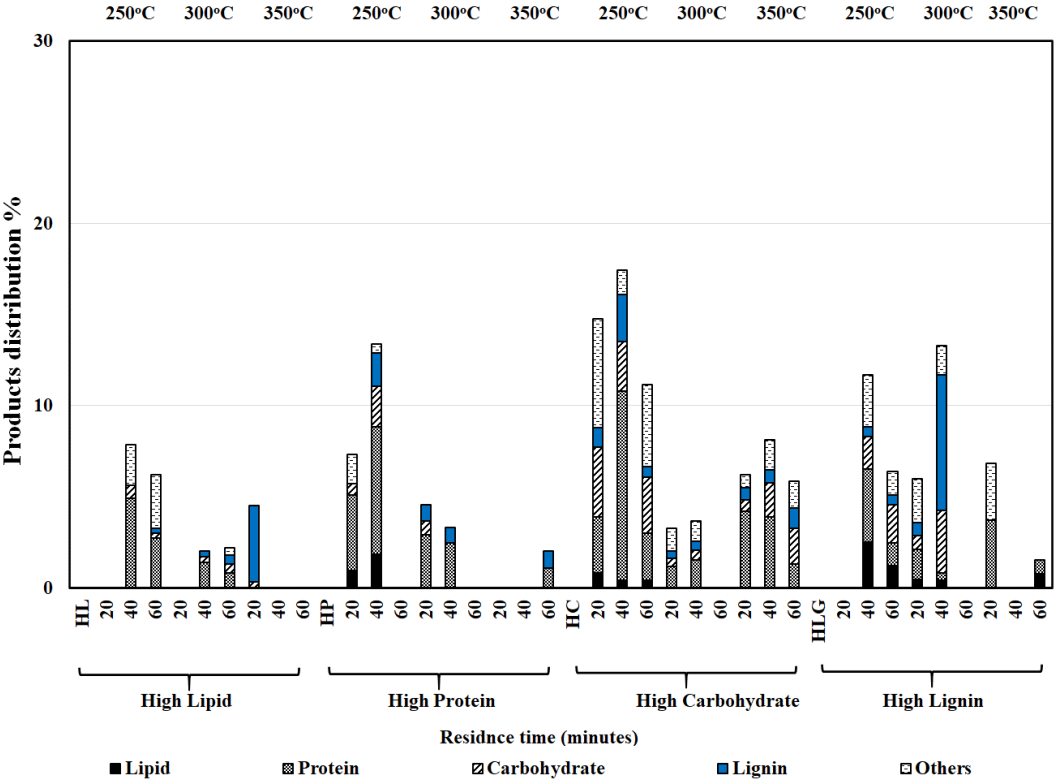

F. Non-renewable oil fractions (below 3 minutes retention time).

Figure 2: Percentage of renewable crude in the boiling point ranges of petroleum fractions for the HTL product of biosolids at 250, 300 and 350 °C and 20, 40 and 60 minutes.

Kerosene-like 205^{o}C to 255^{o}C

The kerosene-like product showed no significant change in the yield from the biosolid samples before the HTL process; it ranged between 8 to 10%. The sources of the kerosene-like compounds in the biosolid samples and the resultant renewable crude oil were mostly produced from protein and lignin. The kerosene-like product yield from the HL sample at 250°C and 300ºC decreased from 8 to 2% and from10 to 3%, respectively with increased residence time. However, at 350°C, the kerosene-like product yield increased from 4 to 39% with increased residence time to 40 minutes, before dropping again to 18% at 60 minutes. The kerosene-like product yield from the HP sample at 250°C and 300ºC had the same trend, and the yield increased from less than 1 to 9%. At 350°C, the kerosene-like product behaved similarly to the HL sample yields at the same HTL conditions, as it increased from 9 to 14% with increased residence time to 40 minutes, before dropping again to 2% at 60 minutes. The kerosene-like product yield from the HC sample ranged from 2 to 7%. In general, at 250°C and 300ºC, the yield decreased from around 4 to 1% with increased residence time. While at 350ºC, the kerosene-like product yield slightly increased from 5 to 7% with increased residence times. The kerosene-like product yield from the HLG sample had a more significant range from 2 to 18%. In general, at 250°C, the yield decreased with increased residence time from 9 to 3%. At 300ºC, the kerosene-like product yield increased from 2 to 13% with increased residence time. At 350ºC, the kerosene-like product yield increased from 6 to 18% with increased residence time to 40 minutes before dropping again to 8% at 60 minutes.

Diesel-like 205°C to 290°C

Generally, there was no significant change in the diesel-like product yield from the biosolid samples before the HTL process, which was around 11%. The diesel-like product yield from the biosolid samples was mostly from the protein constituents. The diesel-like product yield in the renewable crude oil from biosolid samples fluctuated depending on the biosolid composition and the HTL reaction conditions, ranging between 1 and 41%. The diesel-like product yield in the renewable crude oil was mostly from the protein constituents with a small contribution from lipid, carbohydrate, and lignin constituents. The diesel-like product yield from the HL sample at 250°C and 300ºC decreased from 16 to 2% and from 15 to 7%, respectively with increased residence times. At 350°C, the diesel-like product yield showed a sharp increase from 5 to 41% with increased residence time to 40 minutes, before dropping again to 22% at 60 minutes.

The diesel-like product yield from the HP sample at 250°C and 300ºC had the same trend and increased from around 1 to 14% with increased residence times. At 350°C, the diesel-like product yield had the same trend and increased from 17 to 20% with increased residence time to 40 minutes, before dropping again to 2% at 60 minutes. The diesel-like product yield from the HC sample at 250°C was around 6 %, despite the change in residence time. At 300ºC, the diesel-like product yield decreased from 6 to 2% with increased residence time. At 350°C, the diesel-like product yield increased from 6 to 13% with increased residence time. The diesel-like yield from the HLG sample at 250°C decreased from 10 to 4% with increased residence time. At 300ºC, the yield was mostly different from 250°C, as the diesel-like product yield increased from 5 to 15% with increased residence time. In comparison, the diesel-like product yield from the HLG sample at 350°C had the same trend as the HL sample, which increased

from 6 to 21% with increased residence time to 40 minutes, before dropping again to 9% at 60 minutes.

Gas oil-like 255^{o}C to 425^{o}C

Prior to the HTL process, the gas oil-like product yield from the biosolid samples ranged between 30 to 42%. The gas oil-like product yield sources were mostly from lipid constituents despite the difference in the biosolids' composition. The gas oil-like product yield in the renewable crude oil fluctuated depending on the HTL conditions, and the primary source of the gas oil-like product was from the lipid constituents. The gas oil-like product yield from the HL sample at 250ºC generally increased from 50 to 61%, with increased residence time. At 300ºC and 350°C, the gas oil-like product yield decreased slightly from 58 to 53% and from 58 to 18% with increased residence time to 40 minutes before it increased again to 80% and 43%, respectively at 60 minutes. The gas oil-like product yield from the HP sample at 250°C slightly decreased from 54 to 50% with increased residence time to 60 minutes. At 300ºC, it was mostly constant at 50%, despite the change in residence time. At 350ºC, the gas oil-like product yield decreased from 50 to 42% with increased residence time to 40 minutes before increasing to 47% at 60 minutes.

The gas oil-like product yield from the HC sample at 250°C decreased from 70 to 66%, with increased residence time to 40 minutes, before increasing again to 78% at 60 minutes. The gas oil-like product yield at 300ºC had the opposite trend at 250ºC and increased from 56 to 65% with increased residence time to 40 minutes before decreasing again to 55% at 60 minutes. At 350ºC, there was a slight decrease from 59 to 57% with increased residence time to 60 minutes. The gas oil-like product yield from the HLG sample at 250°C and 350ºC decreased from 44 to

39% and from 53 to 40% with increased residence time to 40 minutes before increasing again to 54% and 69%, respectively at 60 minutes. The gas oil-like product yield at 300ºC had the opposite behaviour at 250°C and increased from 36 to 60% with increased residence time to 40 minutes before decreasing to 50% at 60 minutes.

Wax, lubricating oil and vacuum gas oil-like yields at 425ºC to 600ºC

The wax, lubricating oil, and vacuum gas oil-like product yield from the biosolid samples before the HTL process ranged between 5 to 50%, where most of its source was from the lipid constituents. The wax, lubricating oil, and vacuum gas oil-like product yield in the renewable crude oil fluctuated depending on the biosolid composition and HTL reaction conditions and ranged between 2 to 48%, with the primary source of the produced yield from the lipid constituents. The wax, lubricating oil, and vacuum gas oil-like product yield from the HL sample at 250°C and 300ºC increased from 8 to 19% and from 10 to 18%, respectively with increased residence time to 40 minutes before dropping again to 16% at 60 minutes. At 350°C, the yields showed an opposite trend and decreased from 8 to 2% with increased residence time to 40 minutes, before increasing again to 6% at 60 minutes. The wax, lubricating oil, and vacuum gas oil-like product yield from the HP sample at 250°C and 300ºC decreased from 23 to 9% and from 30 to 9%, respectively, with increased residence time to 60 minutes. At 350ºC, the yield decreased from 9 to 7% with increased residence time to 40 minutes before increasing again to 12% at 60 minutes. The wax, lubricating oil, and vacuum gas oil-like product yield from the HC sample at 250°C and 300ºC decreased from 24 to 14%, and from 20 to 11% with increased residence time to 40 minutes, before increasing again to 24% and 18%, respectively, at 60 minutes. At 350ºC, the yield decreased from 10 to 6% with increased residence time to 60 minutes. The wax, lubricating oil, and vacuum gas oil-like product yield from the HLG

sample at 250°C increased from 8 to 37% with increased residence time to 40 minutes before decreasing again to 22% at 60 minutes. At 300ºC and 350ºC, the yield decreased from 48 to 8% and from 13 to 10%, respectively, with increased residence time.

Non-renewable oil fractions below 3 minutes' retention time

It was noticeable that whilst identifying the compounds in the produced renewable crude oil via the HTL of biosolids; there were compounds produced below a 3-minute retention time. Retention time ranges for the boiling point distributions of the renewable crude oil were assigned by reference to saturated hydrocarbon standards containing nC_6 to nC_{40}, where compounds below 3-minute retention time were classified as non-renewable crude oil. Most of these compounds are gasses or components that cannot be classified as renewable crude oil and are mainly produced from protein and carbohydrate.

To summarise, it was evident that the biosolid composition and HTL reaction conditions significantly affect the renewable crude oil composition. The outcomes of this research could assist in optimising the HTL conditions regarding the organic composition of biosolids to maximise the target renewable crude oil fractions.

- Gasoline and naphtha-like: HL, HP samples produced the highest yield at 350°C and 40 minutes, while the highest yield HLG sample was at 250°C and 20 minutes.
- Kerosene-like: the HL, HP and HLG samples produced the highest yield at 350°C and 40 minutes.
- Diesel-like: the HL, HP and HLG samples produced the highest yield at 350°C and 40 minutes; whereas the HC sample produced the highest yield at 350ºC and 60 minutes.

- Gas oil-like: HL samples produced the highest yield at 300ºC and 60 minutes, while the highest yield from the HC sample was at 250°C and 60 minutes. HLG samples produced the highest yield at 350ºC and 60 minutes; while the HP sample produced the highest yield at 250°C and 20 minutes.
- Wax, lubricating oil and vacuum gas oil-like: the HL and HC samples produced the highest yield at 250°C and 20 minutes. The HP and HLG samples produced the highest yield at 300ºC and 20 minutes.

4. Conclusion

Hydrothermal liquefaction of biosolids with different lipid, protein, carbohydrate and lignin fractions resulted in markedly different renewable crude oil compositions, containing a complex mixture of >300 major compounds identified using GC-MS. The results allowed identification of how the lipid, protein, carbohydrate and lignin fractions contribute to renewable crude oil composition. This information is recognised based on a particular set of conditions, specifically temperature and residence time. GC−MS results identified that the predominant components were from the lipid constituents, such as cyclic terpanes and terpenes, accompanied by other compounds produced from the protein, carbohydrate and lignin constituents, such as nitrogenous oxygenated, ketones, aldehydes, and phenolic components. Also, the HTL of biosolids can be optimised to produce a targeted fraction of renewable crude oil. The best gasoline and naphtha-like and diesel-like yields were generated from samples with high protein and lipid content at 350°C and 40 minutes, and at the same HTL conditions; the kerosene-like best yield was produced from the high lipid sample. The highest gas oil-like yield was generated from a high carbohydrate sample at 250°C and 60 minutes, while the high lipid sample was produced at 300ºC and 60 minutes. The greatest yield of wax, lubricating oil and

vacuum gas oil-like was produced from the high lignin sample at 300ºC and 20 minutes. These findings highlight the influence of biosolid composition and HTL conditions on the renewable crude oil composition and show the necessity for a better understanding of renewable crude oil chemistries when considering renewable crude oil uses and upgrading requirements for heavy transportation fuels.

5. Author information

Corresponding Author:

Mr. Jasim Al-juboori

School of Chemical Engineering & Advanced Materials

Faculty of Engineering, Mathematical and Computer Sciences

University of Adelaide

Adelaide, South Australia 5005

+61 8 831 33093

Jasim.al-juboori@adelaide.edu.au

The manuscript was written through the contributions of all authors. All authors have given approval to the final version of the manuscript.

6. Acknowledgements

The authors would like to acknowledge Dr Rosmala Lewis and Melbourne Water, Werribee, Victoria, Australia for providing the feedstocks.

Funding: This work was supported by the Australian Research Council and Southern Oil Refining Pty Ltd [Grant numbers LP150101241].

7. Abbreviations

HTL, Hydrothermal Liquefaction; GC-MS, Gas chromatography-mass spectrometry; TGA, thermogravimetric analysis; Daf, dry-ash free; SRA, Source Rock Analyser; OM, organic matter; HC, high carbohydrate; HP, high proteins; HL, high lipids; HLG, high lignin.

8. References

1. EIA, U., Energy Information Administration: Annual Energy Outlook 2015 with projections to 2040. *US Energy Information Administration, Office of Integrated and International Energy Analysis, US Department of Energy, Washington, DC* **2015,** *20585*.

2. Tully, A., BP's latest estimate says world's oil will last 53.3 years. Diperoleh: 2015.

3. Ullah, K.; Ahmad, M.; Sofia; Sharma, V. K.; Lu, P.; Harvey, A.; Zafar, M.; Sultana, S.; Anyanwu, C. N., Algal biomass as a global source of transport fuels: Overview and development perspectives. *Progress in Natural Science: Materials International* **2014,** *24* (4), 329-339.

4. Tuck, C. O.; Pérez, E.; Horváth, I. T.; Sheldon, R. A.; Poliakoff, M., Valorization of biomass: deriving more value from waste. *Science* **2012,** *337* (6095), 695-699.

5. Dimitriadis, A.; Bezergianni, S., Hydrothermal liquefaction of various biomass and waste feedstocks for biocrude production: A state of the art review. *Renewable and Sustainable Energy Reviews* **2017,** *68*, 113-125.

6. Dote, Y.; Sawayama, S.; Inoue, S.; Minowa, T.; Yokoyama, S.-y., Recovery of liquid

fuel from hydrocarbon-rich microalgae by thermochemical liquefaction. *Fuel* **1994,** *73* (12), 1855-1857.

7. Suzuki, A.; Nakamura, T.; Yokoyama, S.; Ogi, T.; Koguchi, K., Conversion of sewage sludge to heavy oil by direct thermochemical liquefaction. *Journal of Chemical Engineering of Japan* **1988,** *21* (3).

8. Xiu, S.; Shahbazi, A.; Shirley, V.; Cheng, D., Hydrothermal pyrolysis of swine manure to bio-oil: effects of operating parameters on products yield and characterization of bio-oil. *Journal of analytical and applied pyrolysis* **2010,** *88* (1), 73-79.

9. Cantrell, K.; Ro, K.; Mahajan, D.; Anjom, M.; Hunt, P. G., Role of thermochemical conversion in livestock waste-to-energy treatments: obstacles and opportunities. *Industrial & engineering chemistry research* **2007,** *46* (26), 8918-8927.

10. Faeth, J. L.; Valdez, P. J.; Savage, P. E., Fast hydrothermal liquefaction of nannochloropsis sp. to produce biocrude. *Energy and Fuels* **2013,** *27* (3), 1391-1398.

11. Albrecht, K. O.; Zhu, Y.; Schmidt, A. J.; Billing, J. M.; Hart, T. R.; Jones, S. B.; Maupin, G.; Hallen, R.; Ahrens, T.; Anderson, D., Impact of heterotrophically stressed algae for biofuel production via hydrothermal liquefaction and catalytic hydrotreating in continuous-flow reactors. *Algal research* **2016,** *14*, 17-27.

12. Biller, P.; Sharma, B. K.; Kunwar, B.; Ross, A. B., Hydroprocessing of bio-crude from continuous hydrothermal liquefaction of microalgae. *Fuel* **2015,** *159*, 197-205.

13. Chen, W.-T.; Zhang, Y.; Zhang, J.; Yu, G.; Schideman, L. C.; Zhang, P.; Minarick, M., Hydrothermal liquefaction of mixed-culture algal biomass from wastewater treatment system into bio-crude oil. *Bioresource technology* **2014,** *152*, 130-139.

14. Liu, D.; Li, Q.; Zhao, A.; Song, L.; Wu, P.; Yan, Z., Hydro-liquefaction of sawdust and its three components in supercritical ethanol with [BMIM] Cl/NiCl2 catalyst. *Chemical*

Engineering Journal **2015,** *279*, 921-928.

15. Chiaramonti, D.; Prussi, M.; Buffi, M.; Rizzo, A. M.; Pari, L., Review and experimental study on pyrolysis and hydrothermal liquefaction of microalgae for biofuel production. *Applied energy* **2017,** *185*, 963-972.

16. Zhao, P.; Shen, Y.; Ge, S.; Yoshikawa, K., Energy recycling from sewage sludge by producing solid biofuel with hydrothermal carbonization. *Energy conversion and management* **2014,** *78*, 815-821.

17. Huber, G. W.; Iborra, S.; Corma, A., Synthesis of transportation fuels from biomass: Chemistry, catalysts, and engineering. *Chemical Reviews* **2006,** *106* (9), 4044-4098.

18. Orbey, H.; Sandler, S. I., The prediction of the viscosity of liquid hydrocarbons and their mixtures as a function of temperature and pressure. *The Canadian Journal of Chemical Engineering* **1993,** *71* (3), 437-446.

19. Demirbas, A., Progress and recent trends in biodiesel fuels. *Energy conversion and management* **2009,** *50* (1), 14-34.

20. Peterson, A. A.; Vogel, F.; Lachance, R. P.; Fröling, M.; Antal Jr, M. J.; Tester, J. W., Thermochemical biofuel production in hydrothermal media: A review of sub- and supercritical water technologies. *Energy and Environmental Science* **2008,** *1* (1), 32-65.

21. Adjaye, J. D.; Sharma, R. K.; Bakhshi, N. N., Characterization and stability analysis of wood-derived bio-oil. *Fuel Processing Technology* **1992,** *31* (3), 241-256.

22. Speight, J. G., *Handbook of petroleum product analysis*. John Wiley & Sons: 2015; Vol. 182.

23. Vardon, D. R.; Sharma, B. K.; Scott, J.; Yu, G.; Wang, Z.; Schideman, L.; Zhang, Y.; Strathmann, T. J., Chemical properties of biocrude oil from the hydrothermal liquefaction of Spirulina algae, swine manure, and digested anaerobic sludge. *Bioresource Technology*

2011, *102* (17), 8295-8303.

24. Jazrawi, C., Hydrothermal Treatment of Algal Biomass: from Batch to Continuous Pilot Plant Operations. **2014**.

25. Arturi, K. R.; Toft, K. R.; Nielsen, R. P.; Rosendahl, L. A.; Søgaard, E. G., Characterization of liquid products from hydrothermal liquefaction (HTL) of biomass via solid-phase microextraction (SPME). *Biomass and Bioenergy* **2016,** *88*, 116-125.

26. Leahy, J. G.; Colwell, R. R., Microbial degradation of hydrocarbons in the environment. *Microbiology and Molecular Biology Reviews* **1990,** *54* (3), 305-315.

27. Dote, Y.; Inoue, S.; Ogi, T.; Yokoyama, S. Y., Distribution of nitrogen to oil products from liquefaction of amino acids. *Bioresource Technology* **1998,** *64* (2), 157-160.

28. Elliott, D., Thermochemical processing of biomass. Chichester, UK: John Wiley & Sons Ltd: 2011.

29. Savage, P.; Levine, R.; Huelsman, C., Hydrothermal processing of biomass. *Thermochemical conversion of biomass to liquid fuels and chemicals* **2010**, 192-221.

30. Tanneru, S. K.; Steele, P. H., Liquefaction of dried distiller's grains with solubles (DDGS) followed by hydroprocessing to produce liquid hydrocarbons. *Fuel* **2015,** *150*, 512-518.

31. Toor, S. S.; Rosendahl, L.; Rudolf, A., Hydrothermal liquefaction of biomass: A review of subcritical water technologies. *Energy* **2011,** *36* (5), 2328-2342.

32. Bauman-Kaszubska, H.; Sikorski, M., Charakterystyka ilościowa i jakościowa osadów ściekowych pochodzących z małych oczyszczalni ścieków w powiecie płockim. *Inżynieria Ekologiczna* **2011**, 20-19.

33. Bień, J.; Neczaj, E.; Worwąg, M.; Grosser, A.; Nowak, D.; Milczarek, M.; Janik, M., Kierunki zagospodarowania osadów w Polsce po roku 2013. *Inżynieria i Ochrona Środowiska*

2011, *14*, 375-384.

34. Królak, E.; Filipek, K.; Biardzka, E., Comparative analysis of sewage sludge from two sewage treatment plants: in Mrozy and Siedlce (Mazowieckie Province)/Porównawcza analiza osadów ściekowych z dwóch oczyszczalni ścieków w Mrozach i Siedlcach (województwo mazowieckie). *Ochrona Środowiska i Zasobów Naturalnych-Environmental Protection and Natural Resources* **2013,** *24* (2), 57-61.

35. Jain, A.; Balasubramanian, R.; Srinivasan, M., Hydrothermal conversion of biomass waste to activated carbon with high porosity: A review. *Chemical Engineering Journal* **2016,** *283*, 789-805.

36. Mtui, G. Y., Recent advances in pretreatment of lignocellulosic wastes and production of value added products. *African Journal of Biotechnology* **2009,** *8* (8).

37. Sánchez, C., Lignocellulosic residues: biodegradation and bioconversion by fungi. *Biotechnology advances* **2009,** *27* (2), 185-194.

38. Alhassan, Y.; Kumar, N.; Bugaje, I. M., Hydrothermal liquefaction of de-oiled Jatropha curcas cake using Deep Eutectic Solvents (DESs) as catalysts and co-solvents. *Bioresource technology* **2016,** *199*, 375-381.

39. Deniel, M.; Haarlemmer, G.; Roubaud, A.; Weiss-Hortala, E.; Fages, J., Energy valorisation of food processing residues and model compounds by hydrothermal liquefaction. *Renewable and Sustainable Energy Reviews* **2016,** *54*, 1632-1652.

40. Elliott, D. C.; Biller, P.; Ross, A. B.; Schmidt, A. J.; Jones, S. B., Hydrothermal liquefaction of biomass: Developments from batch to continuous process. *Bioresource Technology* **2015,** *178*, 147-156.

41. Akhtar, J.; Amin, N. A. S., A review on process conditions for optimum bio-oil yield in hydrothermal liquefaction of biomass. *Renewable and Sustainable Energy Reviews* **2011,** *15*

(3), 1615-1624.

42. Biller, P.; Ross, A., Potential yields and properties of oil from the hydrothermal liquefaction of microalgae with different biochemical content. *Bioresource technology* **2011,** *102* (1), 215-225.

43. Brown, T. M.; Duan, P.; Savage, P. E., Hydrothermal liquefaction and gasification of Nannochloropsis sp. *Energy and Fuels* **2010,** *24* (6), 3639-3646.

44. Yin, S.; Tan, Z., Hydrothermal liquefaction of cellulose to bio-oil under acidic, neutral and alkaline conditions. *Applied Energy* **2012,** *92*, 234-239.

45. Zhou, D.; Zhang, L.; Zhang, S.; Fu, H.; Chen, J., Hydrothermal liquefaction of macroalgae Enteromorpha prolifera to bio-oil. *Energy & Fuels* **2010,** *24* (7), 4054-4061.

46. Xu, C.; Etcheverry, T., Hydro-liquefaction of woody biomass in sub-and super-critical ethanol with iron-based catalysts. *Fuel* **2008,** *87* (3), 335-345.

47. Fujihara, S.; Kasuga, A.; Aoyagi, Y., Nitrogen-to-protein conversion factors for common vegetables in Japan. *Journal of food science* **2001,** *66* (3), 412-415.

48. Folch, J.; Lees, M.; Sloane Stanley, G., A simple method for the isolation and purification of total lipids from animal tissues. *J biol Chem* **1957,** *226* (1), 497-509.

49. Safařík, I.; Šantrůčková, H., Direct determination of total soil carbohydrate content. *Plant and Soil* **1992,** *143* (1), 109-114.

50. Hietala, D. C.; Faeth, J. L.; Savage, P. E., A quantitative kinetic model for the fast and isothermal hydrothermal liquefaction of Nannochloropsis sp. *Bioresource technology* **2016,** *214*, 102-111.

51. Peters, K. E.; Walters, C. C.; Moldowan, J. M., *The biomarker guide: Volume 1, Biomarkers and isotopes in the environment and human history*. Cambridge university press: 2007.

52. Harborne, J. B., *Methods in plant biochemistry. Volume 1. Plant phenolics*. Academic Press Ltd.: 1989.

53. Koester, S. The Interaction Between Market and Non-market Based Energy and Environmental Regulations to Reduce Carbon Emissions: A Case Study of California and British Columbia. Tufts University, 2019.

54. Alvarez, J.; Lopez, G.; Amutio, M.; Bilbao, J.; Olazar, M., Bio-oil production from rice husk fast pyrolysis in a conical spouted bed reactor. *Fuel* **2014,** *128*, 162-169.

55. Chan, Y. H.; Yusup, S.; Quitain, A. T.; Uemura, Y.; Sasaki, M., Bio-oil production from oil palm biomass via subcritical and supercritical hydrothermal liquefaction. *The Journal of Supercritical Fluids* **2014,** *95*, 407-412.

56. Chen, Y.; Zhao, N.; Wu, Y.; Wu, K.; Wu, X.; Liu, J.; Yang, M., Distributions of organic compounds to the products from hydrothermal liquefaction of microalgae. *Environmental Progress & Sustainable Energy* **2017,** *36* (1), 259-268.

57. Lian, X.; Xue, Y.; Zhao, Z.; Xu, G.; Han, S.; Yu, H., Progress on upgrading methods of bio-oil: a review. *International Journal of Energy Research* **2017,** *41* (13), 1798-1816.

58. Xu, Y.; Long, J.; Liu, Q.; Li, Y.; Wang, C.; Zhang, Q.; Lv, W.; Zhang, X.; Qiu, S.; Wang, T., In situ hydrogenation of model compounds and raw bio-oil over Raney Ni catalyst. *Energy Conversion and Management* **2015,** *89*, 188-196.

59. Madsen, R. B.; Biller, P.; Jensen, M. M.; Becker, J.; Iversen, B. B.; Glasius, M., Predicting the chemical composition of aqueous phase from hydrothermal liquefaction of model compounds and biomasses. *Energy & Fuels* **2016,** *30* (12), 10470-10483.

60. Ying, G.; CHEN, H.-p.; Jun, W.; Tao, S.; Hai-Ping, Y.; Xian-Hua, W., Characterization of products from hydrothermal liquefaction and carbonation of biomass model compounds and real biomass. *Journal of Fuel Chemistry and Technology* **2011,** *39* (12),

893-900.

61. Jindal, M. K.; Jha, M. K., Effect of process parameters on hydrothermal liquefaction of waste furniture sawdust for bio-oil production. *RSC advances* **2016,** *6* (48), 41772-41780.

62. Saisu, M.; Sato, T.; Watanabe, M.; Adschiri, T.; Arai, K., Conversion of lignin with supercritical water− phenol mixtures. *Energy & Fuels* **2003,** *17* (4), 922-928.

63. Wang, Z., Reaction mechanisms of hydrothermal liquefaction of model compounds and biowaste feedstocks. Zhang, Y., Ed. ProQuest Dissertations Publishing: 2011.

64. McConnell, B., Kinetics of Lipid Extraction from Microalgae. **2013**.

65. Madsen, R. B.; Bernberg, R. Z. K.; Biller, P.; Becker, J.; Iversen, B. B.; Glasius, M., Hydrothermal co-liquefaction of biomasses – quantitative analysis of bio-crude and aqueous phase composition. *Sustainable Energy Fuels* **2017,** *1* (4), 789-805.

66. Obeid, R.; Lewis, D. M.; Smith, N.; Hall, T.; van Eyk, P., Reaction Kinetics and Characterization of Species in Renewable Crude from Hydrothermal Liquefaction of Mixtures of Polymer Compounds To Represent Organic Fractions of Biomass Feedstocks. *Energy & Fuels* **2019,** *34* (1), 419-429.

67. Lee, N.; Foustoukos, D. I.; Sverjensky, D. A.; Cody, G. D.; Hazen, R. M., The effects of temperature, pH and redox state on the stability of glutamic acid in hydrothermal fluids. *Geochimica et Cosmochimica Acta* **2014,** *135*, 66-86.

68. Déniel, M.; Haarlemmer, G.; Roubaud, A.; Weiss-Hortala, E.; Fages, J., Energy valorisation of food processing residues and model compounds by hydrothermal liquefaction. *Renewable and Sustainable Energy Reviews* **2016,** *54*, 1632-1652.

69. Obeid, R.; Lewis, D.; Smith, N.; van Eyk, P., The elucidation of reaction kinetics for hydrothermal liquefaction of model macromolecules. *Chemical Engineering Journal* **2019,** *370*, 637-645.

70. Maddi, B.; Panisko, E.; Wietsma, T.; Lemmon, T.; Swita, M.; Albrecht, K.; Howe, D., Quantitative characterization of aqueous byproducts from hydrothermal liquefaction of municipal wastes, food industry wastes, and biomass grown on waste. *ACS Sustainable Chemistry & Engineering* **2017,** *5* (3), 2205-2214.

71. Srokol, Z.; Bouche, A.-G.; van Estrik, A.; Strik, R. C.; Maschmeyer, T.; Peters, J. A., Hydrothermal upgrading of biomass to biofuel; studies on some monosaccharide model compounds. *Carbohydrate Research* **2004,** *339* (10), 1717-1726.

72. Kruse, A.; Maniam, P.; Spieler, F., Influence of proteins on the hydrothermal gasification and liquefaction of biomass. 2. Model compounds. *Industrial & Engineering Chemistry Research* **2007,** *46* (1), 87-96.

73. Madsen, R. B.; Zhang, H.; Biller, P.; Goldstein, A. H.; Glasius, M., Characterizing semivolatile organic compounds of biocrude from hydrothermal liquefaction of biomass. *Energy & Fuels* **2017,** *31* (4), 4122-4134.

74. Ander, P.; Eriksson, K.-E., Methanol formation during lignin degradation by Phanerochaete chrysosporium. *Applied microbiology and biotechnology* **1985,** *21* (1), 96-102.

75. Hemme, D.; Richard, J., Utilization of L-methionine and production of methanethiol by bacteria isolated from raw milk Camembert cheese. *Le lait* **1986,** *66* (2), 135-142.

76. Yaylayan, V. A.; Keyhani, A., Origin of carbohydrate degradation products in L-alanine/D-[13C] glucose model systems. *Journal of Agricultural and Food Chemistry* **2000,** *48* (6), 2415-2419.

77. Wexler, P.; Anderson, B. D.; Gad, S. C.; Hakkinen, P. B.; Kamrin, M.; De Peyster, A.; Locey, B.; Pope, C.; Mehendale, H. M.; Shugart, L. R., *Encyclopedia of toxicology*. Academic Press: 2005; Vol. 1.

78. Meldau, D. G.; Meldau, S.; Hoang, L. H.; Underberg, S.; Wünsche, H.; Baldwin, I.

T., Dimethyl disulfide produced by the naturally associated bacterium Bacillus sp B55 promotes Nicotiana attenuata growth by enhancing sulfur nutrition. *The Plant Cell* **2013,** *25* (7), 2731-2747.

79. Gollakota, A.; Kishore, N.; Gu, S., A review on hydrothermal liquefaction of biomass. *Renewable and Sustainable Energy Reviews* **2018,** *81*, 1378-1392.

80. Teri, G.; Luo, L.; Savage, P. E., Hydrothermal treatment of protein, polysaccharide, and lipids alone and in mixtures. *Energy & fuels* **2014,** *28* (12), 7501-7509.

81. Lange, J. P.; Price, R.; Ayoub, P. M.; Louis, J.; Petrus, L.; Clarke, L.; Gosselink, H., Valeric biofuels: a platform of cellulosic transportation fuels. *Angewandte Chemie International Edition* **2010,** *49* (26), 4479-4483.

82. Déniel, M.; Haarlemmer, G.; Roubaud, A.; Weiss-Hortala, E.; Fages, J., Hydrothermal liquefaction of blackcurrant pomace and model molecules: understanding of reaction mechanisms. *Sustainable Energy & Fuels* **2017,** *1* (3), 555-582.

83. Zhang, B.; Huang, H.-J.; Ramaswamy, S., Reaction kinetics of the hydrothermal treatment of lignin. In *Biotechnology for Fuels and Chemicals*, Springer: 2007; pp 487-499.

84. Geor, R. J., Nutritional management of the equine athlete. *Equine Exercise Physiology. The Science of Exercise in the Athletic Horse. New York: Saunders Elsevier* **2008**, 301-325.

85. Tang, S.; Shi, Z.; Tang, X.; Yang, X., Hydrotreatment of biocrudes derived from hydrothermal liquefaction and lipid extraction of the high-lipid Scenedesmus. *Green Chemistry* **2019,** *21* (12), 3413-3423.

86. Yang, C.; Wang, S.; Yang, J.; Xu, D.; Li, Y.; Li, J.; Zhang, Y., Hydrothermal liquefaction and gasification of biomass and model compounds: A review. *Green Chemistry* **2020**.

87. Kolawole, F.; Kolawole, S.; Agunsoye, J.; Bello, S.; Adebisi, J.; Okoye, O.; Hassan,

S., Cassava leaf nanoparticles (CLNPs) as a potential additive to anti-corrosion coatings for oil and gas pipeline. **2017**.

88. Cao, Q.; Liu, Z.; Xiong, Y.; Zhong, Z.; Ye, Q., Multiple Roles of 25-Hydroxycholesterol in Lipid Metabolism, Antivirus Process, Inflammatory Response, and Cell Survival. *Oxidative Medicine and Cellular Longevity* **2020,** *2020*.

89. Chen, E.; Song, H.; Li, Y.; Chen, H.; Wang, B.; Che, X.; Zhang, Y.; Zhao, S., Analysis of aroma components from sugarcane to non-centrifugal cane sugar using GC-O-MS. *RSC Advances* **2020,** *10* (54), 32276-32289.

90. Hu, Y. M.; Sze, S. C.-W.; Zhang, X. Q.; Tong, Y., Simultaneous Analysis of Lipid-Soluble Constituents of Erxian Decoction by GC–MS. *Chromatographia* **2009,** *70* (7), 1171-1177.

91. Jacoby, E., Biphenyls as potential mimetics of protein α-helix. *Bioorganic & medicinal chemistry letters* **2002,** *12* (6), 891-893.

92. Medicine, N. L. o., *Index Medicus*. US Department of Health, Education, and Welfare, Public Health Service …: 2004.

93. Alhassan, Y.; Hornung, U.; Bugaje, I. M., Lignin Hydrothermal Liquefaction into Bifunctional Chemicals: A Concise Review. *Biorefinery Concepts, Energy and Products* **2020**.

94. Bhaskar, T.; Sera, A.; Muto, A.; Sakata, Y., Hydrothermal upgrading of wood biomass: influence of the addition of K2CO3 and cellulose/lignin ratio. *Fuel* **2008,** *87* (10-11), 2236-2242.

95. Peng, C.; Zhang, G.; Han, J.; Li, X., Hydrothermal conversion of lignin and black liquor for phenolics with the aids of alkali and hydrogen donor. *Carbon Resources Conversion* **2019,** *2* (2), 141-150.

96. Lee, S. R.; Choi, J. H.; Ryoo, R.; Kim, J.-C.; Pang, C.; Kim, S.-H.; Kim, K. H.,

Ergostane-Type Steroids from Korean Wild Mushroom Xerula furfuracea that Control Adipocyte and Osteoblast Differentiation. *Journal of Microbiology and Biotechnology* **2020,** *30* (11), 1769-1776.

97. Stransky, K.; Nemec, V.; Sláma, K., Lipid composition of the seeds of an ecdysteroid-containing plant, Leuzea carthamoides (Willd.) DC (Asteraceae). *Russian journal of plant physiology* **1998,** *45* (3), 333-338.

98. Rushdi, A. I.; Ritter, G.; Grimalt, J. O.; Simoneit, B. R., Hydrous pyrolysis of cholesterol under various conditions. *Organic Geochemistry* **2003,** *34* (6), 799-812.

99. Czochanska, Z.; Sheppard, C. M.; Weston, R. J.; Woolhouse, A. D., A biological marker study of oils and sediments from the West Coast, South Island, New Zealand. *New Zealand Journal of Geology and Geophysics* **1987,** *30* (1), 1-17.

100. Hietala, D. C.; Savage, P. E., Reaction pathways and kinetics of cholesterol in high-temperature water. *Chemical Engineering Journal* **2015,** *265*, 129-137.

101. Brooks, C.; Henderson, W.; Steel, G., The use of trimethylsilyl ethers in the characterization of natural sterols and steroid diols by gas chromatography-mass spectrometry. *Biochimica et Biophysica Acta (BBA)-Lipids and Lipid Metabolism* **1973,** *296* (2), 431-445.

102. Gelders, G.; Vanderstukken, T.; Goesaert, H.; Delcour, J., Amylose–lipid complexation: a new fractionation method. *Carbohydrate Polymers* **2004,** *56* (4), 447-458.

103. Madan, R., *Organic Reactions Conversions Mechanisms & Problems*. S. Chand Publishing: 2009.

104. Long, J.; Xu, Y.; Wang, T.; Yuan, Z.; Shu, R.; Zhang, Q.; Ma, L., Efficient base-catalyzed decomposition and in situ hydrogenolysis process for lignin depolymerization and char elimination. *Applied Energy* **2015,** *141*, 70-79.

105. Miliotti, E.; Dell'Orco, S.; Lotti, G.; Rizzo, A. M.; Rosi, L.; Chiaramonti, D.,

Lignocellulosic ethanol biorefinery: Valorization of lignin-rich stream through hydrothermal liquefaction. *Energies* **2019,** *12* (4), 723.

106. Zhang, C.; Tang, X.; Sheng, L.; Yang, X., Enhancing the performance of Co-hydrothermal liquefaction for mixed algae strains by the Maillard reaction. *Green Chemistry* **2016,** *18* (8), 2542-2553.

107. Poger, D.; Caron, B.; Mark, A. E., Effect of methyl-branched fatty acids on the structure of lipid bilayers. *The Journal of Physical Chemistry B* **2014,** *118* (48), 13838-13848.

108. Aierzhati, A.; Stablein, M. J.; Wu, N. E.; Kuo, C.-T.; Si, B.; Kang, X.; Zhang, Y., Experimental and model enhancement of food waste hydrothermal liquefaction with combined effects of biochemical composition and reaction conditions. *Bioresource technology* **2019,** *284*, 139-147.

109. Schutyser, W.; Renders, a. T.; Van den Bosch, S.; Koelewijn, S.-F.; Beckham, G.; Sels, B. F., Chemicals from lignin: an interplay of lignocellulose fractionation, depolymerisation, and upgrading. *Chemical Society Reviews* **2018,** *47* (3), 852-908.

110. Arturi, K. R.; Strandgaard, M.; Nielsen, R. P.; Søgaard, E. G.; Maschietti, M., Hydrothermal liquefaction of lignin in near-critical water in a new batch reactor: Influence of phenol and temperature. *The Journal of Supercritical Fluids* **2017,** *123*, 28-39.

111. Gao, Y., Lignin Conversion to Value-added Products via Heterogeneous Catalysts. **2018**.

112. Diéguez, M.; Pàmies, O.; Ruiz, A.; Díaz, Y.; Castillón, S.; Claver, C., Carbohydrate derivative ligands in asymmetric catalysis. *Coordination chemistry reviews* **2004,** *248* (21-24), 2165-2192.

113. Pedersen, T. H.; Jensen, C. U.; Sandström, L.; Rosendahl, L. A., Full characterization of compounds obtained from fractional distillation and upgrading of a HTL biocrude. *Applied*

Energy **2017,** *202*, 408-419.

114. Todd, J. D.; Rogers, R.; Li, Y. G.; Wexler, M.; Bond, P. L.; Sun, L.; Curson, A. R.; Malin, G.; Steinke, M.; Johnston, A. W., Structural and regulatory genes required to make the gas dimethyl sulfide in bacteria. *Science* **2007,** *315* (5812), 666-669.

115. Brand, S.; Kim, J., Liquefaction of major lignocellulosic biomass constituents in supercritical ethanol. *Energy* **2015,** *80*, 64-74.

116. Chen, H.; He, Z.; Zhang, B.; Feng, H.; Kandasamy, S.; Wang, B., Effects of the aqueous phase recycling on bio-oil yield in hydrothermal liquefaction of Spirulina Platensis, α-cellulose, and lignin. *Energy* **2019,** *179*, 1103-1113.

117. Ramirez, J. A.; Brown, R. J.; Rainey, T. J., A review of hydrothermal liquefaction bio-crude properties and prospects for upgrading to transportation fuels. *Energies* **2015,** *8* (7), 6765-6794.

118. Ye, Z.; Zhao, J.; ying Huang, H.; Ma, F.; Zhang, R., Decomposition of dimethylamine gas with dielectric barrier discharge. *Journal of hazardous materials* **2013,** *260*, 32-39.

119. Amarasekara, A. S.; Reyes, C. D. G., Pd/C catalyzed room-temperature, atmospheric pressure hydrogenation of furanic bio-oils from acidic ionic liquid catalyzed liquefaction of biomass in acetone. *Fuel Processing Technology* **2020,** *200*, 106320.

120. Fu, J.; Yang, C.; Wu, J.; Zhuang, J.; Hou, Z.; Lu, X., Direct production of aviation fuels from microalgae lipids in water. *Fuel* **2015,** *139*, 678-683.

121. Yamashita, K.; Yamamoto, N.; Mizukoshi, A.; Noguchi, M.; Ni, Y.; Yanagisawa, Y., Compositions of volatile organic compounds emitted from melted virgin and waste plastic pellets. *Journal of the Air & Waste Management Association* **2009,** *59* (3), 273-278.

122. Vardon, D. R. Hydrothermal liquefaction for energy recovery from high-moisture waste biomass. University of Illinois at Urbana-Champaign, 2012.

123. Elvers, B., Handbook of fuels. Energy sources for transportation. **2008**.

124. Minowa, T.; Yokoyama, S. y.; Kishimoto, M.; Okakura, T., Oil production from algal cells of Dunaliella tertiolecta by direct thermochemical liquefaction. *Fuel* **1995,** *74* (12), 1735-1738.

125. Neveux, N.; Yuen, A. K. L.; Jazrawi, C.; Magnusson, M.; Haynes, B. S.; Masters, A. F.; Montoya, A.; Paul, N. A.; Maschmeyer, T.; de Nys, R., Biocrude yield and productivity from the hydrothermal liquefaction of marine and freshwater green macroalgae. *Bioresource Technology* **2014,** *155*, 334-341.

126. Zheng, C.; Zhao, L.; Zhou, X.; Fu, Z.; Li, A., Treatment technologies for organic wastewater. In *Water Treatment*, Intech: 2013.

127. Speight, J. G.; Speight, J., *Handbook of petroleum analysis*. Wiley-Interscience New York: 2001; Vol. 156.

128. Minowa, T.; Kondo, T.; Sudirjo, S. T., Thermochemical liquefaction of Indonesian biomass residues. *Biomass and Bioenergy* **1998,** *14* (5), 517-524.

CHAPTER 7

CONCLUSION

7.1 Conclusion

This thesis provides an advanced understanding of the effect of using different fractions of biosolids' compositions with different HTL conditions, particularly reaction temperature and residence time, on the HTL product yields and distributions and renewable crude oil composition. The first major contribution is developing and modifying methods to determine the biosolids' content of twenty-one samples and measuring the inorganic content. The second significant contribution is developing a set of reaction conditions, which can be applied to predict the yields and distribution of HTL products, such as renewable crude oil, solids residue, aqueous and gas, depending on the organic composition of the biosolids. The applied reaction conditions were set for temperatures of 250, 300 and 350°C and reaction times from 0 to 60 minutes, pressure at 200 bar and the heating rate was 80 ºC/min with different biosolids contents. Fixing the HTL reaction conditions was an approach to simplify the hundreds of complex reactions during the HTL processes, which can help determine the optimum reaction conditions for the HTL of biosolids. The third significant contribution is the characterisation composition of the produced renewable crude oil from different biosolids fractions. The conclusions of each part of the research are illustrated below.

7.1.1 The effect of biochemical composition on the renewable crude oil produced from hydrothermal liquefaction of biosolids

This study involved providing developed and modified methods to determine the biosolids' content of twenty-one samples, particularly lipids, proteins, carbohydrates, and lignins, and measuring the inorganic content. The study also provided a clear understanding of the biosolids' characterisation and how the composition of biosolids affects the product yields and the quality of the resultant renewable crude oil, , alongside determining the level of produced

renewable crude oil at different boiling points. HTL experiments using eight different biosolids samples HC, LC, HP, LP, HL, LP, HLG and LLG, represent the samples that have the highest and lowest carbohydrates, proteins, lipids and lignin contents, respectively. The effect of reaction temperature and residence time on the product yields and distributions and the renewable crude oil's boiling point distribution was analysed. The following conclusions are illustrated below:

1. Biosolids have different organic content associated with the biosolids' age. The biosolids' chemical composition was varied due to the various sources and the initial wastewater treatments.
2. Applying a Van Krevelen diagram to compare biosolids with other biomass showed that only a few biosolids samples contain characteristics similar to those of biomass. The majority of the biosolid samples differ characteristically from other biomass types. The differences in the biosolids' organic content characteristics depend on the sewage sludge sources and the treatment process.
3. HTL of biosolids results showed that biosolids' composition affects the HTL yield, and lipids and proteins positively affect the renewable crude oil yield. In contrast, carbohydrates and insoluble lignin negatively impacted the renewable crude oil yield and carbohydrates and insoluble lignin led to an increase in the solid residue.
4. The renewable crude oil quality was also affected by the differences in the organic composition of biosolids. The renewable crude oil contained a high amount of high-boiling point materials compared with the low-boiling point materials for all biosolids samples used in this study.

7.1.2 Elucidation of the effect of reaction conditions and biosolids' composition on conversion to renewable crude oil via hydrothermal liquefaction

This study provided a new understating of HTL products' characterisation from biosolids and assesses the effects of HTL conditions, particularly reaction temperature and residence time, and different compositions of biosolids on the HTL products' yields and characterisation of the boiling point fractions of the renewable crude produced. A simulated distillation of the renewable crude oil was also utilised to establish the approximate fuel fractions. The following conclusions were made:

1. The HTL products' yields and the quality of the renewable crude oil from the HTL of biosolids were affected by the HTL conditions, particularly reaction temperature, residence time and biosolids' compositions. The differences in biosolids' compositions had the main effects on HTL yields; specifically, the renewable crude oil yield and its characteristics were influenced by the lipids', proteins', carbohydrates' and lignins' contents of biosolids.
2. The effect of the HTL conditions, particularly reaction temperature, was significant. The renewable crude oil yield increased with the increase in temperature until a specific temperature was reached, at which point the renewable crude oil yield started to decrease. Various residence times also affected the renewable crude oil yields significantly. The optimum residence times of the HTL process depended on the selected biosolids sample and temperature.
3. The simulated distillation by TGA of the produced renewable crude oil showed that the desired products from the HTL of biosolids could differ depending on the biosolids' composition and the HTL conditions. For example, the gasoline and naphtha-like yields

from the HL and HP samples have an opposite response to the increase in reaction temperature and residence time. In comparison, the HC and HLG samples were similar but with low yields. The highest yields of the kerosene-like and the diesel-like were mostly similar across all the samples, and only the HL sample showed a decrease with the increase in reaction temperature and residence time. The gas oil-like yields were high in all biosolids samples, but HP, HC, and HLG declined with the increase in reaction temperature. The wax, lubricating oil, and vacuum gas oil-like yields from most biosolids samples were similar; only the HL sample yield increased with the increase in residence time at 300ºC.

7.1.3 Characterisation of chemical properties of the produced organic fractions via hydrothermal liquefaction of biosolids

This work provided a better understating of the produced renewable crude oil composition via the HTL of biosolids. It performed extensive composition characterisation on the produced renewable crude oil to assess the influences of using a particular set of HTL temperatures and residence times and biosolids with different organic fractions of proteins, lipids, carbohydrates and lignins on the composition and the fractions of the produced renewable crude oil. The following conclusions were made:

1. Qualitative characterisation of renewable crude oil was applied using gas chromatography-mass spectrometry analysis. GC-MS identified a complex mixture of >300 major compounds in the produced renewable crude oil. The predominant components were from lipids' constituents, such as cyclic terpanes and terpenes, accompanied by other compounds produced from proteins', carbohydrates' and lignins'

constituents, such as nitrogenous oxygenated, ketones, aldehydes, and phenolic components.

2. Based on the boiling point of the produced compounds, the produced crude oil fractions differed depending on the HTL conditions and the biosolids' composition. The greatest gasoline and naphtha-like, and diesel-like yields were produced from samples with high lipids and proteins contents. The best yield of kerosene-like was generated from the high lipids sample. The highest gas oil-like yield was generated from the high lipids and high carbohydrates sample. While a high-yield of wax, lubricating oil and vacuum gas oil-like were produced from the high lignins sample.
3. The HTL of biosolids can be optimised to produce a targeted fraction of renewable crude oil. The best gasoline and naphtha-like and diesel-like yields were generated from samples with high protein and lipid content at 350°C and 40 minutes, and at the same HTL conditions; the kerosene-like best yield was produced from the high lipid sample. The highest gas oil-like yield was generated from a high carbohydrate sample at 250°C and 60 minutes, while the high lipid sample was produced at 300ºC and 60 minutes. The greatest yield of wax, lubricating oil and vacuum gas oil-like was produced from the high lignin sample at 300ºC and 20 minutes.
4. The outcomes of this work provide a better vision of understating the optimum HTL conditions for specific biosolids' compositions to produce the best yield and quality of the target renewable crude oil fractions via the HTL process, especially when the production of renewable crude oil reaches the commercial stage.

7.2 Recommendations for future work

This thesis provides an advanced understanding of both the biosolids' content and the produced products from the HTL of biosolids, specifically renewable crude oil. It also provides a clear understating of the effects of the reactions' conditions, particularly the reaction temperature and residence time and biosolids' composition on the product yields and distribution and the produced renewable crude oil composition. However, further research is needed to provide more information for the existing knowledge of the HTL of biosolids:

1. The HTL experiments' outcomes have some limitations, such as the batch reactor's configuration, which was only 11 mL volume, and the limitations of applying one heating rate and one loading mass during the HTL process. Therefore, further HTL experiments with different loadings and heating rates could provide further explanation of the HTL reactions of biosolids.
2. The separation methods greatly affect the distribution of HTL products. Therefore, it is essential to apply better separation methods when using the HTL process at an industrial scale for better products distribution, which is yet to be determined and requires more research.
3. The components of biosolids are very complex and vary widely. Biosolids' compositions could be the key factors that affect the HTL process. Therefore, HTL conditions should be selected based on biosolids compositions. Thus, more research into different biosolids compositions' effects on the reaction pathways with different HTL conditions to produce specific renewable crude oil compositions is required. Although this research could require hundreds of specific HTL experiments, it could be useful, especially for targeted compositions of renewable crude oil.
4. Biosolids contain high oxygen compounds, representing a serious concern for the storage instability of renewable crude oil due to oxygen polymerisation. Therefore,

determining the oxygenated compounds before the renewable crude upgrading processes is essential, especially as it is associated with the operating severity and hydrogen consumption.

5. The produced renewable crude oil via the HTL process could contain high nitrogen elements that affect renewable crude oil quality. Further research is required into renewable crude oil upgrading using physical and chemical methods, such as hydrotreating, supercritical fluids, emulsification, solvent addition and catalytic cracking.
6. Inorganic contents in biosolids require further research because they may affect the produced HTL products. HTL experiments with adding inorganics contents to the used samples could help identify their HTL process effect.
7. Techno-economic analysis (TEA) is suggested to be studied in-depth to analyse the economic performance and feaseablity of HTL plants.
8. Finally, the variation between the processes when using batch and continuous reactors in the HTL requires more research for a better understanding of the scientific literature. Therefore, a comparison is needed by applying experiments on continuous systems with the same biosolids composition and HTL reaction conditions to determine product yields and distributions, and renewable crude oil compositions, as the outcome results of continuous processes may be more representative of the industrial stage.

REFERENCES

The following references are cited in Chapters 1, 2, 3 and 7. References for Chapters 4-6 are included within each of these chapters.

REFERENCES

1. Dimitriadis, A.; Bezergianni, S., Hydrothermal liquefaction of various biomass and waste feedstocks for biocrude production: A state of the art review. *Renewable and Sustainable Energy Reviews* **2017,** *68*, 113-125.

2. Tekin, K.; Karagöz, S., Non-catalytic and catalytic hydrothermal liquefaction of biomass. *Research on Chemical Intermediates* **2013,** *39* (2), 485-498.

3. Elliott, D., Thermochemical processing of biomass. Chichester, UK: John Wiley & Sons Ltd: 2011.

4. Outlook, A. E., with Projection to 2050, US Energy Information Administration (EIA), Feb 6, 2018. 2018.

5. Tully, A., BP's latest estimate says world's oil will last 53.3 years. Diperoleh: 2015.

6. Karak, T.; Bhagat, R.; Bhattacharyya, P., Municipal solid waste generation, composition, and management: the world scenario. *Critical Reviews in Environmental Science and Technology* **2012,** *42* (15), 1509-1630.

7. GOH, N.; SHORT, M. D.; BOLAN, N. S.; SAINT, C. P., Solutions for solid wastes. *Unmaking Waste 2015 Conference Proceedings* **2015**, 342-356.

8. Federation, W. E. Questions and Answers on Land Application of Biosolids. (accessed 01 May).

9. Ullah, K.; Ahmad, M.; Sofia; Sharma, V. K.; Lu, P.; Harvey, A.; Zafar, M.; Sultana, S.; Anyanwu, C. N., Algal biomass as a global source of transport fuels: Overview and development perspectives. *Progress in Natural Science: Materials International* **2014,** *24* (4), 329-339.

10. Akhtar, J.; Amin, N. A. S., A review on process conditions for optimum bio-oil yield in hydrothermal liquefaction of biomass. *Renewable and Sustainable Energy Reviews* **2011,** *15* (3), 1615-1624.

11. Zmierczak, W. W.; Miller, J. D., Processes for catalytic conversion of lignin to liquid

bio-fuels and novel bio-fuels. Google Patents: 2011.

12. Goyal, H. B.; Seal, D.; Saxena, R. C., Bio-fuels from thermochemical conversion of renewable resources: A review. *Renewable and Sustainable Energy Reviews* **2008,** *12* (2), 504-517.

13. Jones, C. W.; Agrawal, P. K., Hydrogen production from biomass. Google Patents: 2011.

14. Chen, Y.; Wang, C.; Lu, W.; Yang, Z., Study of the co-deoxy-liquefaction of biomass and vegetable oil for hydrocarbon oil production. *Bioresource technology* **2010,** *101* (12), 4600-4607.

15. Lynd, L. R.; Cushman, J. H.; Nichols, R. J.; Wyman, C. E., Fuel ethanol from cellulosic biomass. *Science* **1991,** *251* (4999), 1318-1323.

16. Tyson, K. *Fuel cycle evaluations of biomass-ethanol and reformulated gasoline. Volume 1*; National Renewable Energy Lab., Golden, CO (United States); Oak Ridge …: 1993.

17. Minowa, T.; Yokoyama, S. y.; Kishimoto, M.; Okakura, T., Oil production from algal cells of Dunaliella tertiolecta by direct thermochemical liquefaction. *Fuel* **1995,** *74* (12), 1735-1738.

18. Corbitt, R. A., Standard handbook of environmental engineering. McGraw-Hill Inc., New York.: 1990.

19. Kalavrouziotis, I. K., *Wastewater and Biosolids Management*. IWA Publishing: 2017.

20. US Environmental Protection, A. Biosolids: Frequently Asked Questions. <http://water.epa.gov/polwaste/wastewater/treatment/biosolids/genqa.cfm> (accessed 1 May).

21. Statistics, A. B. o. Waste Management Services. <http://www.abs.gov.au/ausstats/abs@.nsf/lookup/8698.0Glossary12009-10>. (accessed 2 May).

22. Mateo-Sagasta, J.; Raschid-Sally, L.; Thebo, A., Global wastewater and sludge

production, treatment and use. In *Wastewater*, Springer: 2015; pp 15-38.

23. Mtui, G. Y., Recent advances in pretreatment of lignocellulosic wastes and production of value added products. *African Journal of Biotechnology* **2009,** *8* (8).

24. Sánchez, C., Lignocellulosic residues: biodegradation and bioconversion by fungi. *Biotechnology advances* **2009,** *27* (2), 185-194.

25. Wang, L. K.; Shammas, N. K.; Hung, Y.-T., *Biosolids treatment processes*. Springer: 2007; Vol. 6.

26. Epstein, E., Land Application of Sewage Sludge and Biosolids. Washington, DC: Lewis, 2003; Vol. 27, p 154.

27. Kiser, M. A.; Westerhoff, P.; Benn, T.; Wang, Y.; Pérez-Rivera, J.; Hristovski, K., Titanium nanomaterial removal and release from wastewater treatment plants. *Environmental Science and Technology* **2009,** *43* (17), 6757-6763.

28. Lu, Q.; He, Z. L.; Stoffella, P. J., Land application of biosolids in the USA: A review. *Applied and Environmental Soil Science* **2012,** *2012*.

29. Paez-Rubio, T.; Xin, H.; Anderson, J.; Peccia, J., Particulate matter composition and emission rates from the disk incorporation of class B biosolids into soil. *Atmospheric Environment* **2006,** *40* (36), 7034-7045.

30. Westerhoff, P. K.; Kiser, A.; Hristovski, K., Nanomaterial removal and transformation during biological wastewater treatment. *Environmental Engineering Science* **2013,** *30* (3), 109-117.

31. Muchovej, R. M.; Obreza, T., *Biosolids: Are These Residuals All the Same?* University of Florida Cooperative Extension Service, Institute of Food and Agriculture Sciences, EDIS: 2001.

32. Singh, R.; Agrawal, M., Potential benefits and risks of land application of sewage sludge. *Waste management* **2008,** *28* (2), 347-358.

33. Zorpas, A. A.; Inglezakis, V. J., *Sewage sludge management: From the past to our century*. Nova Science Publishers, Inc.: 2012.

34. Lee, D.; Spinosa, L.; He, P.; Chen, T., Sludge production and management processes: case study in China. *Water science and technology* **2006,** *54* (5), 189-196.

35. Ilani, T.; Herrmann, I.; Karnieli, A.; Arye, G., Characterization of the biosolids composting process by hyperspectral analysis. *Waste management* **2016,** *48*, 106-114.

36. Smith, K.; Fowler, G.; Pullket, S.; Graham, N. J. D., Sewage sludge-based adsorbents: a review of their production, properties and use in water treatment applications. *Water research* **2009,** *43* (10), 2569-2594.

37. Hargreaves, J.; Adl, M.; Warman, P., A review of the use of composted municipal solid waste in agriculture. *Agriculture, Ecosystems & Environment* **2008,** *123* (1-3), 1-14.

38. Moral, R.; Paredes, C.; Bustamante, M.; Marhuenda-Egea, F.; Bernal, M., Utilisation of manure composts by high-value crops: Safety and environmental challenges. *Bioresource Technology* **2009,** *100* (22), 5454-5460.

39. Shah, Z.; Jani, Y. M.; Khan, F., Evaluation of organic wastes for composting. *Communications in soil science and plant analysis* **2014,** *45* (3), 309-320.

40. Mahro, B.; Timm, M., Potential of biowaste from the food industry as a biomass resource. *Engineering in Life Sciences* **2007,** *7* (5), 457-468.

41. Spinosa, L.; Vesilind, P. A., *Sludge into biosolids*. IWA publishing: 2001.

42. Torri, S. I.; Cabrera, M. N., The environmental impact of biosolids land application. In *Organic waste: management strategies, environmental impact and emerging regulations*, Nova Science Publishers, Inc. Hauppauge, NY 11788: 2017; pp 185-208.

43. Kalogo, Y.; Monteith, H., *Energy and resource recovery from sludge*. IWA Publishing: 2012.

44. Klass, D. L., *Biomass for renewable energy, fuels, and chemicals*. Elsevier: 1998.

45. Wyman, C.; Decker, S.; Himmel, M.; Brady, J.; Skopec, C.; Viikari, L., Polysaccharides: structural diversity and functional versatility. *Dekker, New York* **2005**, 995-1033.

46. Brand, S.; Hardi, F.; Kim, J.; Suh, D. J., Effect of heating rate on biomass liquefaction: differences between subcritical water and supercritical ethanol. *Energy* **2014,** *68*, 420-427.

47. Chiaramonti, D.; Prussi, M.; Buffi, M.; Rizzo, A. M.; Pari, L., Review and experimental study on pyrolysis and hydrothermal liquefaction of microalgae for biofuel production. *Applied energy* **2017,** *185*, 963-972.

48. Faeth, J. L.; Valdez, P. J.; Savage, P. E., Fast hydrothermal liquefaction of nannochloropsis sp. to produce biocrude. *Energy and Fuels* **2013,** *27* (3), 1391-1398.

49. Kumar, M.; Olajire Oyedun, A.; Kumar, A., A review on the current status of various hydrothermal technologies on biomass feedstock. *Renewable and Sustainable Energy Reviews* **2017**.

50. Darvodelsky, P., Biosolids snapshot (p. 35). Canberra, Australia: Department of Sustainability, Environment, Water. *Population and Communities* **2012**.

51. Villadsen, S. R.; Dithmer, L.; Forsberg, R.; Becker, J.; Rudolf, A.; Iversen, S. B.; Iversen, B. B.; Glasius, M., Development and application of chemical analysis methods for investigation of bio-oils and aqueous phase from hydrothermal liquefaction of biomass. *Energy and Fuels* **2012,** *26* (11), 6988-6998.

52. Xue, Y.; Chen, H.; Zhao, W.; Yang, C.; Ma, P.; Han, S., *A review on the operating conditions of producing bio-oil from hydrothermal liquefaction of biomass*. International Journal of Energy Research: Wiley Online Library, 2016; Vol. 20.

53. Savage, P.; Levine, R.; Huelsman, C., Hydrothermal processing of biomass. *Thermochemical conversion of biomass to liquid fuels and chemicals* **2010**, 192-221.

54. Singh, A.; Nigam, P. S.; Murphy, J. D., Renewable fuels from algae: An answer to

debatable land based fuels. *Bioresource Technology* **2011,** *102* (1), 10-16.

55. Toor, S. S.; Rosendahl, L.; Rudolf, A., Hydrothermal liquefaction of biomass: A review of subcritical water technologies. *Energy* **2011,** *36* (5), 2328-2342.

56. Patil, V.; Tran, K.-Q.; Giselrød, H. R., Towards sustainable production of biofuels from microalgae. *International journal of molecular sciences* **2008,** *9* (7), 1188-1195.

57. Gollakota, A.; Kishore, N.; Gu, S., A review on hydrothermal liquefaction of biomass. *Renewable and Sustainable Energy Reviews* **2018,** *81*, 1378-1392.

58. Chen, K.; Lyu, H.; Hao, S.; Luo, G.; Zhang, S.; Chen, J., Separation of phenolic compounds with modified adsorption resin from aqueous phase products of hydrothermal liquefaction of rice straw. *Bioresource Technology* **2015,** *182*, 160-168.

59. Linghong, Z.; Chunbao, X.; Champagne, P.; Mabee, W., Overview of current biological and thermo-chemical treatment technologies for sustainable sludge management. *Waste Management & Research* **2014,** *32* (7), 586-600.

60. Peterson, A. A.; Vogel, F.; Lachance, R. P.; Fröling, M.; Antal Jr, M. J.; Tester, J. W., Thermochemical biofuel production in hydrothermal media: A review of sub- and supercritical water technologies. *Energy and Environmental Science* **2008,** *1* (1), 32-65.

61. Demirbaş, A., Effect of lignin content on aqueous liquefaction products of biomass. *Energy Conversion and Management* **2000,** *41* (15), 1601-1607.

62. Zhang, L.; Xu, C. C.; Champagne, P., Overview of recent advances in thermo-chemical conversion of biomass. *Energy Conversion and Management* **2010,** *51* (5), 969-982.

63. Zhong, C.; Wei, X., A comparative experimental study on the liquefaction of wood. *Energy* **2004,** *29* (11), 1731-1741.

64. Biller, P.; Riley, R.; Ross, A., Catalytic hydrothermal processing of microalgae: decomposition and upgrading of lipids. *Bioresource technology* **2011,** *102* (7), 4841-4848.

65. Hadhoum, L.; Balistrou, M.; Burnens, G.; Loubar, K.; Tazerout, M., Hydrothermal

liquefaction of oil mill wastewater for bio-oil production in subcritical conditions. *Bioresource technology* **2016,** *218*, 9-17.

66. Xu, C.; Etcheverry, T., Hydro-liquefaction of woody biomass in sub-and super-critical ethanol with iron-based catalysts. *Fuel* **2008,** *87* (3), 335-345.

67. Elliott, D. C.; Biller, P.; Ross, A. B.; Schmidt, A. J.; Jones, S. B., Hydrothermal liquefaction of biomass: Developments from batch to continuous process. *Bioresource Technology* **2015,** *178*, 147-156.

68. Huber, G. W.; Iborra, S.; Corma, A., Synthesis of transportation fuels from biomass: Chemistry, catalysts, and engineering. *Chemical Reviews* **2006,** *106* (9), 4044-4098.

69. López Barreiro, D.; Prins, W.; Ronsse, F.; Brilman, W., Hydrothermal liquefaction (HTL) of microalgae for biofuel production: State of the art review and future prospects. *Biomass and Bioenergy* **2013,** *53*, 113-127.

70. Ramirez, J. A.; Brown, R. J.; Rainey, T. J., A review of hydrothermal liquefaction bio-crude properties and prospects for upgrading to transportation fuels. *Energies* **2015,** *8* (7), 6765-6794.

71. Zhang, L.; Xu, C.; Champagne, P., Overview of recent advances in thermo-chemical conversion of biomass. *Energy Conversion and Management* **2010,** *51* (5), 969-982.

72. Frank, E. D.; Elgowainy, A.; Han, J.; Wang, Z., Life cycle comparison of hydrothermal liquefaction and lipid extraction pathways to renewable diesel from algae. *Mitigation and Adaptation Strategies for Global Change* **2013,** *18* (1), 137-158.

73. Beckman, D.; Elliott, D. C., Comparisons of the yields and properties of the oil products from direct thermochemical biomass liquefaction processes. *The Canadian Journal of Chemical Engineering* **1985,** *63* (1), 99-104.

74. Tran, K.-Q., Fast hydrothermal liquefaction for production of chemicals and biofuels from wet biomass–The need to develop a plug-flow reactor. *Bioresource technology* **2016,** *213*,

327-332.

75. Biller, P.; Ross, A., Potential yields and properties of oil from the hydrothermal liquefaction of microalgae with different biochemical content. *Bioresource technology* **2011,** *102* (1), 215-225.

76. Garcia Alba, L.; Torri, C.; Samorì, C.; Van Der Spek, J.; Fabbri, D.; Kersten, S. R. A.; Brilman, D. W. F., Hydrothermal treatment (HTT) of microalgae: Evaluation of the process as conversion method in an algae biorefinery concept. *Energy and Fuels* **2012,** *26* (1), 642-657.

77. Ross, A. B.; Biller, P.; Kubacki, M. L.; Li, H.; Lea-Langton, A.; Jones, J. M., Hydrothermal processing of microalgae using alkali and organic acids. *Fuel* **2010,** *89* (9), 2234-2243.

78. Madsen, R. B.; Bernberg, R. Z. K.; Biller, P.; Becker, J.; Iversen, B. B.; Glasius, M., Hydrothermal co-liquefaction of biomasses – quantitative analysis of bio-crude and aqueous phase composition. *Sustainable Energy Fuels* **2017,** *1* (4), 789-805.

79. Jena, U.; Das, K. C.; Kastner, J. R., Effect of operating conditions of thermochemical liquefaction on biocrude production from Spirulina platensis. *Bioresource Technology* **2011,** *102* (10), 6221-6229.

80. Valdez, P. J.; Nelson, M. C.; Wang, H. Y.; Lin, X. N.; Savage, P. E., Hydrothermal liquefaction of Nannochloropsis sp.: Systematic study of process variables and analysis of the product fractions. *Biomass and Bioenergy* **2012,** *46*, 317-331.

81. Suzuki, A.; Nakamura, T.; Yokoyama, S.; Ogi, T.; Koguchi, K., Conversion of sewage sludge to heavy oil by direct thermochemical liquefaction. *Journal of Chemical Engineering of Japan* **1988,** *21* (3).

82. Brown, T. M.; Duan, P.; Savage, P. E., Hydrothermal liquefaction and gasification of Nannochloropsis sp. *Energy and Fuels* **2010,** *24* (6), 3639-3646.

83. McKendry, P., Energy production from biomass (part 2): conversion technologies.

Bioresource technology **2002,** *83* (1), 47-54.

84. Bühler, W.; Dinjus, E.; Ederer, H.; Kruse, A.; Mas, C., Ionic reactions and pyrolysis of glycerol as competing reaction pathways in near-and supercritical water. *The Journal of supercritical fluids* **2002,** *22* (1), 37-53.

85. Lehr, V.; Sarlea, M.; Ott, L.; Vogel, H., Catalytic dehydration of biomass-derived polyols in sub-and supercritical water. *Catalysis Today* **2007,** *121* (1-2), 121-129.

86. Wang, Z., Reaction mechanisms of hydrothermal liquefaction of model compounds and biowaste feedstocks. Zhang, Y., Ed. ProQuest Dissertations Publishing: 2011.

87. McConnell, B., Kinetics of Lipid Extraction from Microalgae. **2013**.

88. Gollakota, A. R. K.; Kishore, N.; Gu, S., A review on hydrothermal liquefaction of biomass. *Renewable and Sustainable Energy Reviews* **2017**.

89. Yaylayan, V.; Kaminsky, E., Isolation and structural analysis of Maillard polymers: caramel and melanoidin formation in glycine/glucose model system. *Food chemistry* **1998,** *63* (1), 25-31.

90. Brunner, G., Near critical and supercritical water. Part I. Hydrolytic and hydrothermal processes. *The Journal of Supercritical Fluids* **2009,** *47* (3), 373-381.

91. Tonoli, G.; Teixeira, E.; Corrêa, A.; Marconcini, J.; Caixeta, L.; Pereira-da-Silva, M.; Mattoso, L., Cellulose micro/nanofibres from Eucalyptus kraft pulp: preparation and properties. *Carbohydrate polymers* **2012,** *89* (1), 80-88.

92. Jazrawi, C., Hydrothermal Treatment of Algal Biomass: from Batch to Continuous Pilot Plant Operations. **2014**.

93. Delmer, D. P.; Amor, Y., Cellulose biosynthesis. *The plant cell* **1995,** *7* (7), 987.

94. Kumar, S.; Gupta, R. B., Hydrolysis of microcrystalline cellulose in subcritical and supercritical water in a continuous flow reactor. *Industrial & Engineering Chemistry Research* **2008,** *47* (23), 9321-9329.

95. Rogalinski, T.; Liu, K.; Albrecht, T.; Brunner, G., Hydrolysis kinetics of biopolymers in subcritical water. *The Journal of Supercritical Fluids* **2008,** *46* (3), 335-341.

96. Rowell, R. M.; Pettersen, R.; Han, J. S.; Rowell, J. S.; Tshabalala, M. A., Cell wall chemistry. *Handbook of wood chemistry and wood composites* **2005,** *2*.

97. Bobleter, O., Hydrothermal degradation of polymers derived from plants. *Progress in polymer science* **1994,** *19* (5), 797-841.

98. Montané, D.; Nabarlatz, D.; Martorell, A.; Torné-Fernández, V.; Fierro, V., Removal of lignin and associated impurities from xylo-oligosaccharides by activated carbon adsorption. *Industrial & engineering chemistry research* **2006,** *45* (7), 2294-2302.

99. Saisu, M.; Sato, T.; Watanabe, M.; Adschiri, T.; Arai, K., Conversion of lignin with supercritical water− phenol mixtures. *Energy & Fuels* **2003,** *17* (4), 922-928.

100. Sasaki, M.; Goto, M., Recovery of phenolic compounds through the decomposition of lignin in near and supercritical water. *Chemical Engineering and Processing: Process Intensification* **2008,** *47* (9-10), 1609-1619.

101. Osada, M.; Sato, T.; Watanabe, M.; Shirai, M.; Arai, K., Catalytic gasification of wood biomass in subcritical and supercritical water. *Combustion Science and Technology* **2006,** *178* (1-3), 537-552.

102. Kanetake, T.; Sasaki, M.; Goto, M., Decomposition of a lignin model compound under hydrothermal conditions. *Chemical Engineering & Technology: Industrial Chemistry-Plant Equipment-Process Engineering-Biotechnology* **2007,** *30* (8), 1113-1122.

103. Vassilev, S. V.; Baxter, D.; Andersen, L. K.; Vassileva, C. G.; Morgan, T. J., An overview of the organic and inorganic phase composition of biomass. *Fuel* **2012,** *94*, 1-33.

104. Ramsurn, H.; Gupta, R. B. In *Two-Step Biomass Hydrothermal Liquefaction Process through Acidic Subcritical-followed by Alkaline Supercritical-Water Treatment*, San Francisco: Tagungsbeitrag International Symposium on Supercritical Fluids, 2012.

105. Chornet, E.; Overend, R. P., Biomass liquefaction: an overview. In *Fundamentals of thermochemical biomass conversion*, Springer: 1985; pp 967-1002.

106. Sanghi, R.; Singh, V., *Green chemistry for environmental remediation*. John Wiley & Sons: 2012.

107. Tanneru, S. K.; Steele, P. H., Liquefaction of dried distiller's grains with solubles (DDGS) followed by hydroprocessing to produce liquid hydrocarbons. *Fuel* **2015,** *150*, 512-518.

108. Meeroff, D. E., Effects of ionizing radiation in wastewater treatment and residuals processing. **2001**.

109. Isikgor, F. H.; Becer, C. R., Lignocellulosic biomass: a sustainable platform for the production of bio-based chemicals and polymers. *Polymer Chemistry* **2015,** *6* (25), 4497-4559.

110. Hietala, D. C.; Faeth, J. L.; Savage, P. E., A quantitative kinetic model for the fast and isothermal hydrothermal liquefaction of Nannochloropsis sp. *Bioresource technology* **2016,** *214*, 102-111.

111. Mante, O. D.; Agblevor, F., Catalytic pyrolysis for the production of refinery-ready biocrude oils from six different biomass sources. *Green Chemistry* **2014,** *16* (6), 3364-3377.

112. Zein, M.; Winter, R., Effect of temperature, pressure and lipid acyl chain length on the structure and phase behaviour of phospholipid–gramicidin bilayers. *Physical Chemistry Chemical Physics* **2000,** *2* (20), 4545-4551.

113. Martin, J.; Kornsulle, R., Process for the extraction of macromolecules from biomass using the stillage. *US Patent* **2011**.

114. Zhang, S.; Yang, X.; Zhang, H.; Chu, C.; Zheng, K.; Ju, M.; Liu, L., Liquefaction of biomass and upgrading of bio-oil: a review. *Molecules* **2019,** *24* (12), 2250.

115. Gollakota, A. R.; Reddy, M.; Subramanyam, M. D.; Kishore, N., A review on the upgradation techniques of pyrolysis oil. *Renewable and Sustainable Energy Reviews* **2016,** *58*,

1543-1568.

116. Shakya, R.; Whelen, J.; Adhikari, S.; Mahadevan, R.; Neupane, S., Effect of temperature and Na2CO3 catalyst on hydrothermal liquefaction of algae. *Algal Research* **2015,** *12*, 80-90.

117. Sun, P.; Heng, M.; Sun, S.; Chen, J., Direct liquefaction of paulownia in hot compressed water: Influence of catalysts. *Energy* **2010,** *35* (12), 5421-5429.

118. Ye, L.; Zhang, J.; Zhao, J.; Tu, S., Liquefaction of bamboo shoot shell for the production of polyols. *Bioresource technology* **2014,** *153*, 147-153.

119. Liu, Z.; Zhang, F.-S., Effects of various solvents on the liquefaction of biomass to produce fuels and chemical feedstocks. *Energy conversion and management* **2008,** *49* (12), 3498-3504.

120. Sugano, M.; Takagi, H.; Hirano, K.; Mashimo, K., Hydrothermal liquefaction of plantation biomass with two kinds of wastewater from paper industry. *Journal of Materials Science* **2008,** *43* (7), 2476-2486.

121. Zhou, D.; Zhang, L.; Zhang, S.; Fu, H.; Chen, J., Hydrothermal liquefaction of macroalgae Enteromorpha prolifera to bio-oil. *Energy & Fuels* **2010,** *24* (7), 4054-4061.

122. Xu, C.; Lancaster, J., Conversion of secondary pulp/paper sludge powder to liquid oil products for energy recovery by direct liquefaction in hot-compressed water. *Water research* **2008,** *42* (6-7), 1571-1582.

123. Xiu, S.; Shahbazi, A.; Shirley, V.; Cheng, D., Hydrothermal pyrolysis of swine manure to bio-oil: effects of operating parameters on products yield and characterization of bio-oil. *Journal of analytical and applied pyrolysis* **2010,** *88* (1), 73-79.

124. Molten, P.; Demmitt, T.; Donovan, J.; Miller, R., Mechanism of conversion of cellulose wastes to liquid in alkaline solution. *Energy from biomass and wastes III. Chicago, IL: Institute of Gas Technology* **1983,** *293*.

125. Goheen, D. W., Lignin Structure and Reactions. *Adv Chem Ser* **1965,** *59*, 205.

126. Jin, B.; Duan, P.; Xu, Y.; Wang, F.; Fan, Y., Co-liquefaction of micro-and macroalgae in subcritical water. *Bioresource technology* **2013,** *149*, 103-110.

127. Clarens, A. F.; Resurreccion, E. P.; White, M. A.; Colosi, L. M., Environmental life cycle comparison of algae to other bioenergy feedstocks. *Environmental science & technology* **2010,** *44* (5), 1813-1819.

128. Shuping, Z.; Yulong, W.; Mingde, Y.; Kaleem, I.; Chun, L.; Tong, J., Production and characterization of bio-oil from hydrothermal liquefaction of microalgae Dunaliella tertiolecta cake. *Energy* **2010,** *35* (12), 5406-5411.

129. Fang, Z.; Sato, T.; Smith Jr, R. L.; Inomata, H.; Arai, K.; Kozinski, J. A., Reaction chemistry and phase behavior of lignin in high-temperature and supercritical water. *Bioresource Technology* **2008,** *99* (9), 3424-3430.

130. Qian, Y.; Zuo, C.; Tan, J.; He, J., Structural analysis of bio-oils from sub-and supercritical water liquefaction of woody biomass. *Energy* **2007,** *32* (3), 196-202.

131. Pandey, A.; Lee, D. J.; Chang, J.-S.; Chisti, Y.; Soccol, C. R., *Biomass, biofuels, biochemicals: biofuels from algae*. Elsevier: 2018.

132. Chan, Y. H.; Yusup, S.; Quitain, A. T.; Tan, R. R.; Sasaki, M.; Lam, H. L.; Uemura, Y., Effect of process parameters on hydrothermal liquefaction of oil palm biomass for bio-oil production and its life cycle assessment. *Energy Conversion and Management* **2015,** *104*, 180-188.

133. Behrendt, F.; Neubauer, Y.; Oevermann, M.; Wilmes, B.; Zobel, N., Direct liquefaction of biomass. *Chemical Engineering & Technology: Industrial Chemistry-Plant Equipment-Process Engineering-Biotechnology* **2008,** *31* (5), 667-677.

134. DESHPANDE, G.; HOLDER, G.; SHAH, Y. In *Effect of solvent density on coal-liquefaction under supercritical conditions*, ABSTRACTS OF PAPERS OF THE AMERICAN

CHEMICAL SOCIETY, AMER CHEMICAL SOC 1155 16TH ST, NW, WASHINGTON, DC 20036: 1985; pp 41-FUL.

135. Chan, Y. H.; Yusup, S.; Quitain, A. T.; Uemura, Y.; Sasaki, M., Bio-oil production from oil palm biomass via subcritical and supercritical hydrothermal liquefaction. *The Journal of Supercritical Fluids* **2014,** *95*, 407-412.

136. Savage, P. E., A perspective on catalysis in sub-and supercritical water. *The Journal of Supercritical Fluids* **2009,** *47* (3), 407-414.

137. Sasaki, M.; Adschiri, T.; Arai, K., Fractionation of sugarcane bagasse by hydrothermal treatment. *Bioresource Technology* **2003,** *86* (3), 301-304.

138. Sun, J.; Yang, J.; Shi, M., Review of denitrogenation of algae biocrude produced by hydrothermal liquefaction. *Transactions of Tianjin University* **2017,** *23* (4), 301-314.

139. LI, R.-d.; LI, B.-s.; YANG, T.-h.; XIE, Y.-h., Liquefaction of rice stalk in sub-and supercritical ethanol. *Journal of Fuel Chemistry and Technology* **2013,** *41* (12), 1459-1465.

140. Özçimen, D.; Karaosmanoğlu, F., Production and characterization of bio-oil and biochar from rapeseed cake. *Renewable energy* **2004,** *29* (5), 779-787.

141. ZHANG, H.-f.; SU, X.-l.; SUN, D.-k.; ZHANG, R.; BI, J.-c., Investigation on degradation of polyethylene to oil in a continuous supercritical water reactor. *Journal of Fuel chemistry and Technology* **2007,** *35* (4), 487-491.

142. Loppinet-Serani, A.; Aymonier, C.; Cansell, F., Current and foreseeable applications of supercritical water for energy and the environment. *ChemSusChem: Chemistry & Sustainability Energy & Materials* **2008,** *1* (6), 486-503.

143. Zhang, B.; von Keitz, M.; Valentas, K., Thermochemical liquefaction of high-diversity grassland perennials. *Journal of Analytical and Applied Pyrolysis* **2009,** *84* (1), 18-24.

144. Qu, Y.; Wei, X.; Zhong, C., Experimental study on the direct liquefaction of Cunninghamia lanceolata in water. *Energy* **2003,** *28* (7), 597-606.

145. Karagöz, S.; Bhaskar, T.; Muto, A.; Sakata, Y.; Uddin, M. A., Low-temperature hydrothermal treatment of biomass: effect of reaction parameters on products and boiling point distributions. *Energy & fuels* **2004,** *18* (1), 234-241.

146. Tumuluru, J. S., *Biomass preprocessing and pretreatments for production of biofuels: mechanical, chemical and thermal methods*. CRC Press: 2018.

147. Gai, C.; Li, Y.; Peng, N.; Fan, A.; Liu, Z., Co-liquefaction of microalgae and lignocellulosic biomass in subcritical water. *Bioresource technology* **2015,** *185*, 240-245.

148. Zheng, J.-L.; Zhu, M.-Q.; Wu, H.-t., Alkaline hydrothermal liquefaction of swine carcasses to bio-oil. *Waste management* **2015,** *43*, 230-238.

149. Zhu, Y.; Biddy, M. J.; Jones, S. B.; Elliott, D. C.; Schmidt, A. J., Techno-economic analysis of liquid fuel production from woody biomass via hydrothermal liquefaction (HTL) and upgrading. *Applied Energy* **2014,** *129*, 384-394.

150. Lu, J.; Li, X.; Yang, R.; Zhao, J.; Liu, Y.; Qu, Y., Liquefaction of fermentation residue of reed-and corn stover-pretreated with liquid hot water in the presence of ethanol with aluminum chloride as the catalyst. *Chemical Engineering Journal* **2014,** *247*, 142-151.

151. Kamio, E.; Sato, H.; Takahashi, S.; Noda, H.; Fukuhara, C.; Okamura, T., Liquefaction kinetics of cellulose treated by hot compressed water under variable temperature conditions. *Journal of materials science* **2008,** *43* (7), 2179-2188.

152. Zhang, B.; von Keitz, M.; Valentas, K., Thermal effects on hydrothermal biomass liquefaction. In *Biotechnology for fuels and chemicals*, Springer: 2008; pp 511-518.

153. Wang, L., *Sustainable bioenergy production*. CRC Press: 2014.

154. Durak, H.; Aysu, T., Effects of catalysts and solvents on liquefaction of Onopordum heteracanthum for production of bio-oils. *Bioresource technology* **2014,** *166*, 309-317.

155. Jindal, M. K.; Jha, M. K., Effect of process parameters on hydrothermal liquefaction of waste furniture sawdust for bio-oil production. *RSC advances* **2016,** *6* (48), 41772-41780.

156. Singh, R.; Prakash, A.; Balagurumurthy, B.; Bhaskar, T., Hydrothermal Liquefaction of Biomass. In *Recent Advances in Thermochemical Conversion of Biomass*, 2015; pp 269-291.

157. Cheng, S.; D'cruz, I.; Wang, M.; Leitch, M.; Xu, C., Highly efficient liquefaction of woody biomass in hot-compressed alcohol− water co-solvents. *Energy & Fuels* **2010,** *24* (9), 4659-4667.

158. Xu, C. C.; Shao, Y.; Yuan, Z.; Cheng, S.; Feng, S.; Nazari, L.; Tymchyshyn, M., Hydrothermal liquefaction of biomass in hot-compressed water, alcohols, and alcohol-water co-solvents for biocrude production. In *Application of hydrothermal reactions to biomass conversion*, Springer: 2014; pp 171-187.

159. Sato, T.; Osada, M.; Watanabe, M.; Shirai, M.; Arai, K., Gasification of alkylphenols with supported noble metal catalysts in supercritical water. *Industrial & engineering chemistry research* **2003,** *42* (19), 4277-4282.

160. Boocock, D. G. B.; Sherman, K. M., Further aspects of powdered poplar wood liquefaction by aqueous pyrolysis. *The Canadian Journal of Chemical Engineering* **1985,** *63* (4), 627-633.

161. Wang, C.; Pan, J.; Li, J.; Yang, Z., Comparative studies of products produced from four different biomass samples via deoxy-liquefaction. *Bioresource technology* **2008,** *99* (8), 2778-2786.

162. He, Y.; Liang, X.; Jazrawi, C.; Montoya, A.; Yuen, A.; Cole, A. J.; Neveux, N.; Paul, N. A.; de Nys, R.; Maschmeyer, T., Continuous hydrothermal liquefaction of macroalgae in the presence of organic co-solvents. *Algal Research* **2016,** *17*, 185-195.

163. Sasaki, M., MEASUREMENT OF THE RATE OF RETRO-ALDOL CONDENSATION OF. *Hydrothermal Reactions and Techniques* **2003**, 169.

164. Løes, A.-K.; Sandquist, J.; Meyer, G., Elemental composition and phosphorus

availability in hydrochars from seaweed and organic waste digestate. *Acta Agriculturae Scandinavica, Section B—Soil & Plant Science* **2018,** *68* (1), 57-66.

165. Bolton, T. F.; Havenhand, J. N., Physiological acclimation to decreased water temperature and the relative importance of water viscosity in determining the feeding performance of larvae of a serpulid polychaete. *Journal of plankton research* **2005,** *27* (9), 875-879.

166. Carlsson, A.; Lindman, B.; Stenberg, O., Use of viscosity-adjusting agent to counteract viscosity decrease upon temperature increase of a water-based system. Google Patents: 1994.

167. Henrikson, J. T.; Chen, Z.; Savage, P. E., Inhibition and acceleration of phenol oxidation by supercritical water. *Industrial & engineering chemistry research* **2003,** *42* (25), 6303-6309.

168. Water, M. Biosolids. https://www.melbournewater.com.au/water-data-and-education/environmental-issues/how-we-generate-energy/biosolids (accessed 25/08/2020).

169. Ameel, J.; Ruzycki, E.; Axler, R., Analytical chemistry and quality assurance procedures for natural water samples. Central Analytical Laboratory. *Natural Resources Research Institute Technical Report NRRI/TR–98/03 revised annually* **1998**.

170. Folch, J.; Lees, M.; Sloane Stanley, G., A simple method for the isolation and purification of total lipids from animal tissues. *J biol Chem* **1957,** *226* (1), 497-509.

171. Zhu, C.; Lee, Y., Determination of biomass dry weight of marine microalgae. *Journal of applied phycology* **1997,** *9* (2), 189-194.

172. Fujihara, S.; Kasuga, A.; Aoyagi, Y., Nitrogen-to-protein conversion factors for common vegetables in Japan. *Journal of food science* **2001,** *66* (3), 412-415.

173. Mariotti, F.; Tomé, D.; Mirand, P. P., Converting nitrogen into protein—beyond 6.25 and Jones' factors. *Critical reviews in food science and nutrition* **2008,** *48* (2), 177-184.

174. Maclean, W.; Harnly, J.; Chen, J.; Chevassus-Agnes, S.; Gilani, G.; Livesey, G.;

Warwick, P. In *Food energy–Methods of analysis and conversion factors*, Food and agriculture organization of the united nations technical workshop report, 2003; pp 8-9.

175. Parmar, N.; Singh, A.; Ward, O., Enzyme treatment to reduce solids and improve settling of sewage sludge. *Journal of Industrial Microbiology and Biotechnology* **2001,** *26* (6), 383-386.

176. Dubois, M.; Gilles, K. A.; Hamilton, J. K.; Rebers, P. t.; Smith, F., Colorimetric method for determination of sugars and related substances. *Analytical chemistry* **1956,** *28* (3), 350-356.

177. Liu, D.; Wong, P.; Dutka, B., Determination of carbohydrate in lake sediment by a modified phenol-sulfuric acid method. *Water research* **1973,** *7* (5), 741-746.

178. Masuko, T.; Minami, A.; Iwasaki, N.; Majima, T.; Nishimura, S.-I.; Lee, Y. C., Carbohydrate analysis by a phenol–sulfuric acid method in microplate format. *Analytical biochemistry* **2005,** *339* (1), 69-72.

179. Safařík, I.; Šantrůčková, H., Direct determination of total soil carbohydrate content. *Plant and Soil* **1992,** *143* (1), 109-114.

180. Stehouwer, R., Land application of sewage sludge in Pennsylvania: Effects of biosolids on soil and crop quality. *Environmental Soil Issues, Pen State College of Agric. Sci., University Park, PA* **2003**.

181. Montgomery, R., Further studies of the phenolsulfuric acid reagent for carbohydrates. *Biochimica et Biophysica Acta* **1961,** *48*, 591-593.

182. Dolson, D. A.; Battino, R.; Letcher, T. M.; Pegel, K.; Revaprasadu, N., Carbohydrate dehydration demonstrations. *Journal of chemical education* **1995,** *72* (10), 927.

183. Hatfield, R. D.; Jung, H. J. G.; Ralph, J.; Buxton, D. R.; Weimer, P. J., A comparison of the insoluble residues produced by the Klason lignin and acid detergent lignin procedures. *Journal of the Science of Food and Agriculture* **1994,** *65* (1), 51-58.

184. Li, Y.; Leow, S.; Fedders, A. C.; Sharma, B. K.; Guest, J. S.; Strathmann, T. J., Quantitative multiphase model for hydrothermal liquefaction of algal biomass. *Green Chemistry* **2017,** *19* (4), 1163-1174.

185. Vo, T. K.; Kim, S.-S.; Ly, H. V.; Lee, E. Y.; Lee, C.-G.; Kim, J., A general reaction network and kinetic model of the hydrothermal liquefaction of microalgae Tetraselmis sp. *Bioresource technology* **2017,** *241*, 610-619.

186. Instruments, M., Mastersizer 2000 user manual. *Worcestershire, United Kingdom: Malvern Instruments* **2007**.

187. Sarma, A.; Ryder, A., Comparison of the fluorescence behavior of a biocrude oil and crude petroleum oils. *Energy & fuels* **2006,** *20* (2), 783-785.

188. Garcia-Perez, M.; Chaala, A.; Pakdel, H.; Kretschmer, D.; Roy, C., Characterization of bio-oils in chemical families. *Biomass and Bioenergy* **2007,** *31* (4), 222-242.

189. Obeid, R.; Lewis, D.; Smith, N.; van Eyk, P., The elucidation of reaction kinetics for hydrothermal liquefaction of model macromolecules. *Chemical Engineering Journal* **2019,** *370*, 637-645.

190. Hecht, N. L.; Duvall, D., *Characterization and utilization of municipal and utility sludges and ashes*. National Environmental Research Center, Office of Research and Development, US Environmental Protection Agency: 1975; Vol. 1.

191. Li, S., Jiang, Y., Snowden-Swan, L.J., Askander, J.A., Schmidt, A.J. and Billing, J.M., 2021. Techno-economic uncertainty analysis of wet waste-to-biocrude via hydrothermal liquefaction. *Applied Energy*, *283*, p.116340.

192. Snowden-Swan, L.J., Zhu, Y., Jones, S.B., Elliott, D.C., Schmidt, A.J., Hallen, R.T., Billing, J.M., Hart, T.R., Fox, S.P. and Maupin, G.D., 2016. *Hydrothermal Liquefaction and Upgrading of Municipal Wastewater Treatment Plant Sludge: A Preliminary Techno-*

Economic Analysis, Rev. 1 (No. PNNL-25464-Rev. 1). Pacific Northwest National Lab.(PNNL), Richland, WA (United States).

APPENDICES

The following section includes appendices from chapter 3, which contains (materials and methods) and chapters 4, 5 and 6.

APPENDIX A:

SUPPLEMENTARY MATRIAL FOR CHAPTER 3

MATERIALS AND METHODS

Table A1: Preparation of standard samples.

Standard Sample (µg/mL)	Volume standard sugar solution (mL)	H_2O (mL)
0	**0**	**10**
10	**0.1**	**9.9**
20	**0.2**	**9.8**
30	**0.3**	**9.7**
40	**0.4**	**9.6**
50	**0.5**	**9.5**
60	**0.6**	**9.4**
70	**0.7**	**9.3**
80	**0.8**	**9.2**
90	**0.9**	**9.1**
100	**1**	**9**

Table A2: The actual measure of carbohydrate.

Sample g/10 mL

0.221 concentration of solids in original sample #1

0.220 concentration of solids in original sample #2

0.222 concentration of solids in original sample #3

0.221 g per 10 mL average concentration of solids in original the 3 samples

0.0221 g per mL average concentration of solids in original 3 samples as grams per mL

22000 ug per mL average concentration of solids in original 3 samples as micrograms per mL

Average of concentration = 0.641 / (0.0091) x10 = 703.8 µg/mL

Fraction = average absorbance multiplied by the average concentration of solids in the original 3 samples as µg/mL

Fraction = 703.8 μg /mL/ 22000 μg per mL = 0.03199

The percentage of Carbohydrate in bio-solids = the fraction x 100 = 3.199%

In the organic materials = (3.199/28.82) x 100% = 11.1%

Table A3: The CHNOS analysis results for the biosolid samples.

No	AFDW%	Carbon%	Hydrogen%	Nitrogen%	Sulphur%	Oxygen%
1	39.8	20.1	3.5	1.7	1.1	13.4
2	35.2	19.2	3.3	1.7	1.2	9.8
3	35.8	18.5	3.3	1.5	1.2	11.3
4	34.3	19.4	3.5	2.0	1.4	8.0
5	32.6	19.3	3.3	1.7	1.1	7.3
6	39.6	20.3	3.3	1.8	1.3	12.9
7	31.5	15.1	2.7	1.3	1.0	11.4
8	30.3	8.1	1.7	1.0	0.8	18.7
9	18.7	8.6	1.8	1.0	0.9	6.5
10	25.5	8.4	1.8	0.9	1.0	13.4
11	41.2	11.5	2.4	1.3	1.7	24.3
12	24.6	12.3	2.3	1.6	1.0	7.4
13	27.7	11.7	2.4	1.4	1.1	11.1
14	27.1	9.2	2.1	1.1	0.9	13.8
15	32.0	15.4	2.9	1.7	1.1	10.9
16	37.6	22.0	3.7	2.9	1.8	7.2
17	41.4	14.0	2.6	1.9	1.4	21.6
18	35.4	18.4	4.3	2.6	1.3	8.9
19	45.1	19.4	3.6	2.4	1.8	18.0
20	34.0	18.1	3.4	2.1	1.5	8.9
21	43.6	24.7	4.4	3.3	2.0	9.3
22	28.3	8.3	5.1	0.7	1.9	12.4
23	25.0	10.1	8.1	0.7	1.5	4.7
24	25.7	11.6	7.8	0.8	1.6	3.9
25	25.1	11.6	6.7	1.1	2.9	2.9
26	34.3	16.5	3.8	1.4	2.0	10.6
27	34.8	17.7	3.5	1.7	3.2	8.7
28	19.9	8.6	1.9	0.9	0.7	7.8
29	11.9	2.2	1.4	0.3	0.5	7.5
30	9.8	0.4	1.4	0.1	0.4	7.5
31	15.5	10.0	2.1	0.8	0.7	1.9
32	20.0	12.9	2.3	1.5	0.9	2.4
33	31.3	21.8	4.0	1.8	1.2	2.5

34	30.1	18.3	3.4	1.7	1.3	5.3
35	29.4	14.2	5.3	1.3	1.3	7.3
36	26.4	16.7	4.4	1.6	1.3	2.3
37	45.6	27.0	4.0	2.5	1.9	10.2
38	43.8	26.5	4.2	2.3	1.2	9.5
39	40.5	24.4	3.9	2.1	1.2	8.9
40	31.0	18.6	4.3	1.5	2.2	4.4
41	46.4	26.4	3.9	1.8	1.4	13.0
42	45.1	23.8	3.6	2.1	1.7	13.9
43	27.5	13.4	6.8	1.5	1.8	3.8
44	20.7	9.9	4.9	0.8	1.3	3.7
45	50.0	34.0	5.1	3.0	1.7	6.2
46	51.2	28.1	4.5	2.5	1.6	14.5
47	38.9	24.9	4.4	2.4	3.0	4.2
48	21.1	8.8	5.9	0.7	3.5	2.3
49	31.2	14.3	2.8	1.3	2.3	10.5
50	47.9	26.7	4.3	2.7	1.5	12.7
51	42.0	24.0	3.9	2.2	1.5	10.3
52	40.1	24.5	4.2	1.9	3.0	6.6
53	41.7	20.6	3.7	1.7	2.4	13.4
54	14.3	1.2	0.4	0.1	0.8	11.8
55	36.9	20.9	3.9	1.8	1.2	9.2
56	17.9	10.8	4.0	1.6	1.2	0.3
57	29.2	21.9	4.1	1.9	1.2	0.2
58	36.1	21.2	3.5	1.9	1.3	8.1
59	30.9	8.1	1.8	0.8	1.6	18.6

APPENDIX B:

SUPPLEMENTARY MATRIAL FOR CHAPTER 4

The effect of biochemical composition on the renewable crude oil produced from hydrothermal liquefaction of biosolids

Jasim M. Al-juboori [a], David M. Lewis [a], Peter J. Ashman [a], Tony Hall [b] and Philip J. van Eyk. [a],*

[a] *School of Chemical Engineering & Advanced Materials, University of Adelaide, Adelaide, SA 5005*

[b] *School of Physical Sciences, University of Adelaide, Adelaide, SA 5005*

* *Corresponding Author: philip.vaneyk@adelaide.edu.au*

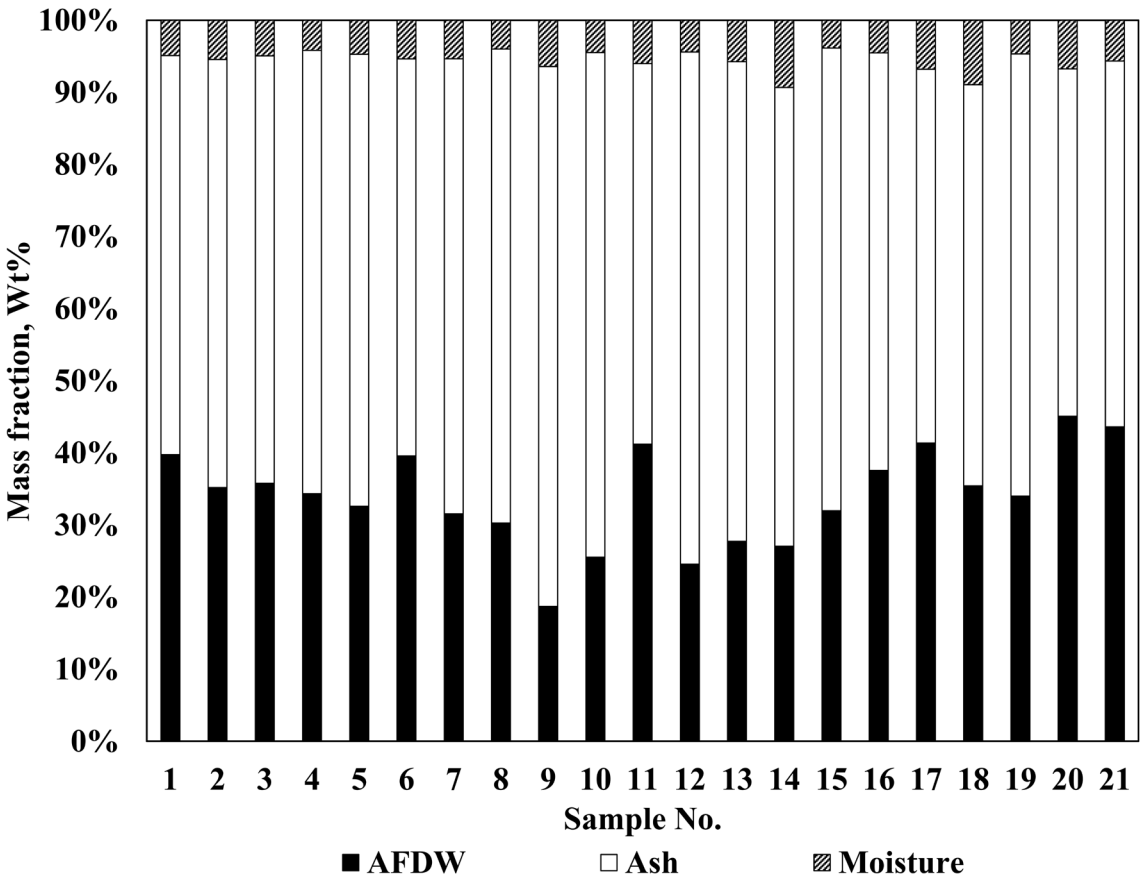

Figure S1: The AFDW and the moisture percentage in the biosolids.

APPENDIX C:

SUPPLEMENTARY MATRIAL FOR CHAPTER 5

Elucidation of the effect of reaction conditions and biosolids composition on conversion to renewable crude oil via hydrothermal liquefaction

Jasim M. Al-juboori [a], Reem Obeid [a], David M. Lewis [a], Tony Hall[b] and Philip J. van Eyk.a [a,*]

[a] School of Chemical Engineering & Advanced Materials, University of Adelaide, Adelaide, SA 5005

[b] School of Physical Sciences, University of Adelaide, Adelaide, SA 5005

** Corresponding Author: philip.vaneyk@adelaide.edu.au*

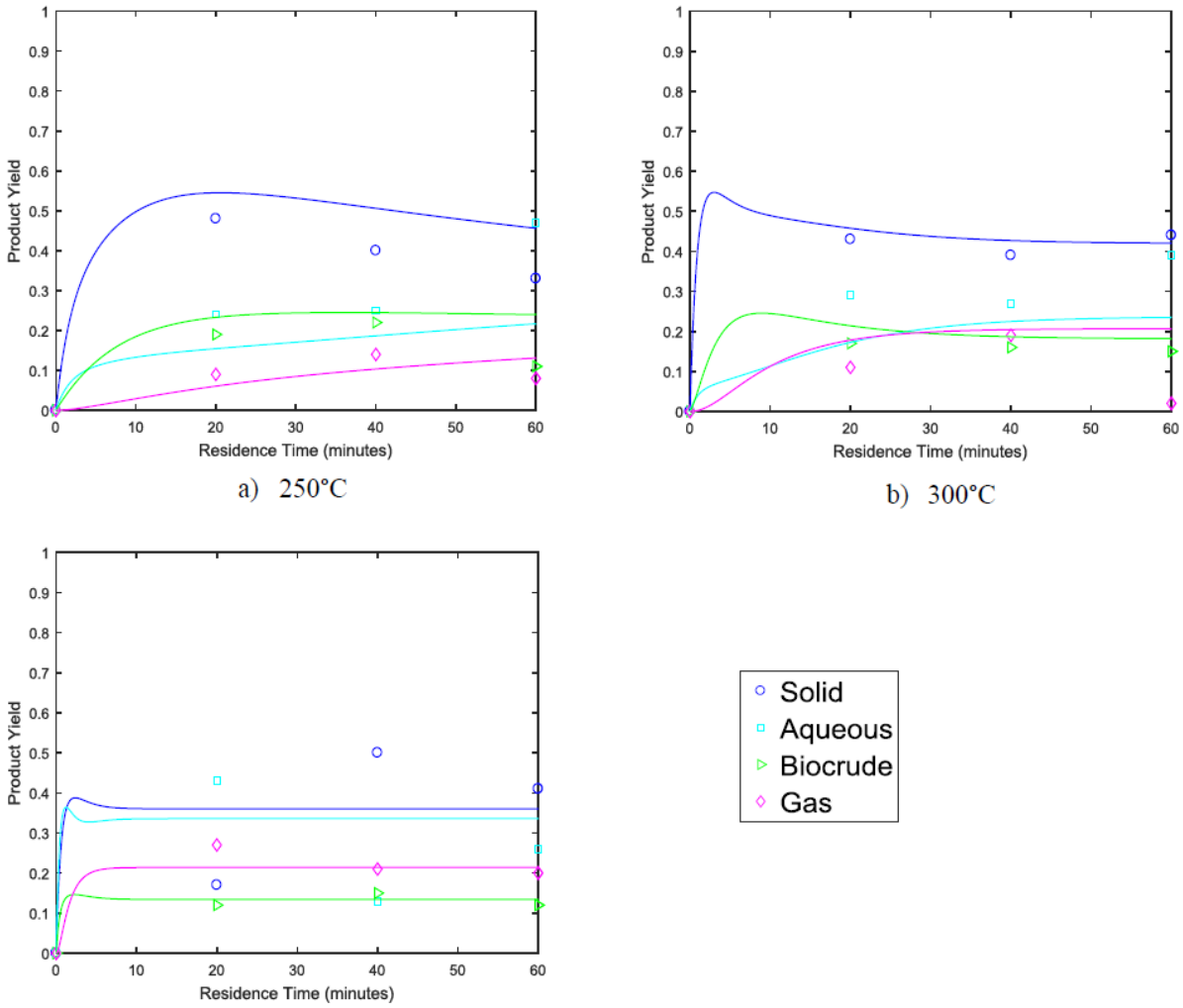

Figure S1: Bulk kinetic with data for high lipid biosolids.

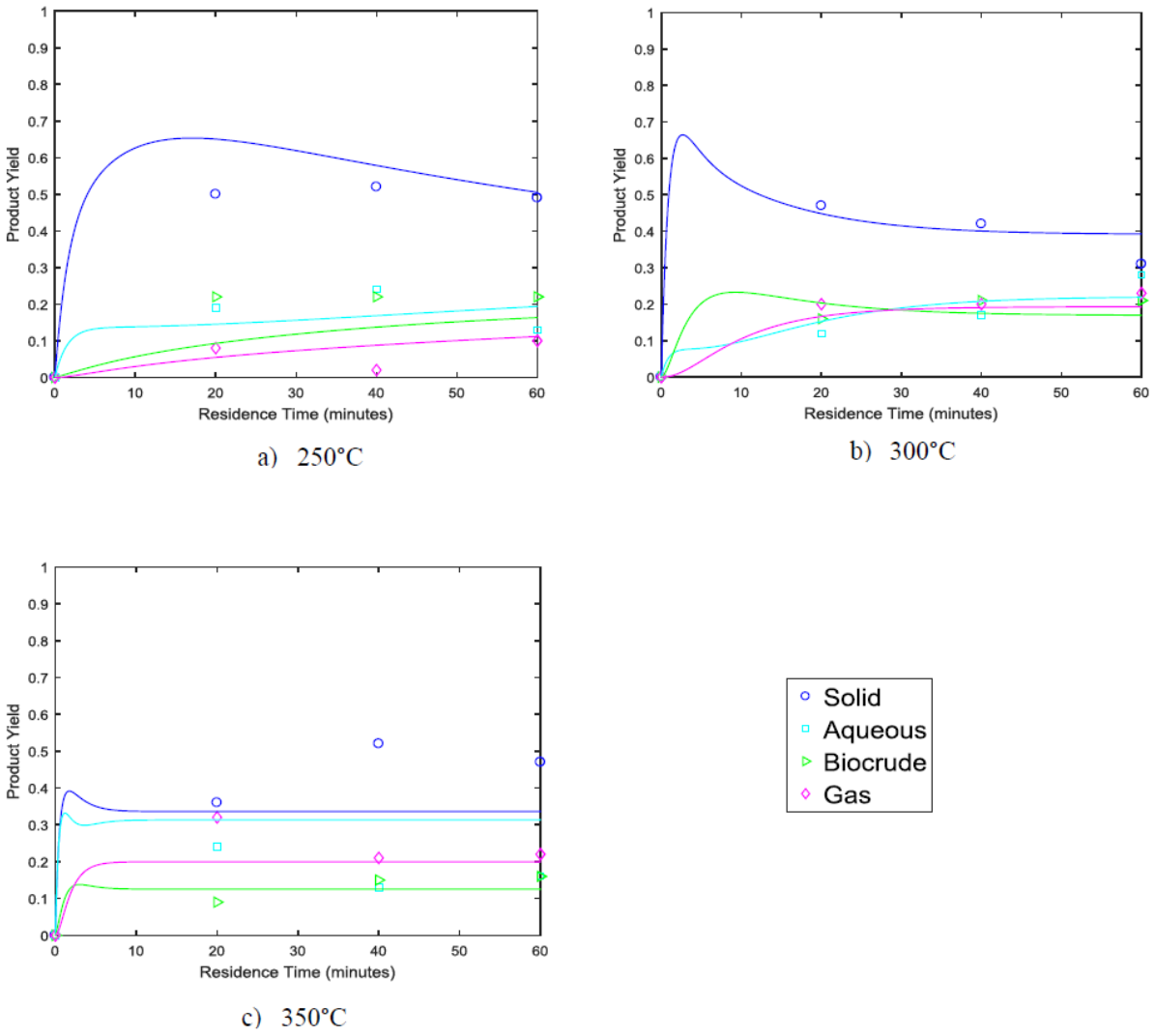

Figure S2: Bulk kinetic with data for high protein biosolids.

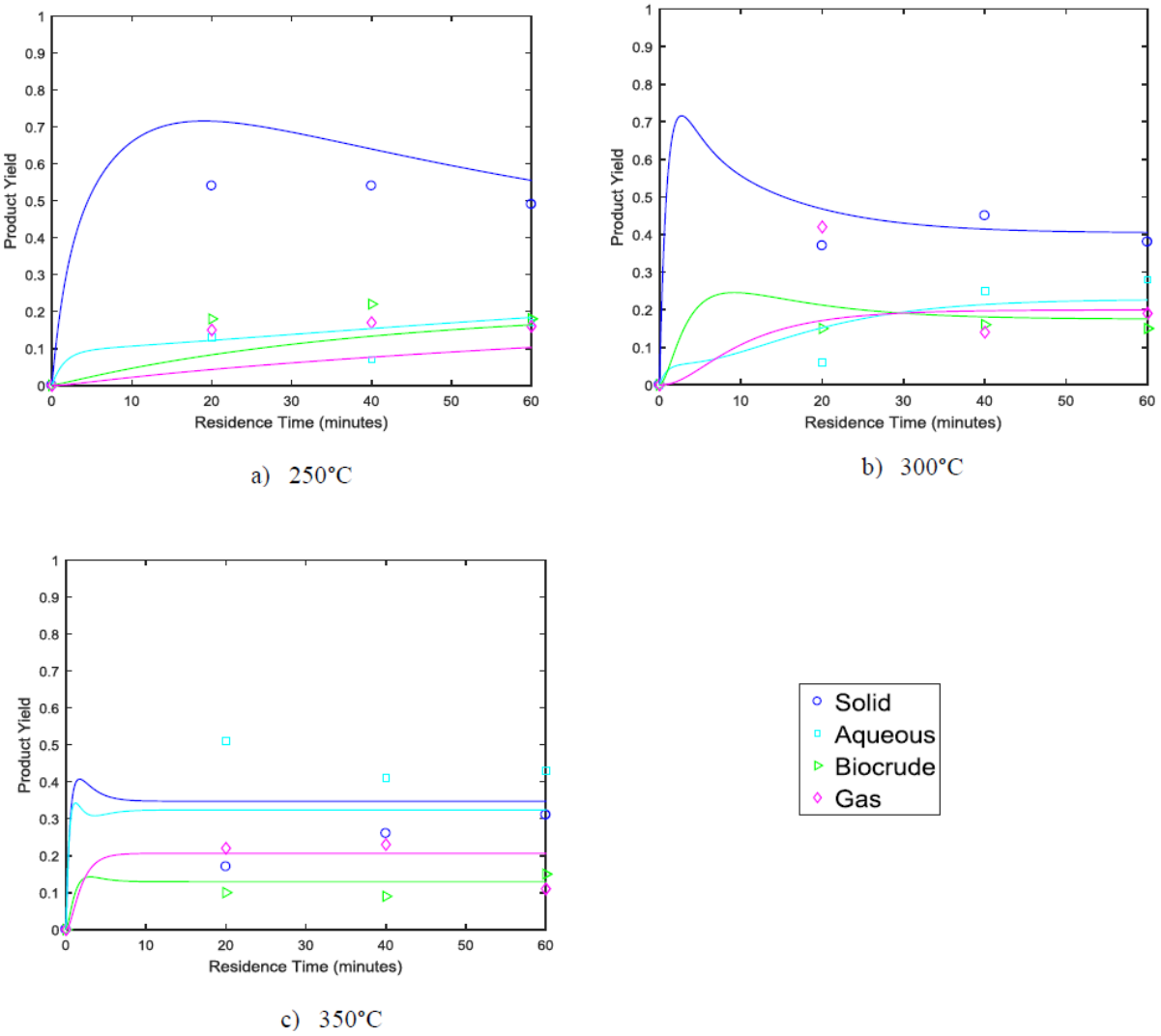

Figure S3: Bulk kinetic with data for high carbohydrate biosolids.

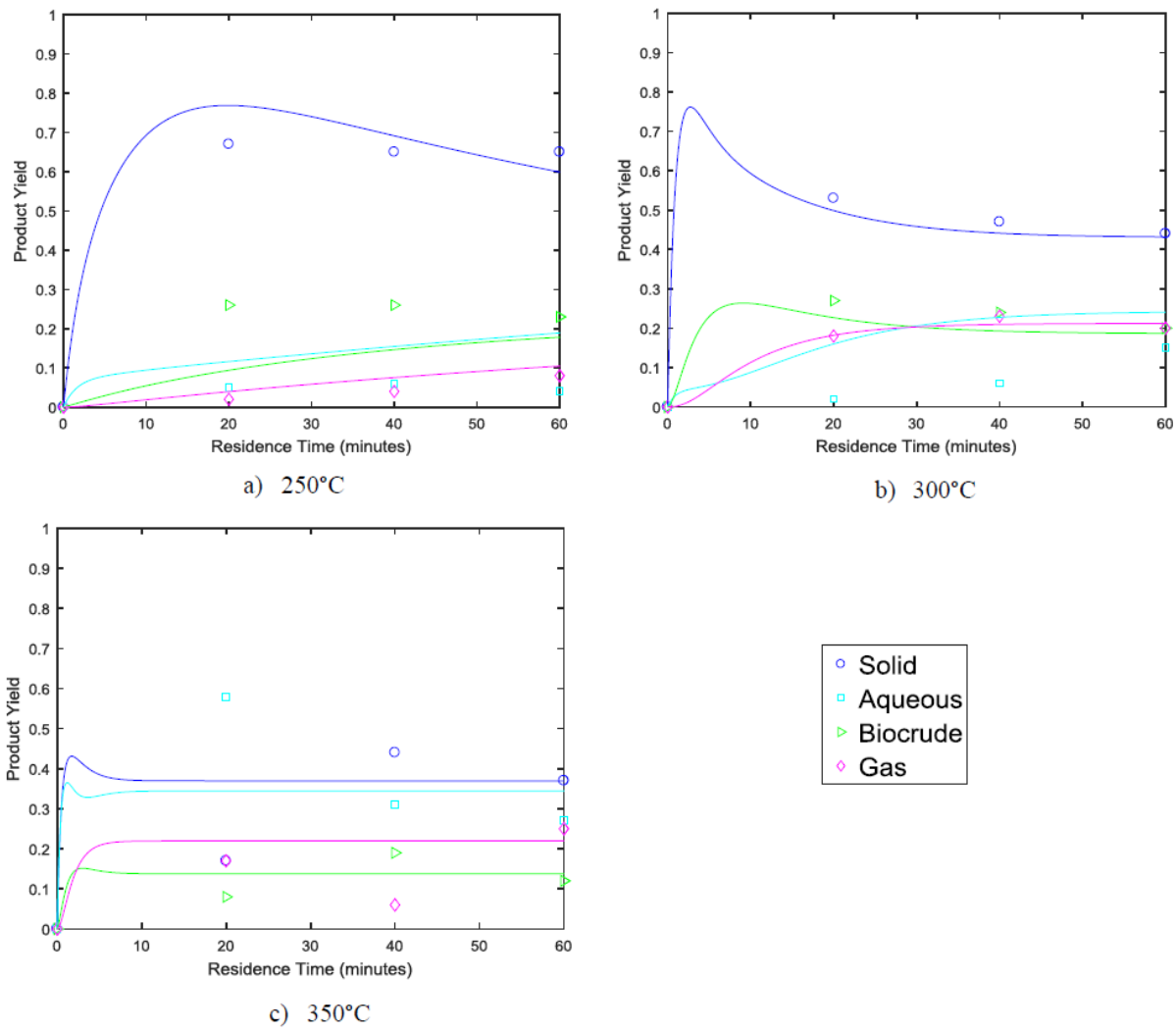

Figure S4: Bulk kinetic with data for high lignin biosolids.

APPENDIX D:

SUPPLEMENTARY MATRIAL FOR CHAPTER 6

CHARACTERISATION OF CHEMICAL PROPERTIES OF THE PRODUCED ORGANIC FRACTIONS VIA HYDROTHERMAL LIQUEFACTION OF BIOSOLIDS

Jasim M. Al-juboori [a,*], David M. Lewis [a], Tony Hall [b] and Philip J. van Eyk [a]

[a] *School of Chemical Engineering & Advanced Materials, University of Adelaide, Adelaide, SA 5005*

[b] *School of Physical Sciences, University of Adelaide, Adelaide, SA 5005*

** Corresponding Author: Jasim.al-juboori@adelaide.edu.au*

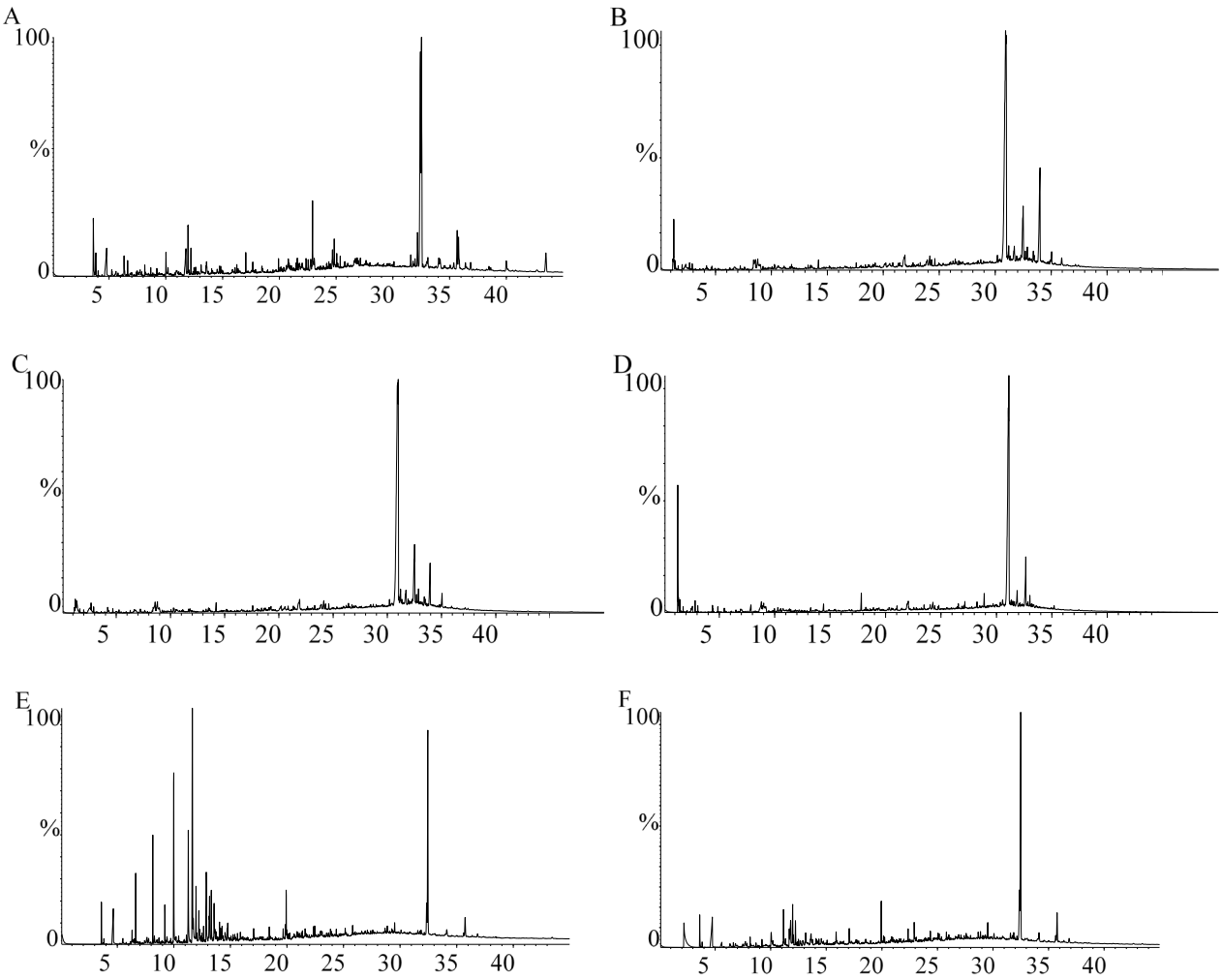

Figure S1: GC-MS of the produced renewable crude oil via the HTL of HL sample: (A) at 300ºC reaction temperature and 20 minutes residence time, (B) at 300ºC and 40 minutes, (C) at 300ºC and 60 minutes, (D) at 350ºC and 20 minutes, (E) at 350ºC and 40 minutes and (F) at 350ºC and 60 minutes.

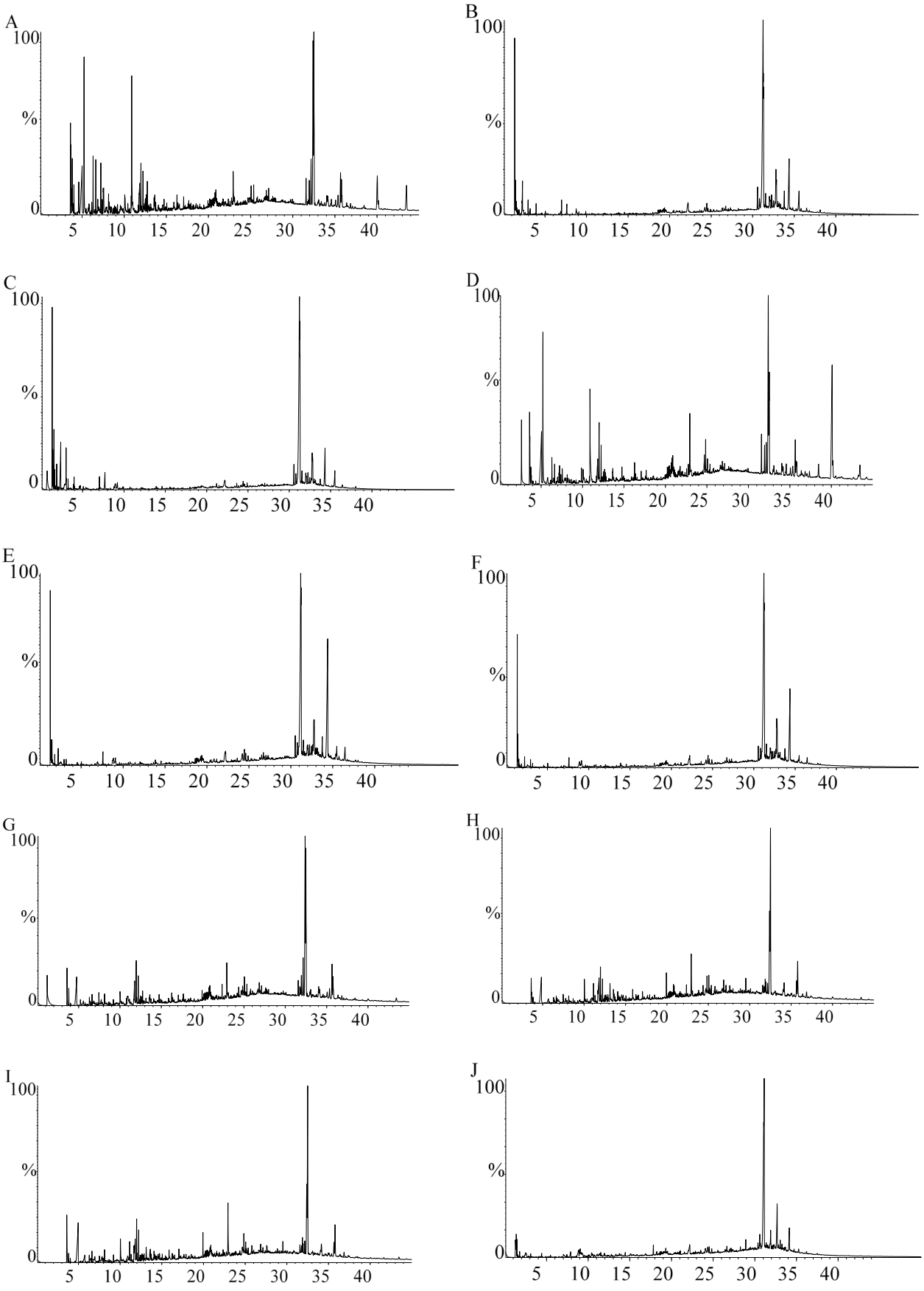
A
B
C
D
E
F
G
H
I
J
100
%
0
5 10 15 20 25 30 35 40

Figure S2: Chromatogram of GC-MS analysis of the HP sample: (A) before the HTL process, (B) for the produced renewable crude oil via the HTL process at 250ºC reaction temperature of and 20 minutes residence time, (C) at 250ºC and 40 minutes, (D) at 250ºC and 60 minutes, (E) at 300ºC and 20 minutes, (F) at 300ºC and 40 minutes, (G) at 300ºC and 60 minutes, (H) at 350ºC and 20 minutes, (I) at 350ºC and 40 minutes, (J) at 350ºC and 60 minutes.

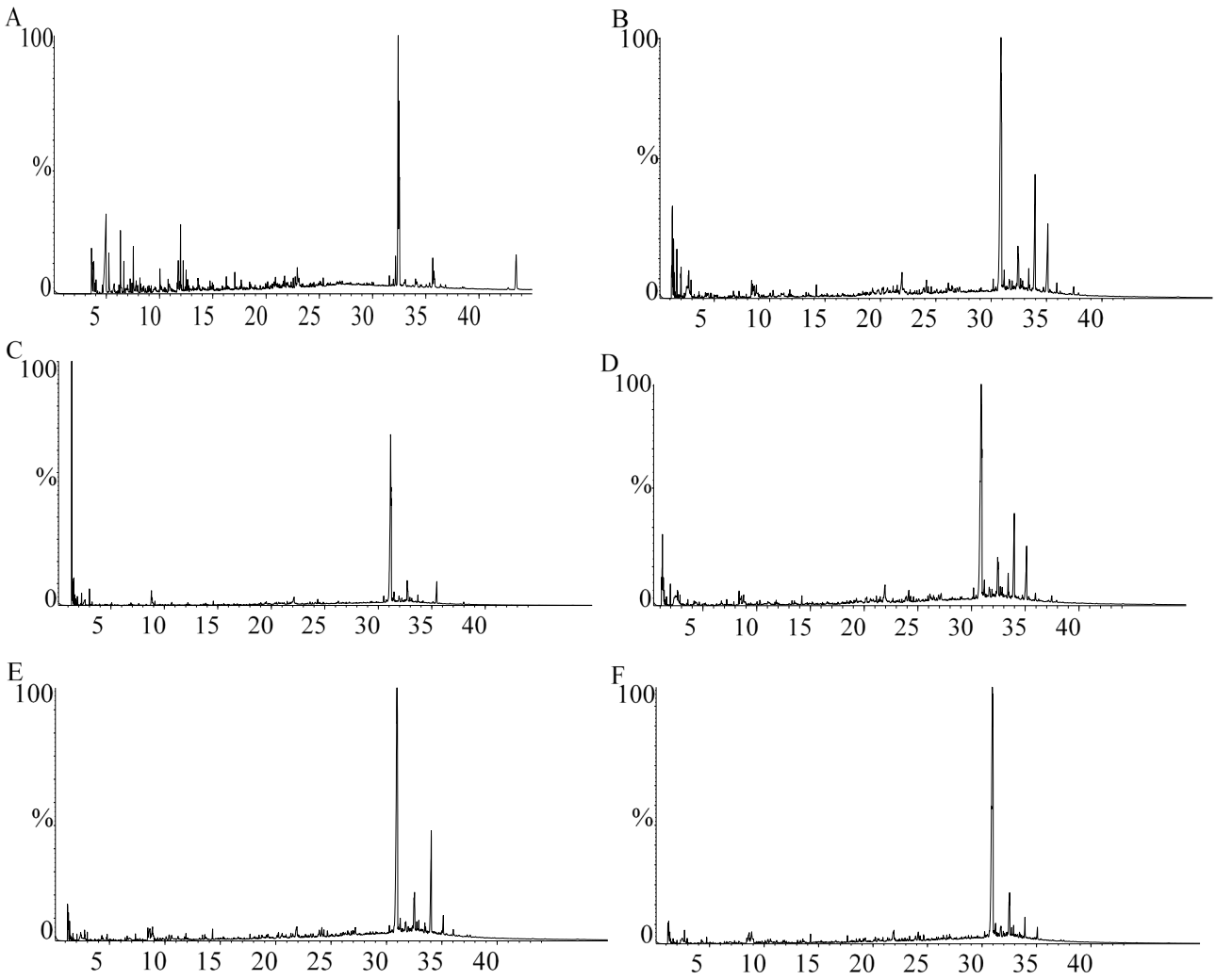

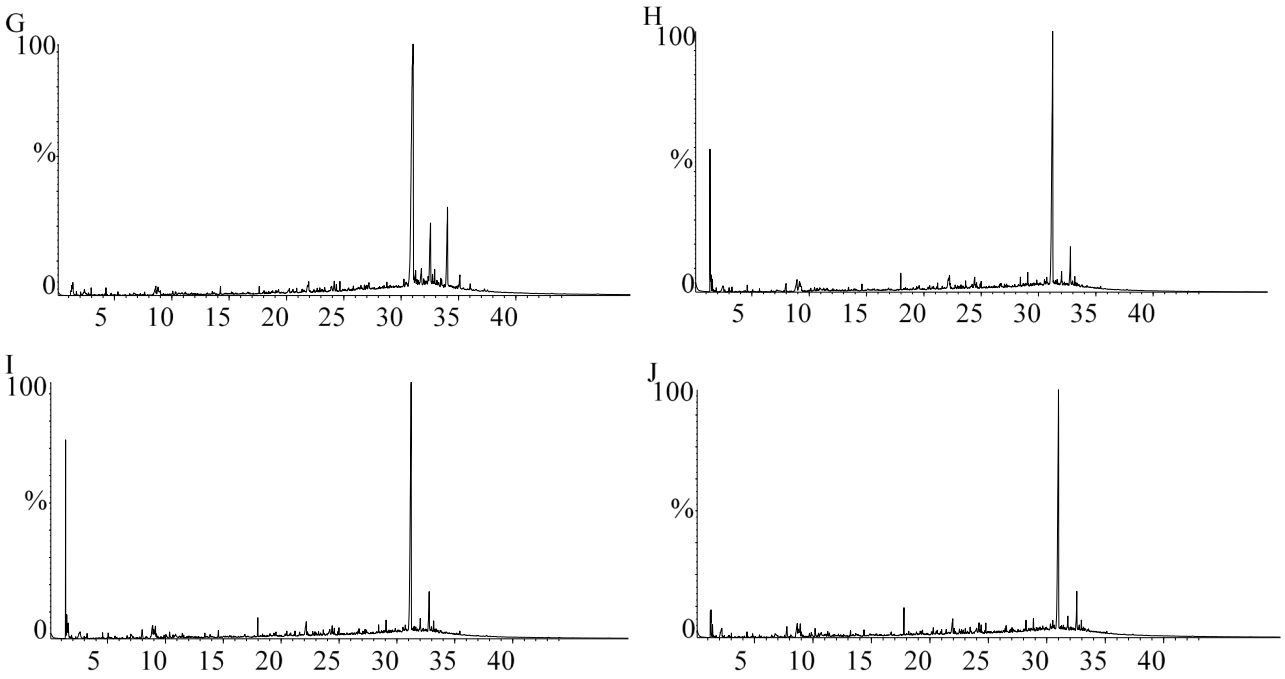

Figure S3: Chromatogram of GC-MS analysis of the HC sample: (A) before the HTL process, (B) for the produced renewable crude oil via the HTL process at 250ºC reaction temperature of and 20 minutes residence time, (C) at 250ºC and 40 minutes, (D) at 250ºC and 60 minutes, (E) at 300ºC and 20 minutes, (F) at 300ºC and 40 minutes, (G) at 300ºC and 60 minutes, (H) at 350ºC and 20 minutes, (I) at 350ºC and 40 minutes, (J) at 350ºC and 60 minutes.

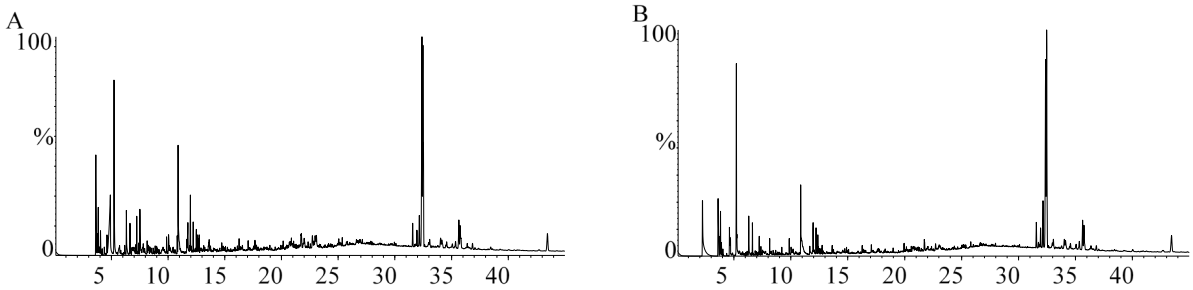

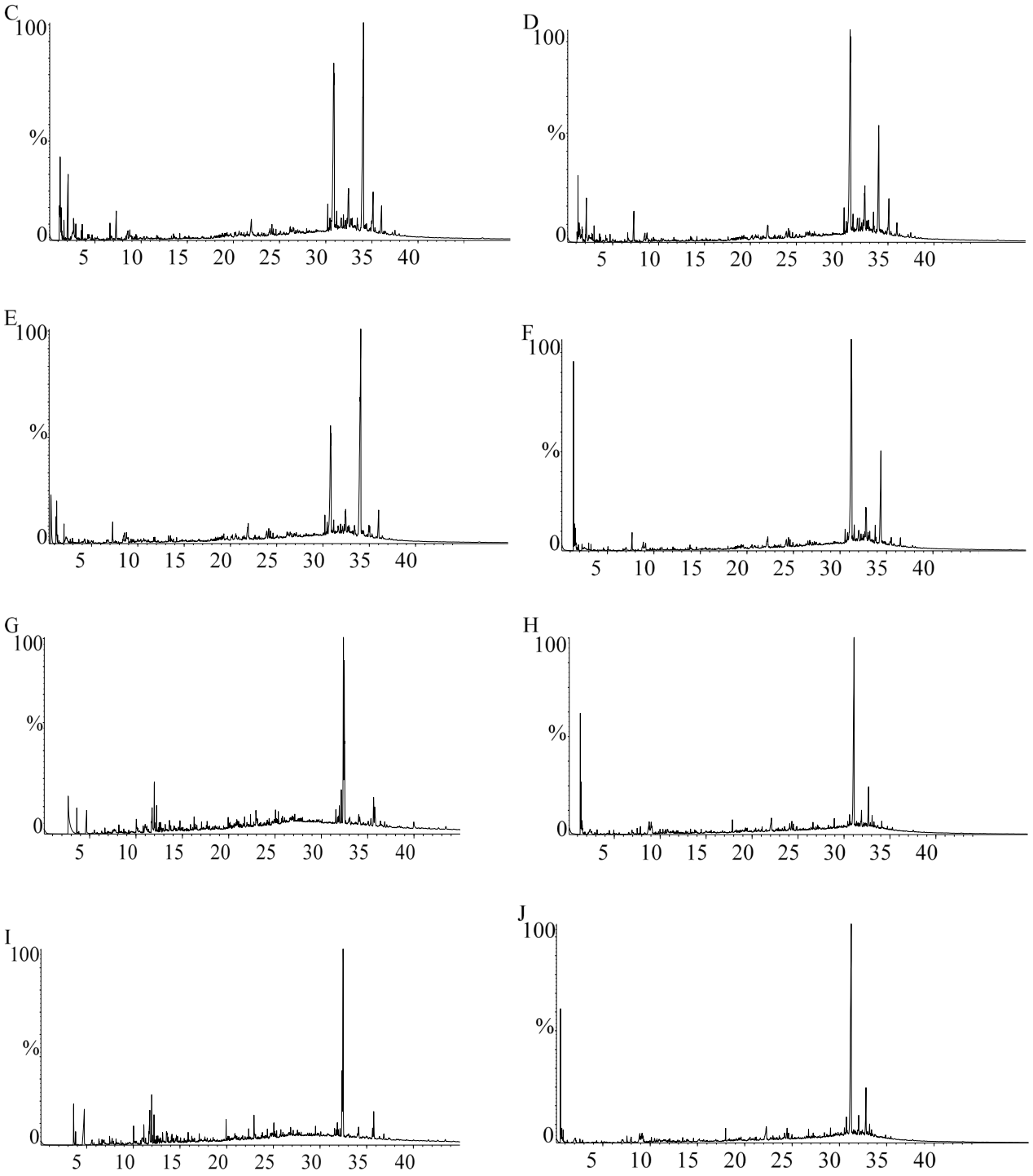

Figure S4: Chromatogram of GC-MS analysis of the HLG sample: (A) before the HTL process, (B) for the produced renewable crude oil via the HTL process at 250ºC reaction temperature of and 20 minutes residence time, (C) at 250ºC and 40 minutes, (D) at 250ºC and 60 minutes, (E) at 300ºC and 20 minutes, (F) at 300ºC and 40 minutes, (G) at 300ºC and 60 minutes, (H) at 350ºC and 20 minutes, (I) at 350ºC and 40 minutes, (J) at 350ºC and 60 minutes.

Table S1: The major identified compounds of the produced renewable crude oil via the HTL process from the HL sample at reaction temperature of 250°C and residence time of 40 minutes using GC-MS analysis.

HL 250°C 40 Mins							
No	**Retention time (mins)**	**Area**	**Area (%)**	**Compound name**	**Molecular formula**	**Molecular weight (g/mol)**	**Classification of compound**
1	1.357	303693014	4.90	Carbon dioxide	CO_2	44	Protein[64, 6]
2	1.461	137785541	2.22	Methanethiol	CH_4S	48	Probably bacterial products[122]
3	1.567	46378756	0.75	Acetone	C_3H_6O	58	Carbohydrate[23]
Total yields %			**7.87**				
1	7.162	22486732	0.33	Phenol	C_6H_6O	94	Protein, Carbohydrate, Lignin[29, 52, 106]
2	8.856	43328088	0.70	Phenol, 2-methoxy-	C7H8O2	124	Lipid, Lignin[64, 10]
3	8.988	44353930	0.72	2,5-Pyrrolidinedione, 1-methyl-	C_5H_7NO	113	Protein[64]
4	9.211	47107397	0.76	Methyl creatinine	$C_4H_7N_3O$	113	Protein[44]
5	10.76	13193000	0.21	Phenol, 2-methoxy-4-methyl-	$C_8H_{10}O_2$	138	Lignin[69]
6	11.483	10270259	0.17	Phenol, 3-(1-methylethyl)-	$C_9H_{12}O$	136	Lipid, Lignin[64, 10]
7	20.53	28876973	0.47	Tetradecanoic acid	$C_{14}H_{28}O_2$	228	Lipid[45, 12]
8	22.266	116189323	1.87	n-Hexadecanoic acid	$C_{16}H_{32}O_2$	256	Lipid, Protein, Carbohydrate[12, 64]
9	24.271	45611953	0.74	Oleic Acid	$C_{18}H_{34}O_2$	282	Lipid[22]
10	24.492	40722637	0.66	Octadecanoic acid	$C_{18}H_{36}O_2$	284	Lipid[22]
11	30.579	34577941	0.56	Cholestene isomer (3?)	$C_{27}H_{46}$	370	Lipid[45, 52, 88, 106]
12	31.294	2828823440	30.44	Cholest-2-ene	$C_{27}H_{46}$	370	Lipid[45, 52, 88, 106]
13	31.315	941998206	15.20	Cholestane	$C_{27}H_{48}$	372	Lipid[45, 52, 88, 106]
14	31.576	86311357	1.39	Cholestadiene isomer	$C_{27}H_{44}$	368	Lipid[45, 52, 88, 106]
15	32.027	47383353	0.76	Ergost-2-ene	$C_{28}H_{48}$	384	Lipid[22]
16	32.072	39509698	0.64	Ergostane	$C_{28}H_{50}$	386	Lipid[123]
17	32.287	65357290	1.05	Stigmastene isomer	$C_{29}H_{50}$	398	Lipid[86]
18	32.501	34555682	0.56	Stigmastene isomer	$C_{29}H_{50}$	398	Lipid[86]
19	32.683	28269300	0.46	Stigmastene isomer	$C_{29}H_{50}$	398	Lipid[86]
20	32.811	154557216	2.49	Stigmast-2-ene, (5.alpha.)-	$C_{29}H_{50}$	398	Lipid[88]
21	32.85	119822246	1.93	Stigmastane	$C_{29}H_{52}$	400	Lipid[88]
22	33.051	55947895	0.90	Cholestenone isomer	$C_{27}H_{44}O$	384	Lipid[45, 52, 88, 106]
23	33.226	35521667	0.57	Cholestanone isomer	$C_{27}H_{46}O$	386	Lipid[22, 75]
24	33.585	29205830	0.47	C30 17a(H)-hopane	$C_{30}H_{52}$	412	Lipid[25]
25	33.821	85950791	1.39	Cholestanone isomer	$C_{27}H_{46}O$	386	Lipid[22, 75]

26	34.169	29616699	0.48	Cholestadienone isomer	$C_{27}H_{42}O$	382	Lipid[124]
27	34.371	193019785	3.11	Cholestanediol isomer	$C_{27}H_{48}O_2$	404	Lipid[22]
28	35.228	28815533	0.46	Diethylcholestene isomer	$C_{31}H_{54}$	426	Lipid[17]
29	35.632	236427020	3.81	Dihydroxychloesterol	$C_{27}H_{46}O_3$	418	Lipid[17]
Total yields %			**73.30**				
Total yields % (oil fraction + non-oil fraction)			**81.17**				

Table S2: The major identified compounds of the produced renewable crude oil via the HTL process from the HL sample at reaction temperature of 250°C and residence time of 60 minutes using GC-MS analysis.

HL 250°C 60 Mins							
No	**Retention time (mins)**	**Area**	**Area (%)**	**Compound name**	**Molecular formula**	**Molecular weight (g/mol)**	**Classification of compound**
1	1.388	283926584	2.72	Carbon dioxide	CO_2	44	Protein[64, 6]
2	1.494	310040690	2.97	Methanethiol	CH_4S	48	Probably bacterial products[122]
3	1.715	55592127	0.53	Acetic acid, methyl ester	$C_3H_6O_2$	74	Carbohydrate, Lignin[99, 5]
Total yields %			**6.22**				

1	5.59	2858642	0.58	Styrene	C_8H_8	104	Protein[64]
2	8.87	78243550	0.75	Phenol, 2-methoxy-	$C_7H_8O_2$	124	Lipid, Lignin[64, 10]
3	9.206	47214409	0.45	Methyl creatinine	$C_4H_7N_3O$	113	Protein[44]
4	10.73	20254928	0.19	Phenol, 2-methoxy-4-methyl-	$C_8H_{10}O_2$	138	Lignin[69]
5	11.46	20331724	0.19	Phenol, 3-(1-methylethyl)-	$C_9H_{12}O$	136	Lipid, Lignin[64, 10]
6	22.335	180889687	1.73	n-Hexadecanoic acid	$C_{16}H_{32}O_2$	256	Lipid, Protein, Carbohydrate[12, 64]
7	24.316	91330990	0.87	Oleic Acid	$C_{18}H_{34}O_2$	282	Lipid[22]
8	24.553	86742054	0.83	Octadecanoic acid	$C_{18}H_{36}O_2$	284	Lipid[22]
9	29.078	54887811	0.53	Docosanoic acid	$C_{22}H_{44}O_2$	340	Lipid[41]
10	30.611	83227011	0.80	Cholestene isomer (3?)	$C_{27}H_{46}$	370	Lipid[45, 52, 88, 106]
11	30.844	65642811	0.63	Cholestene isomer (4?)	$C_{27}H_{46}$	370	Lipid[45, 52, 88, 106]
12	31.294	2951420015	28.25	Cholest-2-ene	$C_{27}H_{46}$	370	Lipid[45, 52, 88, 106]
13	31.315	1473497549	14.10	Cholestane	$C_{27}H_{48}$	372	Lipid[45, 52, 88, 106]
14	31.632	127406604	1.22	Cholestadiene isomer	$C_{27}H_{44}$	368	Lipid[45, 52, 88, 106]
15	31.711	58011756	0.56	Cholestenone isomer	$C_{27}H_{44}O$	384	Lipid[45, 52, 88, 106]
16	31.882	69597650	0.67	Cholestanone isomer	$C_{27}H_{46}O$	386	Lipid[22, 75]

17	32.072	85595822	0.82	Ergost-2-ene	$C_{28}H_{48}$	384	Lipid[22]
18	32.113	73823668	0.71	Ergostane	$C_{28}H_{50}$	386	Lipid[123]
19	32.328	85030770	0.81	Stigmastene isomer	$C_{29}H_{50}$	398	Lipid[86]
20	32.715	52131799	0.50	Stigmastene isomer	$C_{29}H_{50}$	398	Lipid[86]
21	32.861	276652270	2.65	Stigmastene isomer	$C_{29}H_{50}$	398	Lipid[86]
22	32.902	184474317	1.77	Stigmast-2-ene, (5.alpha.)-	$C_{29}H_{50}$	398	Lipid[88]
23	33.097	100192224	0.96	Stigmastane	$C_{29}H_{52}$	400	Lipid[88]
24	33.271	62268721	0.60	Cholestenone isomer	$C_{27}H_{44}O$	384	Lipid[45, 52, 88, 106]
25	33.352	49713092	0.48	Cholestanone isomer	$C_{27}H_{46}O$	386	Lipid[22, 75]
26	33.621	56717048	0.54	C30 17a(H)-hopane	$C_{30}H_{52}$	412	Lipid[25]
27	33.874	149801489	1.43	Cholestanone isomer	$C_{27}H_{46}O$	386	Lipid[22, 75]
28	34.378	134331783	1.29	Cholestanediol isomer	$C_{27}H_{48}O_2$	404	Lipid[22]
29	35.272	55815151	0.53	Diethylcholestene isomer	$C_{31}H_{54}$	426	Lipid[17]
30	35.672	288723149	2.76	Dihydroxychloesterol	$C_{27}H_{46}O_3$	418	Lipid[17]
Total yields %			**68.19**				
Total yields % (oil fraction + non-oil fraction)			**74.41**				

Table S3: The major identified compounds of the produced renewable crude oil via the HTL process from the HL sample at reaction temperature of 300ºC and residence time of 20 minutes using GC-MS analysis.

HL 300°C 20 Mins							
No	**Retention time (mins)**	**Area**	**Area (%)**	**Compound name**	**Molecular formula**	**Molecular weight (g/mol)**	**Classification of compound**
1	3.613	15482231	3.14	Carbon dioxide	CO_2	44	Protein[64, 6]
2	3.838	3943585	0.80	Methanethiol	CH_4S	48	Probably bacterial products[122]
3	4.788	17185473	3.48	Acetic acid	CH_3COOH	60	Carbohydrate, Lignin[64]
4	6.327	5639564	1.14	Disulfide, dimethyl	$C_2H_6S_2$	94	Probably bacterial products[21]
5	10.012	5681776	1.15	Phenol	C_6H_6O	94	Protein, Carbohydrate, Lignin[29, 52, 106]
6	11.775	14471098	2.93	p-Cresol	C_7H_8O	108	Protein, Carbohydrate[64, 6]
7	11.967	14559852	2.95	2,5-Pyrrolidinedione, 1-methyl-	C_5H_7NO	113	Protein[64]
8	12.213	4206760	0.85	Methyl creatinine	$C_4H_7N_3O$	113	Protein[44]
9	13.581	6098313	1.24	2,5-Pyrrolidinedione, 1-propyl-	$C_7H_{11}NO_2$	141	Protein[64]
10	17.042	3745353	0.76	1H-Isoindole-1,3(2H)-dione,2-methyl-	$C_9H_7NO_2$	161	Protein[64]
11	22.768	5305303	1.07	Biphenylol isomer	$C_{12}H_{10}O$	170	Lipid, Protein, Carbohydrate[31, 22]

12	22.928	16315540	3.31	n-Hexadecanoic acid	$C_{16}H_{32}O_2$	256	Lipid, Protein, Carbohydrate[12, 64]
13	24.68	7277797	1.47	Oleic Acid	$C_{18}H_{34}O_2$	282	Lipid[22]
14	24.841	5870291	1.19	Octadecanoic acid	$C_{18}H_{36}O_2$	284	Lipid[22]
15	31.571	3493955	0.71	Cholestene isomer (3?)	$C_{27}H_{46}$	370	Lipid[45, 52, 88, 106]
16	32.169	11391754	2.31	Cholestene isomer (4?)	$C_{27}H_{46}$	370	Lipid[45, 52, 88, 106]
17	32.436	110472294	22.38	Cholest-2-ene	$C_{27}H_{46}$	370	Lipid[45, 52, 88, 106]
18	32.522	88907524	18.01	Cholestane	$C_{27}H_{48}$	372	Lipid[45, 52, 88, 106]
19	33.088	3626963	0.73	Cholestadiene isomer	$C_{27}H_{44}$	368	Lipid[45, 52, 88, 106]
20	34.05	3839376	0.78	Ergost-2-ene	$C_{28}H_{48}$	384	Lipid[22]
21	34.156	4842665	0.98	Ergostane	$C_{28}H_{50}$	386	Lipid[123]
22	35.673	14989523	3.04	Stigmastene isomer (2?)	$C_{29}H_{50}$	398	Lipid[51]
23	35.791	12730085	2.58	Stigmastane	$C_{29}H_{52}$	400	Lipid[88]
24	39.989	4958480	1.00	Cholestanediol isomer	$C_{27}H_{48}O_2$	404	Lipid[22]
25	43.472	10781032	2.18	Dihydroxychloesterol	$C_{27}H_{46}O_3$	418	Lipid[17]
Total yields %			**80.20**				

Table S4: The major identified compounds of the produced renewable crude oil via the HTL process from the HL sample at reaction temperature of 300ºC and residence time of 40 minutes using GC-MS analysis.

HL 300°C 40 Mins							
No	**Retention time (mins)**	**Area**	**Area (%)**	**Compound name**	**Molecular formula**	**Molecular weight (g/mol)**	**Classification of compound**
1	1.282	156027839	1.40	2-Propanamine	C_3H_9N	59	Protein[125]
2	2.347	67962678	0.61	Acetic acid	CH_3COOH	60	Carbohydrate, Lignin[64]
Total yields %			**2.01**				

1	7.616	41363730	0.46	2-Pyrrolidinone, 1-methyl-	C_5H_9NO	99	Protein[29]
2	8.574	90057407	0.81	2-Hexanone, 4-methyl-	$C_7H_{14}O$	114	Lignin[126]
3	8.782	90832658	0.81	Phenol, 2-methoxy-	C7H8O2	124	Lipid, Lignin[64, 10]
4	10.614	36223688	0.32	Creosol	$C_8H_{10}O_2$	138	Lignin[65]
5	14.208	33193656	0.30	1H-Isoindole-1,3(2H)-dione,2-methyl-	$C_9H_7NO_2$	161	Protein[64]
6	20.576	64136876	0.57	Tetradecanoic acid	$C_{14}H_{28}O_2$	228	Lipid[45, 12]
7	21.865	98627303	0.88	d-Proline, n-butoxycarbonyl-, butyl ester	$C_{14}H_{25}NO_4$	271	Lipid, Protein, Carbohydrate[116]

8	21.932	72099951	0.65	n-Hexadecanoic acid	$C_{16}H_{32}O_2$	256	Lipid, Protein, Carbohydrate[12, 64]
9	23.934	65867248	0.59	Oleic Acid	$C_{18}H_{34}O_2$	282	Lipid[22]
10	24.161	85994444	0.77	Octadecanoic acid	$C_{18}H_{36}O_2$	284	Lipid[22]
11	30.2	80285492	0.72	Cholestene isomer	$C_{27}H_{46}$	370	Lipid[45, 52, 88, 106]
12	30.438	71493828	0.64	Cholestene isomer (3?)	$C_{27}H_{46}$	370	Lipid[45, 52, 88, 106]
13	30.931	2866750278	25.67	Cholest-2-ene	$C_{27}H_{46}$	370	Lipid[45, 52, 88, 106]
14	30.976	936425218	8.39	Cholestane	$C_{27}H_{48}$	372	Lipid[45, 52, 88, 106]
15	31.212	156752831	1.40	Cholestadiene isomer	$C_{27}H_{44}$	368	Lipid[45, 52, 88, 106]
16	31.71	208816399	1.87	Cholestenone isomer	$C_{27}H_{44}O$	384	Lipid[45, 52, 88, 106]
17	31.919	78185759	0.70	Cholestanone isomer	$C_{27}H_{46}O$	386	Lipid[22, 75]
18	32.177	76530580	0.69	Ergostane	$C_{28}H_{50}$	386	Lipid[123]
19	32.301	86943726	0.78	Stigmastene isomer	$C_{29}H_{50}$	398	Lipid[86]
20	32.499	539676396	4.83	Stigmastene isomer	$C_{29}H_{50}$	398	Lipid[86]
21	32.694	105628378	0.95	Stigmastene isomer	$C_{29}H_{50}$	398	Lipid[86]
22	32.873	95968181	0.86	Stigmast-2-ene, (5.alpha.)-	$C_{29}H_{50}$	398	Lipid[88]
23	33.21	92517421	0.83	Cholestenone isomer	$C_{27}H_{44}O$	384	Lipid[45, 52, 88, 106]
24	33.409	75312741	0.67	Cholestanone isomer	$C_{27}H_{46}O$	386	Lipid[22, 75]
25	33.48	66604842	0.60	C30 17a(H)-hopane	$C_{30}H_{52}$	412	Lipid[25]
26	34.001	820445857	7.35	Cholestadienone isomer	$C_{27}H_{42}O$	382	Lipid[124]
27	35.046	106266495	0.95	Cholestanediol isomer	$C_{27}H_{48}O_2$	404	Lipid[22]
Total yields %			**64.06**				
Total yields % (oil fraction + non-oil fraction)			**66.06**				

Table S5: The major identified compounds of the produced renewable crude oil via the HTL process from the HL sample at reaction temperature of 300ºC and residence time of 60 minutes using GC-MS analysis.

HL 300°C 60 Mins							
No	**Retention time (mins)**	**Area**	**Area (%)**	**Compound name**	**Molecular formula**	**Molecular weight (g/mol)**	**Classification of compound**
1	1.145	2249395	0.38	Carbon dioxide	CO_2	44	Protein[64, 6]
2	1.231	2311484	0.39	Methanethiol	CH_4S	48	Probably bacterial products[122]
3	2.534	5864412	0.99	Acetic acid	CH_3COOH	60	Carbohydrate, Lignin[64]
4	2.684	2537247	0.43	Pyridine	C_5H_5N	79	Protein[64]
Total yields %			**2.19**				

1	4.265	2385651	0.40	Pyridine, 3-methyl-	C_6H_7N	93	Protein[64]
2	6.668	2457677	0.42	Phenol	C_6H_6O	94	Protein, Carbohydrate, Lignin[29, 52, 106]
3	8.591	5291493	0.90	2-Hexanone, 4-methyl-	$C_7H_{14}O$	114	Lignin[126]
4	8.805	5843191	0.99	Phenol, 2-methoxy-	$C_7H_8O_2$	124	Lipid, Lignin[64, 10]
5	8.976	3155850	0.53	2,5-Pyrrolidinedione, 1-methyl-	C_5H_7NO	113	Protein[64]
6	10.279	2252185	0.38	Creosol	$C_8H_{10}O_2$	138	Lignin[65]
7	14.221	3758532	0.64	1H-lsoindole-1,3(2H)-dione,2-methyl-	$C_9H_7NO_2$	161	Lipid[22]
8	16.582	1941058	0.33	Dodecanoic acid	$C_{12}H_{24}O_2$	200	Lipid, Protein[127]
9	20.856	2105030	0.36	Tetradecanoic acid	$C_{14}H_{28}O_2$	228	Lipid[45, 12]
10	21.336	2464956	0.42	Complex Pyrrolidinedione isomer	$C_{14}H_{34}NO_2$	250	Protein[64]
11	21.849	7584325	1.28	d-Proline, n-butoxycarbonyl-, butyl ester	$C_{14}H_{25}NO_4$	271	Lipid, Protein, Carbohydrate[116]
12	21.913	4738080	0.80	n-Hexadecanoic acid	$C_{16}H_{32}O_2$	256	Lipid, Protein, Carbohydrate[12, 64]
13	24.146	5839347	0.99	Oleic Acid	$C_{18}H_{34}O_2$	282	Lipid[22]
14	24.306	2362266	0.40	Octadecanoic acid	$C_{18}H_{36}O_2$	284	Lipid[22]
15	24.605	2450333	0.41	Hexadecanamide	$C_{16}H_{33}NO$	255	Protein[64]
16	30.193	2720153	0.46	Cholestene isomer	$C_{27}H_{46}$	370	Lipid[45, 52, 88, 106]
17	30.866	109872973	18.60	Cholest-2-ene	$C_{27}H_{46}$	370	Lipid[45, 52, 88, 106]
18	30.962	219745947	37.19	Cholestane	$C_{27}H_{48}$	372	Lipid[45, 52, 88, 106]
19	31.218	7080737	1.20	Cholestadiene isomer	$C_{27}H_{44}$	368	Lipid[45, 52, 88, 106]
20	31.72	12098202	2.05	Cholestenone isomer	$C_{27}H_{44}O$	384	Lipid[45, 52, 88, 106]
21	32.319	2385738	0.40	Stigmastene isomer	$C_{29}H_{50}$	398	Lipid[86]
22	32.511	47638701	8.06	Stigmastene isomer	$C_{29}H_{50}$	398	Lipid[86]
23	32.693	3209304	0.54	Stigmastene isomer	$C_{29}H_{50}$	398	Lipid[86]
24	32.874	4508547	0.76	Stigmast-2-ene, (5.alpha.)-	$C_{29}H_{50}$	398	Lipid[88]
25	33.408	3259455	0.55	Cholestanone isomer	$C_{27}H_{46}O$	386	Lipid[22, 75]
26	33.943	26416623	4.47	Cholestadienone isomer	$C_{27}H_{42}O$	382	Lipid[124]
27	35.043	8089107	1.37	Cholestanediol isomer	$C_{27}H_{48}O_2$	404	Lipid[22]
Total yields %			**84.90**				
Total yields % (oil fraction + non-oil fraction)			**87.10**				

Table S6: The major identified compounds of the produced renewable crude oil via the HTL process from the HL sample at reaction temperature of 350°C and residence time of 20 minutes using GC-MS analysis.

APPENDICES

HL 350°C 20 Mins							
No	**Retention time (mins)**	**Area**	**Area (%)**	**Compound name**	**Molecular formula**	**Molecular weight (g/mol)**	**Classification of compound**
1	1.255	293650456	3.89	Methanol	CH_3OH	32	Lignin[68]
2	2.581	47443841	0.63	Acetic acid	CH_3COOH	60	Carbohydrate, Lignin[64]
Total yields %			**4.51**				
1	7.857	48304009	0.64	2-Pyrrolidinone, 1-methyl-	C_5H_9NO	99	Protein[29]
2	8.805	115984543	1.53	Phenol, 2-methoxy-	$C_7H_8O_2$	124	Lipid, Lignin[64, 10]
3	9.008	81551840	1.08	2,5-Pyrrolidinedione, 1-methyl	C_5H_7NO	113	Protein[64]
4	9.188	43043646	0.57	Pyrrolidinedinone, dimethyl isomer	$C_6H_9NO_2$	127	Protein[64]
5	14.41	32248270	0.43	1H-Isoindole-1,3(2H)-dione,2-methyl-	$C_9H_7NO_2$	161	Protein[64]
6	17.819	66253362	0.88	Benzene,1,1-(1,3-propanediyl) bis-	$C_{15}H_{16}$	196	Carbohydrate[2]
7	22.055	112023328	1.48	n-Hexadecanoic acid	$C_{16}H_{32}O_2$	256	Lipid, Protein, Carbohydrate[12, 64]
8	24.032	51302900	0.68	Oleic Acid	$C_{18}H_{34}O_2$	282	Lipid[22]
9	24.283	71989347	0.95	Octadecanoic acid	$C_{18}H_{36}O_2$	284	Lipid[22]
10	28.258	48651449	0.64	Cholestene isomer (3?)	$C_{27}H_{46}$	370	Lipid[45, 52, 88, 106]
11	28.907	71918895	0.95	Docosanoic acid	$C_{22}H_{44}O_2$	340	Lipid[41]
12	30.015	38936084	0.52	Cholestene isomer	$C_{27}H_{46}$	370	Lipid[45, 52, 88, 106]
13	30.134	40563243	0.54	Cholestene isomer	$C_{27}H_{46}$	370	Lipid[45, 52, 88, 106]
14	30.362	53899870	0.71	Cholestene isomer	$C_{27}H_{46}$	370	Lipid[45, 52, 88, 106]
15	30.497	36158692	0.48	Cholest-2-ene	$C_{27}H_{46}$	370	Lipid[45, 52, 88, 106]
16	30.564	72317383	0.96	Cholestane	$C_{27}H_{48}$	372	Lipid[45, 52, 88, 106]
17	31.083	1825200123	24.15	Cholestadiene isomer	$C_{27}H_{44}$	368	Lipid[45, 52, 88, 106]
18	31.132	948908024	12.56	Cholestenone isomer	$C_{27}H_{44}O$	384	Lipid[45, 52, 88]
19	31.491	41390031	0.55	Cholestanone isomer	$C_{27}H_{46}O$	386	Lipid[22, 75]
20	31.638	44577423	0.59	Ergost-2-ene	$C_{28}H_{48}$	384	Lipid[22]
21	31.877	165482742	2.19	Ergostane	$C_{28}H_{50}$	386	Lipid[123]
22	32.335	42395941	0.56	Stigmastene isomer	$C_{29}H_{50}$	398	Lipid[86]
23	32.424	40168462	0.53	Stigmastene isomer	$C_{29}H_{50}$	398	Lipid[86]
24	32.657	336428336	4.45	Stigmastane	$C_{29}H_{52}$	400	Lipid[88]
25	32.841	49665537	0.66	Stigmastdiene isomer	$C_{29}H_{50}$	398	Lipid[86]
26	33.027	62509732	0.83	Cholestenone isomer	$C_{27}H_{44}O$	384	Lipid[45, 52, 88, 106]
27	33.217	43163062	0.57	Cholestanone isomer	$C_{27}H_{46}O$	386	Lipid[22, 75]
28	35.215	15464695	0.20	Diethylcholestene isomer	$C_{31}H_{54}$	426	Lipid[17]

Total yields %	**60.88**
Total yields % (oil fraction + non-oil fraction)	**65.39**

Table S7: The major identified compounds of the produced renewable crude oil via the HTL process from the HL sample at reaction temperature of 350°C and residence time of 40 minutes using GC-MS analysis.

HL 350°C 40 Mins							
No	**Retention time (mins)**	**Area**	**Area (%)**	**Compound name**	**Molecular formula**	**Molecular weight (g/mol)**	**Classification of compound**
1	3.602	4011174	1.71	Carbon dioxide	CO_2	44	Protein[64, 6]
2	4.66	8393789	3.57	Acetic acid	CH_3COOH	60	Carbohydrate, Lignin[64]
3	6.316	1507510	0.64	Disulfide, dimethyl	$C_2H_6S_2$	94	Probably bacterial products[21]
4	6.636	4737327	2.02	Toluene	C_7H_8	92	Lipid, Protein, Carbohydrate[64]
5	8.153	7650739	3.26	Styrene	C_8H_8	104	Protein[64]
6	9.211	2647329	1.13	2-Pyrrolidinone, 1-methyl-	C_5H_9NO	99	Protein[29]
7	10.002	17744059	7.56	Phenol	C_6H_6O	94	Protein, Carbohydrate, Lignin[29, 52, 106]
8	11.284	13186345	5.62	o-Cresol	C_7H_8O	108	Protein, Lignin[127 81]
9	11.647	31763913	13.53	m-Cresol	C_7H_8O	108	Protein, Lignin[127 81]
10	11.722	4266015	1.82	p-Cresol	C_7H_8O	108	Protein, Carbohydrate[64, 6]
11	11.967	6042528	2.57	2,5-Pyrrolidinedione, 1-methyl-	C_5H_7NO	113	Protein[64]
12	12.224	2734986	1.16	Methyl creatinine	$C_4H_7N_3O$	113	Protein[44]
13	12.875	10104314	4.30	Phenol, 2,5-dimethyl-	$C_8H_{10}O$	122	Lipid, Protein, Carbohydrate, Lignin[99,118,64,22]
14	13.164	7893102	3.36	Phenol, 3,5-dimethyl-	$C_8H_{10}O$	122	Lipid, Protein, Carbohydrate, Lignin[99,118,64,22]
15	13.324	5121278	2.18	Phenol, 2,3-dimethyl-	$C_8H_{10}O$	122	Lipid, Protein, Carbohydrate, Lignin[99,118,64,22]
16	13.57	4104361	1.75	Phenol, 3,4-dimethyl-	$C_8H_{10}O$	122	Lipid, Protein, Carbohydrate, Lignin[99,118,64,22]
17	14.051	1881109	0.80	p-Cumenol	$C_6H_{12}O$	136	Lignin[7]
18	14.264	2247924	0.96	Phenol, 2-(1-methylethyl)-	$C_9H_{12}O$	136	Lipid, Protein, Carbohydrate, Lignin[99,118,64,22]
19	14.531	2085115	0.89	Phenol, 2,3,5-trimethyl-	$C_9H_{12}O$	136	Lipid, Protein, Carbohydrate, Lignin[99,118,64,22]
20	19.894	1507218	0.64	Dibenzofuran, 4-methyl-	$C_{13}H_{10}O$	182	Carbohydrate, Lignin[99, 5]
21	19.937	3853488	1.64	Benzene,1,1'-(1,3-propanediyl)bis-	$C_{15}H_{16}$	196	Carbohydrate[2]
22	32.351	5030589	2.14	Cholest-2-ene	$C_{27}H_{46}$	370	Lipid[45, 52, 88, 106]

23	32.458	26777446	11.40	Cholestane	$C_{27}H_{48}$	372	Lipid[79, 80, 85, 87]
24	34.124	1504190	0.64	Ergostane	$C_{28}H_{50}$	386	Lipid[68]
25	35.748	3582661	1.53	Stigmastane	$C_{29}H_{52}$	400	Lipid[88]
Total yields %			**76.82**				

Table S8: The major identified compounds of the produced renewable crude oil via the HTL process from the HL sample at reaction temperature of 350°C and residence time of 60 minutes using GC-MS analysis.

HL 350°C 60 Mins							
No	**Retention time (mins)**	**Area**	**Area (%)**	**Compound name**	**Molecular formula**	**Molecular weight (g/mol)**	**Classification of compound**
1	3.613	6598717	2.01	Carbon dioxide	CO_2	44	Protein[64, 6]
2	4.746	20183374	6.15	Acetic acid	CH_3COOH	60	Carbohydrate, Lignin[64]
3	5.601	2864168	0.87	Propanoic acid	$C_3H_6O_2$	74	Lipid, Protein[101]
4	6.316	2265812	0.69	Disulfide, dimethyl	$C_2H_6S_2$	94	Probably bacterial products[21]
5	7.727	2830242	0.86	Pentanoic Acid	$C_5H_{10}O_2$	102	Lipid[55]
6	10.045	7001185	2.13	Phenol	C_6H_6O	94	Protein, Carbohydrate, Lignin[29, 52, 106]
7	11.145	9166422	2.79	2-Pyrrolidinone, 1-methyl-	C_5H_9NO	99	Protein[29]
8	11.669	4407833	1.34	m-Cresol	C_7H_8O	108	Protein, Lignin[127 81]
9	11.786	10515876	3.21	p-Cresol	C_7H_8O	108	Protein, Carbohydrate[64, 6]
10	11.978	10584729	3.23	2,5-Pyrrolidinedione, 1-methyl-	C_5H_7NO	113	Protein[64]
11	12.224	5530858	1.69	Methyl creatinine	$C_4H_7N_3O$	113	Protein[44]
12	13.143	5430403	1.66	Phenol, 4-ethyl-	$C_8H_{10}O$	122	Lipid, Protein, Carbohydrate, Lignin[99,118,64,22]
13	13.634	6168310	1.88	2,5-Pyrrolidinedione, 1-propyl-	$C_7H_{11}NO_2$	141	Protein[64]
14	15.888	2728233	0.83	2,2-Dimethyl-1-pyrrolidin-1-ylpropan-1-one	$C_9H_{17}NO$	155	Carbohydrate[30]
15	17.064	3434504	1.05	1H-Isoindole-1,3(2H)-dione,2-methyl-	$C_9H_7NO_2$	161	Protein[64]
16	19.948	7553887	2.30	Benzene,1,1'-(1,3-propanediyl) bis-	$C_{15}H_{16}$	196	Carbohydrate[2]
17	22.907	5592576	1.70	n-Hexadecanoic acid	$C_{16}H_{32}O_2$	256	Lipid, Protein, Carbohydrate[12, 64]
18	28.666	2341045	0.71	Cholesteneone isomer (14?)	$C_{27}H_{44}O$	384	Lipid[45, 52, 88, 106]
19	29.531	3618010	1.10	Cholesteneone isomer (24?)	$C_{27}H_{44}O$	384	Lipid[45, 52, 88, 106]
20	32.373	18797947	5.73	Cholest-2-ene	$C_{27}H_{46}$	370	Lipid[45, 52, 88, 106]
21	32.49	82445784	25.13	Cholestane	$C_{27}H_{48}$	372	Lipid[45, 52, 88, 106]
22	34.135	4610757	1.41	Ergostane	$C_{28}H_{50}$	386	Lipid[123]

23	35.642	2328459	0.71	Stigmastene isomer (2?)	$C_{29}H_{50}$	398	Lipid[51]
24	35.77	10679105	3.26	Stigmastane	$C_{29}H_{52}$	400	Lipid[88]
25	36.849	2396529	0.73	Cholestan-3-one, (5.alpha.)-	$C_{27}H_{46}O$	386	Lipid[22]
Total yields %			**73.18**				

Table S9: The major identified compounds of the produced renewable crude oil from the HP sample before the HTL process using GC-MS analysis.

HP S							
No	**Retention time (mins)**	**Area**	**Area (%)**	**Compound name**	**Molecular formula**	**Molecular weight (g/mol)**	**Classification of compound**
1	3.624	27684878	3.94	Carbon dioxide	CO_2	44	Protein[64, 6]
2	3.837	10679170	1.52	Methanethiol	CH_4S	48	Probably bacterial products[122]
3	4.03	6778508	0.96	Acetone	C_3H_6O	58	Carbohydrate[23]
4	4.607	6632895	0.94	2-Butanone	C_4H_8O	72	Carbohydrate[107]
5	5.002	41656471	5.93	Acetic acid	CH_3COOH	60	Carbohydrate, Lignin[64]
6	5.237	44794249	6.37	Propanoic acid	$C_3H_6O_2$	74	Lipid, Protein[101]
7	6.305	11064979	1.57	Disulfide, dimethyl	$C_2H_6S_2$	94	Probably bacterial products[21]
8	6.626	8163636	1.16	Toluene	C_7H_8	92	Lipid, Protein, Carbohydrate[64]
9	7.224	7636558	1.09	Acetic acid, butyl ester	$C_6H_{12}O_2$	116	Carbohydrate[67]
10	7.566	16214477	2.31	Pyrazine, methyl-	$C_5H_6N_2$	94	Protein[44, 52]
11	10.066	10541264	1.50	Phenol	C_6H_6O	94	Protein, Carbohydrate, Lignin[29, 52, 106]
12	10.888	31610000	4.50	2-Pyrrolidinone, 1-methyl-	C_5H_9NO	99	Protein[29]
13	11.829	17185193	2.44	p-Cresol	C_7H_8O	108	Protein, Carbohydrate[64, 6]
14	11.989	13616661	1.94	2,5-Pyrrolidinedione, 1-methyl-	C_5H_7NO	113	Protein[64]
15	12.213	2535773	0.97	Methyl creatinine	$C_4H_7N_3O$	113	Protein[44]
16	22.928	10451579	1.49	n-Hexadecanoic acid	$C_{16}H_{32}O_2$	256	Lipid, Protein, Carbohydrate[12, 64]
17	31.582	7738176	1.10	Cholestene isomer (3?)	$C_{27}H_{46}$	370	Lipid[45, 52, 88, 106]
18	31.956	7117988	1.01	Cholestene isomer (7?)	$C_{27}H_{46}$	370	Lipid[45, 52, 88, 106]
19	32.169	14951606	2.13	Cholestene isomer (4?)	$C_{27}H_{46}$	370	Lipid[45, 52, 88, 106]
20	32.404	69379438	9.87	Cholest-2-ene	$C_{27}H_{46}$	370	Lipid[45, 52, 88, 106]
21	32.5	72519846	10.32	Cholestane	$C_{27}H_{48}$	372	Lipid[45, 52, 88, 106]
22	35.673	15021301	2.14	Stigmastene isomer (2?)	$C_{29}H_{50}$	398	Lipid[51]
23	35.78	14282610	2.03	Stigmastane	$C_{29}H_{52}$	400	Lipid[88]
24	40.032	20028096	2.85	Cholestanediol isomer	$C_{27}H_{48}O_2$	404	Lipid[22]

25	43.504	16972982	2.41	Dihydroxychloesterol	$C_{27}H_{46}O_3$	418	Lipid[17]
Total yields %			**72.48**				

Table S10: The major identified compounds of the produced renewable crude oil via the HTL process from the HP sample at reaction temperature of 250ºC and residence time of 20 minutes using GC-MS analysis.

HP 250°C 20 Mins							
No	**Retention time (mins)**	**Area**	**Area (%)**	**Compound name**	**Molecular formula**	**Molecular weight (g/mol)**	**Classification of compound**
1	1.356	266324175	3.24	Carbon dioxide	CO_2	44	Protein[64, 6]
2	1.453	132533491	1.61	Methanethiol	CH_4S	48	Probably bacterial products[122]
3	1.564	50183572	0.61	Acetone	C_3H_6O	58	Carbohydrate[23]
4	2.288	154090209	1.87	Propanoic acid	$C_3H_6O_2$	74	Lipid, Protein[101]
Total yields %			**7.33**				

1	7.629	49582378	0.60	1-Hexene, 4-methyl-	C_8H_{14}	98	Lignin[22]
2	8.755	39287729	0.48	Phenol, 2-methoxy-	$C_7H_8O_2$	124	Lipid, Lignin[64, 10]
3	10.65	8215644	0.10	Creosol	$C_8H_{10}O_2$	138	Lignin[65]
4	16.865	8302226	0.10	Dodecanoic acid	$C_{12}H_{24}O_2$	200	Lipid, Protein[127]
5	22.216	153420767	1.86	n-Hexadecanoic acid	$C_{16}H_{32}O_2$	256	Lipid, Protein, Carbohydrate[12, 64]
6	24.244	78089711	0.95	Oleic Acid	$C_{18}H_{34}O_2$	282	Lipid[22]
7	24.483	83748883	1.02	Octadecanoic acid	$C_{18}H_{36}O_2$	284	Lipid[22]
8	26.351	57746000	0.70	9-Octadecenamide, (Z)-	$C_{18}H_{35}NO$	281	Protein[64]
9	29.326	70316999	0.85	Docosanoic acid	$C_{22}H_{44}O_2$	340	Lipid[41]
10	29.466	49879492	0.61	Cholestene isomer	$C_{27}H_{46}$	370	Lipid[45, 52, 88, 106]
11	29.781	57782737	0.70	Cholesteneone isomer (24?)	$C_{27}H_{44}O$	384	Lipid[45, 52, 88, 106]
12	30.589	138000541	1.68	Cholestene isomer (3?)	$C_{27}H_{46}$	370	Lipid[45, 52, 88, 106]
13	30.822	120399839	1.46	Cholestene isomer	$C_{27}H_{46}$	370	Lipid[45, 52, 88, 106]
14	31.085	774548516	9.41	Cholest-2-ene	$C_{27}H_{46}$	370	Lipid[45, 52, 88, 106]
15	31.254	1549097031	18.82	Cholestane	$C_{27}H_{48}$	372	Lipid[45, 52, 88, 106]
16	31.56	139218148	1.69	Cholestadiene isomer	$C_{27}H_{44}$	368	Lipid[45, 52, 88]
17	32.017	172617606	2.10	Ergost-2-ene	$C_{28}H_{48}$	384	Lipid[127]
18	32.283	116140121	1.41	Stigmastene isomer	$C_{29}H_{50}$	398	Lipid[86]
19	32.501	90464556	1.10	Stigmastene isomer	$C_{29}H_{50}$	398	Lipid[86]

20	32.679	93489984	1.14	Stigmastene isomer	$C_{29}H_{50}$	398	Lipid[86]
21	32.805	239838396	2.91	Stigmast-2-ene, (5.alpha.)-	$C_{29}H_{50}$	398	Lipid[88]
22	32.849	191626035	2.33	Stigmastane	$C_{29}H_{52}$	400	Lipid[88]
23	33.045	68100147	0.83	Cholestenone isomer	$C_{27}H_{44}O$	384	Lipid[45, 52, 88, 106]
24	33.362	65836625	0.80	Cholestanone isomer	$C_{27}H_{46}O$	386	Lipid[22, 75]
25	33.575	74250502	0.90	C30 17a(H)-hopane	$C_{30}H_{52}$	412	Lipid[25]
26	33.81	115270208	1.40	Cholestanone isomer	$C_{27}H_{46}O$	386	Lipid[22, 75]
27	34.389	414582960	5.04	Cholestanediol isomer	$C_{27}H_{48}O_2$	404	Lipid[22]
28	35.582	179286483	2.18	Dihydroxychloesterol	$C_{27}H_{46}O_3$	418	Lipid[17]
29	36.5	54658419	0.66	Stigmastanediol isomer	$C_{29}H_{52}O_2$	432	Lipid[88]
Total yields %			**63.84**				
Total yields % (oil fraction + non-oil fraction)			**71.17**				

Table S11: The major identified compounds of the produced renewable crude oil via the HTL process from the HP sample at reaction temperature of 250ºC and residence time of 40 minutes using GC-MS analysis.

HP 250°C 40 Mins							
No	**Retention time (mins)**	**Area**	**Area (%)**	**Compound name**	**Molecular formula**	**Molecular weight (g/mol)**	**Classification of compound**
1	1.324	355323339	5.17	Carbon dioxide	CO_2	44	Protein[64, 6]
2	1.398	92059728	1.34	Methanol	CH_3OH	32	Lignin[68]
3	1.534	72048193	1.05	Acetone	C_3H_6O	58	Carbohydrate[23]
4	1.597	35268574	0.51	Dimethyl sulfide	C_2H_6S	62	Gas[91]
5	1.863	51823665	0.75	2-Butanone	C_4H_8O	72	Carbohydrate[107]
6	2.35	251843350	3.66	Propanoic acid	$C_3H_6O_2$	74	Lipid, Protein[101]
7	2.88	63062300	0.92	Acetic acid	C2H4O2	60	Carbohydrate, Lignin[64]
Total yields %			**13.40**				

1	3.003	143662836	2.09	Disulfide, dimethyl	$C_2H_6S_2$	94	Probably bacterial products[21]
2	7.035	33428773	0.49	Phenol	C_6H_6O	94	Protein, Carbohydrate, Lignin[29, 52, 106]
3	7.704	82034007	1.19	1-Hexene, 4-methyl-	C_8H_{14}	98	Lignin[22]
4	8.984	53959409	0.78	2,5-Pyrrolidinedione, 1-methyl-	C_5H_7NO	113	Protein[64]
5	9.212	52256013	0.76	Methyl creatinine	$C_4H_7N_3O$	113	Protein[44]
6	10.744	12182351	0.18	Creosol	$C_8H_{10}O_2$	138	Lignin[65]

7	13.906	12748409	0.19	N-[2-Hydroxyethyl]succinimide	$C_6H_9NO_3$	143	Protein[94]
8	22.207	103837696	1.51	n-Hexadecanoic acid	$C_{16}H_{32}O_2$	256	Lipid, Protein, Carbohydrate[12, 64]
9	24.424	31288731	0.45	Octadecanoic acid	$C_{18}H_{36}O_2$	284	Lipid[22]
10	30.57	107769642	1.57	Cholestene isomer (3?)	$C_{27}H_{46}$	370	Lipid[45, 52, 88, 106]
11	30.803	83722010	1.22	Cholestene isomer	$C_{27}H_{46}$	370	Lipid[45, 52, 88, 106]
12	31.171	810469759	11.78	Cholest-2-ene	$C_{27}H_{46}$	370	Lipid[45, 52, 88, 106]
13	31.238	1620939517	23.57	Cholestane	$C_{27}H_{48}$	372	Lipid[45, 52, 88, 106]
14	31.54	116884822	1.70	Cholestadiene isomer	$C_{27}H_{44}$	368	Lipid[45, 52, 88, 106]
15	31.997	77234392	1.12	Cholestanone isomer	$C_{27}H_{46}O$	386	Lipid[22, 75]
16	32.046	57495878	0.84	Ergost-2-ene	$C_{28}H_{48}$	384	Lipid[22]
17	32.26	82548705	1.20	Stigmastene isomer	$C_{29}H_{50}$	398	Lipid[86]
18	32.475	62655277	0.91	Stigmastene isomer	$C_{29}H_{50}$	398	Lipid[86]
19	32.656	66248571	0.96	Stigmastene isomer	$C_{29}H_{50}$	398	Lipid[86]
20	32.778	196567180	2.86	Stigmast-2-ene, (5.alpha.)-	$C_{29}H_{50}$	398	Lipid[88]
21	32.825	145383247	2.11	Stigmastane	$C_{29}H_{52}$	400	Lipid[88]
22	33.018	61142359	0.89	Cholestenone isomer	$C_{27}H_{44}O$	384	Lipid[45, 52, 88, 106]
23	33.323	30341089	0.44	Cholestanone isomer	$C_{27}H_{46}O$	386	Lipid[22, 75]
24	33.542	41634541	0.61	C30 17a(H)-hopane	$C_{30}H_{52}$	412	Lipid[25]
25	33.752	40235826	0.59	Cholestanone isomer	$C_{27}H_{46}O$	386	Lipid[22, 75]
26	34.329	243661564	3.54	Cholestanediol isomer	$C_{27}H_{48}O_2$	404	Lipid[22]
27	35.52	102162667	1.49	Dihydroxychloesterol	$C_{27}H_{46}O_3$	418	Lipid[17]
Total yields %			**65.03**				
Total yields % (oil fraction + non-oil fraction)			**78.43**				

Table S12: The major identified compounds of the produced renewable crude oil via the HTL process from the HP sample at reaction temperature of 250ºC and residence time of 60 minutes using GC-MS analysis.

HP 250°C 60 Mins							
No	**Retention time (mins)**	**Area**	**Area (%)**	**Compound name**	**Molecular formula**	**Molecular weight (g/mol)**	**Classification of compound**
1	3.603	10831072	2.20	Carbon dioxide	CO_2	44	Protein[64, 6]
2	3.816	3553068	0.72	Methanethiol	CH_4S	48	Probably bacterial products[122]
3	4.767	22086959	4.48	Acetic acid	CH_3COOH	60	Carbohydrate, Lignin[64]
4	7.459	3601771	0.73	Pyridine, 2-methyl-	C_6H_7N	93	Protein[64]

5	10.012	5585181	1.13	Phenol	C_6H_6O	94	Protein, Carbohydrate, Lignin[29, 52, 106]
6	10.931	9540535	1.93	2-Pyrrolidinone, 1-methyl-	C_5H_9NO	99	Protein[29]
7	11.775	11763869	2.38	p-Cresol	C_7H_8O	108	Protein, Carbohydrate[64, 6]
8	11.978	12866980	2.61	2,5-Pyrrolidinedione, 1-methyl-	C_5H_7NO	113	Protein[64]
9	12.224	6310776	1.28	Methyl creatinine	$C_4H_7N_3O$	113	Protein[44]
10	13.634	3773343	0.76	2,5-Pyrrolidinedione, 1-propyl-	$C_7H_{11}NO_2$	141	Protein[64]
11	20.717	3674285	0.74	C9-phenol isomer	$C_{15}H_{24}O$	220	Lipid, Protein, Carbohydrate, Lignin[99,118,64,22]
12	20.792	4505699	0.91	C9-phenol isomer	$C_{15}H_{24}O$	220	Lipid, Protein, Carbohydrate, Lignin[99,118,64,22]
13	22.928	12976720	2.63	n-Hexadecanoic acid	$C_{16}H_{32}O_2$	256	Lipid, Protein, Carbohydrate[12, 64]
14	24.702	3869472	0.78	Oleic Acid	$C_{18}H_{34}O_2$	282	Lipid[22]
15	25.054	4201969	0.85	Hexadecanamide	$C_{16}H_{33}NO$	255	Protein[64]
16	31.571	5222524	1.06	Cholestene isomer (3?)	$C_{27}H_{46}$	370	Lipid[45, 52, 88, 106]
17	31.956	6710425	1.36	Cholestene isomer (7?)	$C_{27}H_{46}$	370	Lipid[45, 52, 88, 106]
18	32.169	14734625	2.99	Cholestene isomer (4?)	$C_{27}H_{46}$	370	Lipid[45, 52, 88, 106]
19	32.404	81255442	16.47	Cholest-2-ene	$C_{27}H_{46}$	370	Lipid[45, 52, 88, 106]
20	32.49	66775717	13.53	Cholestane	$C_{27}H_{48}$	372	Lipid[45, 52, 88, 106]
21	34.05	5190367	1.05	Cholestadiene isomer	$C_{27}H_{44}$	368	Lipid[45, 52, 88, 106]
22	34.156	5646555	1.14	Ergostane	$C_{28}H_{50}$	386	Lipid[123]
23	35.353	5271842	1.07	Stigmastene isomer	$C_{29}H_{50}$	398	Lipid[86]
24	35.663	15598886	3.16	Stigmastene isomer (2?)	$C_{29}H_{50}$	398	Lipid[51]
25	35.78	12351425	2.50	Stigmastane	$C_{29}H_{52}$	400	Lipid[88]
Total yields %			**68.49**				

Table S13: The major identified compounds of the produced renewable crude oil via the HTL process from the HP sample at reaction temperature of 300ºC and residence time of 20 minutes using GC-MS analysis.

HP 300°C 20 Mins							
No	**Retention time (mins)**	**Area**	**Area (%)**	**Compound name**	**Molecular formula**	**Molecular weight (g/mol)**	**Classification of compound**
1	1.32	230726277	2.93	Carbon dioxide	CO_2	44	Protein[64, 6]
2	1.393	72691629	0.92	Methanol	CH_3OH	32	Lignin[68]
3	1.525	57424949	0.73	Acetone	C_3H_6O	58	Carbohydrate[23]
Total yields %			**4.58**				

1	8.849	49848120	0.63	2,5-Pyrrolidinedione, 1-methyl-	C_5H_7NO	113	Protein[64]

2	9.092	55794391	0.71	2,5-Pyrrolidinedione, dimethyl	$C_6H_9NO_2$	127	Protein[64]
3	10.842	15679473	0.20	1-Hexanol, 2-ethyl	$C_8H_{18}O$	130	Carbohydrate, Lignin[67]
4	16.913	15294375	0.19	Dodecanoic acid	$C_{12}H_{24}O_2$	200	Lipid, Protein[127]
5	22.183	90030314	1.14	n-Hexadecanoic acid	$C_{16}H_{32}O_2$	256	Lipid, Protein, Carbohydrate[12, 64]
6	24.234	82257381	1.04	Oleic acid	$C_{18}H_{34}O_2$	282	Lipid[22]
7	24.466	72352233	0.92	Octadecanoic acid	$C_{18}H_{36}O_2$	284	Lipid[22]
8	30.529	100773516	1.28	Cholestene isomer (3?)	$C_{27}H_{46}$	370	Lipid[45, 52, 88, 106]
9	30.78	111176310	1.41	Cholestene isomer	$C_{27}H_{46}$	370	Lipid[45, 52, 88, 106]
10	31.18	1495481142	18.99	Cholest-2-ene	$C_{27}H_{46}$	370	Lipid[45, 52, 88, 106]
11	31.221	503059439	6.39	Cholestane	$C_{27}H_{48}$	372	Lipid[45, 52, 88, 106]
12	31.498	126232073	1.60	Cholestadiene isomer	$C_{27}H_{44}$	368	Lipid[45, 52, 88, 106]
13	31.964	66174641	0.84	Cholestanone isomer	$C_{27}H_{46}O$	386	Lipid[22, 75]
14	32.004	51913654	0.66	Ergost-2-ene	$C_{28}H_{48}$	384	Lipid[22]
15	32.225	121313254	1.54	Stigmastene isomer	$C_{29}H_{50}$	398	Lipid[86]
16	32.447	95425554	1.21	Stigmastene isomer	$C_{29}H_{50}$	398	Lipid[86]
17	32.632	103368175	1.31	Stigmastene isomer	$C_{29}H_{50}$	398	Lipid[86]
18	32.789	365710346	4.64	Stigmastane	$C_{29}H_{52}$	400	Lipid[88]
19	32.99	94589373	1.20	Cholestenone isomer	$C_{27}H_{44}O$	384	Lipid[45, 52, 88, 106]
20	33.305	54662628	0.69	Cholestanone isomer	$C_{27}H_{46}O$	386	Lipid[22, 75]
21	33.75	105589955	1.34	C30 17a(H)-hopane	$C_{30}H_{52}$	412	Lipid[25]
22	33.814	70203133	0.89	Cholestanone isomer	$C_{27}H_{46}O$	386	Lipid[22, 75]
23	34.394	1018498488	12.94	Cholestanediol isomer	$C_{27}H_{48}O_2$	404	Lipid[22]
24	35.369	50162363	0.64	Dihydroxychloesterol	$C_{27}H_{46}O_3$	418	Lipid[17]
25	35.481	80028589	1.02	Diethylcholestene isomer	$C_{31}H_{54}$	426	Lipid[17]
26	36.462	99684483	1.27	Stigmastanediol isomer	$C_{29}H_{52}O_2$	432	Lipid[88]
Total yields %			**64.71**				
Total yields % (oil fraction + non-oil fraction)			**69.30**				

Table S14: The major identified compounds of the produced renewable crude oil via the HTL process from the HP sample at reaction temperature of 300ºC and residence time of 40 minutes using GC-MS analysis.

HP 300°C 40 Mins							
No	**Retention time (mins)**	**Area**	**Area (%)**	**Compound name**	**Molecular formula**	**Molecular weight (g/mol)**	**Classification of compound**

1	1.35	222859277	2.45	Carbon dioxide	CO_2	44	Protein[64, 6]
2	1.399	78319305	0.86	Methanol	CH_3OH	32	Lignin[68]
Total yields %			**3.31**				

1	7.616	41363730	0.46	1-Hexene, 4-methyl-	C_8H_{14}	98	Lignin[22]
2	8.908	68120922	0.75	2,5-Pyrrolidinedione, 1-methyl-	C_5H_7NO	113	Protein[64]
3	9.145	67630720	0.74	Pyrrolidinedinone, dimethyl isomer	$C_6H_9NO_2$	127	Protein[64]
4	10.868	20506963	0.23	1-Hexanol, 2-ethyl	$C_8H_{18}O$	130	Carbohydrate, Lignin[67]
5	13.87	20569422	0.23	N-[2-Hydroxyethyl]succinimide	$C_6H_9NO_3$	143	Protein[94]
6	22.157	72124049	0.79	n-Hexadecanoic acid	$C_{16}H_{32}O_2$	256	Lipid, Protein, Carbohydrate[12, 64]
7	22.243	74591222	0.82	Hexadecanoic acid	$C_{16}H_{32}O_2$	256	Protein[64]
8	24.467	88101142	0.97	Oleic Acid	$C_{18}H_{34}O_2$	282	Lipid[22]
9	26.524	67688487	0.74	9-Octadecenamide	$C_{18}H_{35}NO$	281	Protein[64]
10	30.549	120222916	1.32	Cholestene isomer (3?)	$C_{27}H_{46}$	370	Lipid[45, 52, 88, 106]
11	30.809	133310142	1.47	Cholestene isomer	$C_{27}H_{46}$	370	Lipid[45, 52, 88, 106]
12	30.975	80704828	0.89	Cholestane	$C_{27}H_{48}$	372	Lipid[45, 52, 88, 106]
13	31.228	1832728156	20.16	Cholest-2-ene	$C_{27}H_{46}$	370	Lipid[45, 52, 88, 106]
14	31.262	557727145	6.14	Cholestane	$C_{27}H_{48}$	372	Lipid[45, 52, 88, 106]
15	31.532	156033474	1.72	Cholestadiene isomer	$C_{27}H_{44}$	368	Lipid[45, 52, 88, 106]
16	31.747	90965475	1.00	Cholestenone isomer	$C_{27}H_{44}O$	384	Lipid[45, 52, 88]
17	31.995	144445664	1.59	Cholestanone isomer	$C_{27}H_{46}O$	386	Lipid[22, 75]
18	32.038	103140314	1.13	Ergost-2-ene	$C_{28}H_{48}$	384	Lipid[22]
19	32.253	110250910	1.21	Stigmastene isomer	$C_{29}H_{50}$	398	Lipid[86]
20	32.491	119127247	1.31	Stigmastene isomer	$C_{29}H_{50}$	398	Lipid[86]
21	32.661	125982667	1.39	Stigmastene isomer	$C_{29}H_{50}$	398	Lipid[86]
22	32.784	260812371	2.87	Stigmast-2-ene, (5.alpha.)-	$C_{29}H_{50}$	398	Lipid[88]
23	32.825	212388998	2.34	Stigmastane	$C_{29}H_{52}$	400	Lipid[88]
24	33.023	85746380	0.94	Cholestenone isomer	$C_{27}H_{44}O$	384	Lipid[45, 52, 88, 106]
25	33.773	91296182	1.00	Cholestan-3-one, (5.alpha.)-	$C_{27}H_{46}O$	386	Lipid[22]
26	34.383	606609821	6.67	Cholestanediol isomer	$C_{27}H_{48}O_2$	404	Lipid[22]
27	35.496	68809453	0.76	Dihydroxychloesterol	$C_{27}H_{46}O_3$	418	Lipid[17]
28	36.471	66669155	0.73	Stigmastanediol isomer	$C_{29}H_{52}O_2$	432	Lipid[88]
Total yields %			**60.38**				
Total yields % (oil fraction + non-oil fraction)			**63.69**				

Table S15: The major identified compounds of the produced renewable crude oil via the HTL process from the HP sample at reaction temperature of 300°C and residence time of 60 minutes using GC-MS analysis.

HP 300°C 60 Mins							
No	**Retention time (mins)**	**Area**	**Area (%)**	**Compound name**	**Molecular formula**	**Molecular weight (g/mol)**	**Classification of compound**
1	3.603	10831072	2.20	Carbon dioxide	CO_2	44	Protein[64, 6]
2	3.816	3553068	0.72	Methanethiol	CH_4S	48	Probably bacterial products[122]
3	4.767	22086959	4.48	Acetic acid	CH_3COOH	60	Carbohydrate, Lignin[64]
4	7.459	3601771	0.73	Pyridine, 2-methyl-	C_6H_7N	93	Protein[64]
5	10.012	5585181	1.13	Phenol	C_6H_6O	94	Protein, Carbohydrate, Lignin[29, 52, 106]
6	10.931	9540535	1.93	2-Pyrrolidinone, 1-methyl-	C_5H_9NO	99	Protein[29]
7	11.775	11763869	2.38	p-Cresol	C_7H_8O	108	Protein, Carbohydrate[64, 6]
8	11.978	12866980	2.61	2,5-Pyrrolidinedione, 1-methyl-	C_5H_7NO	113	Protein[64]
9	12.224	6310776	1.28	Methyl creatinine	$C_4H_7N_3O$	113	Protein[44]
10	13.634	3773343	0.76	2,5-Pyrrolidinedione, 1-propyl-	$C_7H_{11}NO_2$	141	Protein[64]
11	20.717	3674285	0.74	C9-phenol isomer	$C_{15}H_{24}O$	220	Lipid, Protein, Carbohydrate, Lignin[99,118,64,22]
12	20.792	4505699	0.91	C9-phenol isomer	$C_{15}H_{24}O$	220	Lipid, Protein, Carbohydrate, Lignin[99,118,64,22]
13	22.928	12976720	2.63	n-Hexadecanoic acid	$C_{16}H_{32}O_2$	256	Lipid, Protein, Carbohydrate[12, 64]
14	24.702	3869472	0.78	Oleic Acid	$C_{18}H_{34}O_2$	282	Lipid[22]
15	25.054	4201969	0.85	Hexadecanamide	$C_{16}H_{33}NO$	255	Protein[64]
16	31.571	5222524	1.06	Cholestene isomer (3?)	$C_{27}H_{46}$	370	Lipid[45, 52, 88, 106]
17	31.956	6710425	1.36	Cholestene isomer (7?)	$C_{27}H_{46}$	370	Lipid[45, 52, 88, 106]
18	32.169	14734625	2.99	Cholestene isomer (4?)	$C_{27}H_{46}$	370	Lipid[45, 52, 88, 106]
19	32.404	81255442	16.47	Cholest-2-ene	$C_{27}H_{46}$	370	Lipid[45, 52, 88, 106]
20	32.49	66775717	13.53	Cholestane	$C_{27}H_{48}$	372	Lipid[45, 52, 88, 106]
21	34.05	5190367	1.05	Cholestadiene isomer	$C_{27}H_{44}$	368	Lipid[45, 52, 88, 106]
22	34.156	5646555	1.14	Ergostane	$C_{28}H_{50}$	386	Lipid[123]
23	35.353	5271842	1.07	Stigmastene isomer	$C_{29}H_{50}$	398	Lipid[86]
24	35.663	15598886	3.16	Stigmastene isomer (2?)	$C_{29}H_{50}$	398	Lipid[51]
25	35.78	12351425	2.50	Stigmastane	$C_{29}H_{52}$	400	Lipid[88]
Total yields %			**68.49**				

Table S16: The major identified compounds of the produced renewable crude oil via the HTL process from the HP sample at reaction temperature of 350ºC and residence time of 20 minutes using GC-MS analysis.

HP 350°C 20 Mins							
No	**Retention time (mins)**	**Area**	**Area (%)**	**Compound name**	**Molecular formula**	**Molecular weight (g/mol)**	**Classification of compound**
1	3.613	8423137	1.74	Carbon dioxide	CO_2	44	Protein[64, 6]
2	4.842	25936595	5.36	Acetic acid	CH_3COOH	60	Carbohydrate, Lignin[64]
3	7.801	4011261	0.83	Pentanoic Acid	$C_5H_{10}O_2$	102	Lipid[61]
4	10.034	8558229	1.77	Phenol	C_6H_6O	94	Protein, Carbohydrate, Lignin[29, 52, 106]
5	11.134	5707161	1.18	2-Pyrrolidinone, 1-methyl-	C_5H_9NO	99	Protein[29]
6	11.807	16925027	3.50	p-Cresol	C_7H_8O	108	Protein, Carbohydrate[64, 6]
7	11.978	10676881	2.21	2,5-Pyrrolidinedione, 1-methyl-	C_5H_7NO	113	Protein[64]
8	12.224	6494073	1.34	Methyl creatinine	$C_4H_7N_3O$	113	Protein[44]
9	13.132	7110963	1.47	Phenol, 4-ethyl-	$C_8H_{10}O$	122	Lipid, Protein, Carbohydrate, Lignin[99,118,64,22]
10	19.937	5820351	1.20	Benzene,1,1'-(1,3-propanediyl) bis-	$C_{15}H_{16}$	196	Carbohydrate[2]
11	20.802	4604690	0.95	C9-phenol isomer	$C_{15}H_{24}O$	220	Lipid, Protein, Carbohydrate, Lignin[99,118,64,22]
12	22.939	16740492	3.46	n-Hexadecanoic acid	$C_{16}H_{32}O_2$	256	Lipid, Protein, Carbohydrate[12, 64]
13	24.691	5571940	1.15	Oleic Acid	$C_{18}H_{34}O_2$	282	Lipid[22]
14	24.841	7549952	1.56	Octadecanoic acid	$C_{18}H_{36}O_2$	284	Lipid[22]
15	25.065	4676608	0.97	Hexadecanamide	$C_{16}H_{33}NO$	255	Protein[64]
16	29.531	4205339	0.87	Cholesteneone isomer (24?)	$C_{27}H_{44}O$	384	Lipid[45, 52, 88, 106]
17	31.87	4936018	1.02	Cholestene isomer (3?)	$C_{27}H_{46}$	370	Lipid[45, 52, 88, 106]
18	31.956	4248195	0.88	Cholestene isomer (7?)	$C_{27}H_{46}$	370	Lipid[45, 52, 88, 106]
19	32.159	4531615	0.94	Cholestene isomer (4?)	$C_{27}H_{46}$	370	Lipid[45, 52, 88, 106]
20	32.394	49366093	10.21	Cholest-2-ene	$C_{27}H_{46}$	370	Lipid[45, 52, 88, 106]
21	32.511	91484917	18.92	Cholestane	$C_{27}H_{48}$	372	Lipid[45, 52, 88, 106]
22	34.156	9110478	1.88	Cholestadiene isomer	$C_{27}H_{44}$	368	Lipid[45, 52, 88, 106]
23	35.663	9170903	1.90	Stigmastene isomer (2?)	$C_{29}H_{50}$	398	Lipid[51]
24	35.791	18804222	3.89	Stigmastane	$C_{29}H_{52}$	400	Lipid[88]
25	36.87	4134503	0.85	Cholestan-3-one, (5.alpha.)-	$C_{27}H_{46}O$	386	Lipid[22]
Total yields %			**70.05**				

Table S17: The major identified compounds of the produced renewable crude oil via the HTL process from the HP sample at reaction temperature of 350°C and residence time of 40 minutes using GC-MS analysis.

HP 350°C 40 Mins							
No	**Retention time (mins)**	**Area**	**Area (%)**	**Compound name**	**Molecular formula**	**Molecular weight (g/mol)**	**Classification of compound**
1	3.603	19268350	3.89	Carbon dioxide	CO_2	44	Protein[64, 6]
2	4.959	40240665	8.13	Acetic acid	CH_3COOH	60	Carbohydrate, Lignin[64]
3	5.761	6694493	1.35	Propanoic acid	$C_3H_6O_2$	74	Lipid, Protein[101]
4	6.476	3891519	0.79	Disulfide, dimethyl	$C_2H_6S_2$	94	Probably bacterial products[21]
5	7.844	4727708	0.96	Pentanoic Acid	$C_5H_{10}O_2$	102	Lipid[61]
6	10.034	9886750	2.00	Phenol	C_6H_6O	94	Protein, Carbohydrate, Lignin[29, 52, 106]
7	10.91	6404556	1.29	2-Pyrrolidinone, 1-methyl-	C_5H_9NO	99	Protein[29]
8	11.134	7324936	1.48	2-Hexanone, 4-methyl-	$C_7H_{14}O$	114	Lignin[126]
9	11.658	6007674	1.21	m-Cresol	C_7H_8O	108	Protein, Lignin[127 81]
10	11.807	14848721	3.00	p-Cresol	C_7H_8O	108	Protein, Carbohydrate[64, 6]
11	11.978	13240552	2.68	2,5-Pyrrolidinedione, 1-methyl-	C_5H_7NO	113	Protein[64]
12	12.224	8318699	1.68	Methyl creatinine	$C_4H_7N_3O$	113	Protein[44]
13	13.121	5691781	1.15	Phenol, 4-ethyl-	$C_8H_{10}O$	122	Lipid, Protein, Carbohydrate, Lignin[99,118,64,22]
14	13.623	5058633	1.02	2,5-Pyrrolidinedione, 1-propyl-	$C_7H_{11}NO_2$	141	Protein[64]
15	19.937	5746187	1.161	Benzene,1,1'-(1,3-propanediyl) bis-	$C_{15}H_{16}$	196	Carbohydrate[2]
16	20.77	5886764	1.19	C9-phenol isomer	$C_{15}H_{24}O$	220	Lipid, Protein, Carbohydrate, Lignin[99,118,64,22]
17	22.939	19032153	3.85	n-Hexadecanoic acid	$C_{16}H_{32}O_2$	256	Lipid, Protein, Carbohydrate[12, 64]
18	24.841	6408891	1.30	Octadecanoic acid	$C_{18}H_{36}O_2$	284	Lipid[22]
19	31.87	5301100	1.07	Cholestene isomer (3?)	$C_{27}H_{46}$	370	Lipid[45, 52, 88, 106]
20	31.945	3447249	0.70	Cholestene isomer (7?)	$C_{27}H_{46}$	370	Lipid[45, 52, 88, 106]
21	32.159	5202534	1.05	Cholestene isomer (4?)	$C_{27}H_{46}$	370	Lipid[45, 52, 88, 106]
22	32.394	39046503	7.89	Cholest-2-ene	$C_{27}H_{46}$	370	Lipid[45, 52, 88, 106]
23	32.501	84906294	17.16	Cholestane	$C_{27}H_{48}$	372	Lipid[45, 52, 88, 106]
24	34.146	7793447	1.58	Cholestadiene isomer	$C_{27}H_{44}$	368	Lipid[45, 52, 88, 106]
25	35.652	7361288	1.49	Stigmastene isomer (2?)	$C_{29}H_{50}$	398	Lipid[51]
26	35.78	17470074	3.53	Stigmastane	$C_{29}H_{52}$	400	Lipid[88]
Total yields %			**72.60**				

Table S18: The major identified compounds of the produced renewable crude oil via the HTL process from the HP sample at reaction temperature of 350°C and residence time of 60 minutes using GC-MS analysis.

HP 350°C 60 Mins							
No	**Retention time (mins)**	**Area**	**Area (%)**	**Compound name**	**Molecular formula**	**Molecular weight (g/mol)**	**Classification of compound**
1	1.265	118552487	1.07	Carbon dioxide	CO_2	44	Protein[64, 6]
2	1.365	103977292	0.94	Methanol	CH_3OH	32	Lignin[68]
Total yields %			**2.01**				
1	7.901	54182065	0.49	Butanoic acid, 3-methyl-	$C_5H_{10}O_2$	102	Carbohydrate, Lignin[109, 18, 128]
2	8.871	118978956	1.07	2,5-Pyrrolidinedione, 1-methyl-	C_5H_7NO	113	Protein[64]
3	9.043	77421945	0.70	Pyrrolidinedinone, dimethyl isomer	$C_6H_9NO_2$	127	Protein[64]
4	11.095	42953526	0.39	1-Hexanol, 2-ethyl	$C_8H_{18}O$	130	Carbohydrate, Lignin[67]
5	11.332	31339492	0.28	1,2-Benzenedicarboxaldehyde	$C_8H_6O_2$	134	Carbohydrate[2]
6	22.186	145324636	1.31	n-Hexadecanoic acid	$C_{16}H_{32}O_2$	256	Lipid, Protein, Carbohydrate[12, 64]
7	24.069	101118994	0.91	Oleic Acid	$C_{18}H_{34}O_2$	282	Lipid[22]
8	26.436	91264112	0.82	9-Octadecenamide, (Z)-	$C_{18}H_{35}NO$	281	Protein[64]
9	26.656	78563073	0.71	Octadecanamide	$C_{18}H_{37}NO$	283	Protein[64]
10	28.276	75084693	0.68	Cholestene isomer (3?)	$C_{27}H_{46}$	370	Lipid[45, 52, 88, 106]
11	30.15	77856888	0.70	Cholestene isomer	$C_{27}H_{46}$	370	Lipid[45, 52, 88, 106]
12	30.392	105239025	0.95	Cholestene isomer	$C_{27}H_{46}$	370	Lipid[45, 52, 88, 106]
13	30.601	167843348	1.51	Cholestene isomer (3?)	$C_{27}H_{46}$	370	Lipid[45, 52, 88, 106]
14	30.677	90518258	0.82	Cholestene isomer (3?)	$C_{27}H_{46}$	370	Lipid[45, 52, 88, 106]
15	31.074	1417799901	12.79	Cholestadiene isomer	$C_{27}H_{44}$	368	Lipid[45, 52, 88, 106]
16	31.131	980489813	8.84	Cholest-2-ene	$C_{27}H_{46}$	370	Lipid[45, 52, 88]
17	31.38	109005784	0.98	Cholestane	$C_{27}H_{48}$	372	Lipid[45, 52, 88, 106]
18	31.911	323358207	2.92	Cholestanone isomer	$C_{27}H_{46}O$	386	Lipid[22, 75]
19	32.104	71763324	0.65	Ergost-2-ene	$C_{28}H_{48}$	384	Lipid[22]
20	32.275	90902971	0.82	Stigmastene isomer	$C_{29}H_{50}$	398	Lipid[86]
21	32.467	80734885	0.73	Stigmastene isomer	$C_{29}H_{50}$	398	Lipid[86]
22	32.687	481040906	4.34	Stigmastene isomer	$C_{29}H_{50}$	398	Lipid[86]
23	32.86	92500453	0.83	Stigmastane	$C_{29}H_{52}$	400	Lipid[88]
24	33.063	114559070	1.03	Cholestenone isomer	$C_{27}H_{44}O$	384	Lipid[45, 52, 88, 106]
25	33.267	88596149	0.80	Cholestanone isomer	$C_{27}H_{46}O$	386	Lipid[22, 75]
26	34.148	239822342	2.16	Cholestadienone isomer	$C_{27}H_{42}O$	382	Lipid[124]

27	34.719	37009445	0.33	Diethylcholestene isomer	$C_{31}H_{54}$	426	Lipid[17]
Total yields %			**48.56**				
Total yields % (oil fraction + non-oil fraction)			**50.57**				

Table S19: The major identified compounds of the produced renewable crude oil from the HC sample before the HTL process using GC-MS analysis.

HC S							
No	**Retention time (mins)**	**Area**	**Area (%)**	**Compound name**	**Molecular formula**	**Molecular weight (g/mol)**	**Classification of compound**
1	3.603	10808030	2.97	Carbon dioxide	CO_2	44	Protein[64, 6]
2	3.774	6388030	1.75	Methanol	CH_3OH	32	Lignin[68]
3	4.981	42448421	11.65	Acetic acid	CH_3COOH	60	Carbohydrate, Lignin[64]
4	5.237	7894210	2.17	2-Butanone	C_4H_8O	72	Carbohydrate[107]
5	5.739	3492518	0.96	Propanoic acid	$C_3H_6O_2$	74	Lipid, Protein[101]
6	6.327	9162365	2.51	Disulfide, dimethyl	$C_2H_6S_2$	94	Probably bacterial products[21]
7	6.647	3222637	0.88	Toluene	C_7H_8	92	Lipid, Protein, Carbohydrate[64]
8	7.534	7956082	2.18	Pyrazine, methyl-	$C_5H_6N_2$	94	Protein[44, 52]
9	7.812	3563811	0.98	Pentanoic Acid	$C_5H_{10}O_2$	102	Lipid[61]
10	10.034	4269931	1.17	Phenol	C_6H_6O	94	Protein, Carbohydrate, Lignin[29, 52, 106]
11	10.889	2675369	0.73	2-Pyrrolidinone, 1-methyl-	C_5H_9NO	99	Protein[29]
12	11.754	7438218	2.04	p-Cresol	C_7H_8O	108	Protein, Carbohydrate[64, 6]
13	11.978	10588344	2.91	2,5-Pyrrolidinedione, 1-methyl-	C_5H_7NO	113	Protein[64]
14	12.213	3567969	0.98	Methyl creatinine	$C_4H_7N_3O$	113	Protein[44]
15	13.591	3562048	0.98	2,5-Pyrrolidinedione, 1-propyl-	$C_7H_{11}NO_2$	141	Protein[64]
16	17.063	2527907	0.69	1H-Isoindole-1,3(2H)-dione,2-methyl-	$C_9H_7NO_2$	161	Protein[64]
17	21.743	3133123	0.86	Complex Pyrrolidinedione isomer	$C_{14}H_{34}NO_2$	250	Protein[64]
18	22.736	3034079	0.83	Biphenylol isomer	$C_{12}H_{10}O$	170	Lipid, Protein, Carbohydrate[31, 22]
19	22.928	5163538	1.42	n-Hexadecanoic acid	$C_{16}H_{32}O_2$	256	Lipid, Protein, Carbohydrate[12, 64]
20	32.159	5920775	1.62	Cholestene isomer (4?)	$C_{27}H_{46}$	370	Lipid[45, 52, 88, 106]
21	32.404	63233043	17.35	Cholest-2-ene	$C_{27}H_{46}$	370	Lipid[45, 52, 88, 106]
22	32.49	50930550	13.98	Cholestane	$C_{27}H_{48}$	372	Lipid[45, 52, 88, 106]
23	35.652	7329734	2.01	Stigmastene isomer (2?)	$C_{29}H_{50}$	398	Lipid[51]
24	35.77	5537607	1.52	Stigmastane	$C_{29}H_{52}$	400	Lipid[88]
25	43.494	14564171	4.00	Dihydroxychloesterol	$C_{27}H_{46}O_3$	418	Lipid[17]
Total yields %			**79.15**				

Table S20: The major identified compounds of the produced renewable crude oil via the HTL process from the HC sample at reaction temperature of 250°C and residence time of 20 minutes using GC-MS analysis.

HC 250°C 20 Mins							
No	**Retention time (mins)**	**Area**	**Area (%)**	**Compound name**	**Molecular formula**	**Molecular weight (g/mol)**	**Classification of compound**
1	1.156	8563279	1.55	Carbon dioxide	CO_2	44	Protein[64, 6]
2	1.231	33015626	5.96	Methanethiol	CH_4S	48	Probably bacterial products[122]
3	1.327	10543610	1.90	Acetone	C_3H_6O	58	Carbohydrate[23]
4	1.413	5044076	0.91	Acetic acid, methyl ester	$C_3H_6O_2$	74	Carbohydrate, Lignin[99, 5]
5	1.626	5004483	0.90	2-Butanone	C_4H_8O	72	Carbohydrate[107]
6	2.011	8878804	1.60	Propanoic acid	$C_3H_6O_2$	74	Lipid, Protein[101]
7	2.513	6601536	1.19	Acetic acid	CH_3COOH	60	Carbohydrate, Lignin[64]
8	2.705	4038120	0.73	Pyridine	C_5H_5N	79	Protein[64]
Total yields %			**14.75**				
1	4.447	2954972	0.53	Acetamide, N-methyl-	C_3H_7NO	73	Protein[64]
2	8.378	5267817	0.95	Phenol, 2-methoxy-	C7H8O2	124	Lipid, Lignin[64, 10]
3	8.464	3722266	0.67	2,5-Pyrrolidinedione, 1-methyl-	C_5H_7NO	113	Protein[64]
4	8.613	4577251	0.83	Pyrrolidinedinone, dimethyl isomer	$C_6H_9NO_2$	127	Protein[64]
5	8.806	5100360	0.92	Pyrrolidinedinone, dimethyl isomer	$C_6H_9NO_2$	127	Protein[64]
6	10.312	3105931	0.56	Creosol	$C_8H_{10}O_2$	138	Lignin[65]
7	14.222	3449620	0.62	1H-Isoindole-1,3(2H)-dione,2-methyl-	$C_9H_7NO_2$	161	Protein[64]
8	21.957	15157523	2.74	n-Hexadecanoic acid	$C_{16}H_{32}O_2$	256	Lipid, Protein, Carbohydrate[12, 64]
9	24.168	4905394	0.89	9-Octadecenamide, (Z)-	$C_{18}H_{35}NO$	281	Protein[64]
10	25.097	2887892	0.52	Hexadecanamide	$C_{16}H_{33}NO$	255	Protein[64]
11	26.134	4327664	0.78	Cholestene isomer (3?)	$C_{27}H_{46}$	370	Lipid[45, 52, 88, 106]
12	26.914	3008145	0.54	Docosanoic acid	$C_{22}H_{44}O_2$	340	Lipid[41]
13	27.138	3773666	0.68	Cholestene isomer	$C_{27}H_{46}$	370	Lipid[45, 52, 88, 106]
14	30.116	1015488	0.18	Cholestene isomer (3?)	$C_{27}H_{46}$	370	Lipid[45, 52, 88, 106]
15	30.183	2030975	0.37	Cholestene isomer	$C_{27}H_{46}$	370	Lipid[45, 52, 88, 106]
16	30.888	255569951	46.14	Cholest-2-ene	$C_{27}H_{46}$	370	Lipid[45, 52, 88, 106]
17	31.176	6693842	1.21	Cholestane	$C_{27}H_{48}$	372	Lipid[45, 52, 88, 106]
18	31.625	7018621	1.27	Cholestanone isomer	$C_{27}H_{46}O$	386	Lipid[22, 75]
19	32.415	15005500	2.71	Stigmastene isomer	$C_{29}H_{50}$	398	Lipid[86]

20	32.661	3423086	0.62	Stigmastene isomer	$C_{29}H_{50}$	398	Lipid[86]
21	33.388	6777466	1.22	Cholestanone isomer	$C_{27}H_{46}O$	386	Lipid[22, 75]
22	33.964	58311397	10.53	Cholestan-3-one, (5.alpha.)-	$C_{27}H_{46}O$	386	Lipid[22]
23	35.118	40859001	7.38	Dihydroxychloesterol	$C_{27}H_{46}O_3$	418	Lipid[17]
24	35.93	4065219	0.73	Diethylcholestene isomer	$C_{31}H_{54}$	426	Lipid[17]
25	37.447	3902534	0.70	Stigmastanediol isomer	$C_{29}H_{52}O_2$	432	Lipid[88]
Total yields %			**84.29**				
Total yields % (oil fraction + non-oil fraction)			**99.04**				

Table S21: The major identified compounds of the produced renewable crude oil via the HTL process from the HC sample at reaction temperature of 250ºC and residence time of 40 minutes using GC-MS analysis.

HC 250°C 40 Mins							
No	**Retention time (mins)**	**Area**	**Area (%)**	**Compound name**	**Molecular formula**	**Molecular weight (g/mol)**	**Classification of compound**
1	1.343	235777593	8.98	Carbon dioxide	CO_2	44	Protein[64, 6]
2	1.405	40740406	1.55	Methanol	CH_3OH	32	Lignin[68]
3	1.44	35136063	1.34	Methanethiol	CH_4S	48	Probably bacterial products[122]
4	1.547	28441206	1.08	Acetone	C_3H_6O	58	Carbohydrate[23]
5	1.63	18843438	0.72	Acetic acid, methyl ester	$C_3H_6O_2$	74	Carbohydrate, Lignin[99, 5]
6	1.87	15097512	0.58	2-Butanone	C_4H_8O	72	Carbohydrate[107]
7	2.266	23179185	0.88	Propanoic acid	$C_3H_6O_2$	74	Lipid, Protein[101]
8	2.553	35203156	1.34	Acetic acid	CH_3COOH	60	Carbohydrate, Lignin[64]
9	2.999	24935811	0.95	Pyridine	C_5H_5N	79	Protein[64]
Total yields %			**17.43**				

1	6.878	9191367	0.35	Phenol	C_6H_6O	94	Protein, Carbohydrate, Lignin[29, 52, 106]
2	8.795	42567895	1.62	Phenol, 2-methoxy-	$C_7H_8O_2$	124	Lipid, Lignin[64, 10]
3	8.863	31566479	1.20	2,5-Pyrrolidinedione, 1-methyl-	C_5H_7NO	113	Protein[64]
4	10.696	10426690	0.40	Creosol	$C_8H_{10}O_2$	138	Lignin[65]
5	14.582	8232878	0.31	1H-Isoindole-1,3(2H)-dione,2-methyl-	$C_9H_7NO_2$	161	Protein[64]
6	19.535	16191792	0.62	Benzene,1,1-(1,3-propanediyl) bis-	$C_{15}H_{16}$	196	Carbohydrate[2]

7	20.486	10716369	0.41	Tetradecanoic acid	$C_{14}H_{28}O_2$	228	Lipid[45, 12]
8	20.701	14391479	0.55	Complex Pyrrolidinedione isomer	$C_{14}H_{34}NO_2$	250	Protein[64]
9	21.983	17612671	0.67	d-Proline, n-butoxycarbonyl-, butyl ester	$C_{14}H_{25}NO_4$	271	Lipid, Protein, Carbohydrate[116]
10	22.138	48583051	1.85	n-Hexadecanoic acid	$C_{16}H_{32}O_2$	256	Lipid, Protein, Carbohydrate[12, 64]
11	24.348	14604321	0.56	Octadecanamide	$C_{18}H_{37}NO$	283	Protein[64]
12	30.517	21670578	0.83	Cholestene isomer (3?)	$C_{27}H_{46}$	370	Lipid[45, 52, 88, 106]
13	30.761	21837960	0.83	Cholestene isomer	$C_{27}H_{46}$	370	Lipid[45, 52, 88, 106]
14	31.162	1188675529	45.30	Cholest-2-ene	$C_{27}H_{46}$	370	Lipid[45, 52, 88, 106]
15	31.32	15463473	0.59	Cholestane	$C_{27}H_{48}$	372	Lipid[45, 52, 88, 106]
16	31.482	50024796	1.91	Cholestadiene isomer	$C_{27}H_{44}$	368	Lipid[45, 52, 88, 106]
17	31.616	13921128	0.53	Cholestanone isomer	$C_{27}H_{46}O$	386	Lipid[22, 75]
18	31.944	50574068	1.93	Cholestanone isomer	$C_{27}H_{46}O$	386	Lipid[22, 75]
19	32.209	29617416	1.13	Stigmastene isomer	$C_{29}H_{50}$	398	Lipid[86]
20	32.468	20105195	0.77	Stigmastene isomer	$C_{29}H_{50}$	398	Lipid[86]
21	32.615	13575659	0.52	Stigmastene isomer	$C_{29}H_{50}$	398	Lipid[86]
22	32.712	124995070	4.76	Stigmast-2-ene, (5.alpha.)-	$C_{29}H_{50}$	398	Lipid[88]
23	32.963	29581651	1.13	Stigmastane	$C_{29}H_{52}$	400	Lipid[88]
24	33.139	13163272	0.50	Cholestenone isomer	$C_{27}H_{44}O$	384	Lipid[45, 52, 88, 106]
25	33.711	23940476	0.91	C30 17a(H)-hopane	$C_{30}H_{52}$	412	Lipid[25]
26	34.07	11502697	0.44	Cholestadienone isomer	$C_{27}H_{42}O$	382	Lipid[124]
27	34.196	12123667	0.46	Cholestanediol isomer	$C_{27}H_{48}O_2$	404	Lipid[22]
28	35.48	89559980	3.41	Diethylcholestene isomer	$C_{31}H_{54}$	426	Lipid[17]
Total yields %			**74.48**				
Total yields % (oil fraction + non-oil fraction)			**91.91**				

Table S22: The major identified compounds of the produced renewable crude oil via the HTL process from the HC sample at reaction temperature of 250ºC and residence time of 60 minutes using GC-MS analysis.

HC 250°C 60 Mins							
No	**Retention time (mins)**	**Area**	**Area (%)**	**Compound name**	**Molecular formula**	**Molecular weight (g/mol)**	**Classification of compound**
1	1.148	8777287	1.52	Carbon dioxide	CO_2	44	Protein[64, 6]
2	1.233	26017237	4.51	Methanethiol	CH_4S	48	Probably bacterial products[122]
3	1.319	11296412	1.96	Acetone	C_3H_6O	58	Carbohydrate[23]
4	1.394	2976313	0.52	2-Butanone	C_4H_8O	72	Carbohydrate[107]

5	1.97	4954805	0.86	Propanoic acid	$C_3H_6O_2$	74	Lipid, Protein[101]
6	2.323	6683654	1.16	Acetic acid	CH_3COOH	60	Carbohydrate, Lignin[64]
7	2.686	3608467	0.63	Pyridine	C_5H_5N	79	Protein[64]
Total yields %			**11.15**				

1	8.359	5428057	0.94	Phenol, 2-methoxy-	C7H8O2	124	Lipid, Lignin[64, 10]
2	8.434	3352156	0.58	2,5-Pyrrolidinedione, 1-methyl-	C_5H_7NO	113	Protein[64]
3	8.797	5430063	0.94	Pyrrolidinedinone, dimethyl isomer	$C_6H_9NO_2$	127	Protein[64]
4	14.213	2949140	0.51	1H-Isoindole-1,3(2H)-dione,2-methyl-	$C_9H_7NO_2$	161	Protein[64]
5	21.959	18528810	3.21	n-Hexadecanoic acid	$C_{16}H_{32}O_2$	256	Lipid, Protein, Carbohydrate[12, 64]
6	23.935	5361250	0.93	Oleic Acid	$C_{18}H_{34}O_2$	282	Lipid[22]
7	24.17	5773363	1.00	Octadecanamide	$C_{18}H_{37}NO$	283	Protein[64]
8	26.125	4158216	0.72	Cholestene isomer (3?)	$C_{27}H_{46}$	370	Lipid[45, 52, 88, 106]
9	26.926	4503991	0.78	Docosanoic acid	$C_{22}H_{44}O_2$	340	Lipid[41]
10	27.183	5698680	0.99	Cholestene isomer	$C_{27}H_{46}$	370	Lipid[45, 52, 88, 106]
11	30.195	3501650	0.61	Cholestene isomer	$C_{27}H_{46}$	370	Lipid[45, 52, 88, 106]
12	30.9	293993629	50.95	Cholestene isomer	$C_{27}H_{46}$	370	Lipid[45, 52, 88, 106]
13	31.01	2596205	0.45	Cholest-2-ene	$C_{27}H_{46}$	370	Lipid[45, 52, 88, 106]
14	31.2	5192411	0.90	Cholestane	$C_{27}H_{48}$	372	Lipid[45, 52, 88, 106]
15	31.648	8177831	1.42	Cholestadiene isomer	$C_{27}H_{44}$	368	Lipid[45, 52, 88, 106]
16	32.428	17747664	3.08	Stigmastene isomer	$C_{29}H_{50}$	398	Lipid[86]
17	32.685	3666993	0.64	Stigmastene isomer	$C_{29}H_{50}$	398	Lipid[86]
18	33.422	10540965	1.83	Cholestanone isomer	$C_{27}H_{46}O$	386	Lipid[22, 75]
19	33.988	60218408	10.44	Cholestan-3-one, (5.alpha.)-	$C_{27}H_{46}O$	386	Lipid[22]
20	35.131	37751501	6.54	Dihydroxychloesterol	$C_{27}H_{46}O_3$	418	Lipid[17]
21	35.954	4358878	0.76	Diethylcholestene isomer	$C_{31}H_{54}$	426	Lipid[17]
22	37.471	3822162	0.66	Stigmastanediol isomer	$C_{29}H_{52}O_2$	432	Lipid[88]
Total yields %			**88.85**				
Total yields % (oil fraction + non-oil fraction)			**100.0**				

Table S23: The major identified compounds of the produced renewable crude oil via the HTL process from the HC sample at reaction temperature of 300ºC and residence time of 20 minutes using GC-MS analysis.

HC 300°C 20 Mins

No	Retention time (mins)	Area	Area (%)	Compound name	Molecular formula	Molecular weight (g/mol)	Classification of compound
1	1.208	63429200	1.19	Carbon dioxide	CO_2	44	Protein[64, 6]
2	1.287	65083560	1.22	Nitrous oxide	N_2O	44	Gas[74]
3	2.389	45755944	0.86	Acetic acid	CH_3COOH	60	Carbohydrate, Lignin[64]
Total yields %			**3.26**				
1	8.454	27884462	0.52	Phenol, 2-methoxy-	C7H8O2	124	Lipid, Lignin[64, 10]
2	8.648	81916496	1.53	2,5-Pyrrolidinedione, 1-methyl-	C_5H_7NO	113	Protein[64]
3	8.88	83337351	1.56	Pyrrolidinedinone, dimethyl isomer	$C_6H_9NO_2$	127	Protein[64]
4	10.605	31183778	0.58	Creosol	$C_8H_{10}O_2$	138	Lignin[65]
5	14.306	24330729	0.46	1H-Isoindole-1,3(2H)-dione,2-methyl-	$C_9H_7NO_2$	161	Protein[64]
6	21.926	81385393	1.52	n-Hexadecanoic acid	$C_{16}H_{32}O_2$	256	Lipid, Protein, Carbohydrate[12, 64]
7	23.937	34443668	0.64	Oleic Acid	$C_{18}H_{34}O_2$	282	Lipid[22]
8	24.176	40620855	0.76	Octadecanamide	$C_{18}H_{37}NO$	283	Protein[64]
9	27.191	39545567	0.74	Cholestene isomer	$C_{27}H_{46}$	370	Lipid[45, 52, 88, 106]
10	30.271	33171298	0.62	Cholesteneone isomer (24?)	$C_{27}H_{44}O$	384	Lipid[45, 52, 88, 106]
11	30.514	34014008	0.64	Cholestene isomer	$C_{27}H_{46}$	370	Lipid[45, 52, 88, 106]
12	30.954	1451071052	27.16	Cholestene isomer (3?)	$C_{27}H_{46}$	370	Lipid[45, 52, 88, 106]
13	30.989	496313640	9.29	Cholestene isomer	$C_{27}H_{46}$	370	Lipid[45, 52, 88, 106]
14	31.252	30029617	0.56	Cholest-2-ene	$C_{27}H_{46}$	370	Lipid[45, 52, 88, 106]
15	31.252	60059233	1.12	Cholestane	$C_{27}H_{48}$	372	Lipid[45, 52, 88]
16	31.492	30584883	0.57	Cholestadiene isomer	$C_{27}H_{44}$	368	Lipid[45, 52, 88, 106]
17	31.72	55499316	1.04	Cholestanone isomer	$C_{27}H_{46}O$	386	Lipid[22, 75]
18	31.759	57149733	1.07	Cholestanone isomer	$C_{27}H_{46}O$	386	Lipid[22, 75]
19	31.977	36381996	0.68	Ergost-2-ene	$C_{28}H_{48}$	384	Lipid[22]
20	32.244	39355529	0.74	Stigmastene isomer	$C_{29}H_{50}$	398	Lipid[86]
21	32.381	51037511	0.96	Stigmastene isomer	$C_{29}H_{50}$	398	Lipid[86]
22	32.542	251694833	4.71	Stigmastene isomer	$C_{29}H_{50}$	398	Lipid[86]
23	32.748	57920129	1.08	Stigmast-2-ene, (5.alpha.)-	$C_{29}H_{50}$	398	Lipid[88]
24	32.928	49448317	0.93	Stigmastane	$C_{29}H_{52}$	400	Lipid[88]
25	33.295	45682166	0.85	Cholestenone isomer	$C_{27}H_{44}O$	384	Lipid[45, 52, 88, 106]
26	33.473	40052561	0.75	Cholestanone isomer	$C_{27}H_{46}O$	386	Lipid[22, 75]
27	34.056	469359783	8.78	Cholestadienone isomer	$C_{27}H_{42}O$	382	Lipid[124]
28	35.14	78398404	1.47	Dihydroxychloesterol	$C_{27}H_{46}O_3$	418	Lipid[17]
Total yields %			**71.34**				
Total yields % (oil fraction + non-oil fraction)			**74.60**				

Table S24: The major identified compounds of the produced renewable crude oil via the HTL process from the HC sample at reaction temperature of 300ºC and residence time of 40 minutes using GC-MS analysis.

HC 300°C 40 Mins							
No	**Retention time (mins)**	**Area**	**Area (%)**	**Compound name**	**Molecular formula**	**Molecular weight (g/mol)**	**Classification of compound**
1	1.182	58325817	0.97	Carbon dioxide	CO_2	44	Protein[64, 6]
2	1.261	65544759	1.09	Dimethylamine	$(CH_3)_2NH$	45	Gas[108]
3	2.499	61370987	1.02	Acetic acid	CH_3COOH	60	Carbohydrate, Lignin[64]
4	2.708	34557634	0.58	Pyridine	C_5H_5N	79	Protein[64]
Total yields %			**3.67**				

1	8.419	16668111	0.28	Phenol, 2-methoxy-	C7H8O2	124	Lipid, Lignin[64, 10]
2	8.64	90184578	1.51	2,5-Pyrrolidinedione, 1-methyl-	C_5H_7NO	113	Protein[64]
3	8.87	103321159	1.72	Pyrrolidinedinone, dimethyl isomer	$C_6H_9NO_2$	127	Protein[64]
4	10.374	26411385	0.44	Methyl creatinine	$C_4H_7N_3O$	113	Protein[44]
5	10.592	28871529	0.48	Creosol	$C_8H_{10}O_2$	138	Lignin[65]
6	21.844	54186175	0.90	d-Proline, n-butoxycarbonyl-, butyl ester	$C_{14}H_{25}NO_4$	271	Lipid, Protein, Carbohydrate[116]
7	21.919	43423887	0.72	n-Hexadecanoic acid	$C_{16}H_{32}O_2$	256	Lipid, Protein, Carbohydrate[12, 64]
8	23.9	34644505	0.58	Oleic Acid	$C_{18}H_{34}O_2$	282	Lipid[22]
9	24.153	59882155	1.00	Octadecanamide	$C_{18}H_{37}NO$	283	Protein[64]
10	24.637	34719250	0.58	Hexadecanamide	$C_{16}H_{33}NO$	255	Protein[64]
11	27.121	49393896	0.82	Cholestene isomer	$C_{27}H_{46}$	370	Lipid[45, 52, 88, 106]
12	29.331	32433592	0.54	Cholestene isomer	$C_{27}H_{46}$	370	Lipid[45, 52, 88, 106]
13	30.24	43919704	0.73	Cholesteneone isomer (24?)	$C_{27}H_{44}O$	384	Lipid[45, 52, 88, 106]
14	30.498	45140270	0.75	Cholestene isomer	$C_{27}H_{46}$	370	Lipid[45, 52, 88, 106]
15	30.946	1958591718	32.70	Cholestene isomer (3?)	$C_{27}H_{46}$	370	Lipid[45, 52, 88, 106]
16	30.996	619955200	10.35	Cholestene isomer	$C_{27}H_{46}$	370	Lipid[45, 52, 88, 106]
17	31.176	30722822	0.51	Cholest-2-ene	$C_{27}H_{46}$	370	Lipid[45, 52, 88, 106]
18	31.239	61445643	1.03	Cholestane	$C_{27}H_{48}$	372	Lipid[45, 52, 88, 106]
19	31.5	54145909	0.90	Cholestadiene isomer	$C_{27}H_{44}$	368	Lipid[45, 52, 88, 106]
20	31.74	124578216	2.08	Cholestanone isomer	$C_{27}H_{46}O$	386	Lipid[22, 75]
21	31.951	42001691	0.70	Ergost-2-ene	$C_{28}H_{48}$	384	Lipid[22]
22	32.222	49474357	0.83	Stigmastene isomer	$C_{29}H_{50}$	398	Lipid[86]
23	32.478	152044936	2.54	Stigmastene isomer	$C_{29}H_{50}$	398	Lipid[86]
24	32.527	155616493	2.60	Stigmastene isomer	$C_{29}H_{50}$	398	Lipid[86]
25	32.721	62411655	1.04	Stigmast-2-ene, (5.alpha.)-	$C_{29}H_{50}$	398	Lipid[88]
26	32.899	51717679	0.86	Stigmastane	$C_{29}H_{52}$	400	Lipid[88]
27	33.242	45881960	0.77	Cholestenone isomer	$C_{27}H_{44}O$	384	Lipid[45, 52, 88, 106]
28	33.936	93607889	1.56	Cholestan-3-one, (5.alpha.)-	$C_{27}H_{46}O$	386	Lipid[22]

29	35.076	48629795	0.81	Dihydroxychloesterol	$C_{27}H_{46}O_3$	418	Lipid[17]
Total yields %			**70.36**				
Total yields % (oil fraction + non-oil fraction)			**74.03**				

Table S25: The major identified compounds of the produced renewable crude oil via the HTL process from the HC sample at reaction temperature of 300ºC and residence time of 60 minutes using GC-MS analysis.

HC 300°C 60 Mins							
No	**Retention time (mins)**	**Area**	**Area (%)**	**Compound name**	**Molecular formula**	**Molecular weight (g/mol)**	**Classification of compound**
1	7.642	19095516	0.14	2-Pyrrolidinone, 1-methyl-	C_5H_9NO	99	Protein[29]
2	8.621	101155136	0.73	Pyrrolidinedinone, dimethyl isomer	$C_6H_9NO_2$	127	Protein[29]
3	8.812	93513650	0.67	Pyrrolidinedinone, dimethyl isomer	$C_6H_9NO_2$	127	Protein[29]
4	14.255	30600392	0.22	1H-Isoindole-1,3(2H)-dione,2-methyl-	$C_9H_7NO_2$	161	Protein[64]
5	17.632	26579173	0.19	Benzene,1,1-(1,3-propanediyl) bis-	$C_{15}H_{16}$	196	Carbohydrate[2]
6	21.836	79211678	0.57	n-Hexadecanoic acid	$C_{16}H_{32}O_2$	256	Lipid, Protein, Carbohydrate[12, 64]
7	23.946	94733733	0.68	Oleic Acid	$C_{18}H_{34}O_2$	282	Lipid[22]
8	24.173	109178328	0.79	Octadecanamide	$C_{18}H_{37}NO$	283	Protein[64]
10	28.76	82418715	0.59	Cholestene isomer	$C_{27}H_{46}$	370	Lipid[45, 52, 88, 106]
11	30.248	135770760	0.98	Cholesteneone isomer (24?)	$C_{27}H_{44}O$	384	Lipid[45, 52, 88, 106]
12	30.429	114659110	0.83	Cholestene isomer	$C_{27}H_{46}$	370	Lipid[45, 52, 88, 106]
13	30.503	84376223	0.61	Cholestene isomer	$C_{27}H_{46}$	370	Lipid[45, 52, 88, 106]
14	31.043	4496395794	32.42	Cholestane	$C_{27}H_{48}$	372	Lipid[45, 52, 88, 106]
15	31.201	66247679	0.48	Cholest-2-ene	$C_{27}H_{46}$	370	Lipid[45, 52, 88, 106]
16	31.268	132495357	0.96	Cholestadiene isomer	$C_{27}H_{44}$	368	Lipid[45, 52, 88, 106]
17	31.498	119784116	0.86	Cholestanone isomer	$C_{27}H_{46}O$	386	Lipid[22, 75]
18	31.769	337061501	2.43	Cholestanone isomer	$C_{27}H_{46}O$	386	Lipid[22, 75]
19	31.971	103187056	0.74	Ergost-2-ene	$C_{28}H_{48}$	384	Lipid[22]
20	32.218	116521434	0.84	Stigmastene isomer	$C_{29}H_{50}$	398	Lipid[86]
21	32.354	126349059	0.91	Stigmastene isomer	$C_{29}H_{50}$	398	Lipid[86]
22	32.562	721190364	5.20	Stigmastene isomer	$C_{29}H_{50}$	398	Lipid[86]

23	32.744	144961948	1.05	Stigmast-2-ene, (5.alpha.)-	$C_{29}H_{50}$	398	Lipid[88]
24	32.929	198547884	1.43	Stigmastane	$C_{29}H_{52}$	400	Lipid[88]
25	33.116	105905443	0.76	Cholestenone isomer	$C_{27}H_{44}O$	384	Lipid[45, 52, 88, 106]
26	33.286	136560570	0.98	Cholestanone isomer	$C_{27}H_{46}O$	386	Lipid[22, 75]
27	33.464	85339243	0.62	C30 17a(H)-hopane	$C_{30}H_{52}$	412	Lipid[25]
28	34.046	763044590	5.50	Cholestadienone isomer	$C_{27}H_{42}O$	382	Lipid[124]
29	35.125	172713482	1.25	Dihydroxychloesterol	$C_{27}H_{46}O_3$	418	Lipid[17]
Total yields %			**63.43**				

Table S26: The major identified compounds of the produced renewable crude oil via the HTL process from the HC sample at reaction temperature of 350ºC and residence time of 20 minutes using GC-MS analysis.

HC 350°C 20 Mins							
No	**Retention time (mins)**	**Area**	**Area (%)**	**Compound name**	**Molecular formula**	**Molecular weight (g/mol)**	**Classification of compound**
1	1.354	163156692	4.19	Carbon dioxide	CO_2	44	Protein[64, 6]
2	1.456	27568070	0.71	Methanethiol	CH_4S	48	Probably bacterial products[122]
3	2.477	51118797	1.31	Acetic acid	CH_3COOH	60	Carbohydrate, Lignin[64]
Total yields %			**6.22**				

1	7.989	35075585	0.90	2-Pyrrolidinone, 1-methyl-	C_5H_9NO	99	Protein[29]
2	8.941	84256717	2.17	2,5-Pyrrolidinedione, 1-methyl	C5H7 NO2	113	Protein[64]
3	9.161	62769721	1.61	Pyrrolidinedinone, dimethyl isomer	C_6H_9 NO2	127	Protein[64]
4	9.245	41623093	1.07	Methyl creatinine	$C_4H_7N_3O$	113	Protein[44]
5	10.976	15860295	0.41	1-Hexanol, 2-ethyl-	$C_8H_{18}O$	130	Carbohydrate, Lignin[67]
6	14.61	16434128	0.42	1H-Isoindole-1,3(2H)-dione,2-methyl-	$C_9H_7NO_2$	161	Protein[64]
7	17.996	33131264	0.85	Benzene,1,1-(1,3-propanediyl) bis-	$C_{15}H_{16}$	196	Carbohydrate[2]
8	22.146	46919355	1.21	d-Proline, n-butoxycarbonyl-, butyl ester	$C_{14}H_{25}NO_4$	271	Lipid, Protein, Carbohydrate[116]
9	22.241	62508710	1.61	n-Hexadecanoic acid	$C_{16}H_{32}O_2$	256	Lipid, Protein, Carbohydrate[12, 64]
10	24.444	48571936	1.25	Octadecanamide	$C_{18}H_{37}NO$	283	Protein[64]
11	28.428	30611616	0.79	Cholestene isomer (3?)	$C_{27}H_{46}$	370	Lipid[45, 52, 88, 106]
12	28.68	31319246	0.80	Docosanoic acid	$C_{22}H_{44}O_2$	340	Lipid[41]

13	29.071	43950486	1.13	Cholestene isomer	$C_{27}H_{46}$	370	Lipid[45, 52, 88, 106]
14	29.604	32982646	0.85	Cholest-23-ene, (5.beta.)-	$C_{27}H_{46}$	370	Lipid[45, 52, 88, 106]
15	29.854	27773462	0.71	Cholestene isomer	$C_{27}H_{46}$	370	Lipid[45, 52, 88, 106]
16	30.179	29374432	0.75	Cholesteneone isomer (24?)	$C_{27}H_{44}O$	384	Lipid[45, 52, 88, 106]
17	30.526	35458243	0.91	Cholestene isomer	$C_{27}H_{46}$	370	Lipid[45, 52, 88, 106]
18	30.725	49740374	1.28	Cholestene isomer	$C_{27}H_{46}$	370	Lipid[45, 52, 88, 106]
19	31.185	446895910	11.49	Cholest-2-ene	$C_{27}H_{46}$	370	Lipid[45, 52, 88]
20	31.242	893791821	22.97	Cholestane	$C_{27}H_{48}$	372	Lipid[45, 52, 88, 106]
21	31.495	37020122	0.95	Cholestadiene isomer	$C_{27}H_{44}$	368	Lipid[45, 52, 88, 106]
22	31.633	29001536	0.75	Cholestanone isomer	$C_{27}H_{46}O$	386	Lipid[22, 75]
23	32.021	93613675	2.41	Ergost-2-ene	$C_{28}H_{48}$	384	Lipid[22]
24	32.266	46185479	1.19	Stigmastene isomer	$C_{29}H_{50}$	398	Lipid[86]
25	32.789	156620658	4.03	Stigmast-2-ene, (5.alpha.)-	$C_{29}H_{50}$	398	Lipid[88]
26	32.979	38669853	0.99	Stigmastane	$C_{29}H_{52}$	400	Lipid[88]
27	33.174	35615964	0.92	Cholestenone isomer	$C_{27}H_{44}O$	384	Lipid[45, 52, 88, 106]
28	33.373	25688376	0.66	Cholestanone isomer	$C_{27}H_{46}O$	386	Lipid[22, 75]
29	35.15	5344804	0.14	Dihydroxychloesterol	$C_{27}H_{46}O_3$	418	Lipid[17]
Total yields %			**65.20**				
Total yields % (oil fraction + non-oil fraction)			**71.42**				

Table S27: The major identified compounds of the produced renewable crude oil via the HTL process from the HC sample at reaction temperature of 350ºC and residence time of 40 minutes using GC-MS analysis.

HC 350°C 40 Mins							
No	**Retention time (mins)**	**Area**	**Area (%)**	**Compound name**	**Molecular formula**	**Molecular weight (g/mol)**	**Classification of compound**
1	1.384	149957005	3.89	Carbon dioxide	CO_2	44	Protein[64, 6]
2	1.479	64005258	1.66	Methanethiol	CH_4S	48	Probably bacterial products[122]
3	1.588	43863613	1.14	Acetone	C_3H_6O	58	Carbohydrate[23]
4	2.635	54932590	1.43	Acetic acid	CH_3COOH	60	Carbohydrate, Lignin[64]
Total yields %			**8.12**				

1	8.001	35596395	0.92	2-Pyrrolidinone, 1-methyl-	C_5H_9NO	99	Protein[29]
2	8.906	71490787	1.86	2,5-Pyrrolidinedione, 1-methyl-	C_5H_7NO	113	Protein[64]

3	9.14	54395928	1.41	Pyrrolidinedinone, dimethyl isomer	C_6H_9NO2	127	Protein[64]
4	10.367	19976116	0.52	Methyl creatinine	$C_4H_7N_3O$	113	Protein[44]
5	10.887	21945262	0.57	Phenol, 3-(1-methylethyl)-	$C_9H_{12}O$	136	Lipid, Lignin[64, 10]
6	17.987	31711380	0.82	Benzene,1,1-(1,3-propanediyl) bis-	$C_{15}H_{16}$	196	Carbohydrate[2]
7	22.17	75821757	1.97	n-Hexadecanoic acid	$C_{16}H_{32}O_2$	256	Lipid, Protein, Carbohydrate[12, 64]
8	24.202	48475619	1.26	9-Octadecenamide, (Z)-	$C_{18}H_{35}NO$	281	Protein[64]
9	24.415	40376293	1.05	Octadecanamide	$C_{18}H_{37}NO$	283	Protein[64]
10	26.521	24151372	0.63	Cholestene isomer (3?)	$C_{27}H_{46}$	370	Lipid[45, 52, 88, 106]
11	26.731	24593177	0.64	Docosanoic acid	$C_{22}H_{44}O_2$	340	Lipid[41]
12	28.425	31445380	0.82	Cholestene isomer	$C_{27}H_{46}$	370	Lipid[45, 52, 88, 106]
13	28.679	35634093	0.93	Cholestene isomer	$C_{27}H_{46}$	370	Lipid[45, 52, 88, 106]
14	29.068	37648487	0.98	Cholestene isomer	$C_{27}H_{46}$	370	Lipid[45, 52, 88, 106]
15	29.858	42494008	1.10	Cholestene isomer	$C_{27}H_{46}$	370	Lipid[45, 52, 88, 106]
16	30.171	24699394	0.64	Cholesteneone isomer (24?)	$C_{27}H_{44}O$	384	Lipid[45, 52, 88, 106]
17	30.525	49168216	1.28	Cholestene isomer	$C_{27}H_{46}$	370	Lipid[45, 52, 88]
18	30.725	38088028	0.99	Cholestene isomer	$C_{27}H_{46}$	370	Lipid[45, 52, 88, 106]
19	31.028	390562555	10.14	Cholest-2-ene	$C_{27}H_{46}$	370	Lipid[45, 52, 88, 106]
20	31.228	781125110	20.29	Cholestane	$C_{27}H_{48}$	372	Lipid[45, 52, 88, 106]
21	31.492	37295227	0.97	Cholestadiene isomer	$C_{27}H_{44}$	368	Lipid[45, 52, 88, 106]
22	31.634	26032384	0.68	Cholestanone isomer	$C_{27}H_{46}O$	386	Lipid[22, 75]
23	32.019	91414490	2.37	Ergost-2-ene	$C_{28}H_{48}$	384	Lipid[22]
24	32.492	26791378	0.70	Stigmastene isomer	$C_{29}H_{50}$	398	Lipid[86]
25	32.787	150113932	3.90	Stigmast-2-ene, (5.alpha.)-	$C_{29}H_{50}$	398	Lipid[88]
26	32.985	35872185	0.93	Stigmastane	$C_{29}H_{52}$	400	Lipid[88]
27	33.177	38832622	1.01	Cholestenone isomer	$C_{27}H_{44}O$	384	Lipid[45, 52, 88, 106]
28	33.376	27341391	0.71	Cholestanone isomer	$C_{27}H_{46}O$	386	Lipid[22, 75]
29	35.441	10053206	0.26	Dihydroxychloesterol	$C_{27}H_{46}O_3$	418	Lipid[17]
Total yields %			**60.33**				
Total yields % (oil fraction + non-oil fraction)			**68.46**				

Table S28: The major identified compounds of the produced renewable crude oil via the HTL process from the HC sample at reaction temperature of 350°C and residence time of 60 minutes using GC-MS analysis.

HC 350°C 60 Mins							
No	**Retention time (mins)**	**Area**	**Area (%)**	**Compound name**	**Molecular formula**	**Molecular weight (g/mol)**	**Classification of compound**
1	1.236	30840471	1.33	Carbon dioxide	CO_2	44	Protein[64, 6]
2	1.287	33455637	1.44	Methanethiol	CH_4S	48	Probably bacterial products[122]
3	1.422	19131280	0.82	Acetone	C_3H_6O	58	Carbohydrate[23]
4	2.213	52396110	2.25	Acetic acid	CH_3COOH	60	Carbohydrate, Lignin[64]
Total yields %			**5.84**				
1	6.788	24585471	1.06	Phenol	C_6H_6O	94	Protein, Carbohydrate, Lignin[29, 52, 106]
2	7.779	37050946	1.59	2-Pyrrolidinone, 1-methyl-	C_5H_9NO	99	Protein[29]
3	8.665	57073065	2.45	2,5-Pyrrolidinedione, 1-methyl-	C_5H_7NO	113	Protein[64]
4	8.754	25088680	1.08	Pyrrolidinedinone, dimethyl isomer	$C_6H_9NO_2$	127	Protein[64]
5	8.924	44518160	1.91	Pyrrolidinedinone, dimethyl isomer	$C_6H_9NO_2$	127	Protein[64]
6	10.191	19937672	0.86	Methyl creatinine	$C_4H_7N_3O$	113	Protein[44]
7	10.724	15580813	0.67	Phenol, 2-methoxy-4-methyl-	$C_8H_{10}O_2$	138	Lignin[69]
8	16.709	12333328	0.53	Dodecanoic acid	$C_{12}H_{24}O_2$	200	Lipid, Protein[127]
9	17.791	36604885	1.57	Benzene,1,1-(1,3-propanediyl) bis-	$C_{15}H_{16}$	196	Carbohydrate[2]
10	20.302	16641653	0.72	Tetradecanoic acid	$C_{14}H_{28}O_2$	228	Lipid[45, 12]
11	21.407	13792732	0.59	d-Proline, n-butoxycarbonyl-, butyl ester	$C_{14}H_{25}NO_4$	271	Lipid, Protein, Carbohydrate[116]
12	21.963	60103770	2.58	n-Hexadecanoic acid	$C_{16}H_{32}O_2$	256	Lipid, Protein, Carbohydrate[12, 64]
13	24.006	31935983	1.37	Oleic Acid	$C_{18}H_{34}O_2$	282	Lipid[22]
14	24.214	30273412	1.30	9-Octadecenamide, (Z)-	$C_{18}H_{35}NO$	281	Protein[64]
15	24.392	14544893	0.63	Octadecanamide	$C_{18}H_{37}NO$	283	Protein[64]
16	24.794	16094685	0.69	Hexadecanamide	$C_{16}H_{33}NO$	255	Protein[64]
17	26.53	15850308	0.68	Cholestene isomer (3?)	$C_{27}H_{46}$	370	Lipid[45, 52, 88, 106]
18	28.228	18986163	0.82	Docosanoic acid	$C_{22}H_{44}O_2$	340	Lipid[41]
19	28.479	14115713	0.61	Cholestene isomer	$C_{27}H_{46}$	370	Lipid[45, 52, 88, 106]
20	28.867	22130651	0.95	Cholesteneone isomer (24?)	$C_{27}H_{44}O$	384	Lipid[45, 52, 88, 106]
21	30.519	27189662	1.17	Cholestene isomer	$C_{27}H_{46}$	370	Lipid[45, 52, 88, 106]
22	31.008	831635495	35.75	Cholestane	$C_{27}H_{48}$	372	Lipid[45, 52, 88, 106]

23	31.809	34804079	1.50	Cholestanone isomer	$C_{27}H_{46}O$	386	Lipid[22, 75]
24	32.573	90246319	3.88	Stigmastene isomer	$C_{29}H_{50}$	398	Lipid[86]
25	32.782	16049813	0.69	Stigmast-2-ene, (5.alpha.)-	$C_{29}H_{50}$	398	Lipid[88]
26	32.965	20185965	0.87	Stigmastane	$C_{29}H_{52}$	400	Lipid[88]
27	35.139	4900148	0.21	Dihydroxychloesterol	$C_{27}H_{46}O_3$	418	Lipid[17]
Total yields %			**66.73**				
Total yields % (oil fraction + non-oil fraction)			**72.57**				

Table S29: The major identified compounds of the produced renewable crude oil from the HLG sample before the HTL process using GC-MS analysis.

HLG S							
No	**Retention time (mins)**	**Area**	**Area (%)**	**Compound name**	**Molecular formula**	**Molecular weight (g/mol)**	**Classification of compound**
1	3.624	22271606	5.34	Carbon dioxide	CO_2	44	Protein[64, 6]
2	3.763	3849389	0.92	Methanol	CH_3OH	32	Lignin[68]
3	3.838	5484231	1.31	Methanethiol	CH_4S	48	Probably bacterial products[122]
4	4.041	3700031	0.89	Acetone	C_3H_6O	58	Carbohydrate[23]
5	4.906	31865700	7.63	Acetic acid	CH_3COOH	60	Carbohydrate, Lignin[64]
6	5.226	30465830	7.30	1-Butanol	$C_4H_{10}O$	74	Probably bacterial products[54]
7	5.718	3700572	0.89	Propanoic acid	$C_3H_6O_2$	74	Lipid, Protein[101]
8	6.316	7476619	1.79	Disulfide, dimethyl	$C_2H_6S_2$	94	Probably bacterial products[21]
9	6.637	3733946	0.89	Toluene	C_7H_8	92	Lipid, Protein, Carbohydrate[64]
10	7.235	3409052	0.82	Acetic acid, butyl ester	$C_6H_{12}O_2$	116	Carbohydrate[67]
11	7.513	8330005	2.00	Pyrazine, methyl-	$C_5H_6N_2$	94	Protein[44, 52]
12	10.034	4292121	1.03	Phenol	C_6H_6O	94	Protein, Carbohydrate, Lignin[29, 52, 106]
13	10.878	19536596	4.68	2-Pyrrolidinone, 1-methyl-	C_5H_9NO	99	Protein[29]
14	11.743	6474712	1.55	p-Cresol	C_7H_8O	108	Protein, Carbohydrate[64, 6]
15	11.968	8833206	2.12	2,5-Pyrrolidinedione, 1-methyl-	C_5H_7NO	113	Protein[64]
16	13.623	4092601	0.98	2,5-Pyrrolidinedione, 1-propyl-	$C_7H_{11}NO_2$	141	Protein[64]
17	21.753	4908729	1.18	Methyldecanone	$C_{11}H_{22}O$	170	Lipid, Protein, Carbohydrate[45, 43, 39]
18	22.726	3847886	0.92	Biphenylol isomer	$C_{12}H_{10}O$	170	Lipid, Protein, Carbohydrate[31, 22]
19	31.582	4415966	1.06	Cholestene isomer (3?)	$C_{27}H_{46}$	370	Lipid[45, 52, 88, 106]
20	32.159	6311719	1.51	Cholestene isomer (4?)	$C_{27}H_{46}$	370	Lipid[45, 52, 88, 106]
21	32.394	51601099	12.36	Cholest-2-ene	$C_{27}H_{46}$	370	Lipid[45, 52, 88, 106]
22	32.479	53774669	12.88	Cholestane	$C_{27}H_{48}$	372	Lipid[45, 52, 88, 106]

23	35.652	7675587	1.84	Stigmastene isomer (2?)	$C_{29}H_{50}$	398	Lipid[51]
24	35.77	8587041	2.06	Stigmastane	$C_{29}H_{52}$	400	Lipid[88]
25	43.451	7177042	1.72	Dihydroxychloesterol	$C_{27}H_{46}O_3$	418	Lipid[17]
Total yields %			**75.67**				

Table S30: The major identified compounds of the produced renewable crude oil via the HTL process from the HLG sample at reaction temperature of 250ºC and residence time of 20 minutes using GC-MS analysis.

HLG 250°C 20 Mins							
No	**Retention time (mins)**	**Area**	**Area (%)**	**Compound name**	**Molecular formula**	**Molecular weight (g/mol)**	**Classification of compound**
1	3.613	14573189	4.07	Carbon dioxide	CO_2	44	Protein[64, 6]
2	3.763	3696985	1.03	Methanol	CH_3OH	32	Lignin[68]
3	3.827	5705292	1.59	Methanethiol	CH_4S	48	Probably bacterial products[122]
4	4.607	3990899	1.11	2-Butanone	C_4H_8O	72	Carbohydrate[107]
5	4.692	4857330	1.36	Acetic acid	CH_3COOH	60	Carbohydrate, Lignin[64]
6	5.215	31860708	8.90	Propanoic acid	$C_3H_6O_2$	74	Lipid, Protein[101]
7	6.305	6394906	1.79	Disulfide, dimethyl	$C_2H_6S_2$	94	Probably bacterial products[21]
8	6.626	3773948	1.05	Toluene	C_7H_8	92	Lipid, Protein, Carbohydrate[64]
9	10.867	19480791	5.44	2-Pyrrolidinone, 1-methyl-	C_5H_9NO	99	Protein[29]
10	11.668	2761026	0.77	p-Cresol	C_7H_8O	108	Protein, Carbohydrate[64, 6]
11	11.957	5348934	1.49	2,5-Pyrrolidinedione, 1-methyl-	C_5H_7NO	113	Protein[64]
12	12.213	3540492	0.99	Methyl creatinine	$C_4H_7N_3O$	113	Protein[44]
13	12.373	2911638	0.81	Decamethylcyclopentasiloxane	$C_{10}H_{30}O_5Si_5$	370	Plastic[105]
14	21.721	2999148	0.84	Methyldecanone	$C_{11}H_{22}O$	170	Lipid, Protein, Carbohydrate[45, 43, 39]
15	31.56	5276825	1.47	Cholestene isomer (3?)	$C_{27}H_{46}$	370	Lipid[45, 52, 88, 106]
16	31.934	4141988	1.16	Cholestene isomer (7?)	$C_{27}H_{46}$	370	Lipid[45, 52, 88, 106]
17	32.148	10749167	3.00	Cholestene isomer (4?)	$C_{27}H_{46}$	370	Lipid[45, 52, 88, 106]
18	32.383	53827447	15.04	Cholest-2-ene	$C_{27}H_{46}$	370	Lipid[45, 52, 88, 106]
19	32.468	54755939	15.30	Cholestane	$C_{27}H_{48}$	372	Lipid[45, 52, 88, 106]
20	33.056	2852669	0.80	Cholestadiene isomer	$C_{27}H_{44}$	368	Lipid[45, 52, 88, 106]
21	34.017	2998727	0.84	Ergost-2-ene	$C_{28}H_{48}$	384	Lipid[22]
22	34.124	3411835	0.95	Ergostane	$C_{28}H_{50}$	386	Lipid[123]
23	35.63	8316340	2.32	Stigmastene isomer (2?)	$C_{29}H_{50}$	398	Lipid[51]

24	35.748	8040862	2.25	Stigmastane	$C_{29}H_{52}$	400	Lipid[88]
25	43.44	7583107	2.12	Dihydroxychloesterol	$C_{27}H_{46}O_3$	418	Lipid[17]
Total yields %			**76.50**				

Table S31: The major identified compounds of the produced renewable crude oil via the HTL process from the HLG sample at reaction temperature of 250ºC and residence time of 40 minutes using GC-MS analysis.

HLG 250°C 40 Mins							
No	**Retention time (mins)**	**Area**	**Area (%)**	**Compound name**	**Molecular formula**	**Molecular weight (g/mol)**	**Classification of compound**
1	1.156	10737773	1.49	Carbon dioxide	CO_2	44	Protein[64, 6]
2	1.231	20600700	2.86	Methanethiol	CH_4S	48	Probably bacterial products[122]
3	1.338	9281071	1.29	Acetone	C_3H_6O	58	Carbohydrate[23]
4	1.637	4366003	0.61	Acetic acid, methyl ester	$C_3H_6O_2$	74	Carbohydrate, Lignin[99, 5]
5	2.096	36022875	5.01	Propanoic acid	$C_3H_6O_2$	74	Lipid, Protein[101]
6	2.545	3228995	0.45	Acetic acid	CH_3COOH	60	Carbohydrate, Lignin[64]
Total yields %			**11.71**				

1	3.624	2664779	0.37	Pyridine, 2-methyl-	C_6H_7N	93	Protein[64]
2	6.626	3425219	0.48	Phenol	C_6H_6O	94	Protein, Carbohydrate, Lignin[29, 52, 106]
3	7.31	14693405	2.04	2-Pyrrolidinone, 1-methyl-	C_5H_9NO	99	Protein[29]
4	8.581	7630204	1.06	2-Hexanone, 4-methyl-	$C_7H_{14}O$	114	Lignin[126]
5	8.784	4728184	0.66	Phenol, 2-methoxy-	$C_{18}H_{36}O_2$	124	Lipid, Lignin[64, 10]
6	10.6	1723624	0.24	Creosol	$C_8H_{10}O_2$	138	Lignin[65]
7	13.506	1690023	0.23	2,5-Pyrrolidinedione, 1-pentyl-	C9H15NO2	169	Protein[45]
8	19.307	2597403	0.36	Dodecanoic acid	$C_{12}H_{24}O_2$	200	Lipid, Protein[127]
9	20.13	2720030	0.38	Tetradecanoic acid	$C_{14}H_{28}O_2$	228	Lipid[45, 12]
10	21.946	13305286	1.85	n-Hexadecanoic acid	$C_{16}H_{32}O_2$	256	Lipid, Protein, Carbohydrate[12, 64]
11	23.965	6171920	0.86	Oleic Acid	$C_{18}H_{34}O_2$	282	Lipid[22]
12	24.178	4378854	0.61	Octadecanoic acid	$C_{18}H_{36}O_2$	284	Lipid[22]
13	26.166	4537224	0.63	Cholestene isomer (3?)	$C_{27}H_{46}$	370	Lipid[45, 52, 88, 106]
14	30.214	9643774	1.34	Cholesteneone isomer (24?)	$C_{27}H_{46}O$	370	Lipid[45, 52, 88, 106]
15	30.45	5961606	0.83	Cholestene isomer	$C_{27}H_{46}$	370	Lipid[45, 52, 88, 106]
16	30.62	2917581	0.41	Cholestene isomer (3?)	$C_{27}H_{46}$	370	Lipid[45, 52, 88, 106]

17	30.866	178707464	24.85	Cholestadiene isomer	$C_{27}H_{44}$	368	Lipid[45, 52, 88, 106]
18	31.176	2826906	0.39	Cholest-2-ene	$C_{27}H_{46}$	370	Lipid[45, 52, 88, 106]
19	31.244	5653811	0.79	Cholestane	$C_{27}H_{48}$	372	Lipid[45, 52, 88]
20	31.646	2967820	0.41	Cholestadiene isomer	$C_{27}H_{44}$	368	Lipid[45, 52, 88, 106]
21	31.913	4813765	0.67	Cholestadiene isomer	$C_{27}H_{44}$	368	Lipid[45, 52, 88, 106]
22	32.469	27479418	3.82	Stigmastene isomer	$C_{29}H_{50}$	398	Lipid[86]
23	33.409	5764871	0.80	C30 17a(H)-hopane	$C_{30}H_{52}$	412	Lipid[25]
24	34.082	186725025	25.96	Cholestadienone isomer	$C_{27}H_{42}O$	382	Lipid[86]
25	34.968	4925525	0.68	Cholestanediol isomer	$C_{27}H_{48}O_2$	404	Lipid[22]
26	35.129	22551854	3.14	Dihydroxychloesterol	$C_{27}H_{46}O_3$	418	Lipid[17]
27	36.037	18100377	2.52	Diethylcholestene isomer	$C_{31}H_{54}$	426	Lipid[17]
28	37.49	3594283	0.50	Stigmastanediol isomer	$C_{29}H_{52}O_2$	432	Lipid[88]
Total yields %			**76.87**				
Total yields % (oil fraction + non-oil fraction)			**88.59**				

Table S32: The major identified compounds of the produced renewable crude oil via the HTL process from the HLG sample at reaction temperature of 250ºC and residence time of 60 minutes using GC-MS analysis.

HLG 250°C 60 Mins							
No	**Retention time (mins)**	**Area**	**Area (%)**	**Compound name**	**Molecular formula**	**Molecular weight (g/mol)**	**Classification of compound**
1	1.226	111077834	1.27	Methanethiol	CH_4S	48	Probably bacterial products[122]
2	1.348	80784366	0.92	Acetone	C_3H_6O	58	Carbohydrate[23]
3	1.58	49322680	0.56	Acetic acid, methyl ester	$C_3H_6O_2$	74	Carbohydrate, Lignin[99, 5]
4	1.666	55007589	0.63	2-Butanone	C_4H_8O	72	Carbohydrate[107]
5	2.137	216166802	2.47	Propanoic acid	$C_3H_6O_2$	74	Lipid, Protein[101]
6	2.419	46851445	0.53	Acetic acid	CH_3COOH	60	Carbohydrate, Lignin[64]
Total yields %			**6.38**				

1	7.307	145550279	1.66	2-Pyrrolidinone, 1-methyl-	C_5H_9NO	99	Protein[29]
2	8.523	75849734	0.87	2-Hexanone, 4-methyl-	$C_7H_{14}O$	114	Lignin[126]
3	8.745	62174584	0.71	Phenol, 2-methoxy-	$C_{18}H_{36}O_2$	124	Lipid, Lignin[64, 10]
4	10.523	33225686	0.38	Creosol	$C_8H_{10}O_2$	138	Lignin[65]
5	13.502	20265122	0.23	Phenol, 2-methoxy-4-methyl-	$C_8H_{10}O_2$	138	Lignin[69]

6	21.892	150238340	1.71	n-Hexadecanoic acid	$C_{16}H_{32}O_2$	256	Lipid, Protein, Carbohydrate[12, 64]
7	23.931	70759337	0.81	Oleic Acid	$C_{18}H_{34}O_2$	282	Lipid[22]
8	24.153	61808182	0.71	Octadecanoic acid	$C_{18}H_{36}O_2$	284	Lipid[22]
9	26.061	54716229	0.62	Cholestene isomer (3?)	$C_{27}H_{46}$	370	Lipid[45, 52, 88, 106]
10	30.219	105838372	1.21	Cholesteneone isomer (24?)	$C_{27}H_{46}O$	370	Lipid[45, 52, 88, 106]
11	30.455	92982994	1.06	Cholestene isomer	$C_{27}H_{46}$	370	Lipid[45, 52, 88, 106]
12	30.874	1612840887	18.41	Cholestene isomer (3?)	$C_{27}H_{46}$	370	Lipid[45, 52, 88, 106]
13	30.918	594129076	6.78	Cholestadiene isomer	$C_{27}H_{44}$	368	Lipid[45, 52, 88, 106]
14	31.124	44099890	0.50	Cholest-2-ene	$C_{27}H_{46}$	370	Lipid[45, 52, 88, 106]
15	31.191	88199780	1.01	Cholestane	$C_{27}H_{48}$	372	Lipid[45, 52, 88]
16	31.695	150086128	1.71	Cholestadiene isomer	$C_{27}H_{44}$	368	Lipid[45, 52, 88, 106]
17	31.92	96728607	1.10	Cholestadiene isomer	$C_{27}H_{44}$	368	Lipid[45, 52, 88, 106]
18	32.14	79308292	0.91	Ergost-2-ene	$C_{28}H_{48}$	384	Lipid[22]
19	32.324	95375709	1.09	Stigmastene isomer	$C_{29}H_{50}$	398	Lipid[86]
20	32.444	179433098	2.05	Stigmastene isomer	$C_{29}H_{50}$	398	Lipid[86]
21	32.48	194932353	2.23	Stigmastene isomer	$C_{29}H_{50}$	398	Lipid[86]
22	32.687	91021416	1.04	Stigmast-2-ene, (5.alpha.)-	$C_{29}H_{50}$	398	Lipid[88]
23	32.865	73434069	0.84	Stigmastane	$C_{29}H_{52}$	400	Lipid[88]
24	33.113	46910517	0.54	Cholestenone isomer	$C_{27}H_{44}O$	384	Lipid[45, 52, 88, 106]
25	33.232	44907668	0.51	Cholestanone isomer	$C_{27}H_{46}O$	386	Lipid[22, 75]
26	33.418	91458935	1.04	C30 17a(H)-hopane	$C_{30}H_{52}$	412	Lipid[25]
27	33.995	767182187	8.76	Cholestanone isomer	$C_{27}H_{46}O$	386	Lipid[22, 75]
28	35.098	197216784	2.25	Dihydroxychloesterol	$C_{27}H_{46}O_3$	418	Lipid[17]
29	35.975	71529845	0.82	Diethylcholestene isomer	$C_{31}H_{54}$	426	Lipid[17]
Total yields %			**61.55**				
Total yields % (oil fraction + non-oil fraction)			**67.93**				

Table S33: The major identified compounds of the produced renewable crude oil via the HTL process from the HLG sample at reaction temperature of 300ºC and residence time of 20 minutes using GC-MS analysis.

HLG 300°C 20 Mins							
No	**Retention time (mins)**	**Area**	**Area (%)**	**Compound name**	**Molecular formula**	**Molecular weight (g/mol)**	**Classification of compound**

1	1.143	5364732	1.19	Carbon dioxide	CO_2	44	Protein[64, 6]
2	1.239	10857464	2.41	Methanethiol	CH_4S	48	Probably bacterial products[122]
3	2.03	4231279	0.94	Propanoic acid	$C_3H_6O_2$	74	Lipid, Protein[101]
4	2.254	6599734	1.46	Acetic acid	CH_3COOH	60	Carbohydrate, Lignin[64]
Total yields %			**6.00**				

1	5	2125987	0.47	Styrene	C_8H_8	104	Protein[64]
2	7.286	7901403	1.75	2-Pyrrolidinone, 1-methyl-	C_5H_9NO	99	Protein[29]
3	8.771	3287418	0.73	Phenol, 2-methoxy-	$C_{18}H_{36}O_2$	124	Lipid, Lignin[64, 10]
4	13.525	2317245	0.51	Phenol, 2-methoxy-4-methyl-	$C_8H_{10}O_2$	138	Lignin[69]
5	13.621	2212024	0.49	Phenol, 3-(1-methylethyl)-	$C_9H_{12}O$	136	Lipid, Lignin[64, 10]
6	19.294	2735462	0.61	Dodecanoic acid	$C_{12}H_{24}O_2$	200	Lipid, Protein[127]
7	20.127	2469152	0.55	Tetradecanoic acid	$C_{14}H_{28}O_2$	228	Lipid[45, 12]
8	20.586	3010684	0.67	Complex Pyrrolidinedione isomer	$C_{14}H_{34}NO_2$	250	Protein[64]
9	21.858	7750027	1.72	n-Hexadecanoic acid	$C_{16}H_{32}O_2$	256	Lipid, Protein, Carbohydrate[12, 64]
10	23.93	5866419	1.30	Oleic Acid	$C_{18}H_{34}O_2$	282	Lipid[22]
11	24.154	5041689	1.12	Octadecanoic acid	$C_{18}H_{36}O_2$	284	Lipid[22]
12	24.315	2156936	0.48	Hexadecanamide	$C_{16}H_{33}NO$	255	Protein[64]
13	30.201	5698309	1.26	Cholesteneone isomer (24?)	$C_{27}H_{46}O$	370	Lipid[45, 52, 88, 106]
14	30.447	4540179	1.01	Cholestene isomer	$C_{27}H_{46}$	370	Lipid[45, 52, 88, 106]
15	30.81	101051973	22.41	Cholestadiene isomer	$C_{27}H_{44}$	368	Lipid[45, 52, 88, 106]
16	31.096	1535165	0.34	Cholest-2-ene	$C_{27}H_{46}$	370	Lipid[45, 52, 88, 106]
17	31.163	3070330	0.68	Cholestane	$C_{27}H_{48}$	372	Lipid[45, 52, 88]
18	31.889	2759121	0.61	Cholestadiene isomer	$C_{27}H_{44}$	368	Lipid[45, 52, 88, 106]
19	32.402	7011710	1.55	Stigmastene isomer	$C_{29}H_{50}$	398	Lipid[86]
20	32.669	2481270	0.55	Stigmastene isomer	$C_{29}H_{50}$	398	Lipid[86]
21	33.395	5345214	1.19	C30 17a(H)-hopane	$C_{30}H_{52}$	412	Lipid[25]
22	34.079	174984371	38.80	Cholestanone isomer	$C_{27}H_{46}O$	386	Lipid[22, 75]
23	34.966	6055042	1.34	Cholestadienone isomer	$C_{27}H_{42}O$	382	Lipid[45, 52, 88, 106]
24	35.041	3218948	0.71	Cholestanediol isomer	$C_{27}H_{48}O_2$	404	Lipid[22]
25	36.013	16355916	3.63	Dihydroxychloesterol	$C_{27}H_{46}O_3$	418	Lipid[17]
26	36.397	2335132	0.52	Diethylcholestene isomer	$C_{31}H_{54}$	426	Lipid[17]
Total yields %			**84.99**				
Total yields % (oil fraction + non-oil fraction)			**90.99**				

Table S34: The major identified compounds of the produced renewable crude oil via the HTL process from the HLG sample at reaction temperature of 300°C and residence time of 40 minutes using GC-MS analysis.

HLG 300°C 40 Mins							
No	**Retention time (mins)**	**Area**	**Area (%)**	**Compound name**	**Molecular formula**	**Molecular weight (g/mol)**	**Classification of compound**
1	1.348	20859273	6.32	Methanol	CH_3OH	32	Lignin[68]
2	1.445	5283194	1.60	Methanethiol	CH_4S	48	Probably bacterial products[54]
3	1.509	5488031	1.66	Acetone	C_3H_6O	58	Carbohydrate[23]
4	1.551	7496032	2.27	Acetic acid, methyl ester	$C_3H_6O_2$	74	Carbohydrate, Lignin[99, 5]
5	1.872	2095396	0.63	2-Butanone	C_4H_8O	72	Carbohydrate[107]
6	2.267	2712937	0.82	Propanoic acid	$C_3H_6O_2$	74	Lipid, Protein[101]
Total yields %			**13.31**				
1	6.989	2198729	0.67	Phenol	C_6H_6O	94	Protein, Carbohydrate, Lignin[29, 52, 106]
2	7.651	6273575	1.90	2-Pyrrolidinone, 1-methyl-	C_5H_9NO	99	Protein[29]
3	8.869	6170937	1.87	2,5-Pyrrolidinedione, 1-methyl-	C_5H_7NO	113	Protein[64]
4	9.104	3379922	1.02	Pyrrolidinedinone, dimethyl isomer	$C_6H_9NO_2$	127	Protein[64]
5	10.856	1863652	0.56	Creosol	$C_8H_{10}O_2$	138	Lignin[65]
6	13.88	1743630	0.53	Phenol, 3-(1-methylethyl)-	$C_9H_{12}O$	136	Lipid, Lignin[64, 10]
7	22.159	3686584	1.12	Complex Pyrrolidinedione isomer	$C_{14}H_{34}NO_2$	250	Protein[64]
8	22.234	4000264	1.21	n-Hexadecanoic acid	$C_{16}H_{32}O_2$	256	Lipid, Protein, Carbohydrate[12, 64]
9	24.242	5555673	1.68	Oleic Acid	$C_{18}H_{34}O_2$	282	Lipid[22]
10	24.467	4352728	1.32	Octadecanoic acid	$C_{18}H_{36}O_2$	284	Lipid[22]
11	24.638	2108009	0.64	Hexadecanamide	$C_{16}H_{33}NO$	255	Protein[64]
12	30.556	3623445	1.10	Cholestadiene isomer	$C_{27}H_{44}$	368	Lipid[45, 52, 88, 106]
13	30.813	2767628	0.84	Cholest-2-ene	$C_{27}H_{46}$	370	Lipid[45, 52, 88, 106]
14	31.219	13462715	40.79	Cholestane	$C_{27}H_{48}$	372	Lipid[45, 52, 88, 106]
15	31.539	5003131	1.52	Cholestadiene isomer	$C_{27}H_{44}$	368	Lipid[45, 52, 88, 106]
16	31.998	2166601	0.66	Cholestadiene isomer	$C_{27}H_{44}$	368	Lipid[45, 52, 88, 106]
17	32.265	1911629	0.58	Ergost-2-ene	$C_{28}H_{48}$	384	Lipid[22]
18	32.49	2409110	0.73	Stigmastene isomer	$C_{29}H_{50}$	398	Lipid[86]
19	32.671	3284299	1.00	Stigmast-2-ene, (5.alpha.)-	$C_{29}H_{50}$	398	Lipid[88]
20	32.778	11493188	3.48	Stigmastane	$C_{29}H_{52}$	400	Lipid[88]
21	33.035	2969647	0.90	Cholestenone isomer	$C_{27}H_{44}O$	384	Lipid[45, 52, 88, 106]

22	33.206	2157396	0.65	Cholestanone isomer	$C_{27}H_{46}O$	386	Lipid[22, 75]
23	33.793	5395249	1.63	C30 17a(H)-hopane	$C_{30}H_{52}$	412	Lipid[25]
24	34.402	53155491	16.10	Cholestadienone isomer	$C_{27}H_{42}O$	382	Lipid[124]
25	35.406	2206125	0.67	Cholestanediol isomer	$C_{27}H_{48}O_2$	404	Lipid[22]
26	35.524	2997292	0.91	Dihydroxychloesterol	$C_{27}H_{46}O_3$	418	Lipid[17]
27	36.507	3997997	1.21	Diethylcholestene isomer	$C_{31}H_{54}$	426	Lipid[17]
Total yields %			**85.29**				
Total yields % (oil fraction + non-oil fraction)			**98.60**				

Table S35: The major identified compounds of the produced renewable crude oil via the HTL process from the HLG sample at reaction temperature of 300ºC and residence time of 60 minutes using GC-MS analysis.

HLG 300°C 60 Mins							
No	**Retention time (mins)**	**Area**	**Area (%)**	**Compound name**	**Molecular formula**	**Molecular weight (g/mol)**	**Classification of compound**
1	3.613	3333249	1.17	Carbon dioxide	CO_2	44	Protein[64, 6]
2	4.671	9752821	3.42	Acetic acid	CH_3COOH	60	Carbohydrate, Lignin[64]
3	10.034	3925006	1.37	Phenol	C_6H_6O	94	Protein, Carbohydrate, Lignin[29, 52, 106]
4	10.985	4446591	1.56	2-Pyrrolidinone, 1-methyl-	C_5H_9NO	99	Protein[29]
5	11.743	10485443	3.67	p-Cresol	C_7H_8O	108	Protein, Carbohydrate[64, 6]
6	11.978	9079096	3.18	2,5-Pyrrolidinedion, 1-methyl	$C_5H_7NO_2$	113	Protein[64]
7	12.224	3686433	1.29	Methyl creatinine	$C_4H_7N_3O$	113	Protein[44]
8	12.64	2491826	0.87	2,5-Pyrrolidinedione, 1-ethyl-	$C_6H_9NO_2$	127	Protein[64]
9	13.613	4136147	1.45	2,5-Pyrrolidinedione, 1-propyl-	$C_7H_{11}NO_2$	141	Protein[64]
10	16.273	2678712	0.94	2,5-Pyrrolidinedione, 1-pentyl-	$C_9H_{15}NO_2$	169	Protein[45]
11	21.721	1907936	0.67	Methyldecanone	$C_{11}H_{22}O$	170	Lipid, Protein, Carbohydrate[45, 43, 39]
12	22.939	4156450	1.46	n-Hexadecanoic acid	$C_{16}H_{32}O_2$	256	Lipid, Protein, Carbohydrate[12, 64]
13	25.054	1978146	0.69	Hexadecanamide	$C_{16}H_{33}NO$	255	Protein[64]
14	25.364	1885755	0.66	Methyl hexadecanamide isomer	$C_{17}H_{33}NO$	269	Protein[64]
15	31.571	2957036	1.04	Cholestene isomer (3?)	$C_{27}H_{46}$	370	Lipid[45, 52, 88, 106]
16	31.945	3454619	1.21	Cholestene isomer (7?)	$C_{27}H_{46}$	370	Lipid[45, 52, 88, 106]
17	32.148	7520093	2.63	Cholestene isomer (4?)	$C_{27}H_{46}$	370	Lipid[45, 52, 88, 106]
18	32.383	51444753	18.02	Cholest-2-ene	$C_{27}H_{46}$	370	Lipid[45, 52, 88, 106]

19	32.468	45337743	15.88	Cholestane	$C_{27}H_{48}$	372	Lipid[45, 52, 88, 106]
20	33.067	2120134	0.74	Cholestadiene isomer	$C_{27}H_{44}$	368	Lipid[45, 52, 88, 106]
21	34.039	2641983	0.93	Ergost-2-ene	$C_{28}H_{48}$	384	Lipid[22]
22	35.353	1837230	0.64	Ergostane	$C_{28}H_{50}$	386	Lipid[123]
23	35.652	8596942	3.01	Stigmastene isomer (2?)	$C_{29}H_{50}$	398	Lipid[51]
24	35.759	6920914	2.42	Stigmastane	$C_{29}H_{52}$	400	Lipid[88]
25	39.979	3248341	1.14	Cholestanediol isomer	$C_{27}H_{48}O_2$	404	Lipid[22]
Total yields %			**70.05**				

Table S36: The major identified compounds of the produced renewable crude oil via the HTL process from the HLG sample at reaction temperature of 350ºC and residence time of 20 minutes using GC-MS analysis.

HLG 350°C 20 Mins							
No	**Retention time (mins)**	**Area**	**Area (%)**	**Compound name**	**Molecular formula**	**Molecular weight (g/mol)**	**Classification of compound**
1	1.307	85744684	2.58	Carbon dioxide	CO_2	44	Protein[64, 6]
2	1.404	103287583	3.11	Methanethiol	CH_4S	48	Probably bacterial products[122]
3	1.503	37771090	1.14	2-Propanamine	C_3H_9N	59	Protein[125]
Total yields %			**6.83**				
1	7.855	23527119	0.71	2-Pyrrolidinone, 1-methyl-	C_5H_9NO	99	Protein[29]
2	8.805	70801804	2.13	2,5-Pyrrolidinedione, 1-methyl-	C_5H_7NO	113	Protein[64]
3	9.024	53515730	1.61	Pyrrolidinedinone, dimethyl isomer	$C_6H_9NO_2$	127	Protein[64]
4	9.076	38483241	1.16	Methyl creatinine	$C_4H_7N_3O$	113	Protein[44]
5	10.786	29052624	0.88	Creosol	$C_8H_{10}O_2$	138	Lignin[65]
6	11.395	12328439	0.37	Phenol, 2-methoxy-4-methyl-	$C_8H_{10}O_2$	138	Lignin[69]
7	22.114	86963067	2.62	n-Hexadecanoic acid	$C_{16}H_{32}O_2$	256	Lipid, Protein, Carbohydrate[12, 64]
8	24.1	34191635	1.03	Oleic Acid	$C_{18}H_{34}O_2$	282	Lipid[22]
9	24.332	41801217	1.26	Octadecanoic acid	$C_{18}H_{36}O_2$	284	Lipid[22]
10	28.953	28783423	0.87	Docosanoic acid	$C_{22}H_{44}O_2$	340	Lipid[41]
11	30.414	29471695	0.89	Cholestene isomer	$C_{27}H_{46}$	370	Lipid[45, 52, 88, 106]
12	30.614	42573702	1.28	Cholestene isomer (3?)	$C_{27}H_{46}$	370	Lipid[45, 52, 88, 106]
13	30.697	27750719	0.84	Cholestadiene isomer	$C_{27}H_{44}$	368	Lipid[45, 52, 88, 106]
14	31.101	943980967	28.45	Cholest-2-ene	$C_{27}H_{46}$	370	Lipid[45, 52, 88, 106]

15	31.38	35693185	1.08	Cholestane	$C_{27}H_{48}$	372	Lipid[45, 52, 88]
16	31.674	23927194	0.72	Cholestadiene isomer	$C_{27}H_{44}$	368	Lipid[45, 52, 88, 106]
17	31.912	99022928	2.98	Cholestadiene isomer	$C_{27}H_{44}$	368	Lipid[45, 52, 88, 106]
18	32.113	26892385	0.81	Ergost-2-ene	$C_{28}H_{48}$	384	Lipid[22]
19	32.283	31810879	0.96	Stigmastene isomer	$C_{29}H_{50}$	398	Lipid[86]
20	32.372	25701571	0.77	Stigmastene isomer	$C_{29}H_{50}$	398	Lipid[86]
21	32.68	157365177	4.74	Stigmast-2-ene, (5.alpha.)-	$C_{29}H_{50}$	398	Lipid[88]
22	32.88	33283134	1.00	Stigmastane	$C_{29}H_{52}$	400	Lipid[88]
23	33.07	41613654	1.25	Cholestenone isomer	$C_{27}H_{44}O$	384	Lipid[45, 52, 88, 106]
24	33.271	33583937	1.01	Cholestanone isomer	$C_{27}H_{46}O$	386	Lipid[22, 75]
25	33.397	30214101	0.91	C30 17a(H)-hopane	$C_{30}H_{52}$	412	Lipid[25]
26	34.116	30977628	0.93	Cholestadienone isomer	$C_{27}H_{42}O$	382	Lipid[124]
27	34.734	12302831	0.37	Cholestanediol isomer	$C_{27}H_{48}O_2$	404	Lipid[22]
Total yields %			**61.65**				
Total yields % (oil fraction + non-oil fraction)			**68.48**				

Table S37: The major identified compounds of the produced renewable crude oil via the HTL process from the HLG sample at reaction temperature of 350ºC and residence time of 40 minutes using GC-MS analysis.

HLG 350°C 40 Mins							
No	**Retention time (mins)**	**Area**	**Area (%)**	**Compound name**	**Molecular formula**	**Molecular weight (g/mol)**	**Classification of compound**
1	3.602	9364817	3.24	Carbon dioxide	CO_2	44	Protein[64, 6]
2	4.745	21706452	7.52	Acetic acid	CH_3COOH	60	Carbohydrate, Lignin[64]
3	5.579	2754583	0.95	Propanoic acid	$C_3H_6O_2$	74	Lipid, Protein[101]
4	7.448	2330072	0.81	Pyrazine, methyl-	$C_5H_6N_2$	94	Protein[44, 52]
5	7.737	2712849	0.94	Pentanoic Acid	$C_5H_{10}O_2$	102	Lipid[61]
6	10.023	4952879	1.72	Phenol	C_6H_6O	94	Protein, Carbohydrate, Lignin[29, 52, 106]
7	10.942	3131506	1.08	2-Pyrrolidinone, 1-methyl-	C_5H_9NO	99	Protein[29]
8	11.123	4206950	1.46	2-Hexanone, 4-methyl-	$C_7H_{14}O$	114	Lignin[126]
9	11.764	16976950	5.88	p-Cresol	C_7H_8O	108	Protein, Carbohydrate[64, 6]
10	11.967	9701884	3.36	2,5-Pyrrolidinedione, 1-methyl-	C_5H_7NO	113	Protein[64]

11	12.213	4585832	1.59	Methyl creatinine	$C_4H_7N_3O$	113	Protein[44]
12	12.63	2784216	0.96	2,5-Pyrrolidinedione, 1-ethyl-	$C_6H_9NO_2$	127	Protein[64]
13	13.132	2544165	0.88	Phenol, 4-ethyl-	$C_8H_{10}O$	122	Lipid, Protein, Carbohydrate, Lignin[99,118,64,22]
14	13.548	3223375	1.12	Phenol, 3,4-dimethyl-	$C_8H_{10}O$	122	Lipid, Protein, Carbohydrate, Lignin[99,118,64,22]
15	14.617	3366463	1.17	Phenol, 2,3,5-trimethyl-	$C_9H_{12}O$	136	Lipid, Protein, Carbohydrate, Lignin[99,118,64,22]
16	19.937	3141847	1.09	Benzene, 1,1'-(1,3-propanediyl) bis-	$C_{15}H_{16}$	196	Carbohydrate[2]
17	22.928	7783725	2.70	n-Hexadecanoic acid	$C_{16}H_{32}O_2$	256	Lipid, Protein, Carbohydrate[12, 64]
18	25.054	2319697	0.80	Hexadecanamide	$C_{16}H_{33}NO$	255	Protein[64]
19	31.859	3284998	8.96	Cholest-2-ene	$C_{27}H_{46}$	370	Lipid[45, 52, 88, 106]
20	32.468	56771728	19.67	Cholestane	$C_{27}H_{48}$	372	Lipid[45, 52, 88, 106]
21	34.135	4804127	1.66	Ergostane	$C_{28}H_{50}$	386	Lipid[123]
22	35.63	3623481	1.26	Stigmastene isomer (2?)	$C_{29}H_{50}$	398	Lipid[51]
23	35.748	9727882	3.37	Stigmastane	$C_{29}H_{52}$	400	Lipid[88]
24	36.838	2622265	0.91	Cholestan-3-one, (5.alpha.)-	$C_{27}H_{46}O$	386	Lipid[22]
Total yields %			**73.11**				

Table S38: The major identified compounds of the produced renewable crude oil via the HTL process from the HLG sample at reaction temperature of 350°C and residence time of 60 minutes using GC-MS analysis.

HLG 350°C 60 Mins							
No	**Retention time (mins)**	**Area**	**Area (%)**	**Compound name**	**Molecular formula**	**Molecular weight (g/mol)**	**Classification of compound**
1	2.086	4840708	1.55	Propanoic acid	$C_3H_6O_2$	74	Lipid, Protein[101]
	Total yields %		**1.55**				

1	7.545	2273127	0.73	2-Pyrrolidinone, 1-methyl-	C_5H_9NO	99	Protein[29]
2	8.004	3980417	1.278	2-Hexanone, 4-methyl-	$C_7H_{14}O$	114	Lignin[126]
3	8.923	7494077	2.406	Phenol, 2-methoxy-	$C_{18}H_{36}O_2$	124	Lipid, Lignin[64, 10]
4	8.998	2195528	0.705	2,5-Pyrrolidinedione, 1-methyl-	C_5H_7NO	113	Protein[64]
5	9.147	5256850	1.688	Pyrrolidinedinone, dimethyl isomer	$C_6H_9NO_2$	127	Protein[64]
6	9.265	3249937	1.043	Methyl creatinine	$C_4H_7N_3O$	113	Protein[44]
7	10.13	1781702	0.572	Creosol	$C_8H_{10}O_2$	138	Lignin[65]
8	10.461	1718382	0.552	Phenol, 2-methoxy-4-methyl-	$C_8H_{10}O_2$	138	Lignin[69]
9	13.442	1582663	0.508	Phenol, 3-(1-methylethyl)-	$C_9H_{12}O$	136	Lipid, Lignin[64, 10]

10	17.982	2904843	0.933	Dodecanoic acid	$C_{12}H_{24}O_2$	200	Lipid, Protein[127]
11	19.392	1356852	0.436	Tetradecanoic acid	$C_{14}H_{28}O_2$	228	Lipid[45, 12]
12	22.277	11388876	3.657	n-Hexadecanoic acid	$C_{16}H_{32}O_2$	256	Lipid, Protein, Carbohydrate[12, 64]
13	24.21	2580270	0.828	Oleic Acid	$C_{18}H_{34}O_2$	282	Lipid[22]
14	24.478	5552605	1.783	Octadecanoic acid	$C_{18}H_{36}O_2$	284	Lipid[22]
15	24.627	2166905	0.696	Hexadecanamide	$C_{16}H_{33}NO$	255	Protein[64]
16	26.742	1983642	0.637	Cholestene isomer (3?)	$C_{27}H_{46}$	370	Lipid[45, 52, 88, 106]
17	29.061	2089404	0.671	Docosanoic acid	$C_{22}H_{44}O_2$	340	Lipid[41]
18	30.535	2348207	0.754	Cholesteneone isomer (24?)	$C_{27}H_{46}O$	370	Lipid[45, 52, 88, 106]
19	30.738	4899341	1.573	Cholestene isomer	$C_{27}H_{46}$	370	Lipid[45, 52, 88, 106]
20	31.251	139422213	44.76	Cholest-2-ene	$C_{27}H_{46}$	370	Lipid[45, 52, 88, 106]
21	31.496	1683445	0.541	Cholestane	$C_{27}H_{48}$	372	Lipid[45, 52, 88, 106]
22	31.934	1506539	0.484	Cholestadiene isomer	$C_{27}H_{44}$	368	Lipid[45, 52, 88]
23	32.031	7341876	2.357	Ergost-2-ene	$C_{28}H_{48}$	384	Lipid[22]
24	32.81	18933337	6.079	Stigmastane	$C_{29}H_{52}$	400	Lipid[88]
25	33.195	2938720	0.944	Cholestenone isomer	$C_{27}H_{44}O$	384	Lipid[45, 52, 88, 106]
26	33.398	2163026	0.694	Cholestanone isomer	$C_{27}H_{46}O$	386	Lipid[22, 75]
Total yields %			**77.31**				
Total yields % (oil fraction + non-oil fraction)			**78.87**				